

**Speciation of Metals in Proteins Using  
Gel Electrophoresis with Laser Ablation – ICP-MS**

**Kerry Tomlinson**

A thesis submitted in partial fulfilment of the  
requirements of the University of Sheffield for the

degree of

**Doctor of Philosophy**

*Department of Chemistry*

*University of Sheffield*

**June 2002**

## **IMAGING SERVICES NORTH**

Boston Spa, Wetherby

West Yorkshire, LS23 7BQ

[www.bl.uk](http://www.bl.uk)

**ORIGINAL COPY TIGHTLY  
BOUND**

*To Darren and Joshua Zachary*

*“Metals: We know so much and we know so little”*

*Arthur Furst 1977*

# Abstract

A study into the applicability of laser ablation inductively coupled plasma-mass spectrometry (LA ICP-MS) coupled with native polyacrylamide gel electrophoresis (PAGE) to metal speciation in proteins is described in this thesis.

Chapter one of the thesis outlines the various roles played by metal ions in clinical samples. Health risks can arise from anthropogenic metal enrichment and metallo-drug therapy is identified as a key source. The use of platinum and gold metallo-drugs is discussed in detail. Speciation of metals in clinical samples is examined, concentrating on some of the techniques currently employed and their limitations. Particular attention is paid to the techniques employed in the study. The aim of the study is outlined – to develop an alternative speciation strategy for the study of metals in proteins. The reagents and instrumentation used are described in chapter two along with all experimental procedures.

Chapter three describes the method development and determination of the analytical performance of the technique. The technique is used to study platinum speciation of protein samples enriched *in vitro*, the metal distribution profiles obtained are shown. The technique is next applied to the analysis of *in vivo* samples obtained from platinum therapy patients and a control source. Chapter four outlines the application of the technique to analysis of gold enriched samples both *in vitro* and *in vivo* from chrysotherapy patients. The gold distribution profiles obtained are shown and discussed. Chapter five looks at multi-element distribution and interactions occurring in serum. Elements naturally occurring at trace levels in serum, such as Cu and Fe, are studied *in vivo*. Other, lower level metals are studied following *in vitro* enrichment.

Chapter six concludes the study. It discusses how the technique was found to be applicable for metal speciation of clinical samples by meeting the criteria laid out at the start of the study. Recommendations for future work are also outlined.

# **Declaration**

I declare that this thesis, submitted in fulfilment of the degree of Doctor of Philosophy at the University of Sheffield, is my own work. It has not been previously submitted for a degree at this or any other university.

**Kerry Tomlinson**

**The University of Sheffield**

**June 2002**

## **Acknowledgements**

I would like to acknowledge, and thank, a number of people without whom this work would not have been possible.

Firstly I would like to express my gratitude to my Supervisor Professor Cameron McLeod for his guidance, advice and continued support throughout. My sincerest thanks also go to everyone in the Centre for Analytical Sciences, in particular Alan Cox and Dr Renli Ma for their scientific advice and encouragement. I would also like to thank Pat Mellor for all her assistance during the preparation of this thesis.

I would like to acknowledge; Hewlett Packard Ltd. Chemical Analysis Group, UK for the provision of the HP 4500 ICP-MS, and in particular Glenn Woods and Ed McCurdy for all their help and advice and CETAC/Transgenomic Inc., USA for the provision of LSX100/200, and in particular Dr Petra Krause and Dr Robert Hutton for all their help and advice.

I would like to thank everyone in the Child Health Department, Sheffield Childrens Hospital, for their help and guidance in particular Dr Hilary Powers and Dr Gareth Evans for all their advice. Thank you to Dr Arthur Moir for his assistance in mastering gel electrophoresis and to Professor Sheila Hancock and Dr Francesa Henshaw for their advice.

Thanks are also due to Professor Barry Hancock from the Department of Clinical Oncology at the Weston Park Hospital for help with the platinum studies and Dr Deborah Bax from the Department of Rheumatology at the Royal Hallamshire Hospital for help with the gold studies.

Finally I would like to thank my family and friends. Special thanks go to my husband Darren and son Joshua for their love, support and limitless patience without which none of this would have been possible.

# Abbreviations

1D	One Dimensional
2D	Two Dimensional
AAS	Atomic Absorption Spectroscopy
AMP	Ammonium Persulphate
amu	Atomic Mass Unit
BSA	Bovine Serum Albumin
CCD	Charge Coupled Device
CE	Capillary Electrophoresis
CRM	Certified Reference Material
Cys	Cysteine
DC	Direct Current
DDTC	Diethyldithiocarbamate
DIN	Direct Injection Nebulisation
DNA	Deoxyribonucleic Acid
EDTA	Ethylenedinitrilotetraacetate
ESR	Electron Spin Resonance
ETV	Electrothermal Vapourisation
FIA	Flow Injection Analysis
GC	Gas Chromatography
GF	Graphite Furnace
HPLC	High Pressure Liquid Chromatography
ICP	Inductively Coupled Plasma
IEF	Isoelectric Focusing
IEP	Immuno-electrophoresis
IPG	Immobilised pH Gradient
IR	Infra-red
IS	Internal Standard
LA	Laser Ablation
LOD	Limit of Detection
MALDI	Matrix Assisted Laser Desorption Ionisation
MCN	Microconcentric Nebulisation
MRI	Magnetic Resonance Imaging



<b>MS</b>	<b>Mass Spectrometry</b>
<b>MWCO</b>	<b>Molecular Weight Cut Off</b>
<b>m/z</b>	<b>Mass to Charge Ratio</b>
<b>NAA</b>	<b>Neutron Activation Analysis</b>
<b>Nd:YAG</b>	<b>Neodymium-Yttrium Aluminium Garnet Laser</b>
<b>NIST</b>	<b>National Institute of Standards and Technology</b>
<b>NMR</b>	<b>Nuclear Magnetic Resonance</b>
<b>OES</b>	<b>Optical Emission Spectroscopy</b>
<b>PAGE</b>	<b>Polyacrylamide Gel Electrophoresis</b>
<b>RA</b>	<b>Rheumatoid Arthritis</b>
<b>RDA</b>	<b>Recommended Daily Allowances</b>
<b>RF</b>	<b>Radio Frequency</b>
<b>RMM</b>	<b>Relative Molecular Mass</b>
<b>RNA</b>	<b>Ribonucleic Acid</b>
<b>Rpm</b>	<b>Revolutions per Minute</b>
<b>PBS</b>	<b>Phosphate Buffered Saline</b>
<b>pI</b>	<b>Isoelectric Point</b>
<b>RSD</b>	<b>Relative Standard Deviation</b>
<b>SDS</b>	<b>Sodium Dodecylsulphate</b>
<b>TB</b>	<b>Tuberculosis</b>
<b>TEMED</b>	<b>N,N,N'N'-tetramethylethylenediamine</b>
<b>TOF</b>	<b>Time of Flight Mass Spectrometry</b>
<b>UV</b>	<b>Ultra-violet</b>
<b>XRF</b>	<b>X-ray Fluorescence</b>

# Table of Contents

<b>Abstract</b>	<b>iv</b>
<b>Declaration</b>	<b>v</b>
<b>Acknowledgements</b>	<b>vi</b>
<b>Abbreviations</b>	<b>vii</b>
<b>Table of Contents</b>	<b>ix</b>
<b>Chapter 1: Introduction</b>	<b>1</b>
<b>1.1 Role of Trace Elements in the Human Body</b>	<b>1</b>
<b>1.2 Metabolism of Trace Elements in the Human Body</b>	<b>6</b>
<b>1.3 Anthropogenically Enriched Elements in the Human Body</b>	<b>10</b>
1.3.1 Platinum Drugs	12
1.3.2 Gold Drugs	18
1.3.3 Other Metal Based Drugs	24
<b>1.4 Trace Element Determination and Speciation in Biological Systems</b>	<b>26</b>
1.4.1 Trace Element Determination	26
1.4.2 Separation	36
1.4.3 Hyphenated Approaches	45
<b>1.5 The Aim of This Study</b>	<b>53</b>
<b>Chapter 2: Experimental</b>	<b>55</b>
<b>2.1 Reagents and Materials</b>	<b>55</b>
2.1.1 Reagents	55
2.1.2 Materials	56
2.1.3 Preparation of Electrophoresis Buffers and Gels	56
<b>2.2 Electrophoresis</b>	<b>59</b>
2.2.1 Equipment	59
2.2.2 Sample Preparation	61
2.2.3 Experimental Procedures	63
<b>2.3 Laser Ablation ICP-MS</b>	<b>69</b>
2.3.1 Instrumentation	69
2.3.2 Experimental Procedures	70

<b>2.4</b>	<b>Flow Injection ICP-MS</b>	<b>74</b>
2.4.1	Instrumentation	74
2.4.2	Experimental Procedure	74
<b>Chapter 3: Characterisation of Platinum Enriched Gels</b>		<b>75</b>
<b>3.1</b>	<b>Introduction</b>	<b>75</b>
<b>3.2</b>	<b>Method Development</b>	<b>78</b>
3.2.1	Flow Injection – ICP-MS	78
3.2.2	Laser Ablation of Gels	80
3.2.3	Electrophoresis	89
3.2.4	Basic Analytical Performance	109
<b>3.3</b>	<b>Application of FI ICP-MS to Clinical Samples</b>	<b>118</b>
3.3.1	<i>In Vitro</i> Studies	118
3.3.2	<i>In Vivo</i> Studies	122
<b>3.4</b>	<b>Application of LA ICP-MS to Clinical Samples</b>	<b>123</b>
3.4.1	<i>In Vitro</i> Studies	123
3.4.2	<i>In Vivo</i> Studies	133
<b>3.5</b>	<b>Main Findings</b>	<b>135</b>
<b>Chapter 4: Characterisation of Gold Enriched Gels</b>		<b>137</b>
<b>4.1</b>	<b>Introduction</b>	<b>137</b>
<b>4.2</b>	<b>Method Development</b>	<b>139</b>
4.2.1	Electrophoresis	140
4.2.2	Basic Analytical Performance	143
<b>4.3</b>	<b>Application of FI ICP-MS to Clinical Samples</b>	<b>147</b>
4.3.1	<i>In Vitro</i> Studies	147
4.3.2	<i>In Vivo</i> Studies	149
<b>4.4</b>	<b>Application of LA ICP-MS to Clinical Samples</b>	<b>150</b>
4.4.1	<i>In Vitro</i> Studies	150
4.4.2	<i>In Vivo</i> Studies	158
<b>4.5</b>	<b>Main Findings</b>	<b>160</b>
<b>Chapter 5: Multi-Element Studies</b>		<b>162</b>
<b>5.1</b>	<b>Introduction</b>	<b>162</b>

<b>5.2</b>	<b>Application of LA ICP-MS to Clinical Samples</b>	<b>163</b>
5.2.1	Essential Metals Naturally Occurring in Serum	164
5.2.2	Anthropogenically Enriched Metals	168
5.2.3	Metal Interactions in Serum	181
<b>5.3</b>	<b>Main Findings</b>	<b>184</b>
<b>Chapter 6: Conclusions and Recommendations for Future Work</b>		<b>186</b>
<b>6.1</b>	<b>Conclusions</b>	<b>186</b>
<b>6.2</b>	<b>Recommendations for Future Work</b>	<b>189</b>
<b>Appendix 1</b>		<b>191</b>
<b>Appendix 1.1: Elemental Composition of a Reference Person</b>		<b>192</b>
<b>Appendix 1.2: The Natural Protein Amino Acids</b>		<b>193</b>
<b>Appendix 1.3: Metallo-drugs used in Sample Enrichment</b>		<b>194</b>
<b>Appendix 1.4: Properties of Serum Proteins</b>		<b>195</b>
<b>Appendix 1.5: Metal Standards used in Sample Enrichment</b>		<b>196</b>
<b>Appendix 1.6: Laser Ablation Parameters</b>		<b>197</b>
<b>Appendix 1.7: Composition of SRM612</b>		<b>198</b>
<b>Appendix 2</b>		<b>199</b>
<b>Appendix 2.1: Protein Assay</b>		<b>200</b>
<b>Appendix 2.2: Calculation of Iron Concentration</b>		<b>203</b>
<b>Appendix 2.3: Metal Profiles for Enriched Serum</b>		<b>204</b>
<b>Appendix 2.4: Metal Distribution in Enriched Serum</b>		<b>209</b>
<b>Appendix 2.5: MALDI TOF Spectra from Albumin Analysis</b>		<b>211</b>
<b>Bibliography</b>		<b>212</b>

# Chapter 1: Introduction

## 1.1 Role of Trace Elements in the Human Body

Within the human body there exist a multitude of elements at a variety of concentrations (see Appendix 1.1). Some of these elements play important biological roles whilst others serve no apparent function. Surprisingly just four elements; carbon, oxygen, hydrogen and nitrogen make up over 99 % of the total number of atoms present in the body<sup>1</sup>. These four elements are known as the bulk elements and are present at the g/kg level. A further 0.9 % is made of a group known as the macro-nutrients. These seven elements are found in the body at g/kg level. All the bulk elements and macro-nutrients are essential to the body. The remaining 0.1 % of the body mass is made up of a number of elements ranging in concentration from mg- $\mu$ g/kg, these are known as the trace elements. Very little is known about the exact biochemical behaviour of most of the trace elements. Table 1.1 shows a classification of elements commonly found in the human body.

<b>Class</b>	<b>Elements</b>
<b>Bulk Elements</b>	C, H, N, O
<b>Macro-nutrients</b>	Ca, Cl, K, Mg, Na, P, S
<b>Essential Trace Elements</b>	Co, Cr, Cu, F, Fe, I, Mn, Mo, Se, Zn
<b>Possibly Essential Trace Elements</b>	Ni, Si, Sn, V
<b>Non-Essential Trace Elements</b>	Ag, Al, As, Au, B, Ba, Cd, Ge, Hg, Li, Pb, Pt, Rb, Sb, Sr

*Table 1.1: Classification of elements present in the human body*

Mertz<sup>2</sup> first classified the trace elements into two groups; those which have been established as essential for life and health, and those for which proof of essentiality does not (yet) exist. To avoid confusion a definition of essentiality was drawn up<sup>3</sup>, it states that an element is regarded as essential when deficient intake consistently results in an impairment of function and when supplementation with physiological levels cures the impairment. Using epidemiological surveys and animal experiments the trace elements found in the human body have been

classified. Non-essentiality is however, hard to determine due to the extremely low concentrations involved and the problems of contamination. Elements previously considered to be non-essential have been found to play important biological roles as a result of advancement in analytical techniques. It is, therefore, prudent to add a third category containing elements, which may possibly be essential. The biologically important elements tend to be the lighter elements, which are most abundant on earth. These elements tend to be bio-available as a result of their solubility in water. All the essential elements should be provided in the diet to prevent deficiency symptoms developing.

The absolute and relative concentrations of elements are crucial for a healthy existence. No element is inherently toxic or beneficial, they all elicit a biphasic response. Each element has its own specific curve of biological response against concentration, see Figure 1.1.

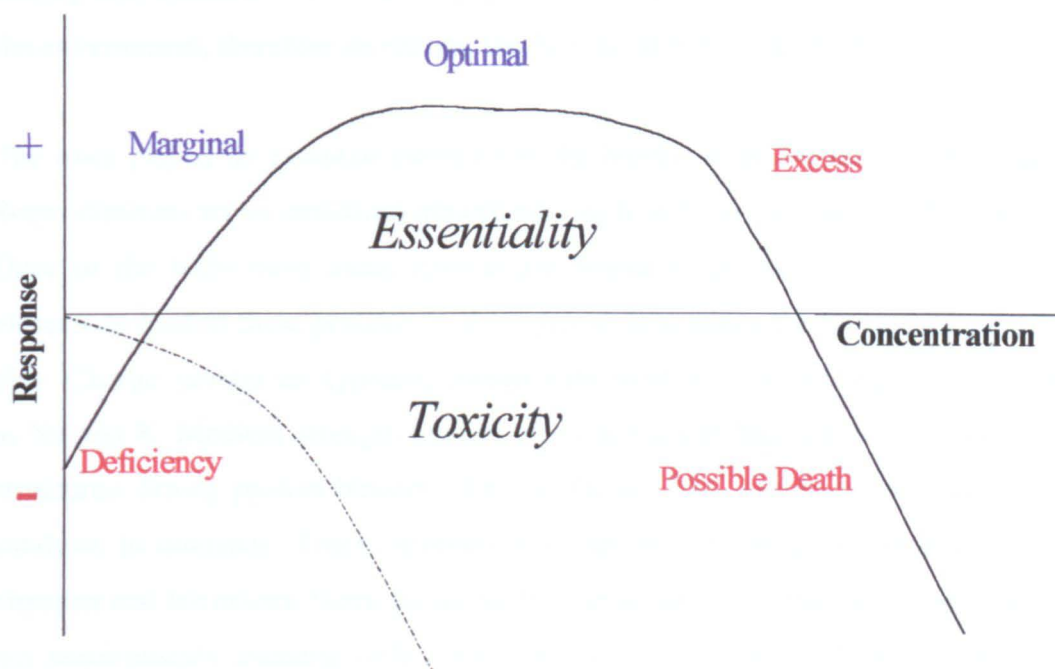


Figure 1.1: Curve of Biological Response vs. Concentration. Solid line - essential elements, dotted line - non-essential elements. Figure adapted from<sup>4</sup>

The balance of elements in a healthy body is very delicate since the difference between beneficial and toxic levels for some essential elements can be quite small. Disorders can occur if this delicate balance is upset and so diagnostic screening of body fluids and tissues is often used. Concentrations of essential elements in the body are under homeostatic control, but for non-essential elements there are no such controls. Extremes in concentration of any element, even the essential elements, can lead to illness or even death, see Table 1.2. Recommended Daily Allowances (RDA) have been drawn up as a guideline to help minimise the occurrence of such toxic effects<sup>5</sup>.

The adequacy of a diet is determined not only by the concentration of an element in the food, but also the bioavailability of that element, that is its ability to be absorbed and utilised by the body. The bioavailability of different elements can vary greatly, Na and K are readily absorbed by the body, whilst strongly hydrostable elements are hardly absorbed at all. For non-essential elements, levels in the body reflect the levels in food and water. Modern day activities such as mining and industrialisation have resulted in the increased release of metals into the environment, therefore increasing the likelihood of toxicity problems.

The roles played by essential elements in the human body are many and varied. Some elements are of structural importance, such as Si in cartilage and F in bone. Once in the body most metal cations are bound to proteins, the ability of an element to bind to these proteins (and enzymes) determines the type of role it will play. Charge carriers are typically metals with weak protein binding ability, such as Na and K. Medium strength binders, such as Ca and Mg, are used to stabilise structures. Strong protein binders, like Cu, Zn and Mo, tend to be used as redox catalysts in enzymes. Trace elements also function as integral components of vitamins and hormones. Some biological processes are very specific in their metal ion requirements meaning only certain metals of specific oxidation states can fulfill the requirements of a catalytic or structural role. Other processes are much less specific in their requirements such that one metal ion can replace another, although this can be at the expense of biological activity.

Element	Deficiency Symptom	Excess Symptom
Ca	Bone Deformities Tetany	Cataract, Gall Stones Atherosclerosis
Co	Anaemia Anorexia Growth Depression	Cardiac Failure Hypothyroidism
Cr	Impaired Glucose Tolerance Elevated Serum Lipids Corneal Opacity	Lung Cancer Contact Dermatitis
Cu	Anaemia Kinky Hair Syndrome Defective Melanin Production Defective Keratinisation Ataxia	Wilson's Disease Liver Cirrhosis Neuropathy Hypertension
F	Dental Caries	Fluorosis
Fe	Anaemia General Weakness	Haemochromatosis Siderosis Liver Cirrhosis
I	Goiter Cretinism	Goiter Thyrotoxicosis
K	Nephropathy Muscular Weakness Respiratory Failure	Addison's Disease
Li	Manic Depression	Hypothyroidism Epileptiform Seizures
Mg	Convulsions	Anaesthesia
Mn	Skeletal and Cartilage Defects Gonadal Dysfunction	Ataxia Manganism Psychiatric Disorders Motor Neurone diseases
Mo	Growth Depression Defective Keratinisation Hyperuricaemia	Anaemia Gout-like Syndrome
Na	Addison's Disease Stomach Cramps	Hypertension Fluid Retention/Swelling
Ni	Growth Depression Impaired Reproduction	Lung Cancer Contact Dermatitis
Se	Liver Necrosis White Muscle Disease Endemic Cardiomyopathy Osteoarthropathy	Selenosis Dermatitis Arthritis Hair Loss
Si	Growth Depression Bone and Cartilage Defects	Silicosis
Sn	Impaired Digestion Growth Depression	Visual Defects Electroencephalographic Abnormalities
V	Growth Depression Failure to Reproduce	Mucosa Membrane Irritation
Zn	Anorexia Growth Depression Sexual Immaturity Hypogonadism Skin Lesions Hyperkeratosis Depression of Immune Response	Pancreatic and Renal Damage Anaemia Skeletal and Tissue Lesions Perinatal Mortality

*Table 1.2: Symptoms of deficiency and excess of some essential elements.*

*Table adapted from<sup>6</sup>*



A large number of complex interdependencies exist between the elements present in a human body. An example of some interdependencies is shown in Figure 1.2. Trace elements can exert stimulatory or antagonistic effects upon one another. Elements of similar ionic radius and electronic configuration are likely to compete, see Table 1.3. Such interactions can include substitution at an active site on an enzyme or competition for binding to a transport or storage protein. As a result of these interdependencies an excess of one element can interfere with the biological activity of another, for some elements such interferences are well documented whilst little is known about others. The presence of complexing agents in the body, such as EDTA, can affect the delicately balanced homeostasis.

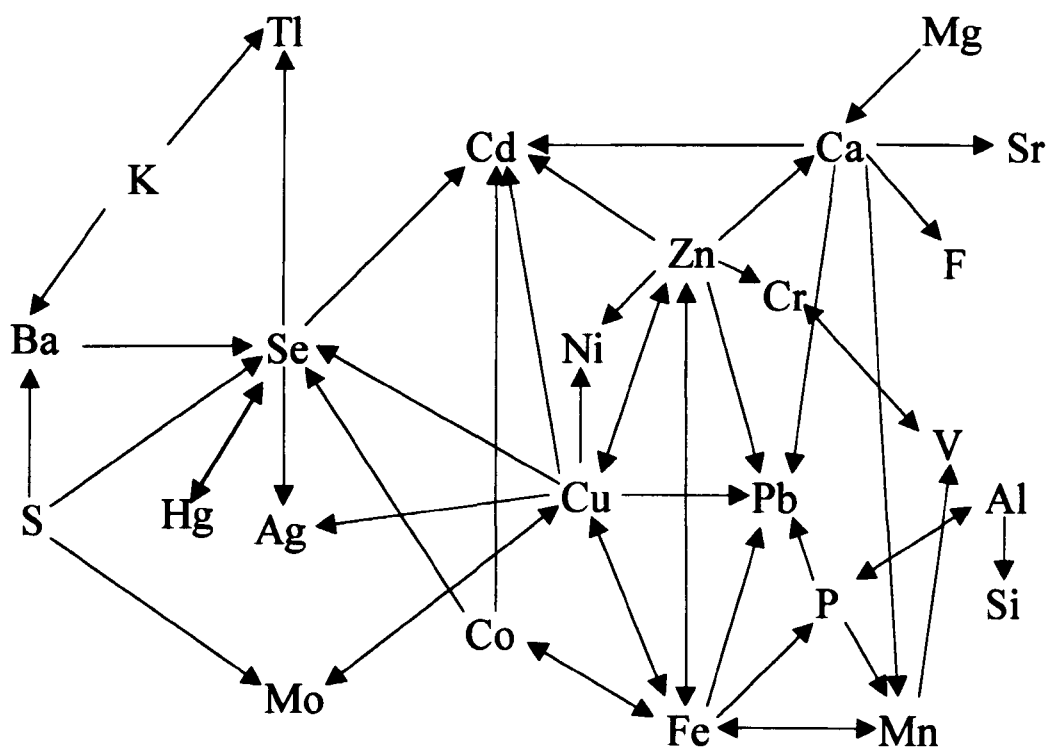


Figure 1.2: Interdependencies of elements in the body. Figure adapted from<sup>7</sup>

Knowledge of these elemental interactions can be useful, an example of such a case is the use of Se to protect against the toxicity of some heavy metals. Se has a high affinity for Hg, Cd and Ag readily complexing these elements and so decreasing their biological activity.

An excess of	Can produce a deficit of
Cd	Se, Zn
Ca	Zn
Fe	Cu, Zn
Mo	Cu
Zn	Cu, Fe

*Table 1.3: Competition between some essential elements, table adapted from<sup>8</sup>*

## **1.2 Metabolism of Trace Elements in the Human Body**

Metals are absorbed into the body by ingestion, inhalation or more rarely by resorption through the skin. Once absorbed metals and their compounds enter the blood where they are mostly bound by blood cells and/or plasma proteins. This is a rapidly reversible process. Plasma protein binding can be specific as in the case of transferrin (Fe) and ceruloplasmin (Cu) or non-specific as in the case of albumin - the most abundant serum protein. The bloodstream then distributes the metals throughout the body. Serum is an important channel of transport for many metabolic entities and so helps maintain metabolic stability within the human body. High molecular mass blood cells and proteins bound to metal ions cannot cross the capillary walls and so the transfer of metal ions to body tissues is dependent upon the diffusible fraction, that is the fraction not bound. Metals can be lost from the body in two ways via the liver or via the kidneys. The manner in which metals are excreted depends upon the individual metal. Sodium and potassium go through the kidneys (i.e. excreted in the urine) along with very small amounts of copper and zinc. In general, however, most of the trace metals are lost via the liver (i.e. in the faeces). Figure 1.3 illustrates the possible pathways of ingested trace metals.

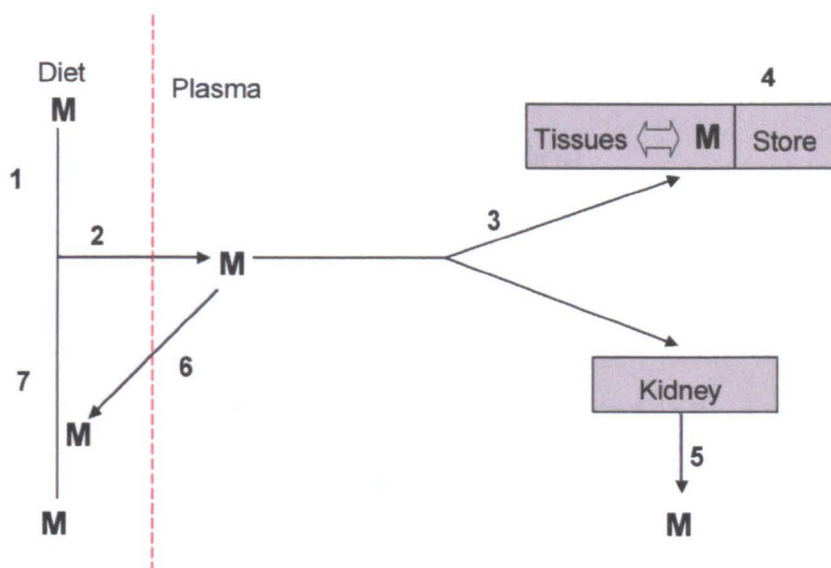
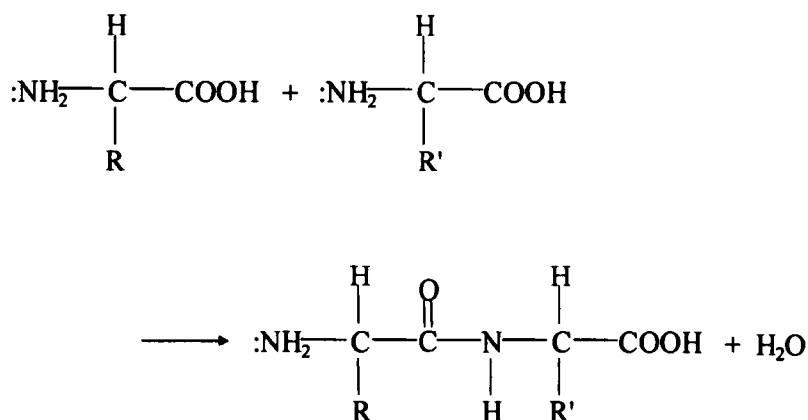


Figure 1.3: Metal ion absorption and excretion

- |                                    |                         |
|------------------------------------|-------------------------|
| 1) Metal intake                    | 5) Urinary excretion    |
| 2) % Absorption                    | 6) Re-excretion by bile |
| 3) Transfer to/Release from tissue | 7) Faecal excretion     |
| 4) Storage                         |                         |

Metal cations found within the body are mostly bound to proteins. The role that each metal ion serves is, therefore, dictated by its ability to bind to these proteins, and in particular enzymes. Metals with weak binding ability, such as sodium and potassium, act as charge carriers. Medium strength binders, such as calcium and magnesium, act to stabilise structures whilst those with very strong binding abilities, such as copper, zinc and molybdenum, act as redox catalysts. Metal toxicity is attributed to metals binding with enzymes and other molecules preventing normal biological functioning.

To understand further the biological/toxic roles of trace metals it is necessary to take a closer look at serum proteins and the possible binding interactions that can occur with trace metals in the body. In general all proteins are able to bind metals on their surface. Proteins are macromolecules, which serve a variety of critical biological functions. The building blocks of proteins are amino acids, polymerised by condensation reactions as shown in Figure 1.4.



*Figure 1.4: Condensation of amino acids to form polypeptides and proteins*

The term ‘metal binding’ is somewhat misleading. The subject of metal adsorption by serum proteins was poorly understood until Langmuir wrote two papers clarifying the subject<sup>9, 10</sup>. It is now known that a considerable amount of metal binding occurs on the surface of the proteins, with covalent bonds (relatively rare but very strong – 40-140 kcal/mole) occurring only in the centre of the protein. When dissolved, proteins are in a colloidal state and so have an enormous surface area for adsorption (1 cm<sup>3</sup> serum = 100 m<sup>2</sup> protein surface)<sup>11</sup>. Despite the fact that most protein-metal interactions are not true bonds the term ‘bond’ is still widely used.

To understand in detail the effects of trace metals on living systems it is necessary to know the nature of the protein binding sites. There are 20 naturally occurring amino acids, each with a different functional group, R (see Appendix 1.2). The amino acids most likely to bind trace elements in serum are aspartic acid, glutamic acid, cysteine (S donor) and histidine (N donor)<sup>12</sup> and possibly lysine (N donor)<sup>13</sup>. Important information about metabolic homeostasis can be obtained from the identification of specific ligand-protein interactions in serum since protein binding controls the distribution of trace metals to tissues, the rate and mechanism of their release and also regulates the metabolism/loss of trace metals. Some typical metal binding sites are given in Table 1.4.

<b>Metal</b>	<b>Ligand</b>
Fe <sup>2+</sup> , Fe <sup>3+</sup>	O, N, S,
alkaline earth metals	O
lanthanides	O
Al <sup>3+</sup> , Cr <sup>3+</sup>	O
di-positive first row transition metals	N
Mn <sup>2+</sup> ⇒ Cu <sup>2+</sup>	N
Zn <sup>2+</sup>	N or S *
Cd <sup>2+</sup> , CH <sub>3</sub> Hg <sup>+</sup> , Pb <sup>2+</sup>	S

*Table 1.4: Favoured metal binding ligands. \* Depending on chelation*

The toxic action of trace elements may be due to the protein complexes formed in the serum. Changes in the molecular structure of proteins result in the appearance of acute metal poisoning. The metals may block active sites, break hydrogen (H) bonds or change the conformation and solubility of the proteins. Toxicity tends to increase with decreasing electron configuration stability, hence, heavy metals are potentially the most toxic elements. This can be explained by the increased affinity of heavy metals for amino, imino and sulphhydryl groups all of which make up the active centres of enzymes and proteins. The exact proteins affected by such heavy metal toxicity are not known.

The chemical forms of trace elements in the body determine their physiological behaviour, much work has been done in this field by Cornelis<sup>14, 15</sup>. These different chemical forms are known as species and their study is known as speciation. The official definition of speciation currently under discussion at IUPAC states that; “Speciation analysis is the process leading to the identification and determination of the different chemical and physical forms of an element existing in a sample”<sup>16</sup>. A prime example of metal toxicity being determined by valence state is the element arsenic, As(V) is relatively harmless whereas As(III) is highly toxic.

Toxicity can also be affected by biomethylation. Metallic mercury does little harm to man, but  $\text{RHg}^+$  compounds, particularly methylmercury cations, are extremely toxic due to their ability to cross the blood-brain barrier. Hence, when analysing biological samples there is a need for speciation, that is a need to know where the element is located and what form it exists in. Total elemental concentration very rarely yields adequate information to determine biological status.

### **1.3 Anthropogenically Enriched Elements in the Human Body**

In recent years levels of elements previously rare in the biosphere have increased, mainly due to industrialisation. Industrialisation has led to the widespread pollution of air and water. This has, in turn, led to pollution of the food chain. As a direct result the occurrence of pollutant trace metals in the human body has increased. Zn smelting has led to a hundred fold increase in Cd levels<sup>17</sup>, whilst the widespread introduction of the automobile has led to an increase in Pb emissions<sup>18</sup>. Many occupations now carry a risk of exposure to such elements and their associated toxic effects. As a result clinical screening is used to warn of such risks. Whilst at the moment there are no known biological roles for elements such as Ta and Zr the increased presence of such elements as contaminants in the environment may lead to their incorporation into biological system. This leads to the need for increased knowledge on the function of such elements in the body and also the future need for toxicological studies.

Another source of increased metal exposure is the use metallo-drugs in medicine. Metallo-drugs are being utilised increasingly, one of the problems associated with their use is the poor characterisation with respect to *in vivo* toxicity. The mode of action, identification of target sites and potential toxicity of the compound are all important details concerning the development of metallo-drugs. The effect of a drug upon biological processes in the body is dependent upon the active site of the drug. Most modern drugs incorporate metal ions as part of their active site (See Table 1.5) and so the mode of action is determined by the type of metal present.

Element	Compound	Use
Ag	Ag(sulfadiazine)	Antibacterial
Al	KAl(SO <sub>4</sub> ) <sub>2</sub> ·12H <sub>2</sub> O	Astringent Antacid
Al	Al(OH) <sub>3</sub>	Antiperspirant
As	As <sub>2</sub> O <sub>3</sub>	Antileukaemic
Au	Au(thioglucose)	Antiarthritic
B	B <sub>12</sub> H <sub>11</sub> SH <sub>2</sub> <sup>-</sup>	Neutron Capture Therapy
Ba	Ba salts	X-ray Diagnosis
Bi	K <sub>3</sub> [Bi(citrate) <sub>2</sub> ]	Antiulcer, Antacid
Ca	CaCO <sub>3</sub>	Antacid
Ce	Ce(NO <sub>3</sub> ) <sub>3</sub>	Burn Wounds
Co	Coenzyme B <sub>12</sub>	Pernicious Anaemia
Cu	CuCO <sub>3</sub>	Dietary Supplement
F	SnF <sub>2</sub> , NaF	Anticaries
Fe	[Fe(Me <sub>4</sub> phen) <sub>3</sub> ] <sup>2+</sup>	Antimicrobial
Fe	Na <sub>2</sub> [Fe(NO)(CN) <sub>5</sub> ]	Vasodilator
Gd	Gd(chelate)	Magnetic Resonance Imaging
Ge	carboxyethyl Ge(IV)	Anticancer
La	La carbonate	Kidney Disease
Li	Li <sub>2</sub> CO <sub>3</sub>	Manic Depression
Mg	MgO	Laxative, Antacid
Mn	Mn(chelate)	Magnetic Resonance Imaging
N	N <sub>2</sub> O	Anesthetic
Os	tetroxide	Antiarthritic
Pt	cis-Pt(NH <sub>3</sub> ) <sub>2</sub> Cl <sub>2</sub>	Anticancer
Ru	[Ru(Me <sub>4</sub> phen) <sub>2</sub> (acac)] <sup>+</sup>	Antimicrobial
S	Na <sub>2</sub> S <sub>2</sub> O <sub>3</sub>	Cyanide Antidote
Sb	NaSb(gluconate)	Antileishmanial
Se	SeS <sub>2</sub>	Antiseborrhoeic
Sn	Sn(protoporphyrin)-(Cl <sub>2</sub> )	Jaundice Treatment
Tc	Tc propyleneamineoxime	Diagnostic Radio Imaging
Xe	Xenon gas	Anaesthetic
Zn	ZnCO <sub>3</sub> , Fe <sub>2</sub> O <sub>3</sub>	Skin Ointment
Zn	Zn sulfate	Wound healing
Zr	Zr lactate	Antiperspirant

Table 1.5: Metallo-drugs in common use. Table adapted from<sup>19</sup>.

The general rules governing which metals bind to which biological sites (as in Table 1.4) hold true for metallo-drugs. Heavy metal complexes tend to act by binding to nucleic acid bases and phosphate groups, and so alter their structure. It is thought that many metallo-drug side effects do not result directly from the mode of action of the drug but are instead caused by their incidental interactions with proteins. Metallo-drugs can be administered in a number of ways; orally, intra-venously, parenterally or topically. Once administered the drugs enter the blood stream. As with all trace metals entering the circulatory system they are reversibly bound to plasma proteins (rapid) or to blood cells (slower). An equilibrium is set up between the bound and unbound forms of the drug, the unbound form is, in general, pharmacologically active. Availability of the drug to the tissues is determined by the position of equilibrium that governs the amount of free (unbound) drug able to diffuse freely between the blood and body tissues. The formation of such a bound drug complex acts to prolong drug action by reducing the amount of free drug available for metabolism. The complex acts as a depository for the drug by slowing down elimination. The more strongly the drug is bound the lower the pharmacological activity due to lower drug concentration reaching the tissues, but these levels will be maintained for longer periods of time than is the case with more weakly bound drugs. Protein-drug binding can also act to protect the body from drug metabolism in the liver and kidneys. Generally only the free drug is metabolised as the protein binding sites usually have a greater affinity for the drug than the metabolising system.

### 1.3.1 Platinum Drugs

Heavy elements rarely occur naturally in biology, that is to say most heavy metals are 'unnatural' in man. This does not mean that they do not occur or have potential uses. Prior to 1969 most cancer research was centred on the potential carcinogenicity of metals and their salts, rather than potential anticancer properties. This is hardly surprising, as medical scientists tended to regard all heavy metal compounds as non-selective poisons. There are, however, a number of metal complexes used in cancer chemotherapy, with a family of neutral platinum complexes being the most important.



The anti-tumour activity of platinum ammine complexes was discovered quite fortuitously by Rosenberg in 1965<sup>20</sup> whilst studying the effect of an electromagnetic field on cell division. A weak alternating current was passed through *Escherichia coli* using inert Pt electrodes in a nutrient medium containing ammonium chloride. The cell division was inhibited whilst cell growth was unaffected leading to filamentous growth of the cells<sup>21</sup>. The effect on the cells was found to be due to electrolysis products of the Pt electrodes within the cell medium, specifically a substance known as Peyrone's chloride<sup>22</sup>, first synthesized in 1845.

Platinum based drugs have been in use since the early 1970's and cisplatin is now one of the most widely used anticancer drugs<sup>23</sup>. In tumour cells genetic control of the cells life span is lost, resulting in the uncontrollable growth of the tumour tissues. Anti-tumour drugs are, therefore, designed to interfere with this cell proliferation by blocking synthesis of DNA, RNA or proteins in the cell nucleus. Reactions involving the drug occurring in other regions, such as with serum proteins, can lead to toxic side effects. These drugs will also damage any normal cells undergoing division, especially susceptible are the dividing cells found within hair follicles and bone marrow. Such side effects limit both the size and the frequency of dosage administered. It should be noted that most of the agents that chemically modify DNA are themselves mutagenic. They must be considered as potential carcinogens and so need to be handled with the utmost care.

The compound cis-diamminedichloroplatinum(II), is commonly known as cisplatin, and its chemical structure is shown in Figure 1.5. It is the parent compound of a family of platinum drugs and is used in the treatment of ovarian, cervical, bronchial, lung, testicular, endometrial, bladder and prostate cancers as well as head and throat tumours. Evidence shows the anti-tumour activity of cisplatin to be due to it reacting and inhibiting the replication of cellular DNA<sup>24</sup>. The trans isomer is found to have no anti-tumour activity and is toxic. Despite its wide field of applicability, the use of cisplatin is severely limited by its numerous side effects, in particular nephrotoxicity<sup>25</sup>, which may be attributed to the inactivation of essential proteins by chelation of platinum to thiol residues<sup>26</sup>. This theory is backed up by the finding that the chelating agent diethyldithiocarbamate

(DDTC) is capable of reducing cisplatin related toxicities without affecting the efficacy of the drug<sup>27</sup>. This is possible because DDTC is capable of reversing cisplatin-protein interactions but is incapable of reacting with bio-complexes involving cisplatin and guanine bases<sup>28</sup>. It is also possible to reduce the severity of the nephrotoxicity, with no effect on the activity of the drug, by hydrating the patients prior to treatment<sup>29</sup>. The use of cisplatin has a number of other disadvantages besides its high toxicity such as the need for administration by intravenous injection and the possibility of patient resistance. Cisplatin resistance is thought to be due to a number of factors which include decreased drug transport, increased cell detoxification due to increased metallothionein levels (known to detoxify heavy metals) and alterations of the apoptotic cell death pathway<sup>30</sup>.

Of the second generation platinum drugs available the most popular is diammine (1,1-cyclobutanedicarboxylato)-platinum(II), commonly known as Carboplatin, see Figure 1.5. Carboplatin shows a similar activity to cisplatin, and is less toxic<sup>31</sup> with respect to the peripheral nervous system and the kidneys – despite the dose levels being higher. The dose limiting side effect for carboplatin is myelosuppression (bone marrow damage). The co-planar structure of carboplatin is thought to be responsible for the delay in its degradation into potentially detrimental derivatives. Since evidence to date suggests cisplatin and carboplatin have the same mechanism of action<sup>32</sup> and produce the same DNA lesions it can be inferred that the differences in toxicity of the two drugs are due to their different pharmacokinetics and distribution properties.

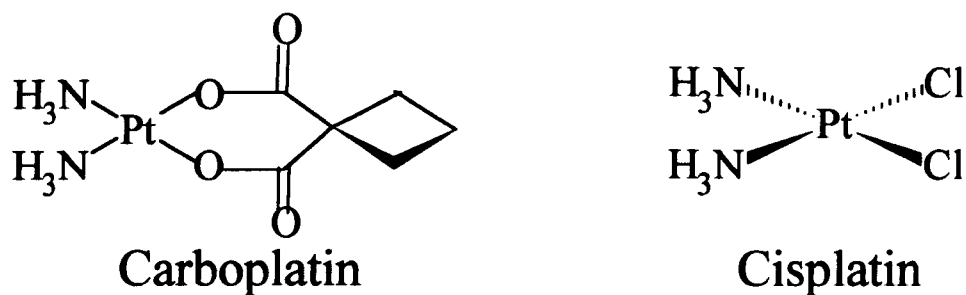


*Figure 1.5: Commonly used platinum anti-tumour drugs*

Third generation drugs are currently under development. In these the platinum complex is coupled to a functional carrier molecule, which improves the selectivity of the drug for the tumour tissue. Cytotoxically active carriers, such as doxorubicin, can synergistically contribute to the efficacy of such platinum drugs<sup>33</sup>. Synthetic, water-soluble, polymeric carriers designed for the binding of antineoplastic co-ordination compounds of the cisplatin type, can be resistant to serum protein binding. This may lead to a reduction in toxic side effects.

Knowledge about the mode of action of cisplatin and the other platinum drugs could lead to information about the mechanisms of toxicity and the structure-activity relationship. This information could then be used to develop more potent, less toxic platinum analogues. It might also be used to improve the scope of activity to include other forms of cancer, such as breast cancer. Figure 1.6 shows the metabolic pathway for cisplatin

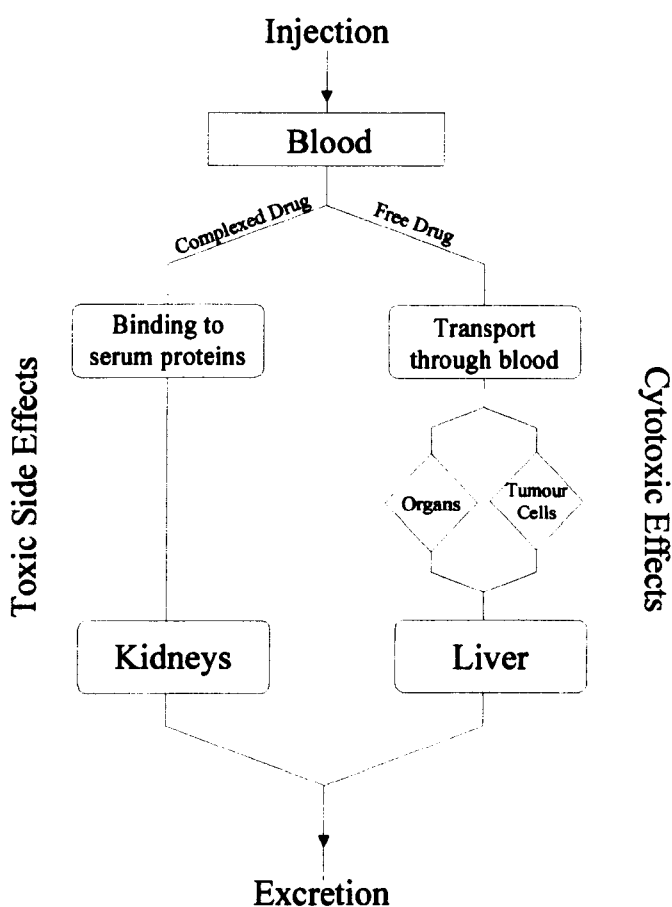


Figure 1.6: Metabolic pathway for cisplatin (Adapted from Ref<sup>34</sup>)

Cisplatin is thought to be cytotoxically active due to its ability to selectively bind to biological molecules, something that is not possible with the trans isomer. The chloride ligands are found to be labile whilst the Pt-amine linkage is found to be very stable against nucleophilic attack. Upon injection cisplatin enters the blood stream. The relatively high chloride ion concentration in human serum (~100 mM)<sup>35</sup> limits the amount of aquation as chlorine substitution reactions are slow. The drug, therefore, remains reasonably intact as it is transported around the body in the blood stream. Whilst in the blood stream reactions with blood proteins may occur, a likely candidate for platinum binding are thiol groups of proteins<sup>36</sup>, which are known to have a high affinity for platinum. It has been shown that 24 hours after injection of cisplatin virtually all the platinum is bound to plasma proteins<sup>37, 38</sup>. Transferrin is thought to act as a carrier for delivering platinum drugs to cancer cells<sup>39</sup> and so maintaining cytotoxicity. However, it has been found that blood platinum binds mainly to albumin resulting in a decrease in the biological activity of cisplatin<sup>40</sup>, and also to globulin<sup>41</sup>.

Once in the blood stream neutral drug compounds are readily able to penetrate the cell membranes. The chloride ion concentration of the intracellular fluid is often relatively low (~4 mM) and so substitution reactions will occur leading to the aquation of the platinum drugs. Aquation is the step necessary to activate the drug. The aquated complex is more labile than the original complex (due to water being a better leaving group with respect to Pt(II) than the chloride ion) and it is able to react with a variety of biological ligands, forming covalent bonds with proteins, DNA, RNA and other nucleophiles in the cell<sup>42</sup>. After reaching the tumour cells cisplatin binds with DNA causing cell death by apoptosis (programmed cell death). After interaction with cell DNA the degradation products of cisplatin are excreted via the liver and kidneys. Carboplatin has been found to aquate at a slower rate than cisplatin<sup>32</sup>, this could explain the reduced toxicity associated with carboplatin therapy.

The precise mechanism of action of cisplatin is still the subject of research. It is generally accepted that the anti-tumour effect of Pt(II) complexes is due to its interaction with DNA. Cisplatin binds to the DNA molecule of tumour cells and so prevents cell replication. There are a number of possible modes of platinum

binding to DNA as shown in Figure 1.7. In theory the cationic Pt(II) species can bind to all sites with lone pairs, but the Guanine N7 sites are the most easily oxidisable DNA sites and as such tend to be favoured over other sites. The bonding of Pt to two N atoms of the same DNA strand<sup>43</sup>, with Guanine as the preferred linkage<sup>44, 45</sup>, is thought to be responsible for the anti-tumour activity. Such an intra-strand linkage is not possible for the trans isomer of cisplatin, giving a possible explanation for its inactivity<sup>46</sup>.

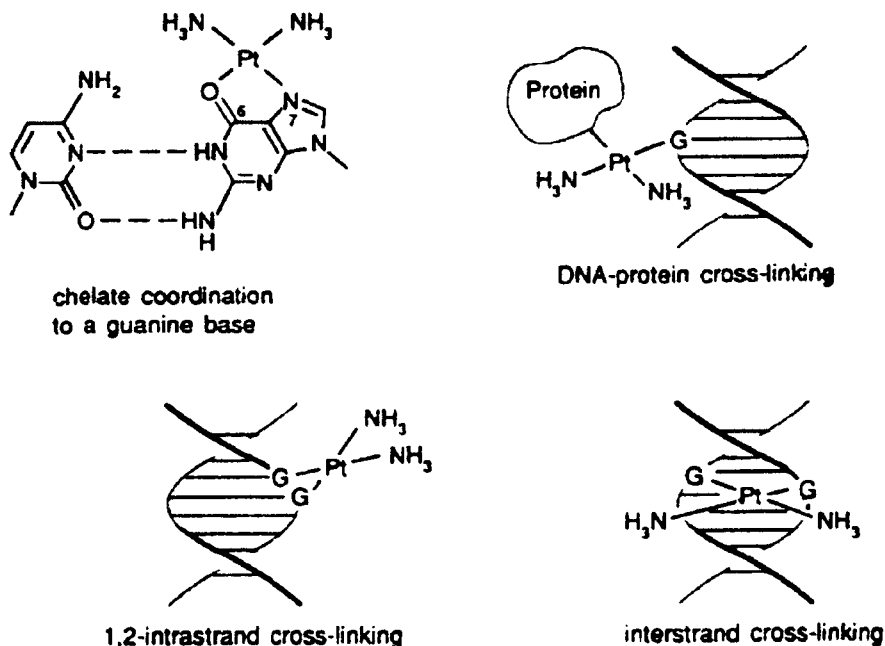


Figure 1.7: Modes of platinum-DNA binding, figure adapted from<sup>34</sup>

Platinated DNA can be analysed by a number of techniques such as NMR, X-ray crystallography and electron microscopy. The results of analysis show the favoured sites of interaction. It can also be determined that cisplatin unwinds the DNA, shortening it by up to 50 % of the original length, and can cause binding and kinking of the DNA helix<sup>47</sup>. Cisplatin damages DNA in a way that healthy cells can repair but which cancerous cells cannot. Despite this a number of toxicities are observed with cisplatin use. Cisplatin is found distributed throughout the kidney, causing it to be toxic above critical levels. Such toxicity may be due to the inhibition of enzymes through co-ordination of platinum to sulphhydryl groups in the proteins.

Most of the current research has been done into the interaction of platinum drugs with DNA<sup>48, 49</sup>, as this is the mechanism whereby this class of platinum complex exerts its specific activity. Next comes research into total platinum serum levels<sup>50, 51</sup>. Relatively few studies into platinum-protein interactions are carried out<sup>52, 53</sup>, this is possibly due to the finding that *in vitro* cytotoxicity of cisplatin is reduced on binding to plasma proteins<sup>54</sup>. As already mentioned cisplatin is found to rapidly react with serum proteins forming complexes with no cytotoxic activity. Such platinum-protein interactions are thought to contribute to the toxic side effects, particularly those involving kidney damage. Knowledge of platinum-protein complex formation is, therefore, important for toxicity studies and was the motivation for this study.

In order to make meaningful correlations between platinum blood levels and drug efficacy and/or toxicity it is necessary to distinguish between free circulating (active) drug and protein bound (inactive) platinum. This can be achieved using ultrafiltration<sup>55</sup>, but for speciation information powerful separation tools such as HPLC are required. Chang et al.<sup>56</sup> reported the first analytical technique capable of quantifying cisplatin in the presence of other platinum species. Cisplatin was isolated by HPLC using a strong anion exchange column. Since then a number of platinum speciation methods have been developed, these being summarised in Section 1.4.

### 1.3.2 Gold Drugs

Chrysotherapy, treatment with gold, gets its name from the Greek χρυσος, meaning gold. Gold, unlike platinum, is an ancient metal and has a long medical history<sup>57</sup>. The tradition of eating gold foil appears to have started in ancient China and then spread to India. The Hindu religion's association of gold with immortality has meant that many modern-day Hindus and some Moslems also eat gold foil in their food. Arab scientists often experimented with various forms of gold in the first millennium AD. In the 8<sup>th</sup> century gold was recommended as a panacea, a view held as recently as 1500 AD by Paracelsus<sup>58</sup>.

By the mid 19<sup>th</sup> century gold therapy was favoured in homeopathy and gold was thought to protect against leprosy. In 1890 Koch<sup>59</sup> found that gold(I) cyanide, AuCN, inhibits the bacteria causing tuberculosis. It was this work done by Koch that put chrysotherapy on a good footing and paved the way for the use of gold salts in the treatment of tuberculosis (TB), syphilis and a number of other pathogenic organisms.

Due to the high toxicity of AuCN it was unsuitable for widespread use and so in 1917 Feldt<sup>60</sup> first tested gold thioglucose (still used today) for the treatment of TB. The first person to use chrysotherapy for non-TB purposes was Landé<sup>61</sup>. He observed the relief of joint pain in patients he was treating with gold thioglucose, and hence suggested its beneficial effects in arthritis. The French physician Jacques Forestier is usually credited with the first treatment of rheumatoid arthritis (RA) by chrysotherapy<sup>62</sup>. Forestier used gold thiopropanol sodium sulphate, and suggested that the effectiveness of the drug lay in the combination of gold with sulphur. In 1934 Forestier recorded a 70-80 % success rate with 500 RA patients<sup>63</sup>.

Au<sup>3+</sup> is isoelectronic with Pt<sup>2+</sup> and so it is of interest as an antineoplastic drug<sup>64</sup>. <sup>195m</sup>Au is used for angiocardigraphy<sup>65</sup>. There are a number of reviews on the various types of gold therapy in use<sup>66-68</sup>. The main application of gold containing drugs is in the treatment of RA, which we will concentrate on here. The gold salts used are known to retard the progression of bone and articular destruction. All gold drugs are Au(I) compounds, since Au(III) is much more toxic to humans. The accumulation of high concentrations of gold in the bloodstream can lead to toxic side effects, and so the monitoring of gold in the serum and urine of patients undergoing such treatment is required. Gold drugs used to treat RA fall into two main groups, oral and parenteral.

Only one of the more modern orally administered gold drug has found widespread acceptance, Auranofin, see Figure 1.8. Auranofin is a lipid-soluble monomer enabling it to be administered orally. It has a gold content of 29 %.

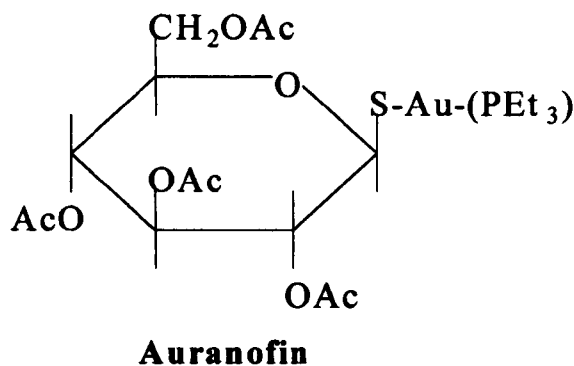


*Figure 1.8: Oral gold drug*

Parenteral drugs are administered by injection and are the older class of gold drugs. There are a number of parenteral drugs available, see Figure 1.9. Of all the parenteral gold drugs available to treat RA the most widely used is sodium aurothiomalate (Myocrisin). Myocrisin is a water-soluble polymeric compound that is insoluble in hydrophobic environments. It is, therefore, administered intramuscularly in the form of an aqueous solution, this prevents hydrolysis by the acidic gastric juices. It has a gold content of around 45 % in the powdered form.

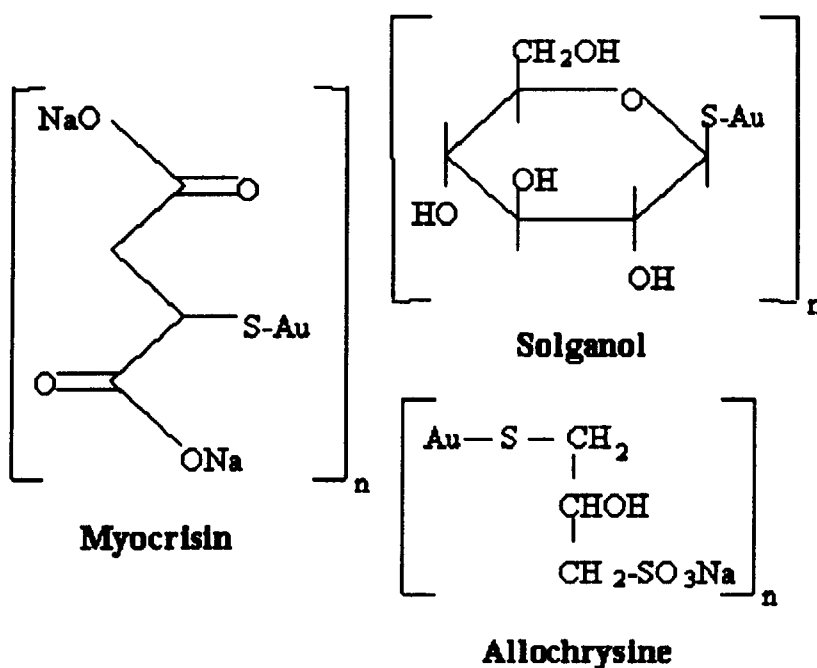


*Figure 1.9: Parenteral gold drugs*



The use of gold thiolate compounds in the treatment of RA is limited by the occurrence of toxic side effects. The side effects resemble allergic reactions on skin and mucous membranes as well as gastrointestinal and renal problems. Such side effects occur in about one third of patients undergoing chrysotherapy with parenteral drugs, a lower toxicity is associated with oral drug treatment. It is assumed that some of the toxic side-effects are due to the formation of Au(III) compounds. Adverse side effects usually disappear after reduction or cessation of dosage. In more severe cases the toxicity of gold drugs may be reduced by the addition of sulphur-chelating agents such as penicillamine, or dimercaprol, since Au(I) is known to form thermodynamically stable complexes with sulphur ligands.

Despite the many tens of millions of people that suffer from RA<sup>69</sup> together with the fact that chrysotherapy, widely used for well over fifty years, has been proven to induce remission<sup>70</sup>, the physiological or chemical mechanisms whereby gold drugs alleviate RA remain elusive<sup>71-73</sup>. However, the pharmacokinetics of parenteral and oral gold drugs are known to differ widely<sup>74</sup>. Gold does not have well defined transport, storage or enzyme functions in the human body. A possible metabolic pathway of gold drugs is outlined in Figure 1.10.

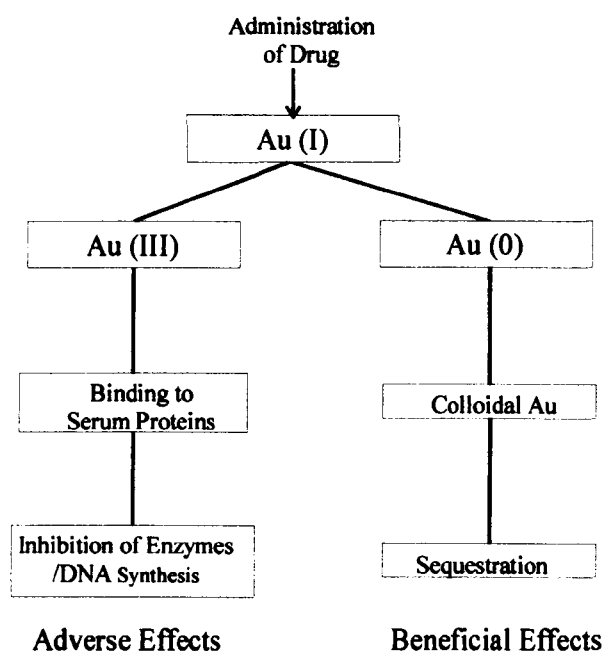


Figure 1.10: Metabolic pathway of gold drugs

Immediately after administration myocrisin in the blood is associated mainly with serum proteins, whilst auranofin is equally distributed between the serum and erythrocytes. After 72 hours auranofin gold is also localised in the serum proteins<sup>75</sup>. Au(I) has a high affinity for thiolate S, but binds only weakly to O and N ligands. As a result, cysteine rich proteins are targets for Au(I) binding, whilst the binding of Au(I) to DNA is weak<sup>76</sup>. In the bloodstream most of the gold from myocrisin is present in the serum, the majority of which (80-90 %) is bound to albumin<sup>77</sup>, whilst most of the remainder is associated with globulins<sup>78</sup>. For myocrisin, the gold content of each protein fraction, isolated by electrophoresis, differs from patient to patient, but remains constant for any one patient as the level of drug in the serum increases during therapy<sup>79</sup>. These findings seem to imply that there are a number of gold binding sites of comparable strength in serum, which are not saturated at the gold levels achieved during therapy. Typical concentrations of gold in the blood of patients are in the range of 0.1-10 µg/mL<sup>80</sup>. The level of gold in the serum reflects the size of the administered dose, total elimination from the body can take over a year after cessation of therapy. Surprisingly no correlation has been found between serum gold levels and clinical response and/or toxicity.

Blood plasma proteins play a role in drug delivery and targeting. Albumin carries 70-95 % of circulating gold in blood of patients treated with gold anti-arthritis drugs<sup>81</sup>, via Cys34<sup>82, 83</sup>. Plasma proteins, principally albumin, act as a major long term pool for a large proportion of the administered gold present in the blood. Some gold is absorbed on albumin, probably as the unchanged or partially metabolised drug. This gives rise to a more active pool of gold which will transfer more easily and so have more clinical relevance than the unbound gold. Myocrisin is also known to react readily with zinc metallothionein *in vitro* with gold replacing the zinc<sup>84</sup>.

RA is an autoimmune disease involving the painful inflammation of tissue surrounding the joints. The areas of inflammation are found to accumulate macrophages and neutrophil polymorphs, the lysosomal enzymes that destroy the articular cartilage<sup>85</sup>. Gold is found to accumulate preferentially in the inflamed

joints<sup>86</sup>, due to the phagocytosis of gold-albumin complexes. Gold is concentrated in the lysosomes, forming aurosomes, where it inhibits the lysosomal enzyme activity. This inhibition is thought to be due to the co-ordination of gold to the thiolate groups present in the enzymes<sup>87</sup>.

The cause of the toxic side effects associated with chrysotherapy is poorly understood. It has been demonstrated that the observed toxicity may be due to the oxidation of Au(I) to Au(III) *in vivo*<sup>88-90</sup>. In inflammatory situations oxidation may be due to the *in vivo* presence of strong oxidants ClO<sup>-</sup> and H<sub>2</sub>O<sub>2</sub>. The aqua complex of Au(I) is unstable and disproportionates thus;



The Au(III) metabolites produced can, in turn, readily oxidise peptide and protein groups and di-sulphide bridges<sup>91</sup> and so may lead to toxic side effects.

Abraham and Himmel<sup>92</sup> have reported on the oral administration of colloidal gold to RA patients not responding to conventional gold therapy. They found this treatment to be effective and found no clinical or laboratory evidence of toxicity. These findings are consistent with the theory that the active ingredient in chrysotherapy is Au(0) and the toxic side effects are caused by Au(III), generated from the oxidation of the Au(I) drug. There is, therefore, a need to develop new speciation tools with which to study Au speciation of patients undergoing chrysotherapy. Speciation data can then be used to further toxicity studies by helping to elucidate the toxic species and the mechanism of toxicity. This knowledge may then be used in the development of new, less toxic drugs.

### 1.3.3 Other Metal Based Drugs

Many other metal based drugs are in use daily, Table 1.5 is in no way exhaustive as there are far too many metallo-drugs to mention in full. The table clearly shows that it is not only the elements essential to good health that are utilised in medicine. Lots of metal based drug therapy involves the use of exogenous metal ions, metals which are non-essential for life, such as Ag, Al, Ge, Li and Sb. A brief description of some of these metal-based drugs follows. Figure 1.11 shows the structures of some metal based drugs; the anti-tumour drug titanocene dichloride, an antimetastatic Ru drug and sodium nitroprusside used as a hypertensive agent during heart surgery.

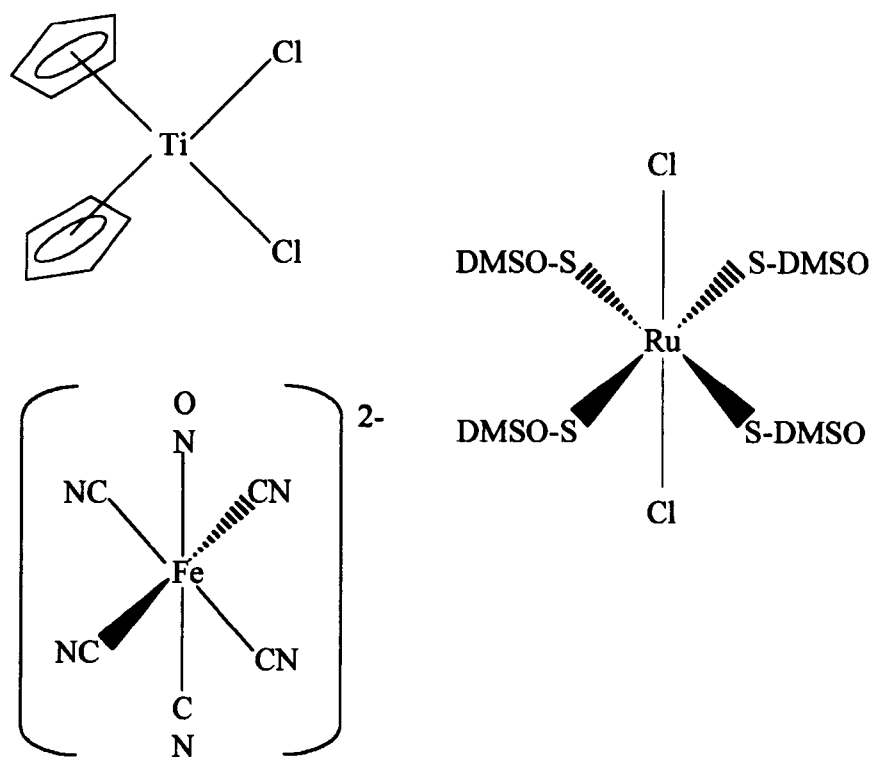


*Figure 1.11: Some examples of metal based drugs*

In their simplest form metal-based drugs are used as dietary supplements to treat the symptoms of essential element deficiency. Metal based drugs can also be administered to counter the effect of an excess of a chemically similar element in the body, although excess metal levels in the body are more frequently treated by chelating agents.

Some metals serve a wide range of therapeutic roles, for example the application of silver in medicine is widespread. It can be used as an anti-bacterial agent, in the treatment of gonococcal infections, and is even used in chewing gum for people wishing to give up smoking.

Some metals have more specific roles, be they anticancer, antiinfective, antiarthritic or neurological. Lithium salts are used in the treatment of manic depressive (bipolar) psychoses and other neurological and psychiatric disorders. Manic depression is thought to be due to too much catecholamine-related activity. Treatment is needed to reduce the activity of dopamine or norepinephrine. Lithium carbonate is particularly effective in the treatment of manic depression as it counteracts both phases in the typically cyclic course. It provides mild sedation without the non-specific tranquilising effect of phenothiazines. Successful lithium treatment requires around 1 mmole  $\text{Li}^+$ /L blood, toxic side effects may be caused by 2 mmoles  $\text{Li}^+$ /L blood, whilst  $\geq 3$  mmoles  $\text{Li}^+$ /L blood can be fatal, giving lithium one of the narrowest therapeutic indexes of commonly used drugs. Lithium salts commonly have a coordination number 6 which means they can easily replace sodium or magnesium in 6 co-ordinate holes, this is done in preference to remaining as the insoluble lithium salt. Lithium is not bound by proteins or metabolised and so virtually all of the lithium administered is excreted in the urine.

Radionuclides have an increasingly important role to play in modern medicine. They are used not only as conventional therapeutic drugs, but also find applicability in diagnostic imaging. Magnetic resonance imaging (MRI) is also a popular diagnostic tool employing metal-based drugs.

The use of metallo-drugs is a very exciting and promising area, creating a great deal of interest. It has only been possible to touch upon the subject briefly here, more detailed information on the role of metal ions in medicine can be obtained from recent reviews<sup>93, 94</sup>.

## **1.4 Trace Element Determination and Speciation in Biological Systems**

In recent times there has been a growth in biological and clinical interest in trace element determination and speciation. This is due to a number of factors;

- improved analytical techniques with low limits of detection
- recognition of essentiality of elements previously considered non-essential
- recognition of deficiency syndromes
- widespread use of metallo-drugs with possible toxic side-effects
- increased exposure to heavy metals due to industrialisation

### **1.4.1 Trace Element Determination**

Humans are exposed to many naturally occurring and anthropogenically enriched metals, all of which are detrimental to health at high enough doses. To help reduce the likelihood of toxicity exposure regulations have been formulated. Determination of metal concentrations in human body fluids and tissues is necessary in order to assess current human exposure, it can also be used for the diagnosis and prognosis of diseases. Such an example is infectious hepatitis where the concentration of copper in serum is directly related to the severity of the disease. Monitoring of metal levels in the blood of patients undergoing metallo-drug therapy is particularly important. Patients receiving lithium treatment may be monitored in this way to help prevent the build up of toxic lithium levels.

Availability of biological samples is usually limited, and the metals of interest are usually at trace levels. As a result of these limitations a suitable technique for trace metal analysis of biological samples needs to be highly sensitive ( $\sim$  ng/L range) requiring  $\mu$ l samples with little or no sample preparation to avoid contamination. The analytical techniques which have been utilised in trace element studies include neutron activation analysis (NAA), X-ray fluorescence (XRF), voltammetry, inductively coupled plasma optical emission spectroscopy/mass spectrometry (ICP-OES or ICP-MS) and atomic absorption spectrometry (AAS). Table 1.6 shows typical relative detection limits for some of these techniques.

<b>Metal</b>	<b>ICP-OES</b>	<b>Flame AAS</b>	<b>GF AAS</b>	<b>Voltammetry</b>	<b>ICP-MS</b>	<b>TXRF</b>	<b>NAA</b>
<b>Ag</b>	1.80	1.50	0.015	0.10	0.03	0.4	2.00
<b>Al</b>	7.00	45.0	0.15	0.03	0.16	-	4.00
<b>As</b>	11.0	30.0	0.60	<0.20	0.04	0.20	0.05
<b>Au</b>	3.00	10.0	0.30	10.0	0.06	0.20	0.005
<b>Be</b>	0.20	3.00	0.015	-	0.10	-	-
<b>Bi</b>	11.0	30.0	0.30	<0.10	0.04	0.20	20.0
<b>Cd</b>	1.00	0.70	0.006	<0.0002	0.03	0.40	1.50
<b>Co</b>	3.00	9.00	0.15	<0.005	0.01	0.10	0.03
<b>Cr</b>	1.50	3.00	0.06	0.02	0.01	0.40	20.0
<b>Cu</b>	1.50	1.50	0.06	0.002	0.02	0.10	0.10
<b>Fe</b>	1.50	7.50	0.06	<0.04	0.20	0.20	6.00
<b>Ga</b>	11.0	150	0.20	0.004	0.08	-	0.06
<b>Ge</b>	9.00	300	0.45	-	0.02	-	0.50
<b>Hg</b>	7.00	300	1.20	0.005	0.02	0.20	0.03
<b>In</b>	25.0	30.0	0.15	-	0.06	-	0.0006
<b>La</b>	2.30	3000	-	-	0.01	-	0.06
<b>Li</b>	1.20	0.70	0.06	-	0.10	-	-
<b>Mg</b>	0.10	0.15	0.012	-	0.13	-	25.0
<b>Mn</b>	0.30	1.50	0.03	40.0	0.03	0.20	0.003
<b>Mo</b>	2.00	45.0	0.12	100	0.04	0.20	10.0
<b>Nb</b>	8.00	3000	-	-	0.02	-	200
<b>Ni</b>	4.00	6.00	0.30	0.001	0.04	0.10	15.0
<b>Pb</b>	15.0	15.0	0.15	0.001	0.01	0.20	3000
<b>Pd</b>	9.00	30.0	0.75	0.02	0.06	-	0.12
<b>Pt</b>	7.00	60.0	1.50	<0.0001	0.08	0.20	1.00
<b>Sb</b>	11.0	45.0	0.60	0.10	0.06	0.50	0.20
<b>Se</b>	20.0	150	0.60	0.02	1.00	0.20	1.1
<b>Sn</b>	10.0	30.0	0.60	<0.03	0.06	0.50	2.00
<b>Ta</b>	8.00	1500	-	-	0.02	-	1.30
<b>Te</b>	155	30.0	0.30	0.06	0.08	1.00	0.50
<b>Th</b>	8.00	-	-	3.00	0.02	-	0.16
<b>Ti</b>	0.60	75.0	1.20	100	0.32	0.40	10.0
<b>Tl</b>	18.0	0.15	0.15	0.015	0.05	0.20	40.0
<b>U</b>	26.0	45000	-	0.03	0.01	0.002	-
<b>V</b>	1.20	60.0	0.60	100	0.03	0.20	0.15
<b>W</b>	8.00	1500	-	1000	0.05	-	0.045
<b>Zn</b>	0.75	1.50	0.03	0.02	0.01	0.10	2.50
<b>Zr</b>	3.30	1500	-	-	0.03	0.30	100

*Table 1.6: Typical relative detection limits for various techniques. Values given in µg/L. Table adapted from<sup>95</sup>.*

NAA works on the principle of exciting the atomic nuclei by particle irradiation within a nuclear reactor. The number of excited atoms depends on the intensity of the irradiation and is directly proportional to the number of atoms present. After excitation the atoms decay and emit  $\alpha$ - or  $\beta$ - particles and/or  $\gamma$ -quanta characteristic of each isotope present. As an analytical method NAA is unique in that it involves the excitation of the atomic nucleus and so the elements are determined independently of their physical and chemical state. Despite it being a very sensitive technique requiring no sample pre-treatment, NAA does not find wide usage mainly due to the limited number of suitable nuclear research reactors. The technique also proves expensive, requiring specially trained and experienced staff, is time consuming and cannot be used for all isotopes due to lack of suitable daughter nuclides. Whilst not used as a routine technique NAA is one of the best methods for the certification of reference materials in the biological field<sup>96</sup>.

XRF is a powerful multielement analysis technique requiring no sample pre-treatment, it can be used to analyse solid samples directly. It uses the principle that atoms subjected to radiation eliminate electrons from the inner atomic shells. Electrons from outer shells drop into the free positions and so emit simple electromagnetic radiation, which is unique to each excited element.

Voltammetry is based on Faraday's law that 1 mole of a compound transformed in an electrode process is equivalent to the electric charge  $n \times 96500\text{C}$  (where  $n$  is the number of electrons transferred). This makes voltammetry potentially a very sensitive and selective technique. However, there are certain drawbacks to the method. The metals for determination need to be completely dissolved in a non-interfering analyte solution of sufficient conductivity. Even residual traces of organic matter can severely interfere and so biological samples must be totally decomposed before analysis. Samples must also be degassed as dissolved oxygen can interfere with results. Since each metal has a certain redox potential at a certain working electrode it is often possible to do sequential simultaneous determination of several metals.



OES is based on the generation of radiation by a host of transitions, resulting in complex spectra. The radiation intensity is directly proportional to the atom concentration. In order to determine elemental concentrations from the multitude of lines proper optical resolution is necessary. OES is well suited to multielement determinations. Inductively coupled plasma is a common excitation source for OES, and such systems can offer sequential or simultaneous multielement determination at the  $\mu\text{g/L}$  level. ICP-OES is a widely used technique due to its ability to perform rapid multielement determinations with relatively low limits of detection with possible automation. Electrothermal vaporisation allows direct sample insertion, which can improve detection limits.

AAS is based on the principle that an atom absorbs radiation at the same wavelength at which it emits radiation. The sample is atomised in the light path of a specific radiation source. The amount of absorption is directly proportional to the number of atoms present. This gives an absorption spectrum, which is much simpler than the equivalent emission spectra. The two main types of AAS are flame atomisation and graphite furnace (GF). GF-AAS is considered accurate and precise and has been used as a reference method. With its multi-element capabilities and its relative cheapness, it has found numerous applications. Flame AAS is not as popular due to poorer limits of detection for many elements, the need to digest organic samples to minimise interference problems and lengthy analysis times. Almost all trace elements of interest in clinical chemistry have been determined in body fluids and tissue samples using AAS.

MS works on the principle of gaseous ion production, either thermally or by an ion current. The ions or molecular fragments are separated by energy-mass focusing, using magnetic fields. The charged particles are then determined qualitatively or quantitatively. MS is a simultaneous multi-element technique, which has been used in combination with a number of techniques. For the determination of trace element concentration in biological samples ICP-MS is one of the most common techniques.

ICP-MS was introduced by Houk et al in 1980<sup>97</sup> and uses the high ionisation efficiency of inductively coupled plasma to ionise the samples. It has sub  $\mu\text{g/L}$  detection limits for many elements. ICP-MS is of particular interest for biological samples due to its rapid sample throughput and isotopic dilution capabilities. Limitations of ICP-MS include non-spectral interferences from the matrix effects and with the quadrupole mass spectrometers isobaric interferences are possible due to the nominal mass resolution. Isobaric interferences lead to complications in determining masses below 80 at low concentration. Some of these problems can be got around by keeping dissolved solids below 0.2 % for continuous nebulisation, and by using internal standards, matrix matching, standard additions or isotope dilution. High resolution MS can also be used for determination of elements below mass 80.

Table 1.7 shows the applicability of the various techniques to total elemental concentration determination in biological samples. In clinical chemistry AAS tends to be favoured for the determination of trace metals due to practicability, time needed for analysis, cost of equipment and possibility for automation.

Analytical Technique	Element	Matrix
XRF	Pt <sup>98, 99</sup>	serum & urine
NAA	multi element <sup>100</sup>	biological samples
Voltammetry	Pt <sup>101, 102</sup>	urine, hair & blood
Glow Discharge MS	Pb & Pt <sup>103</sup>	urine
AAS	Au <sup>104-106</sup>	plasma
ICP-MS	Pt <sup>107-110</sup>	biofluids
	multi element <sup>111, 112</sup>	serum
	Ag, Cd, Co, Pb & Sb <sup>113</sup>	liver
ICP-OES	multi element <sup>114-117</sup>	serum

*Table 1.7: Determination of total elemental concentration in biological samples*

The analytical procedure of choice depends on the trace metal of interest, the matrix and the concentration. AAS is generally limited to liquids and is suited to single element determinations. Since becoming commercially available ICP-MS has proved very effective in determining trace elements in biological samples. Table 1.6 shows ICP-MS is one of the most versatile and sensitive techniques available. Only NAA and voltammetry offer some limits of detection lower than ICP-MS. Both these techniques have problems with cost and sample preparation/applicability, respectively, which prevent their widespread use in biological analysis. Since ICP-MS is such a powerful, multielement technique which was used throughout the study it will be discussed here in more detail. The first paper published on ICP-MS was in 1980<sup>97</sup>, and in 1983 Perkin-Elmer SCIEX introduced the first commercially available ICP-MS instrument. Today the technique is used daily in many laboratories as a routine analytical tool offering lower detection limits and higher productivity than optical ICP techniques. A further advantage of ICP-MS over AAS and ICP-OES is its ability to determine individual isotopes of elements.

ICP-MS can measure most elements in the periodic table. The high temperature of the plasma ion source completely breaks apart the molecules of the sample and so ICP-MS detects only elemental ions. An advantage of ICP-MS over other inorganic techniques for elemental determination, such as ICP-OES and AAS, is its ability to determine individual isotopes of each element. ICP-MS tends to have less interference problems than ICP-OES and is faster than AAS when carrying out multielement determination. Detection limits are generally much lower than with ICP-OES and AAS, and with computer control an ICP-MS system can be run virtually 24 hours a day, 7 days a week. ICP-MS is a powerful multi-element technique for both qualitative and quantitative analysis. The sample, in aerosol form, is first injected into the inductively coupled plasma. The resulting elemental ions are then extracted into the mass spectrometer for detection. A schematic of the HP4500 instrument used is shown in Figure 1.12.

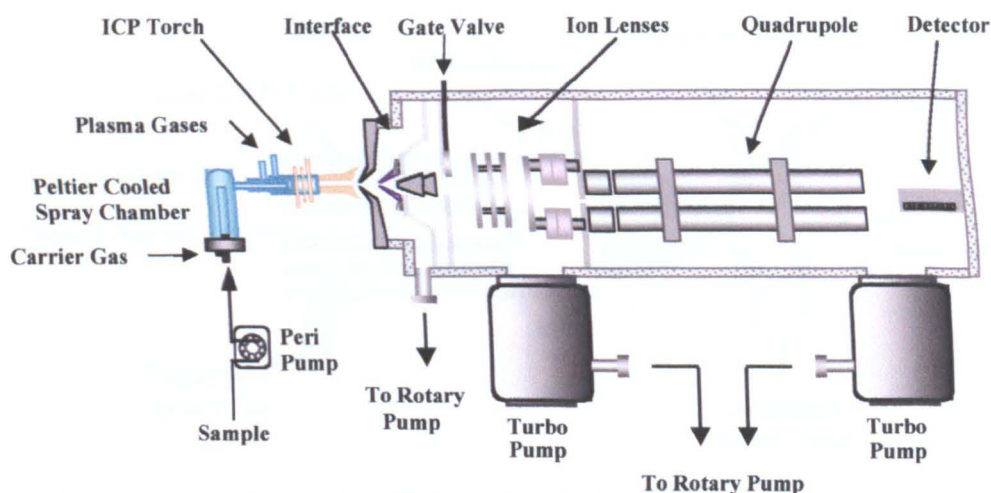


Figure 1.12: Schematic of HP4500 ICP-MS

Most of the samples analysed by ICP-MS are liquids. The nebuliser converts the sample to an aerosol, which is passed through the spray chamber and into the plasma by the carrier gas. As well as conventional nebulisation a number of ‘hyphenated’ techniques exist. These include microconcentric nebulisation (MCN), direct injection nebulisation (DIN), flow injection analysis (FIA) and laser ablation (LA) which is covered in detail in the next section.

The plasma is generated by passing argon through the ICP torch, a series of three concentric quartz tubes encircled at one end by a water cooled, copper radio frequency (RF) load coil. The RF energy couples with the argon of the middle tube to produce the plasma. The outer tube carries a tangential flow of argon, this cools the torch to prevent it from melting and also positions the plasma. The sample aerosol is introduced into the plasma through the innermost injector tube. The sample punches a hole in the plasma and a toroidal plasma is produced with a central axial channel. This plasma formation ensures homogeneous sample introduction. The sample is first atomised and, on absorbing more energy, the atoms release an electron to form singly charged ions (doubly charged ions are also observed for some elements). In quantitative analysis it is important to have an efficient and reproducible excitation source. An ICP source achieves this thanks to the high temperatures present in the plasma, 6000 – 10000 K. The ions produced are extracted from the plasma into the interface region, see Figure 1.13.

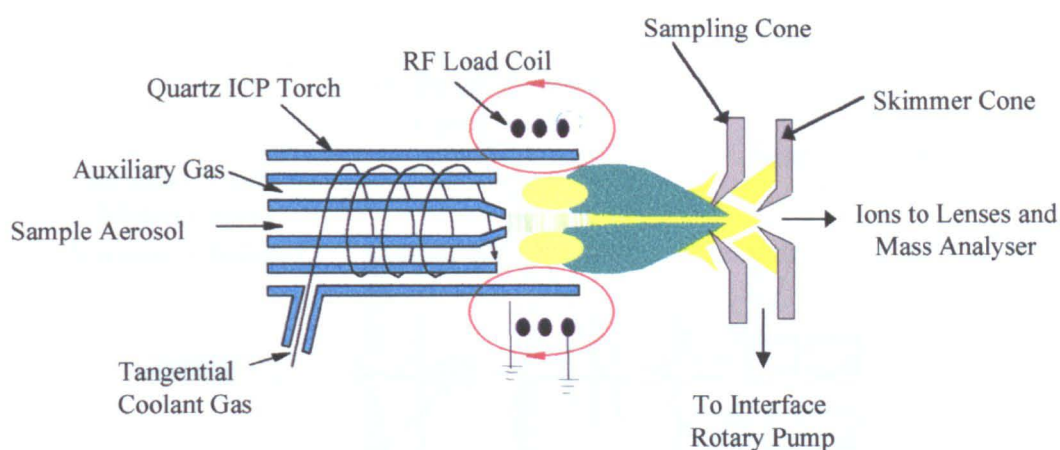


Figure 1.13: Torch and interface region of ICP-MS

An interface region is necessary to compensate for the high temperature and pressure differences that exist between the plasma region and the MS region of the instrument. The ion interface consists of two cones, an outer sampling cone, which is positioned in the analytical zone of the plasma. The skimmer cone is positioned several millimetres behind the sampling cone. The cones are typically made of nickel due to its high thermal conductivity, and robustness (although platinum can be used where nickel is inappropriate), and are water cooled to prevent damage from the heat of the plasma. The orifices of the cones are <1mm in diameter, large enough to prevent them clogging yet small enough to maintain a vacuum and minimise contamination of the mass spectrometer. The pressure difference between the plasma (atmospheric pressure) and the MS (high vacuum  $\sim 10^{-6}$  torr,  $10^{-4}$  Pa) causes the ions in the plasma to be extracted through the cones into the ion lens region.

The ion lens region is positioned immediately behind the interface and acts to focus ions into the quadrupole region. The positive ions produced in the plasma tend to repel each other and so lenses are needed to keep the ion beam from diverging. The HP4500 ICP-MS uses a unique type of lens system, known as the off axis system shown in Figure 1.14. Two extraction lenses accelerate the ion beam before the Einzel lenses focus the ions. Next the Omega + and Omega – lenses bend the focused ion beam allowing the quadrupole and detector to be positioned off axis. This off axis set up reduces the random background noise, and so gives a higher sensitivity.

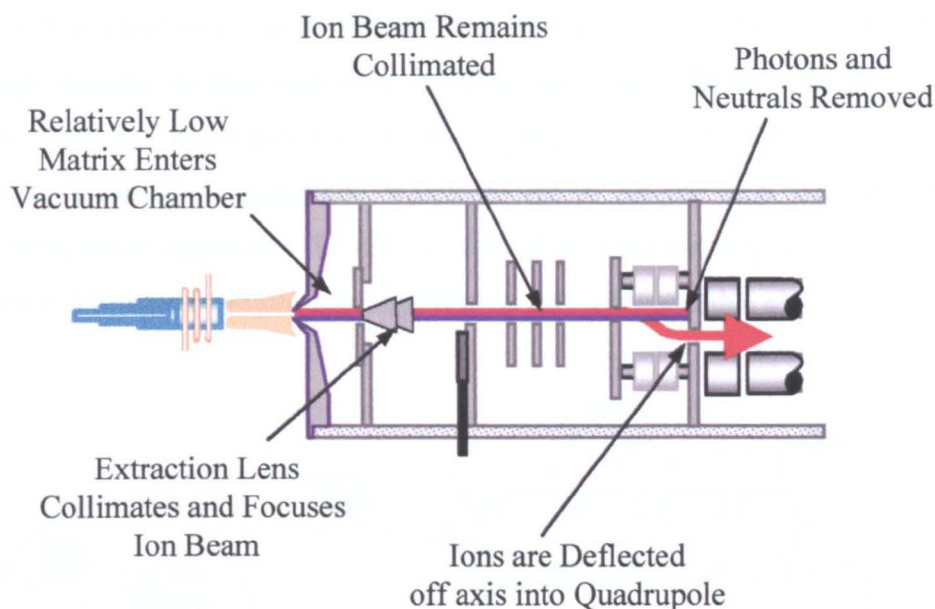


Figure 1.14: Off axis lens system

The ion beam is next fed into the mass analyser which separates, by mass, the singly charged ions. The HP4500 uses a quadrupole mass analyser as shown in Figure 1.15. This is basically a mass filter consisting of four parallel, hyperbolic Mo rods to which are applied a constant voltage and a RF oscillating voltage. A hyperbolic electric field is generated inside the quadrupole, which allows only ions of a specific mass to charge ratio ( $m/z$ ) to pass through to the detector. Other ions do not have a stable path and are lost or neutralised by the quadrupole rods.

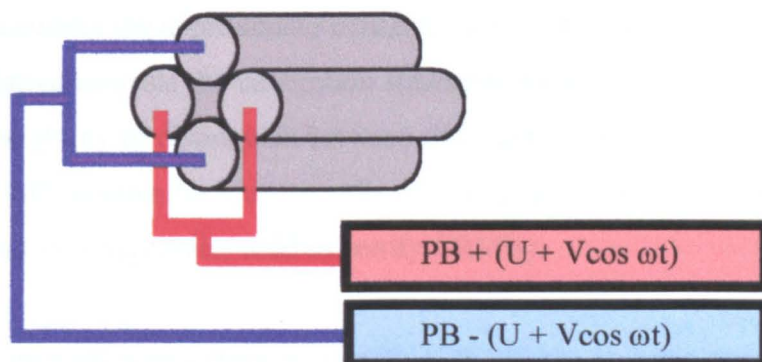


Figure 1.15: Quadrupole mass analyser

Ions exiting from the mass analyser next enter the detector, which generates a measurable electronic signal proportional in intensity to the number of ions. Discrete dynode electron multiplier detectors are used in the HP4500, as shown in Figure 1.16. An ion enters the electron multiplier and hits the first dynode. A flurry of electrons is generated which go on to hit the next dynode, in turn generating more electrons. The electrons generated are eventually detected by the collector. The signal obtained is amplified to give a measurable electronic signal.

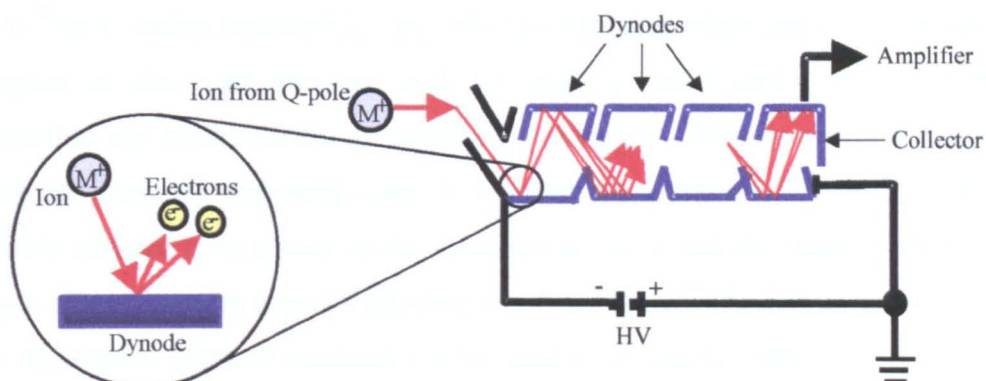


Figure 1.16: Discrete dynode detector

Computers with specially designed software are needed to control the plasma and mass spectrometer and also to interpret the data collected. HP 4500 software is specially designed and so is capable of a number of modes of analysis. Time resolved analysis is usually used with flow injection or laser ablation as it can monitor signal intensity as a function of time. For semi-quantitative analysis a calibration solution is made up containing as few as three elements, and the software calculates the approximate concentrations of the elements of interest. For full quantitative analysis the calibration standards must contain every element of interest. The ability to distinguish between different isotopes of the same element makes ICP-MS suitable for isotope ratio work (e.g. geological dating) and isotope dilution work (very accurate, used to certify CRM's).

The major interferences experienced with ICP-MS are isobaric overlaps, oxides and other polyatomic species, doubly charged ions and matrix effects. Isobaric overlap occurs when isotopes of two different elements have the same  $m/z$  ratio such that they can not be resolved by the mass discriminator. Quadrupole mass

analysers typically operate at low resolution (1 amu), more expensive high resolution ICP-MS systems are available at the cost of sensitivity. Such problems can be got around by using a different isotope of the element of interest or by using specially designed correction software. Interference from polyatomics can be more problematic. Oxides commonly appear, mainly from aqueous sample solutions and so these can be minimised by reducing solvent loading. Laser ablated samples rarely suffer from oxide interferences due to the lack of solvent. Polyatomic argon species also occur, these can cause interferences up to mass 80 ( $^{40}\text{Ar}^{40}\text{Ar}^+$ ). Argon polyatomics are often problematic when analysing biological samples as they can interfere with Cr and Fe. Such interferences are best controlled by manipulation of operating parameters. Doubly charged ions can occur for elements with sufficiently low ionisation potentials, i.e. Ca, Sr, and Ba. Doubly charged ions appear in the mass spectrum at half the mass of the parent singly charged ion. In general, interferences from doubly charged ions are few and can be avoided. Internal standards can be used to correct for matrix effects. Ideally internal standards should not occur naturally in the sample and should not be likely contaminants in the laboratory, Rh and In are popular choices.

## 1.4.2 Separation

In order to gain an insight into the activity of specific metals in the environment, especially those in contact with biological organisms, the total metal concentration of a sample is not always sufficient. In such cases it is useful to gain an indication of the metals various chemical and physical forms, as these determine its biological effect. This is the case in the majority of treatments involving metals. Analytical techniques are needed which can characterise the products of metallo-drug metabolism and so a better understanding of the interactions of metallo-drugs with transport proteins and DNA can be achieved. Successful therapy often involves selectivity and so it is the concentration of one or more specific forms of the metal that is important rather than its total concentration. Table 1.8 shows how the biological effects of certain elements can depend upon their chemical speciation.



<b>Element</b>	<b>Predominantly Beneficial Species</b>	<b>Potentially Toxic Species</b>
As	As(V) compounds	As(III) compounds
Ba	Chloride	Nitrate
C	Widespread in biochemistry	Cyanide ion
Cr	Cr(III) compounds	Cr(VI) compounds
Cu	Carbonate	Chloride

*Table 1.8: Dependence of biological effect on chemical species. Table taken from<sup>118</sup>*

Successful speciation of a biological sample involves a fractionation scheme whereby the concentrations of the element that are, for example, protein bound, bound to low molecular mass components and present as aquated ions, are estimated. There has been an increase of interest in speciation in recent years, as suitably sensitive analytical techniques have become more widely available. Speciation studies are important in a number of different fields, including biochemistry<sup>119</sup>, environmental science<sup>120</sup>, food science<sup>121</sup> and hydrochemistry<sup>122</sup>. An indication of the importance of speciation studies is reflected in the large number of review papers available on the subject<sup>15, 123-126</sup>.

Here we will concentrate on the importance of speciation in biological systems. Identification of specific ligand-protein interactions in serum can yield important information about metabolic homeostasis. Diagnostic information concerning a number of serum binding proteins is important in clinical diagnosis whilst the identification of drug transport proteins yields important therapeutic information. In occupational health speciation plays an important role, especially in the identification of potentially toxic chemical species in the workplace.

A simple way of separating free and protein bound metal ions is by filtration. Depending on the grade of filter used a wide variety of biomolecules can be separated, see Table 1.9.

Size	Mr	Example	Membrane Process
100 $\mu\text{m}$		Pollen	Microfiltration (10 $\mu\text{m}$ -0.02 $\mu\text{m}$ )
10 $\mu\text{m}$		Starch Blood cells Typical bacteria	
1 $\mu\text{m}$		Smallest bacteria	
1000 A		DNA viruses	
100 A	100 kDa 10 kDa 1 kDa	Albumin Vit B12	Ultrafiltration (0.03 $\mu\text{m}$ -0.001 $\mu\text{m}$ )
10 A		Glucose	Reverse Osmosis (0.001 $\mu\text{m}$ -0.0001 $\mu\text{m}$ )
1 A		Water, NaCl	

*Table 1.9: Variety of filters available for separation of biomolecules*

In ultrafiltration the sample is filtered using a filter with a known molecular weight cut off (MWCO) i.e. 30 kDa. The filtrate consists of small particles and molecules with molecular mass less than the cut off, whilst the large molecular mass fraction is retained by the filter. It is assumed that metal found in the filtrate is in the unbound (active if a drug) form. It is possible for metals to bind to low molecular mass fractions such as citrate and so for a true determination of 'free' and 'bound' levels more sophisticated methods of separation are needed.

Chromatography works on the principle that different compounds travel at different speeds through a column, under distinct conditions. Discrete fractions are eluted to give sharp peaks in the time/concentration profile. There are a number of classes of chromatography available, from gas chromatography (GC), for the separation of volatile compounds to high-performance liquid chromatography (HPLC), for non-volatile compound separation.

A more sophisticated separation technique, capable of separating proteins, is electrophoresis. Electrophoresis is a technique that separates charged molecules by migration in an electrical field. Proteins carry a net charge at pH's other than their isoelectric point (pI). The rate of protein migration depends upon the charge density, the higher the ratio of charge to mass the faster the migration. Electrophoresis is a well-established technique first used by Tiselius<sup>127</sup> in 1933 to analyse serum proteins.

The pioneering work done by Tiselius was carried out in free solution, but this suffered from diffusion and convection currents. A support medium was introduced to minimise these effects such that the sample components remained in sharp zones. The earliest supports used were of filter paper and cellulose acetate soaked in buffer. The next major advancement in support media was the introduction of starch gels, still used on occasion. Nowadays most electrophoresis is carried out on agarose or polyacrylamide gels.

Electrophoresis units are available in horizontal or vertical orientation. Vertical mini gel units as shown in Figure 1.17 are available commercially for the separation of proteins. The mini gel system (gel length ~ 10 cm) is well suited to native protein separation as the small format reduces electrophoresis and processing time, thus minimising the likelihood of protein denaturation.

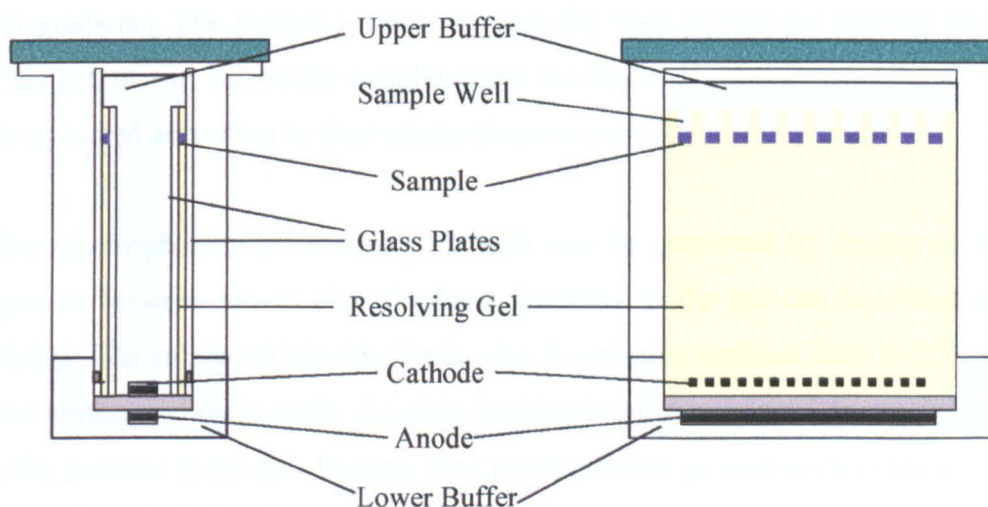


Figure 1.17: Typical vertical mini gel system

Resolving gels are cast between glass plates, typically 1 mm apart, using plastic combs to form the sample wells. When the gel system is assembled the buffer is placed in the upper and lower chambers. In continuous systems the same buffer is used throughout. Discontinuous systems use different upper and lower buffers and include a stacking gel above the resolving gel<sup>128</sup>. The role of the stacking gel is to focus the sample loaded on the gel, but when separating serum proteins the stacking gel can cause the proteins to aggregate and precipitate out. This being the case continuous gels were used throughout. Sample buffer is added to the samples prior to loading. The sample buffer generally contains a tracking dye (bromophenol blue) which aids sample loading and moves with the solvent front thus indicating when electrophoresis is complete. The sample buffer also contains glycerol which, being more dense than the running buffer, allows the samples to sit in the wells and so prevents diffusion into the upper buffer. Once the samples are loaded into the sample wells the appropriate DC voltage is applied via platinum electrodes.

Rapid separation is desirable to preserve protein band sharpness. The higher the voltage applied the faster the rate of migration, but the greater the Joule heating which can distort the protein bands. A compromise is needed to minimise the heating but maximise the migration rate. The design of the system is such that the upper buffer is between the gels being run and so can cool them and minimise heat gradients. The voltage is removed once the tracking dye has reached the end of the gel, that is, before the samples reach the electrode. This ensures the proteins are separated according to their electrophoretic mobility.

After electrophoresis is complete the gels can be preserved by drying on filter paper or between sheets of cellophane. Proteins in the gel can be detected by staining. The sulphated trimethylamine dye Coomassie Brilliant Blue R-250 is the most common protein stain. An acid-methanol-dye mix is used to precipitate or fix the proteins in the gel. The dye then penetrates the gel and binds to the proteins within the gel. A destaining solution is used to remove surplus dye. After staining gels can be dried in the usual manner.

The electrolyte buffer used in electrophoresis is very important as it determines the power requirements and affects separation. Proteins vary in size, shape and charge. Being amphoteric, proteins take on the characteristics of the buffer. In acidic buffers (pH's below their pI)  $\text{NH}_3^+$  groups are produced, whilst in alkaline buffers (pH's above their pI)  $\text{COO}^-$  groups are produced, see Figure 1.18.

When separating proteins there is no definitive buffer, but buffers of pH 8.6, such as Tris-HCl/glycine<sup>129</sup>, are widely used in native PAGE as they render the proteins quite soluble and the proteins retain their native form. At pH 8.6 most proteins have a net negative charge and so will migrate towards the anode.

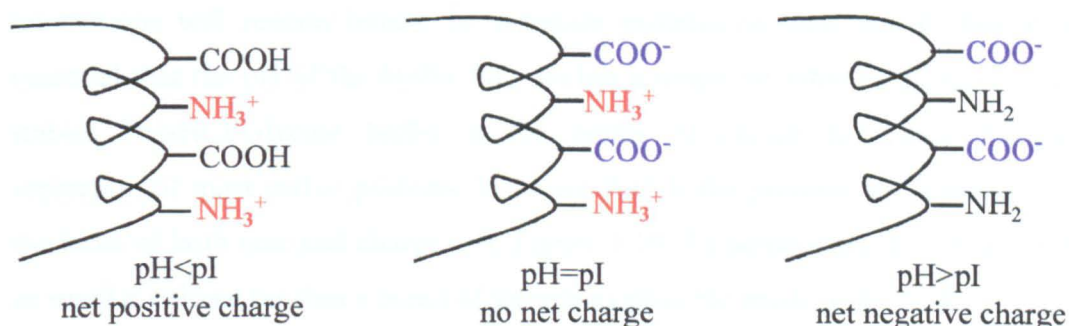


Figure 1.18: Amphoteric nature of proteins

Polyacrylamide gel electrophoresis (PAGE) is the most common matrix medium used for the separation of proteins. Its popularity lies in the fact that it is optically clear, chemically inert, electrically neutral, is stable over a wide range of temperature, pH and ionic strength, and is available in a wide range of pore sizes. Polyacrylamide gel is made up of long linear polyacrylamide chains crosslinked with bis-acrylamide (bis) to create a network of pores. Polyacrylamide gels are characterised by T %, the weight percentage of total monomer including crosslinker. T % gives an indication of the pore size, in general as T % increases the pore size decreases. A protein's ability to move through the gel depends on its size and structure relative to the pore size; as a rule, larger molecules tend to migrate more slowly than smaller ones. No single concentration will give maximum separation for the components of a complex protein mixture such as serum. Gradient gels can also be used, these have a linear pore gradient along the

length of the gel. T % increases, and so pore size decreases in the direction of migration. Gradient gels act as molecular sieves, the proteins are continually entering regions of the gel with smaller pore sizes and so the advancing edge migrates slower than the trailing edge resulting in sharper bands<sup>130</sup>. Gradient gels are especially suited to complex protein mixtures as they increase the molecular mass range that can be separated on a single gel.

Proteins can be separated in a number of ways. Native PAGE uses non-dissociating buffers which separate the proteins in such a way that sub-unit interactions, biological activity and native protein conformation are all preserved. This approach is appropriate when studying metal speciation as any metal-protein interactions will remain intact. To maintain proteins in their native state it is essential that the pH of the buffer falls within a range for which the proteins are stable. Tris-HCl/Glycine buffer is the buffer of choice for electrophoretic separation of most native proteins. In native PAGE the proteins are separated on the basis of both size and charge, see Figure 1.19. To achieve the best resolution as small a volume (as thin a zone) of sample as possible needs to be loaded.

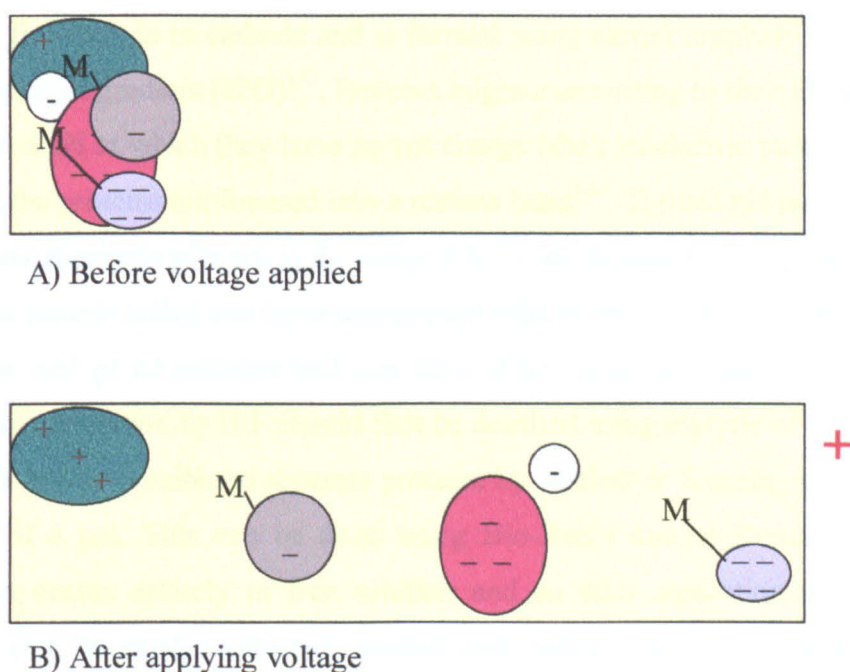


Figure 1.19: Electrophoresis on basis of protein mass and charge

One of the most popular gel systems for separating proteins is SDS-PAGE, described in 1967,<sup>131</sup> it was introduced in its current form in 1970<sup>132</sup>. The proteins are denatured using a buffer containing the strong anionic, protein-dissociating detergent, sodium dodecyl sulphate (SDS) and a thiol reducing agent such as 2-mercaptoethanol. The proteins are dissociated into individual, rod shaped, polypeptide units which bind SDS in a constant weight ratio (1.4 g SDS/g polypeptide<sup>133</sup>). SDS effectively masks the intrinsic charge of the polypeptide chains giving them a constant net negative charge per unit mass, hence proteins migrate as a function of their molecular mass. The high resolution achievable with SDS-PAGE relative to native-PAGE comes at the expense of protein activity and native structure. When studying metal-protein interactions protein denaturation is undesirable since it leads to the breakdown of disulphide bridges and hydrogen bonds. This can cause the proteins to uncoil exposing weak ligand binding sites previously inaccessible. In the case of albumin, an important transport protein, binding sites made up from the sub-unit arrangement are lost on denaturation.

Isoelectric focusing (IEF) is a high-resolution electrophoretic method, which separates proteins in the presence of a continuous pH gradient. The pH gradient increases from anode to cathode and is formed using carrier ampholytes<sup>134</sup> or an immobilised pH gradient (IPG)<sup>135</sup>. Proteins migrate according to their charge until they reach a pH at which they have no net charge (their isoelectric point – pI). At this point the proteins are focused into a narrow band<sup>136</sup>. Typical pH ranges are 3-10 while most protein pI's are in the range 4-6<sup>137</sup>, see Appendix 1.3. Small mobile ions in the sample (salts) can have detrimental effects on IEF as they can alter the net charge and pI of proteins and can slow down migration rates. As a result samples for separation by IEF should first be desalted using dialysis or a desalting column. It is also possible to separate proteins by isoelectric focusing without the presence of a gel. This can be done using Bio-Rad's unique Rotofor system. Separation occurs entirely in free solution and so after separation the sample fractions can be easily collected, pooled and refractionated if required. The proteins remain in their native form as they remain in solution throughout the separation.

One dimensional (1D) electrophoresis gives only limited resolution and protein bands often overlap. In 1975 two dimensional (2D) electrophoresis was developed<sup>138</sup> with high-resolution capabilities. 2D electrophoresis generally combines IEF, separating proteins according to pI, and SDS, separating proteins according to molecular mass. This technique is capable of resolving up to 10000 spots, but a drawback is that it is a technically demanding and labour intensive procedure. Despite 2D electrophoresis having the highest resolving power, 1D electrophoresis is the more widespread technique. In many situations the resolution achieved with 1D is fit for purpose and it is much easier to use with the added advantage of being able to run samples simultaneously for comparison.

Quantitative analysis of metal ions associated with proteins is difficult when protein molecules are enclosed in the gel. Areas of the gel containing proteins of interest can be excised and digested before analysis, but this is at best a qualitative technique. Alternatively proteins separated by PAGE can be recovered from the gel. This can be done either by Western blotting (poor or no protein transfer for high molecular mass proteins) or by electrophoretic elution. Simultaneous electro-elution of multiple protein bands separated by electrophoresis can be achieved using the mini whole gel eluter, as developed by Bio-Rad. Proteins are electrophoretically transferred from the gel across a dialysis membrane, to be collected in one of 14 buffer filled chambers. A reasonable amount of protein is recovered in this way, although not all. Some protein remains in the gel, whilst proteins can also be lost by adsorption to the dialysis membrane. The protein concentration of the recovered fractions can be determined using standard biochemical techniques.



### 1.4.3 Hyphenated Approaches

Speciation of biological samples typically involves a sample pre-treatment step followed by a selective biocompound separation step and finally a sensitive, metal specific, detection step. An inherent drawback with such hybrid systems lies in the fact that biological separation procedures were not originally designed to meet the requirements of trace element determinations and so they present a large contamination/element leaching hazard. Speciation studies generally assume that biomolecules and trace metals detected in the same fraction of a sample are associated with each other.

Speciation of biological samples can be troublesome due to a number of factors;

- low metal concentrations
- small sample volume availability
- complex matrices
- poor specificity for biocompound separation
- contamination
- possible loss of integrity of metal-ligand binding

As a result successful speciation techniques require;

- high sensitivity, with respect to metal detection
- good selectivity, with respect to biocompound separation
- mild conditions, to maintain sample species integrity

A landmark paper written in 1979 by Van Loon<sup>139</sup> regarding hyphenated techniques (as they later came to be known) led to a surge of interest in speciation. However, this is not to say speciation work was not carried out prior to this date. Despite poor limits of detection, proteins were being separated and analysed for metal ions as early as the 1960's<sup>140</sup>.

Early speciation work was done, in general, using gel electrophoresis to separate the metal species<sup>141</sup>. Off-line detection could then be carried out directly on the gel. Alternatively proteins were extracted (blotted) from the gel prior to detection. Speciation by coupling chromatography to a suitable detection system has generally become a favoured approach. The separation technique used is determined by the physico-chemical properties of the analyte, e.g. GC favours volatile analytes. The choice of detection method is determined by the level of analyte in the sample, whilst the matrix dictates the sample preparation strategy. Table 1.10 lists techniques widely used.

<b>Separation Techniques</b>	<b>Detection Techniques</b>
Supercritical Fluid Chromatography	Fluorescence
Liquid Chromatography <i>Reversed Phase</i> <i>Ion Exchange</i> <i>Size Exclusion</i> <i>Affinity</i>	Absorption Spectrometry <i>Graphite Furnace</i> <i>Quartz Furnace</i> <i>Flame</i>
Gas Chromatography <i>Packed Column</i> <i>Megabore Column</i> <i>Capillary Column</i>	Mass Spectrometry <i>Inductively Coupled Plasma</i> <i>Electrospray Ionisation</i>
Electro Chromatography <i>Gel Electrophoresis</i> <i>Micellar Electrokinetic</i> <i>Capillary Zone Electrophoresis</i> <i>Field-Flow Fractionation</i>	Emission Spectroscopy <i>Inductively Coupled Plasma</i> <i>Microwave Induced Plasma</i> <i>Direct Current Plasma</i>
Filtration <i>Dialysis</i> <i>Ultrafiltration</i>	Electrochemistry <i>Ion Selective Electrode</i> <i>Voltammetry</i>
Flow Injection Analysis	Nuclear Magnetic Resonance
	Neutron Activation Analysis

*Table 1.10: Techniques widely used in metal ion speciation.*

Capillary electrophoresis (CE) is becoming more widespread, although there are still a few problems associated with the interface when coupling to elemental detectors such as ICP-MS. In general the combination utilised is dictated by the nature of the compounds being separated. Table 1.11 shows a selection of speciation studies carried out on biological samples and the main metal species detected.

Analytical Technique	Element	Matrix	Species
2D IEP/ Autoradiography	Fe, Zn, Cd, Ni & Ca <sup>142</sup>	serum	Fe-transferrin, Ca-albumin and 7 other proteins, 9 Zn binding proteins, 4 Cu binding proteins and 2 Ni binding proteins
	Ni <sup>143</sup>	serum	Several Ni binding proteins, including albumin
Electrophoresis/ ET-AAS	Au <sup>144</sup>	serum	Au binding to albumin and globulins
	Cu <sup>145</sup>	serum	Cu mainly bound to ceruloplasmin also $\alpha^2$ -protein fraction
HPLC / ET-AAS	Se <sup>146</sup>	serum	Selenoprotein-P, glutathione and albumin
HPLC / Flame-AAS	Au <sup>147</sup>	urine	Au bound to albumin and high molecular mass species
HPLC / HG-AAS	As <sup>148</sup>	serum	Separate monomethylarsonic acid (MMA), As(III), As(V) and dimethylarsinic acid (DMA)
HPLC / ICP-MS	Pt <sup>149, 150</sup>	serum	Separation of Pt drugs and metabolites
	Zn <sup>151</sup>	serum	Zn binding to transferrin and $\alpha_2$ -macroglobulin
	Au <sup>152</sup>	urine	Au drug/metabolite separation
	multi element <sup>153</sup>	milk	Preferential binding of elements to high and/or low molecular mass fractions
CE / ICP-MS	I <sup>154</sup>	serum	Separated iodine, thyroxine and triiodothyroxine
Electrophoresis/ ICP-MS	Pt <sup>155, 156</sup>	serum	Inconclusive
	Co <sup>157</sup>	serum	Co bound to albumin, $\alpha_2$ -macroglobulin, $\alpha_1$ -lipoprotein, $\alpha_1$ -antitrypsin and $\beta_1$ -lipoprotein

Table 1.11: Analytical techniques used in metal speciation of biological samples

By using hyphenation it is possible to couple the high protein resolving power of gel electrophoresis with the high trace element sensitivity of ICP-MS. This can be achieved by ablating the dried electrophoresis gels using laser ablation, a well established solid sample introduction technique for ICP-MS. Since laser ablation was used throughout the study to interrogate dried gels it will be described here in further detail.

Solution nebulisation is the main method of sample introduction used in ICP analysis. Unfortunately many samples are not suitable for nebulisation into ICP systems and the necessary sample digestion procedures can be time consuming and lead to sample contamination or loss. With this driving force methods for solid sample introduction were investigated. A number of techniques have been developed for use with ICP systems including direct sample insertion<sup>158</sup>, electrothermal vaporization (ETV)<sup>159</sup>, arc and spark ablation<sup>160</sup>, and laser ablation<sup>161</sup>. A particular interest in laser ablation developed due to the fact that, unlike alternative solid sample introduction systems, it is able to sample both conducting and non-conducting samples. This makes it applicable to a wide range of organic and inorganic solids of varying geometries, with little or no sample preparation<sup>162</sup>. Laser ablation is also capable of sampling liquid samples<sup>163</sup>.

Laser radiation has some special qualities other energy sources do not possess, it is monochromatic, unidirectional, intense, coherent, and has low beam divergence. As a result of these qualities laser ablation lends itself to a variety of applications including bulk analysis, micro features analysis, surface mapping and depth profiling. Coupling ICP with a laser ablation system has the advantage of separating the sample ablation step from the sample ionisation. Since the sample will be atomised and ionised in the plasma the ablated material may be in any chemical state, unlike laser induced plasma emission spectrometry (LIPS). By coupling ICP-MS to laser ablation the amount of interference due to oxide and hydrogen molecular species can be reduced due to the lack of water being introduced into the ICP compared to solution analysis<sup>164</sup>.

Laser Ablation has been used with ICP-OES systems since 1978<sup>165</sup>, and in 1985 Gray made the first major investigation into its use with ICP-MS<sup>166</sup>. Gray used a ruby laser emitting a beam with approximately a 1 mm diameter, emitting at a wavelength of 694 nm. ICP-MS studies progressed to using the neodymium-yttrium aluminium garnet laser (Nd:YAG), at its fundamental IR wavelength of 1064 nm<sup>167</sup>.

Simultaneous independent parallel research carried out at British Geological Survey<sup>168</sup>, and Memorial University, Newfoundland<sup>169</sup>, showed that superior performance could be achieved by using the frequency quadrupled Nd:YAG operating in the far UV at 266 nm. Others have since confirmed this using Nd:YAG lasers and Excimer lasers. Excimer lasers (UV) use gas-filled cells instead of the usual rod. A choice of output wavelengths is available depending upon the type of gas used. (i.e. XeCl: 308 nm, KrF: 248 nm, ArF: 193 nm). These days commercial laser ablation systems typically use frequency quadrupled Nd:YAG lasers, operating in the Q-switched mode. Nd:YAG lasers tend to be favoured over Excimers as they are easier to operate, cheaper and more robust. This may change as Excimers become more reliable and user friendly.

In laser ablation energy from a pulsed laser beam is focused on a target surface. The sample is vaporised due to interaction of the laser photons with the solid material. The vapour and particulates released from the sample surface are then swept into the plasma, via the Ar carrier gas flow, for atomisation and ionisation. The amount of material ablated depends upon the sample type, the surface conditions and also certain laser properties such as the energy and focus of the laser. The amount of ablated material reaching the ICP depends upon the geometry of the ablation chamber and its connection to the ICP. Signal intensity is directly related to the amount of ablated material transported into the ICP. Calibration curves can be constructed using matrix matched solid samples<sup>170</sup> or even liquid calibration standards<sup>171</sup>. The upper concentration limit is usually determined by the maximum amount of material the laser can ablate from the sample surface.

A transient signal is produced which needs to be monitored in the time resolved analysis mode. Precision can be degraded relative to conventional nebulisation due to heterogeneous sample surfaces and poor shot-to-shot reproducibility of the laser. This can sometimes be overcome by the addition of a suitable internal standard. The spatial resolution achievable depends on the wavelength and quality of the light used, decreasing the wavelength (i.e. going from IR to UV) can decrease the size of the craters produced, see Table 1.12, and can also increase the irradiance (power per unit area). The crater size also determines the limits of detection.

<b>Laser</b>	<b>Emission Wavelength</b>	<b>Crater Diameter</b>
Ruby, IR <sup>172</sup>	694 nm	100 $\mu\text{m}$
Nd YAG, IR <sup>173</sup>	1064 nm	30 $\mu\text{m}$
Frequency Doubled Nd:YAG, UV <sup>174</sup>	532 nm	6-10 $\mu\text{m}$
Frequency Quadrupled Nd:YAG, UV <sup>175</sup>	266 nm	$\sim 1 \mu\text{m}$
ArF Excimer, UV <sup>176</sup>	193 nm	sub- $\mu\text{m}$

*Table 1.12: Crater diameters produced by different lasers*

Several specific parameters determine the suitability of a laser for sample ablation including, lasing wavelength, sufficient power output, repetition rate, shot-to-shot reproducibility, ease of alignment and operation, thermal stability and cost. Nd:YAG laser is widely used, especially when frequency quadrupled to emit at 266 nm. UV emission is found to be better than IR for microanalysis as it produces a fine sample aerosol, has a high transport efficiency, less memory effects, and an improved signal stability. Since UV lasers have shorter wavelength emissions they are absorbed more efficiently. Unlike IR emission where the energy is mostly converted to thermal heating and melting of the sample, the high photon energy of UV makes thermal heating negligible<sup>177</sup>. Nd:YAG lasers can be thermally sensitive and so cooling systems are needed, but they are good lasers for micro-sample analysis as they are rugged, absorbed by most materials, easy to operate, small, inexpensive, have a high degree of reproducibility and a high pulse rate without loss of energy.

The key components for laser ablation include an excitation source (i.e. a rod of Nd doped YAG), a xenon flash lamp and a resonance cavity<sup>178</sup>. A schematic for a typical laser ablation system is shown in Figure 1.20. The excitation medium is housed in the resonance cavity, with a mirror positioned at each end of the rod. The xenon flash lamps, aligned parallel to the rod, act as an optical pump to excite the electrons. The mirrors are positioned an integral number of half wavelengths apart so that a system of standing waves can be established between them. One of the mirrors is half silvered to allow the emission of laser light from the cavity. The resonator is essentially monochromatic, as light of differing wavelengths is lost from the system. In order to produce an emission of 266 nm the output frequency of a Nd:YAG laser needs to be quadrupled. This is achieved by properly aligning two frequency-doubling crystals in the optical path of the laser.

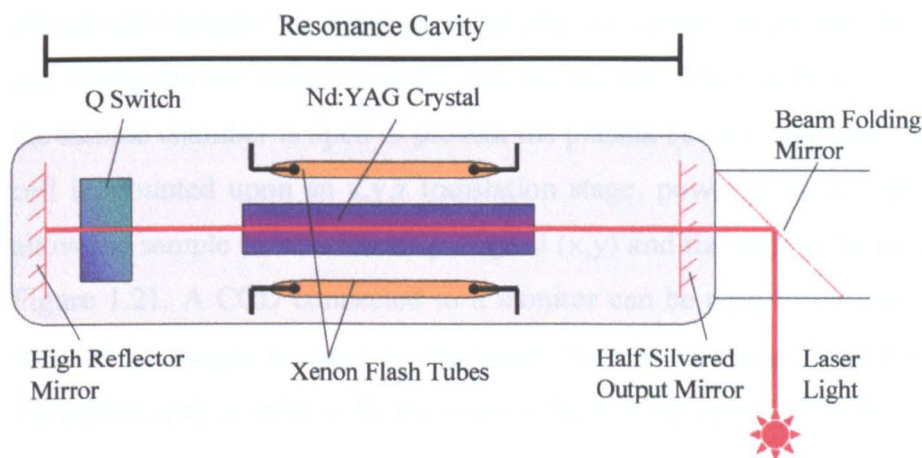


Figure 1.20: Schematic of typical Q-switched Nd:YAG laser

The laser has two different modes of operation, ‘fixed Q’ and ‘Q switching’ mode. In the fixed Q mode the laser is pumped by the flash tubes and light is emitted when the threshold conditions for the laser are reached, typical pulse time  $\mu\text{s}$ 's. Q switching means changing the Q (quality factor) of the resonant cavity, defined as the energy stored in the cavity divided by the energy lost from the cavity per cycle. A high Q cavity will store energy well while a low Q cavity will emit stored energy well. Rapid extraction at high energy can be achieved by switching rapidly

from high to low Q. Q switching is achieved using a Q-switch, an electro-optical device containing a Pockells cell. When a voltage (i.e. 5 kV) is applied across the cell it becomes opaque. By placing the cell within the resonant cavity Q switching can be controlled. When the cell is opaque resonance cannot occur and the energy is stored, when the voltage is removed a short high intensity pulse of light is emitted, typical pulse time ns's. The style of crater produced depends upon the mode of laser operation, with Q-switching the craters are wide and shallow, whilst with fixed-Q mode produces narrow, deep craters<sup>179</sup>.

In laser ablation the emitted light is focused upon a sample, a portion of which will be vaporised. The sample is mounted on a small stage, covered by a quartz window (transparent to the laser wavelength). Cell design is critical for efficient sample transport into the ICP. The cell volume should be kept small enough to minimise diffusion, but be large enough to prevent the sample sputtering onto the cell walls (which can lead to memory effects). In ICP the sample chamber effectively replaces the spray chamber, the Ar carrier gas passes through the cell and transports the ablated sample into the plasma. The gas flow is diverted when the sample chamber is open to prevent the plasma being extinguished. The sample cell is mounted upon an x,y,z translation stage, powered by a stepper motor, to allow the sample to be accurately aligned (x,y) and the laser to be focused (z), see Figure 1.21. A CCD connected to a monitor can be used to provide a magnified view of the sample to assist in alignment. Sample illumination can be from above via a fibre optic system or by transmitted light in the case of thin section samples.

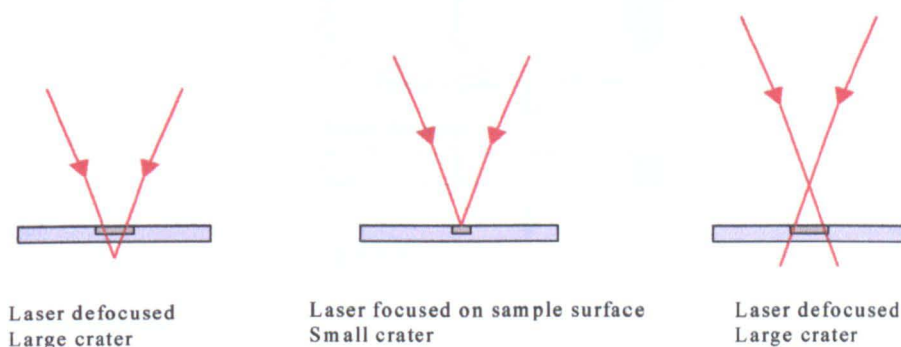


Figure 1.21: Effect of laser focus on crater size



## 1.5 The Aim of This Study

From a study of the literature available it is apparent that there is a need for an analytical technique capable of detecting metal species present in biological samples. Such a technique would find applications in a diverse selection of fields including environmental chemistry, clinical chemistry, pharmacology and associated health studies. It was decided to concentrate upon metal-protein species occurring in human serum.

To achieve such a goal the analytical technique needs to fulfill certain criteria;

- The separation technique needs to employ suitably mild conditions so as to maintain the integrity of metal-protein species throughout speciation
- The technique needs to be able to separate the metal-proteins of interest
- The technique needs to be suitably sensitive to detect the low metal concentrations present in serum samples
- The technique needs to be able to cope with the small sample volumes available

The good selectivity of native PAGE and the high sensitivity of ICP-MS present a novel technique for speciating metal ions in clinical samples when coupled using laser ablation. Figure 1.22 shows a diagrammatic representation of the technique.

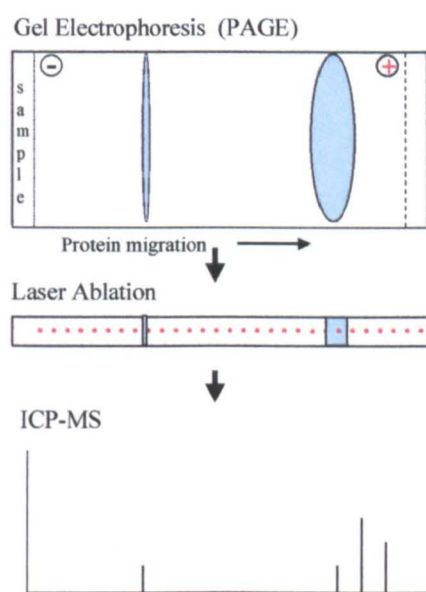


Figure 1.22: Diagrammatic representation of metal speciation in serum

The aim of the study was to develop an analytical technique for the study of metal-protein binding in human serum. Once developed the technique was to be used to study several metal-protein interactions occurring *in vitro*. The ultimate aim of the study was to apply such a technique to the analysis of clinical samples in the form of serum taken from patients receiving metallo-drug therapy. The following chapters will discuss all aspects of the work.

## Chapter 2: Experimental

### 2.1 Reagents and Materials

#### 2.1.1 Reagents

Pure lyophilised forms of human serum albumin,  $\alpha_2$ -macroglobulin and transferrin (Fluka, Switzerland) were used for *in vitro* protein studies. Phosphate buffered saline solution (Sigma, UK) was used to reconstitute the proteins. Control serum samples were obtained from the Children's Hospital, Sheffield. Serum from patients undergoing platinum therapy was obtained from the Department of Clinical Oncology, Weston Park Hospital, Sheffield. Serum from chrysotherapy patients was obtained from the Department of Rheumatology, Royal Hallamshire Hospital, Sheffield.

*In vitro* enrichment of proteins and serum was carried out using metallo-drugs, metals and colloidal gold. Cisplatin (David Bull Laboratories, Victoria) and carboplatin (Bristol Myers Pharmaceuticals, UK), were obtained from the Weston Park Hospital, Sheffield. Myocrisin (JHC Healthcare Limited, Dublin), was obtained from the Royal Hallamshire Hospital, Sheffield. Details of metallo-drugs used given in Appendix 1.3. Chloroplatinic acid standard (1000 mg/L as Pt), chloroauric acid standard (1000 mg/L as Au) and other inorganic metal stock solutions (1000-10000 mg/L) were purchased from BDH, UK. Colloidal gold (10 nm, 0.01 % H<sub>2</sub>AuCl<sub>4</sub>) was purchased from Sigma. Bio-Lyte 3/10 ampholyte (40%) and pre-prepared IEF cathodic buffer were purchased from Bio-Rad, UK. Acetic acid, isopropanol, methanol and sodium hydroxide were all purchased from BDH, UK, whilst hydrochloric acid and phosphoric acid were purchased from Sigma, UK. The following reagents were purchased from Fluka, Switzerland. 2-mercaptoethanol, acrylamide:bis solution (37.5:1), ammonium persulphate (AMP), bromophenol blue, Coomassie brilliant blue R-250, crocein scarlet 7B, glycerol, glycine, phosphate buffer saline solution (PBS), sodium dodecylsulphate (SDS), N,N,N',N'-tetramethylethylenediamine (TEMED), Tris base and triton X100.

## 2.1.2 Materials

10 well, Tris 4-15 % gradient ready gels (Bio-Rad, UK) were used for routine native gel electrophoresis. 2D-prep, Tris 4-15 % gradient ready gels (Bio-Rad, UK) were used for electrophoresis of samples for electro-elution. 10 well, IEF pH 3-10 ready gels (Bio-Rad, UK) were used for isoelectric focusing of samples. VectaSpin Micro filters with a 30 kDa molecular weight cut off (Whatman International, UK) were used in ultra-centrifugation of serum samples.

## 2.1.3 Preparation of Electrophoresis Buffers and Gels

The gels for electrophoresis need to be made in house when not using pre-cast gels. Below are the recipes used to cast 7.5 % and 15 % continuous gels as well as the recipe used to cast enriched gels. The exact procedure followed is described in section 2.2.3. Preparation of the many buffers needed in electrophoresis is also given in this section.

### *Continuous Gels*

	7.5 %	15 %
Deionised Water	4.95 mL	3.45 mL
1.5M Tris-HCl, pH8.8	2.5 mL	2.5 mL
Acryl/Bis (37.5:1)	2.5 mL	4.0 mL
10% AMP*	50 µL	50 µL
TEMED**	5 µL	5 µL

### *Pt Enriched Gel*

	15 %
Deionised Water	3.35 mL
PtCl <sub>4</sub> (100 µg/mL Pt)	0.10 mL
1.5M Tris-HCl, pH8.8	2.5 mL
Acryl/Bis (37.5:1)	4.0 mL
10% AMP*	50 µL
TEMED**	5 µL



***Native Running Buffer (x10 Conc)/ Electro-elution Buffer (x10 Conc)***

Tris Base	15.0 g
Glycine	72.0 g
Deionised Water	make up to 500 mL

***SDS Sample Buffer***

Deionised Water	2.9 mL
0.5 M Tris-HCl, pH6.8	1.0 mL
Glycerol	2.0 mL
10 % (w/v) SDS	1.6 mL
$\beta$ -mercaptoethanol	0.4 mL
1.0 % Bromophenol Blue	0.1 mL

***SDS Running Buffer (x10)***

As native Running Buffer (x10) adding 5.0 g SDS before making up to 500 mL

***IEF Sample Buffer***

50 % Glycerol (v/v)

***IEF Anode Buffer***

Phosphoric Acid	4.2 mL
Deionised Water	make up to 1 L

***Rotofor Buffer***

<b><i>Cathodic</i></b>	<b><i>Anodic</i></b>
0.1 M NaOH	0.1 M H <sub>3</sub> PO <sub>4</sub>

***SDS/Native Stain Solution***

Methanol	400 mL
Acetic Acid	100 mL
Coomassie Blue R-250	1.0 g
Deionised Water	500 mL

### ***IEF Stain Solution***

Isopropanol	270 mL
Acetic acid	100 mL
Coomassie Blue R-250	0.4 g
Crocein Scarlet	0.5 g
Deionised Water	630 mL

### ***SDS/Native/IEF Destain Solution***

Methanol	400 mL
Acetic Acid	100 mL
Deionised water	500 mL

## **2.2 Electrophoresis**

### **2.2.1 Equipment**

Vertical electrophoresis of mini-gels was carried out using a Mini Protean II powered by a Power/Pac 3000 (Bio-Rad, UK).

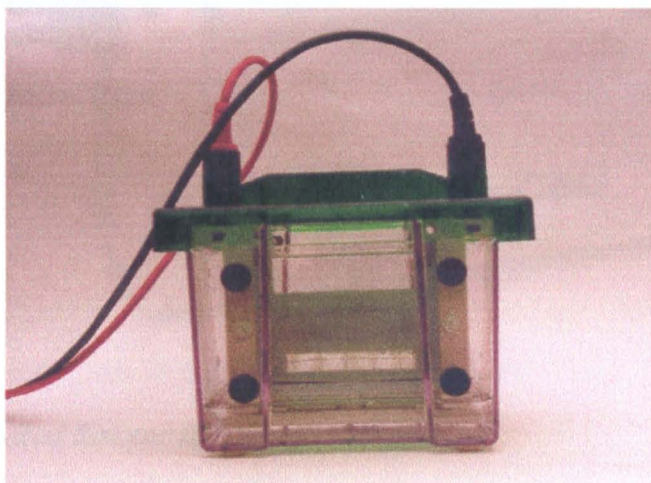


*Figure 2.1: Bio-Rad Mini Protean II System*

Electro-elution of mini-gels was carried out using a Mini-Whole Gel Eluter powered by a Power/Pac 3000 (Bio-Rad, UK).

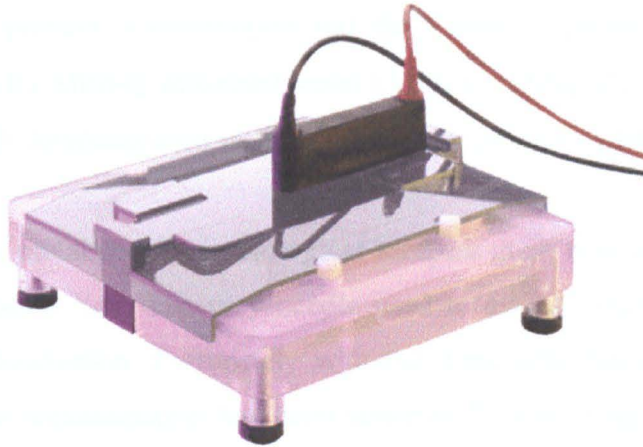


*Figure 2.2: Bio-Rad mini whole gel eluter*

Serum samples for liquid IEF separation were first desalted using Sephadex G-25M columns (Pharmacia Biotech, UK). Liquid IEF separation was then carried out using a Rotofor system powered by a Power/Pac 3000 (Bio-Rad, UK).

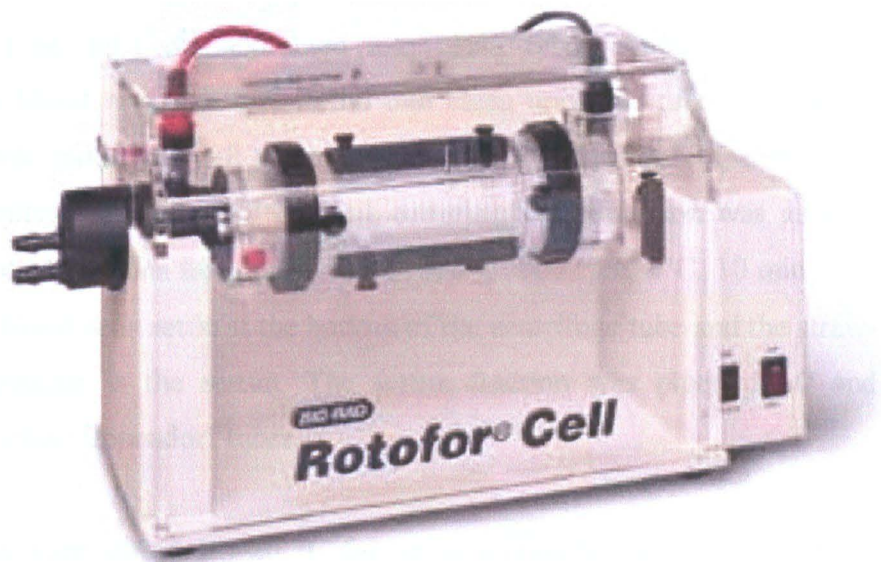


*Figure 2.3: Bio-Rad Rotofor IEF system*

Following electrophoresis polyacrylamide gels were dried using a Geldryer Minidry (Biometra Ltd., UK).



### 2.2.2 Sample Preparation

Powder free polyethylene gloves were worn at all times when handling samples and/or gels to prevent contamination and the transfer of proteins from the skin. Ultrapure 18 M $\Omega$  Milli-Q deionised water (Milli-Q, Millipore, France) was used throughout. All chemicals used were of the highest purity available.

When studying metal species in biological samples great care was taken over the sample preparation step. The very needle used to extract whole blood can be a source of contamination. Fortunately with the disposable butterfly type needles used very little contamination has been reported<sup>180</sup>. Anti-coagulants used in the collection of plasma, such as Li-heparin and K-EDTA, are possible contamination sources. With the anti-coagulant K-EDTA there is the added complication that EDTA, being a strong complexing agent, may disrupt metal-protein binding<sup>181</sup>. As a result serum samples were used throughout the study. Unlike plasma, serum lacks fibrinogen but contains all the proteins and substances not involved in clotting.

Whole blood (~60 mL) was extracted into clean tubes containing no anti-coagulant. The blood was then transferred into clean universal tubes. To isolate the serum, whole blood was left to coagulate naturally at room temperature for around 20 minutes. Once the clotting was complete centrifugation was used to separate the red blood cells from the serum (1000 g/3000 rpm, 4°C, 10 minutes). The dense red blood cells settle at the bottom of the centrifuge tube and the straw-coloured supernatant is the serum. The serum fraction was pipetted off and aliquotted into clean Eppendorf tubes.

Serum samples were stored at -20 °C for up to 6 months. When required the serum samples were removed from the freezer and allowed to thaw naturally at room temperature. After thawing, the serum samples were spun on a vortex spinner for a few minutes to re-homogenise the serum. After thawing any unused sample was discarded as repeated freezing and thawing can denature the proteins.

The average concentration of protein in human serum is 70  $\mu\text{g}/\mu\text{L}$ , after sample enrichment (1 part spike to 9 parts serum) and addition of sample buffer (1:1) the concentration of serum proteins loaded onto the gel was  $\sim 31.5 \mu\text{g}/\mu\text{L}$ . Pure proteins, albumin, transferrin and  $\alpha_2$ -macroglobulin, were acquired in the lyophilised form. The lyophilised proteins were stored at 4 °C until required. They were then reconstituted to the required concentration using phosphate buffered saline (PBS), which is isotonic to serum and has a physiological pH of 7.47. Protein samples were diluted to approximate physiological concentrations (see Appendix 1.4) in order to be comparable with human serum. The concentration of the albumin stock solution was 250  $\mu\text{g}/\mu\text{L}$ . This was diluted using phosphate buffered saline to yield a concentration of 50  $\mu\text{g}/\mu\text{L}$ . After sample enrichment, and addition of sample buffer the concentration of the albumin samples loaded on the gel was 22.5  $\mu\text{g}/\mu\text{L}$ . The concentration of the transferrin stock solution was 20  $\mu\text{g}/\mu\text{L}$ . This was diluted using phosphate buffered saline to give a transferrin concentration of 3  $\mu\text{g}/\mu\text{L}$ . After sample enrichment, and addition of sample buffer the concentration of the transferrin samples loaded on the gel was 1.35  $\mu\text{g}/\mu\text{L}$ . The concentration of the  $\alpha_2$ -macroglobulin stock solution was 20  $\mu\text{g}/\mu\text{L}$ . This was diluted using phosphate buffered saline to yield a sample concentration of 4  $\mu\text{g}/\mu\text{L}$ . After sample enrichment, and addition of sample buffer the concentration of the  $\alpha_2$ -macroglobulin samples loaded on the gel was 1.8  $\mu\text{g}/\mu\text{L}$ .

*In vitro* studies were carried out using serum and protein samples. Enriched samples were compared to un-enriched samples. Elements used to enrich protein samples included Pt, Au, La, Cr, Ni, Ga, Pb, Co, Cd, Zn, Cu, Fe and V. Spike solutions were obtained by diluting the appropriate metal standard solution with ultra-pure water to the desired concentration. Since the standard metal solutions are generally made up in acid care was taken to ensure the pH of the final spike solution was  $\text{pH } 7 \pm 1$ . This was necessary to prevent denaturation of the serum proteins from exposure to extreme pH values. Samples were enriched by adding 10  $\mu\text{L}$  of an appropriate spike solution to 90  $\mu\text{L}$  of sample. To correct for protein dilution the un-spiked samples were prepared by adding 10  $\mu\text{L}$  ultra-pure water to 90  $\mu\text{L}$  sample.

After enrichment the samples were homogenised using a vortex spinner. Samples were then left to equilibrate for at least 3 hours at room temperature or alternatively for 24 hours at 4°C.

In general, platinum studies were carried out using protein and serum samples enriched with 5 µg/mL Pt. Stock solutions of cisplatin (650 µg/mL Pt) and carboplatin (5255 µg/mL Pt) and an inorganic Pt(IV) solution (1000 µg/mL stock in HCl), were diluted to give 50 µg/mL spike solutions. The spike solutions were used to enrich the samples as described above. Gold studies were, in general, carried out using protein and serum samples enriched with 2 µg/mL Au. Gold has lower detection limits with ICP-MS than Pt due to it being mono-isotopic, hence enrichment was possible at a lower level. Stock solutions of myocrisin (26830 µg/mL Au), colloidal Au (57.97 µg/mL Au) and an inorganic Au(III) solution (1000 µg/mL stock in HCl) were diluted to give 20 µg/mL Au spike solutions. The spike solutions were used to enrich the samples as described above. Studies of other metal ions were carried out using protein and serum samples enriched using inorganic metal solutions (1000-10000 µg/mL stock) see Appendix 1.5. The samples were enriched using spike solutions as described above.

Ultrafiltration of protein and serum samples was carried out using microfilters (Whatman International, UK) with a molecular weight cut-off of 30 kDa and a thermostatically controlled microcentrifuge system. The samples were centrifuged at 13000 rpm and a steady 4°C was maintained, for approximately 15 minutes or until sample filtering was complete.

### 2.2.3 Experimental Procedures

#### Gel Preparation

Polyacrylamide gels of different concentrations were cast to compare protein separation after electrophoresis. Polyacrylamide gels enriched with various elements at a range of concentrations were also cast to optimise and calibrate the LA ICP-MS system. Gels were cast in the following way, all the reagents except ammonium persulphate (AMP) and N,N,N',N'-tetramethylethylenediamine

(TEMED), were placed in a clean universal tube and degassed. The casting stand was prepared with glass plates and 1 mm spacers. Immediately prior to casting fresh AMP and TEMED were added to the monomer solution. The solution was mixed thoroughly and then carefully poured into the gel mould. The comb for forming sample wells was added and the gel was left to polymerise for 1 hour. Once polymerised the comb was removed and the sample wells were rinsed out with ultra-pure water. Pre-cast 4-15 % Ready Gel™ plates (Bio-Rad) with 10 sample wells were used to separate samples in general, these were stored at 4 °C prior to use.

### Electrophoresis

1D native PAGE was used to separate serum proteins on the basis of size and charge, using the Mini-PROTEAN® II electrophoresis cell (Bio-Rad). The gel(s) was loaded into the electrophoresis chamber. The upper and lower buffer chambers were then filled with the native running buffer, Tris-Glycine pH 8.6. Bubbles in the running buffer were carefully eliminated to ensure good electrical contact. Next 5 µL of pre-prepared sample mixture were loaded into the sample wells using specially designed elongated micro-pipette tips (Alpha Labs. UK). A constant 200 V voltage was applied to the gel. Gels were run for 45 minutes or until the tracking dye contained in the sample buffer reached the end of the gel, the exact time taken depending upon the experimental conditions. After electrophoresis the gels were carefully removed from the electrophoresis system and were rinsed in fresh running buffer.

SDS PAGE was carried out in much the same way as native PAGE, the main difference being the buffers used. SDS sample buffer was added to samples in the ratio 2:1. The diluted sample was then heated to 95 °C for 5 minutes. The running buffer was added to the upper and lower chambers as described above and 7.5 µL of sample mixture were loaded per sample well. A larger sample volume was loaded compared to native PAGE to maintain the protein loading concentration. A constant voltage (200 V) was applied until electrophoresis was complete, the gel was then removed and rinsed.

IEF separation was carried out using pre-cast 5 % gels with a 3-10 pH range. An equal volume of sample buffer was added to the samples for electrophoresis. After loading the gels in the system the upper (cathodic) and lower (anodic) sample buffers were added. 5  $\mu$ L of sample mixture were then loaded into the sample wells. Next a stepwise voltage profile was applied to the gel(s). 100 V was applied for 1 hour, next 250 V was applied for a further hour and finally 500 V was applied for the final 30 minutes. The total run time was 2.5 hours.

### Electro-elution

Samples for electro-elution were run as 1D native PAGE but using 2D/Prep gels. These gels consisted of a single large 450  $\mu$ L sample well and a 15  $\mu$ L standard well. 75  $\mu$ L of sample mixture were loaded into the sample well and the gel was run as previously described. After electrophoresis the gel was removed and equilibrated in elution buffer for 20 minutes to minimise swelling during elution and to allow the exchange of buffers. The relevant portion of the gel was then excised.

Careful assembly of the Mini Whole Gel Eluter system, (Bio-Rad) is essential for the efficient elution of proteins, see Figure 2.4. The eluter must be level, well aligned and free from air bubbles. To assemble the system the bottom electrode was placed in the base. Next two sheets of filter paper soaked in elution buffer and a pre-soaked (over night) sheet of dialysis membrane were placed on the electrode. Air bubbles were worked out with a roller. The elution chamber core was then inserted and the hex screws finger tightened. Buffer was added until all the chambers were covered, avoiding air bubbles. The excised gel was placed in the elution chamber with the protein bands lying parallel to the channels. Two sheets of filter paper soaked in buffer were laid on top of the gel and air bubbles again worked out using a roller. Excess buffer was blotted off and the aspiration ports were dried before sealing. Finally the upper electrode assembly was placed on top of the chamber and clamped into place. A constant current of 100 mA was applied for 30 minutes. The sealing tabs were then removed carefully to avoid disturbing the samples and the fractions were collected using disposable plastic transfer pipettes. After collection the fractions were analysed by FI ICP-MS.

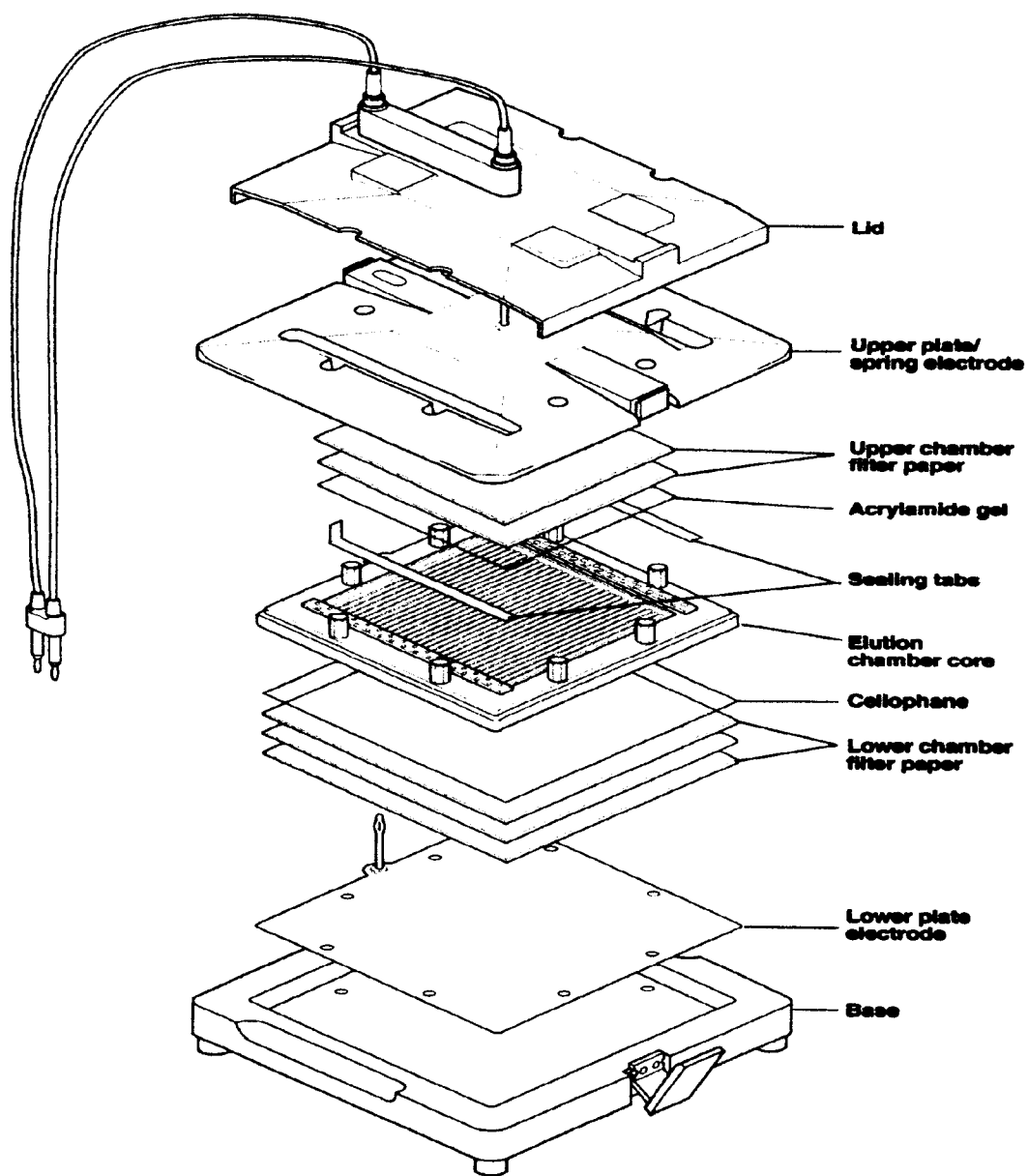


*Figure 2.4 Schematic of Mini Whole Gel Eluter System (Bio-Rad)*

## Liquid IEF

IEF can be carried out entirely in solution using the Rotofor<sup>®</sup> System (Bio-Rad). Before separation samples need to be de-salted by passing 1 mL of serum through disposable PD-10 Sephadex G25 M columns, followed by subsequent 1 mL aliquots of ultra-pure water, till a volume of 19 mL was acquired. 1 mL of a 2 % ampholyte 3/10 solution in ultra-pure water was then added to the sample. The first step in setting up the Rotofor system was the assembly of the electrolyte chambers. Once assembled the chambers were filled with their respective buffers. The anode electrode assembly was then positioned over the ceramic cooling finger, followed by the membrane core and then the focusing chamber. Finally the cathode electrode assembly was added. The collection ports in the focusing chamber were sealed. The sample, 18 mL, was then loaded through the filling ports, ensuring no air bubbles were present, then the ports were sealed. Whilst fractionating the proteins the system was cooled, via the cooling finger, to prevent protein denaturation. A constant 12 W was applied to the system for 3-5 hours. Progress was monitored by observing the voltage increase. When the voltage stabilised the run was complete. The system was left to run a further 30 minutes before harvesting the fractions with the harvesting equipment attached to a vacuum pump.

The 20 fractions acquired can be analysed in a number of ways. A form of 2D electrophoresis can be achieved by separating the fractions using conventional 1D native PAGE, loading 25 µL of recovered sample per lane. The fractions were analysed by FI ICP-MS. Prior to analysis fractions were diluted 1:1 with a 1 % HCl solution containing 20 µg/mL of the internal standards Sc, Ir and Rh.

## Gel Manipulation

Once run, polyacrylamide gels can be stained to show the position of proteins on the gel. Staining is a two step procedure, staining and destaining the gel. For staining the gel is immersed in the stain solution and gently agitated for 1 hour (45 minute maximum for IEF staining). The gels are then immersed in the destain solution and gently agitated for 2-3 hours. During the destaining process, the destain solution needs to be replaced frequently, until the background is clear.

Electrophoresed gels, stained or not, can be dried in two ways. Gels for analysis by laser ablation (preferably not stained) need to be dried on a solid support. The gels were placed carefully on a sheet of blotting paper and covered with heatproof Saran wrap. The gel was then placed on the mini-gel drier, the rubber cover carefully placed over it and the vacuum applied. Gels were dried at 40 °C for around 2 hours (too rapid drying can cause the gels to crack). Stained gels were dried between sheets of cellophane as this method minimised gel cracking and aided viewing. Gels were soaked in 2 % glycerol solution along with two sheets of cellophane. The first sheet of cellophane was placed on a sheet of glass. The gel was carefully placed on top, then covered with a second sheet of cellophane taking care to remove any air bubbles. A second glass sheet was placed on top and clamped together and left over-night to dry out.

Individual lanes from gels dried on blotting paper were cut out, and carefully cut in half to allow mounting in the laser ablation chamber. The two pieces of gel were mounted in the ablation chamber using double sided adhesive tape, see Figure 2.5. The Saran wrap covering the gel was easily peeled off prior to ablation.

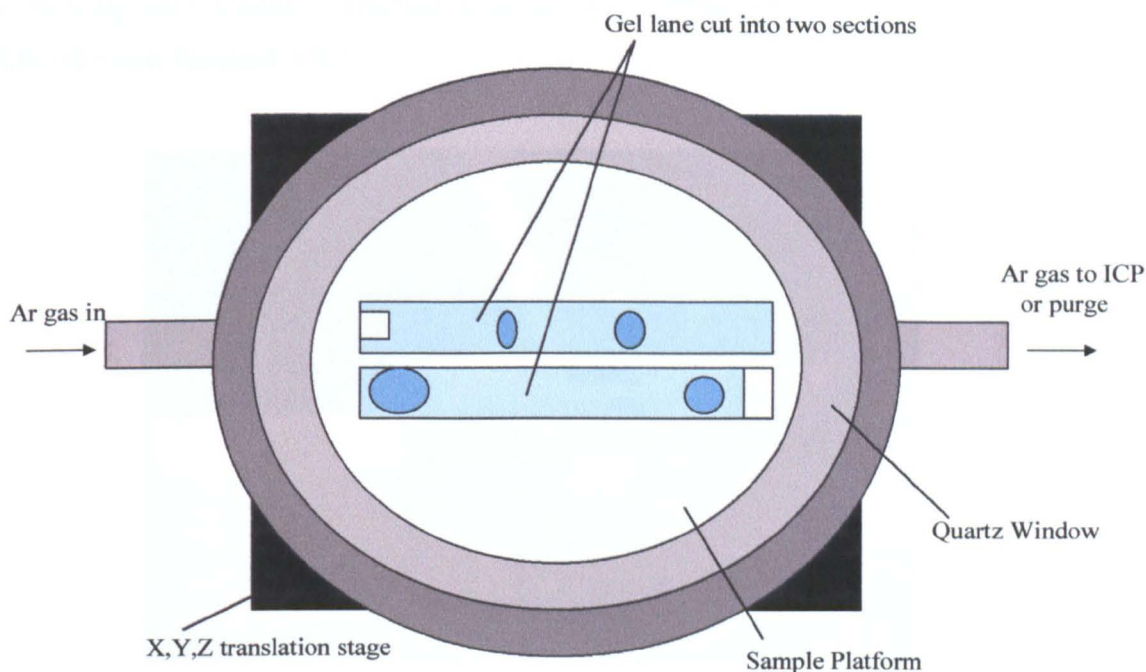


Figure 2.5: Sample of polyacrylamide gel mounted in laser ablation chamber



## 2.3 Laser Ablation ICP-MS

### 2.3.1 Instrumentation

Laser ablation of polyacrylamide gels was carried out using the LSX100 and the LSX200 (CETAC Technologies, Omaha, USA).

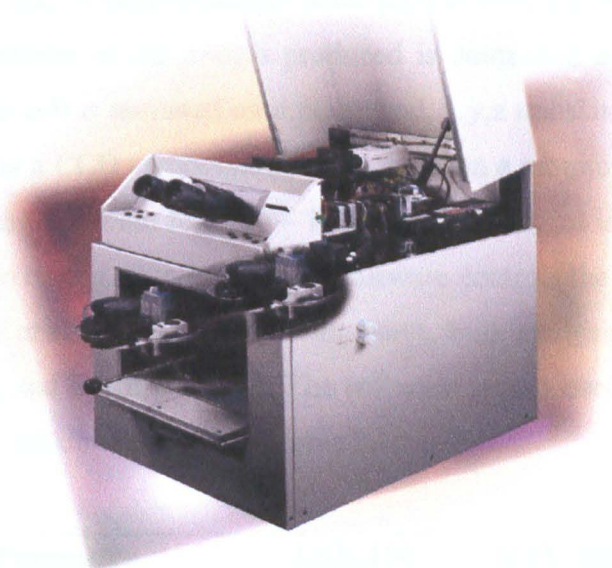


*Figure 2.6: LSX200 Laser ablation system*

Following laser ablation elemental detection was carried out using a HP4500 ICP-MS (Hewlett Packard, USA).



*Figure 2.7: HP4500 ICP-MS*

## 2.3.2 Experimental Procedures

### Laser Ablation

The ablation systems used in this study were the CETAC LSX-100 and the CETAC LSX-200. The LSX-100 laser is a frequency-quadrupled Nd:YAG laser operating at 266 nm. A near-Gaussian beam profile with a 8 ns pulse duration is emitted. The diameter of the craters produced is controlled by the focus of the laser. The sample cell is mounted on a motorised, x,y,z translation stage. Samples can be viewed via a CCD camera image displayed on a monitor. Motorised zoom control allows magnification from 20 – 128x. Sample aerosol is transported to the plasma via Tygon tubing. Windows based software controls the system and allows the sample to be analysed in the following ways, bulk analysis, feature analysis, surface mapping and depth profiling. The software is also used to adjust the key laser parameters, which are shown in Table 2.1.

<b>Parameter</b>	<b>LSX-100</b>	<b>LSX-200</b>
<b>Shot Rate</b>	1-20 Hz	1-20 Hz
<b>Scan Rate</b>	1-100 $\mu\text{m/s}$	1-100 $\mu\text{m/s}$
<b>Number of Shots</b>	1-100 shots	1-100 shots
<b>Focus</b>	$\pm 2000$ steps*	N/A
<b>Aperture Size</b>	N/A	1-7**
<b>Power</b>	1-20**	1-20**

*Table 2.1: Key parameters for LSX100 and LSX200*

\*1 step = 1.25  $\mu\text{m}$

\*\*arbitrary units,

A schematic of the LSX-200 is shown in Figure 2.8. The LSX-200 laser uses a frequency quadrupled Nd:YAG laser operating at 266 nm. A flat-top laser beam profile yields a laser pulse width < 6 ns and features Q-switched laser frequency selection and variable pulse repetition rate from 1-20 Hz. The diameter of the craters produced is controlled by the polarizing beam attenuator (10-300  $\mu\text{m}$ , see Appendix 1.6). An energy probe is incorporated into the system, which measures laser energy directly using a post-attenuated beam.

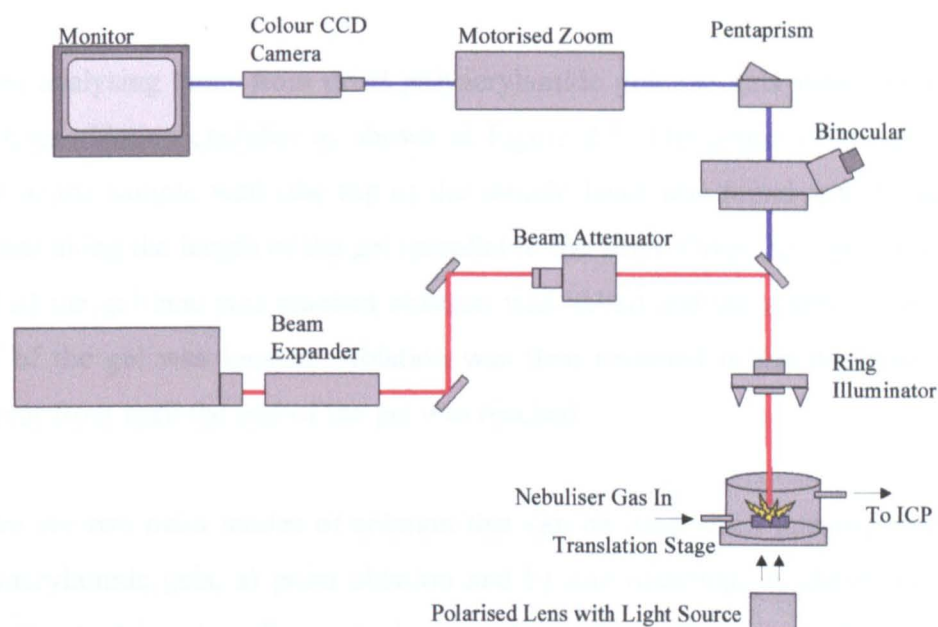


Figure 2.8: Schematic of LSX-200 laser ablation system

The sample cell is mounted on a motorised, x,y,z translation stage with <1 mm resolution. Samples can be viewed with a binocular microscope or by a CCD camera image, using transmitted or reflected light. Motorised zoom control allows magnification from 80 – 800x. Sample aerosol is transported to the plasma via Tygon tubing. Windows based software controls the system and allows the sample to be analysed in the following ways, scanning, rastering, single point analysis, depth profiling, single line scanning and single line rastering of the sample.

Platinum enriched gels were used to determine the best laser parameters to achieve stable, sensitive, representative signals. The parameters were systematically altered whilst monitoring signal response. The optimal conditions for the two types of laser ablation systems used are shown in Table 2.2.

Parameter	LSX100	LSX200
Laser Energy	0.65 mJ	0.8 mJ
Laser Shot Rate	20 Hz	20 Hz
Aperture Size	N/A	260 $\mu\text{m}$
Laser Defocus	-3000 $\mu\text{m}$	N/A
Scan Rate	50 $\mu\text{m/s}$	50 $\mu\text{m/s}$

Table 2.2: Optimised laser ablation parameters

When analysing lanes from dried polyacrylamide gels the gels were mounted in the laser ablation chamber as shown in Figure 2.5. The centre of the gel at the base of the sample well (the top of the sample lane) was found and the gel was ablated along the length of the gel (parallel to the lane). Once the end of the upper half of the gel lane was reached ablation was halted and the centre of the lower half of the gel was located. Ablation was then resumed in the direction of the solvent front until the end of the gel was reached.

There are two main modes of ablation that can be used when interrogating dried polyacrylamide gels, a) point ablation and b) line rastering, as shown in Figure 2.9. The first involves firing the laser at discrete, evenly spaced sites along the length of the gel. It is necessary to leave a crater width space between subsequent shot sites to avoid surface contamination by previously ablated material. The line rastering mode involves firing the laser continuously whilst slowly scanning along the length of the gel lane. This is achieved using the programmable translation stage upon which the ablation chamber is mounted.

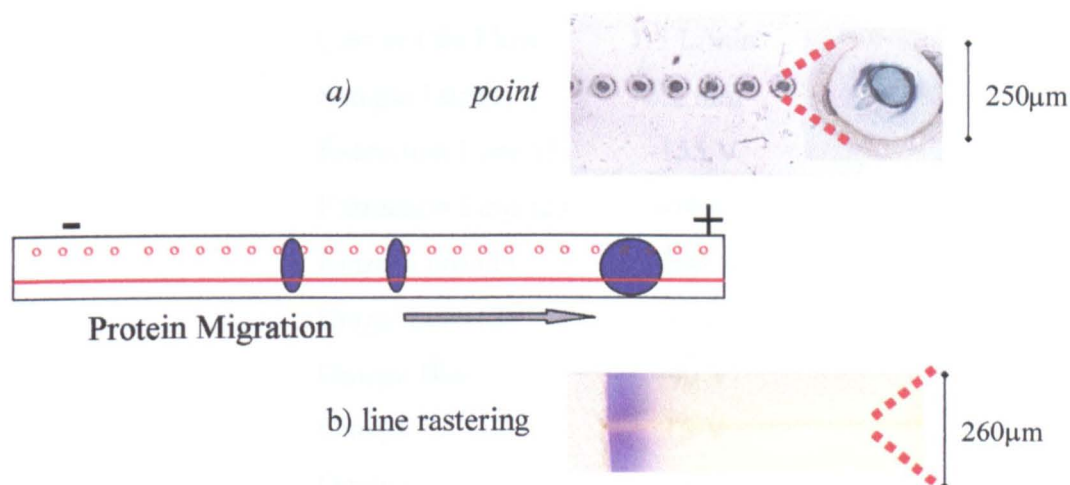


*Figure 2.9: Alternative modes of gel interrogation*

*a) point ablation, laser fired shotwise whilst rastering along length of the gel*

*b) line rastering, laser fired continuously whilst rastering along length of the gel*

## ICP-MS

The operating parameters for the ICP-MS were optimised on a daily basis by ablating a ‘National Institute of Standards and Technology’ reference glass, NIST SRM612, containing many elements at known concentrations (see Appendix 1.7). The software was set for the ICP-MS to monitor  $m/z$  values  $^{59}\text{Co}$ ,  $^{139}\text{La}$ , and  $^{232}\text{Th}$ , all present in the glass, in a time resolved fashion. The laser parameters were set such that the largest crater possible was produced, with high lasing energy, slowly rastering across the surface of the glass whilst ablating continuously. The ICP-MS parameters were varied until a stable, sensitive signal was achieved for the three masses of interest whilst maintaining low oxide and doubly charged ion concentrations. Typical ICP-MS operating parameter for laser analysis are given in Table 2.3.

<b>Parameter</b>	<b>Value</b>
RF Power	1300 W
Reflected Power	0 W
Coolant Gas Flow	16.0 L/min
Auxiliary Gas Flow	1.0 L/min
Carrier Gas Flow	1.5 L/min
Sample Depth	6.2 mm
Extraction Lens (1)	-155 V
Extraction Lens (2)	-64 V
Einzel Lens (1)	-100 V
Einzel Lens (2)	6 V
Omega Bias	-40 V
Omega +	15 V
Omega -	-3 V
Plate Bias	-10
Pole Bias	-10
Integration Time	0.1 s

*Table 2.3: Typical HP4500 parameters*

## **2.4 Flow Injection ICP-MS**

### **2.4.1 Instrumentation**

Flow injection ICP-MS was carried out using a Gilson Miniplus 3 peristaltic pump (Gilson, UK) with a 6 port rotary flow injection valve (Omnifit, UK). This was coupled to a HP4500 ICP-MS system (HP, USA).

Flow injection analysis (FIA) has been a popular sample introduction technique since the 1970s<sup>182</sup>. In flow injection ICP-MS a discrete, reproducible volume of the sample, is transported via a closed circuit by a continuously flowing carrier to the ICP-MS. The main benefits of such a sample introduction system are low limits of detection, good precision, small sample volume and rapid analysis time. FIA is a well-established technique; a typical system is comprised of a peristaltic pump, rotary flow-injection valve and an interface to the analyser. The sample is loaded into the sample loop, then injected into the ICP-MS via a continuously flowing carrier stream. The size of the sample loop can be varied as can the flow rate of the carrier. Both these parameters affect the sensitivity of the technique

### **2.4.2 Experimental Procedure**

Optimisation of carrier flow rate and sample volume, the two main parameters effecting signal response, was carried out using a platinum enriched solution. Both parameters were altered individually and the effect on signal response was noted. The flow rate and sample volume giving the most sensitive response were used throughout.

The carrier solution used for flow injection ICP-MS analysis of protein samples was 0.1 % Triton X100. Memory effects can occur when gold is analysed by ICP-MS and so a wash out step using 2 %HCl / 2 %HNO<sub>3</sub> was performed at the end of each analysis run.

## **Chapter 3: Characterisation of Platinum Enriched Gels**

### **3.1 Introduction**

Despite being one of the rarest elements in the earth's crust (~1 ng/g)<sup>183</sup>, platinum has been widely used for the past hundred years. Known as a 'noble' metal, platinum actually forms a wide variety of complexes with inorganic compounds and biological systems making it of interest not only in terms of mineral exploration, but also in microbiology and clinical medicine. Levels of platinum occurring in the environment, foodstuff and in living organisms are extremely low and, unlike most other heavy metals, platinum is generally regarded as non-toxic. However, in certain situations where platinum is handled, it can pose an occupational hazard. Excessive exposure to soluble platinum compounds can lead to platinumosis, and so knowledge of the bio-availability, bio-accumulation and toxicity of platinum is becoming increasingly important. Platinum baseline levels in humans were found to be 0.8-6.9 ng/L in blood and 0.5-14.3 ng/L in urine<sup>184</sup>. These levels are found to be significantly higher in workers exposed to platinum<sup>110</sup>.

Since its discovery in 1735 platinum has found a number of applications including jewellery, thermocouples, electrodes, fuel cells, surgical implants, corrosion resistant wares, heterogeneous and homogeneous catalysts and cancer chemotherapy. All these applications are potential sources of anthropogenic platinum emission. There has been a rapid increase in use and, as a result, emission of platinum in recent years. This increase can be attributed to two specific sources, the introduction of catalytic converters for the exhaust system of motor cars in 1974 and the first use of platinum chemotherapeutic drugs in 1971.

Platinum is widely used in the automobile industry as an exhaust catalyst that oxidises harmful combustion by-products. Surface abrasion of the catalyst results in the emission of platinum into the environment; this is usually in the form of platinum metal or oxide particulates<sup>185</sup>. Platinum emissions can be detected in the

aerosol from the car exhaust<sup>186</sup>. Once airborne, platinum can contaminate plant life<sup>187</sup>. The platinum content of road dust in areas of south London has been found to be 0.42-29.8 ng/g<sup>188</sup>, significantly higher than crustal levels. A correlation was found between platinum concentration in roadside dust and traffic flow, hence, even higher platinum concentrations might be detected alongside motorways and in inner city areas. The presence of chemical and biological agents in soil can result in the emitted platinum being transformed into bio-available species<sup>189</sup>. There is evidence of platinum uptake by plants growing on contaminated roadside soil<sup>190</sup>, thus providing a mechanism by which platinum can enter the food chain.

Platinum(II) drugs are widely used in the treatment of various cancers. These are also known to contribute to the problem of platinum emission into the environment. Studies show elevated platinum levels in hospital waste water and sewage sludge<sup>191</sup> due to the use of such platinum drugs. Increased emissions of platinum in recent years make it necessary to determine its effect on living organisms and the environment. To achieve this aim, analytical techniques capable of determining the trace and ultra-trace levels of platinum present in the environment need to be developed. Platinum speciation is also required to help elucidate metabolism reaction pathways and products. The detection limits of the traditional techniques for determining platinum, such as fire assay, are too high for such measurements and so instrumentation with lower detection limits is employed. Being relatively cheap and versatile, GF-AAS is the method of choice for the routine determination of platinum in biological fluids. ICP-MS, however, is more sensitive, (see Table 3.1). High sensitivity, combined with rapid, simultaneous multi-element capability makes ICP-MS the preferred technique for ultra-trace analysis. Alternative techniques offering comparable detection limits, such as NAA and PIXE, are costly and require highly specialised equipment in comparison.

	Flame AAS	GF-AAS	ICP-OES	ICP-MS
LOD ( $\mu\text{g/L}$ )	60.0	1.50	7.00	0.08

*Table 3.1: Limits of detection for platinum. Table adapted from<sup>95</sup>*



There are a number of naturally occurring platinum isotopes, their masses and relative abundances are;

$^{190}\text{Pt}$ - 0.01 %	$^{192}\text{Pt}$ - 0.79 %	$^{194}\text{Pt}$ - 32.9 %
$^{195}\text{Pt}$ - 33.8 %	$^{196}\text{Pt}$ - 25.3 %	$^{198}\text{Pt}$ - 7.2 %

ICP-MS is capable of detecting all of these isotopes. In order to obtain the highest sensitivity, however, the most abundant mass is normally monitored, i.e.  $^{195}\text{Pt}$ . Examples of platinum studies involving ICP-MS are numerous, with a high proportion of the samples analysed being biological, in particular urine<sup>192, 193</sup>, and blood<sup>108, 109, 194</sup>.

Besides contributing to platinum emissions into the environment platinum based drugs, such as cisplatin and carboplatin, can also pose a potential health risk to those undergoing therapy. Once in the body Pt(II) tends to bind to sulphur rich amino acids found in proteins when the tertiary structure of the proteins makes this possible. Such interactions are particularly relevant to the toxic side effects of the drugs, especially those involving the kidneys. Cisplatin is known to bind extensively to albumin<sup>36</sup> and to transferrin to a lesser degree<sup>195</sup>. An understanding of the molecular mechanism of such interactions may help optimise cisplatin therapy, making platinum speciation knowledge of clinical, as well as environmental, interest.

Most of the current clinical research concerning platinum focuses on interactions occurring between platinum drugs and DNA. In contrast the results in this chapter focus on the interactions between platinum and serum proteins. PAGE coupled with LA ICP-MS was used to detect and speciate platinum anti-cancer drug metabolites in human serum. Other work in this area done using similar technology<sup>155, 156</sup> experienced problems with high platinum blank concentration levels. This platinum contamination was probably due to the use of a flat bed electrophoresis system utilising sheet type platinum electrodes with large surface areas. No such contamination problems were observed using the vertical Bio-Rad electrophoresis system.

## 3.2 Method Development

Before embarking on the analysis of ‘real’ samples it was necessary to perform initial feasibility studies. The aim of which was to demonstrate the suitability of utilising gel electrophoresis followed by LA ICP-MS for metal speciation in biological samples. The studies were also used to identify some of the key operational parameters. This optimisation of the system was essential to ensure representative sampling of the biological samples (important to maintain metal-protein binding) and to demonstrate adequate species resolution and sensitivity.

### 3.2.1 Flow Injection – ICP-MS

To obtain quantitative data on the platinum content of serum and protein samples analysis was carried out using flow injection – ICP-MS. Optimisation of operating parameters was necessary prior to analysis. The key parameters affecting signal response are the volume of sample injected and the sample flow rate.

#### 3.2.1.a Sample Volume

To determine the optimal sample volume replicate injections were made using a Pt standard solution ( $\text{PtCl}_4$ ,  $50 \mu\text{g/L Pt}$ )<sup>□</sup>. The sample volume was altered with each injection. The ion time responses are given in Figure 3.1.

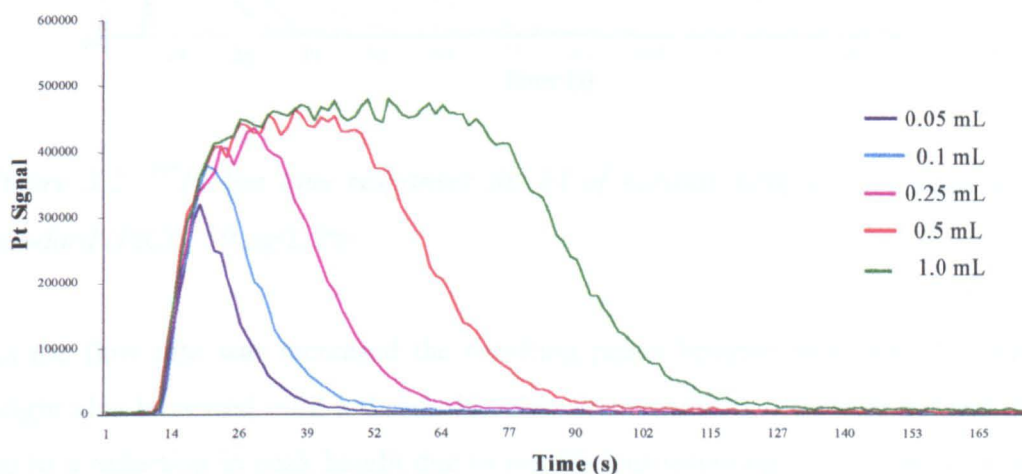


Figure 3.1:  $^{195}\text{Pt}$  Ion time responses for FI of various sample volumes of Pt standard ( $\text{PtCl}_4$ ,  $50 \mu\text{g/L Pt}$ )

<sup>□</sup> Platinum species in Pt standard solutions referred to as  $\text{PtCl}_4$  but more likely to exist as  $\text{PtCl}_6^{2-}$ .

As the sample volume was increased so the peak height increased until a threshold height was reached. Increasing the sample volume further led to peak broadening. The sample volume of 0.1 mL was decided upon as the optimal sample volume giving both well formed peaks and a suitable sensitivity.

### 3.2.1.b Flow Rate

To determine the optimal flow rate replicate injections were made using a Pt standard solution ( $\text{PtCl}_4$ , 50  $\mu\text{g/L}$  Pt). The flow rate was increased with each injection. The ion time responses are given in Figure 3.2.

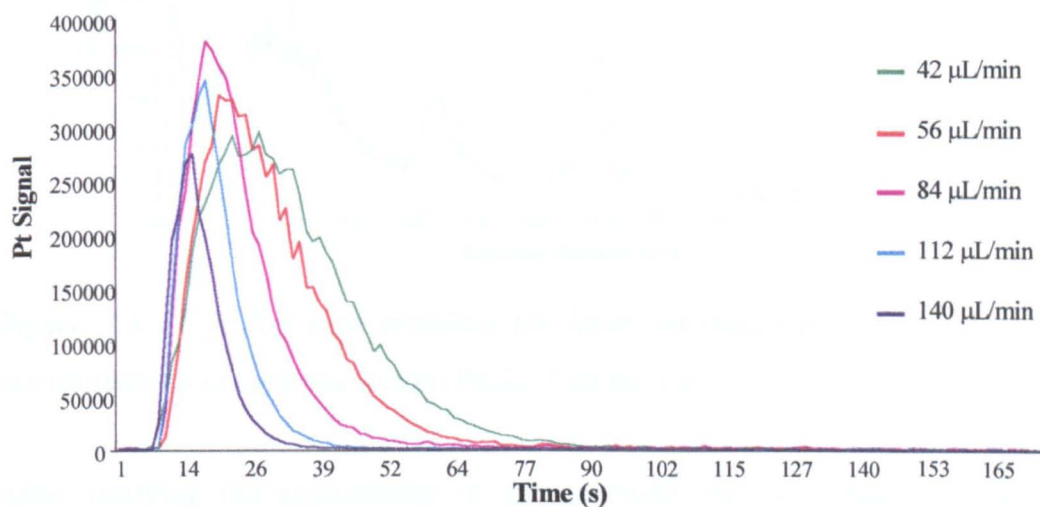


Figure 3.2:  $^{195}\text{Pt}$  Ion time responses for FI of various sample flow rates of Pt standard ( $\text{PtCl}_4$ , 50  $\mu\text{g/L}$  Pt)

As the flow rate was increased the resulting peaks became narrower. The peak height also increased until a threshold value. Increasing the flow rate beyond this led to a reduction in peak height due to insufficient sampling times. The flow rate of 84  $\mu\text{L/min}$ , corresponding to a pump speed of 0.3 rps was decided upon as the optimal flow rate giving both well formed peaks and a suitable sensitivity.

### 3.2.2 Laser Ablation of Gels

To ascertain the applicability of the combined strategy a serum sample, enriched to contain inorganic platinum ( $\text{PtCl}_4$ , 5  $\mu\text{g/mL Pt}$ ), was subjected to electrophoresis and the dried gel was analysed by LA ICP-MS. The Pt distribution profile obtained, Figure 3.3, showed that platinum did bind to serum proteins and also that the system was suitably sensitive to detect platinum in the gel.

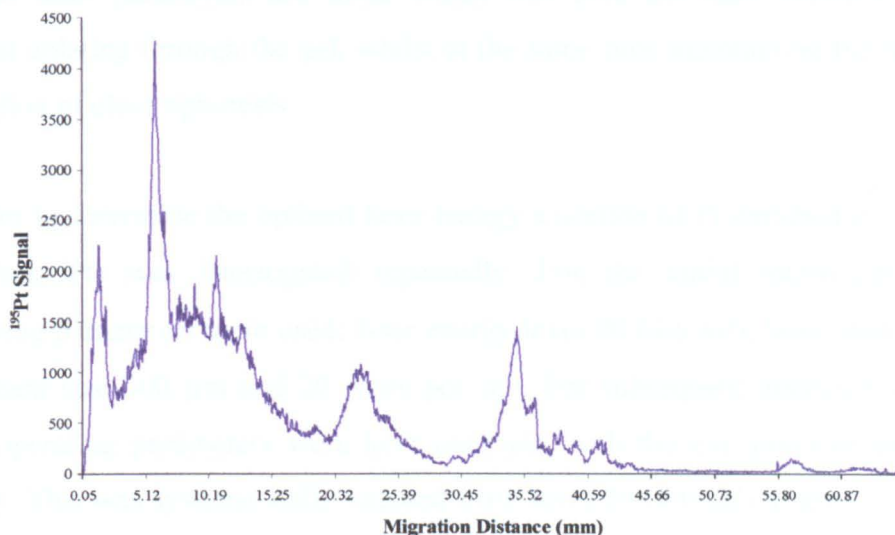


Figure 3.3:  $^{195}\text{Pt}$  Ion time response for laser interrogation of gel following electrophoresis of enriched serum ( $\text{PtCl}_4$ , 5  $\mu\text{g/mL Pt}$ )

After verifying the applicability of the approach, the next stage in method development was to study the gel interrogation strategy. In particular it was necessary to determine whether the sample ablated, could then be analysed by the ICP-MS, to give representative, reproducible results. To investigate this various operating parameters were examined with a view to signal optimisation.

When considering with laser ablation, there are several laser parameters that affect the laser coupling efficiency and transfer of ablated product to the ICP. These include; laser energy, laser shot rate, beam size and number of laser shots per site. The efficiency of laser coupling is dependent also upon the sample matrix. To establish the best laser parameters for the analysis of dried electrophoresis gels a matrix matched enriched gel was prepared (see section 2.2.3).

A gel was cast containing inorganic Pt ( $\text{PtCl}_4$ , 1  $\mu\text{g/mL}$  Pt). After drying, a section of the enriched gel was mounted in the ablation chamber. The gel was then interrogated whilst monitoring  $m/z$  195 (Pt). The laser parameters were systematically altered until the optimal laser parameters had been determined. As the dried gel has a finite depth of 0.2 mm, the amount of sample available for ablation and hence the analyte signal achievable is finite. If the sample is ablated excessively the paper supporting the dried gel then undergoes ablation. The optimal laser parameters are those which will give the most sensitive signal without ablating through the gel, whilst at the same time maintaining the inherent resolution of electrophoresis.

In order to determine the optimal laser energy a section of Pt enriched gel ( $\text{PtCl}_4$ , 1  $\mu\text{g/mL}$  Pt) was interrogated repeatedly. For the initial interrogation the following parameters were used; laser energy level 20 (4.6 mJ), laser shot rate 20 Hz, beam size 300  $\mu\text{m}$  and 20 shots per site. For subsequent interrogations the laser operating parameters were kept constant, with the exception of the laser energy. This was systematically reduced from level 20 (4.6 mJ) to level 1 (0 mJ). The ion time responses obtained can be seen in Figure 3.4. It was noted that as the laser energy decreased so the observed signal decreased. This was as a direct result of a decrease in the amount of sample ablated. Figure 3.4 shows a linear relationship between laser energy and the observed signal intensity. Visual assessment of the ablated gel highlighted excessive ablation when energy levels exceeding 1.7 mJ were used. The optimal laser energy was identified as the laser energy at which maximum analyte signal was achieved without excessive ablation of the gel, as such the optimal laser energy of the LSX-200 was found to be 1.7 mJ. This energy was used for all further gel interrogations, unless otherwise stated. The optimal laser shot rate was determined by repeatedly interrogating a section of Pt enriched gel ( $\text{PtCl}_4$ , 1  $\mu\text{g/mL}$  Pt), whilst systematically altering the shot rate from an initial shot rate of 20 Hz to 1 Hz. In each case equal areas of gel were ablated. Figure 3.5 shows the ion time response obtained. As the shot rate was decreased so the total number of laser shots fired decreased and the signal intensity was also found to decrease. The optimal shot rate for gel interrogation was found to be 20 Hz as this gave the greatest sensitivity.

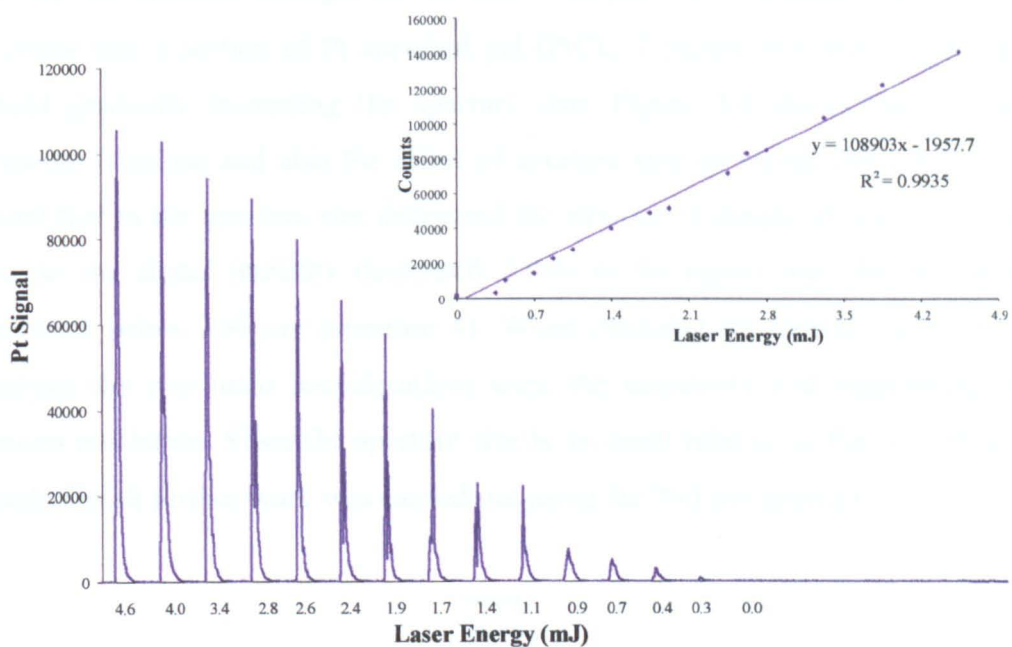


Figure 3.4:  $^{195}\text{Pt}$  Ion time responses for Pt enriched gel ( $\text{PtCl}_4$ ,  $1\ \mu\text{g/mL}$  Pt) at various laser energies      Inset: Integrated Pt peak area vs laser energy

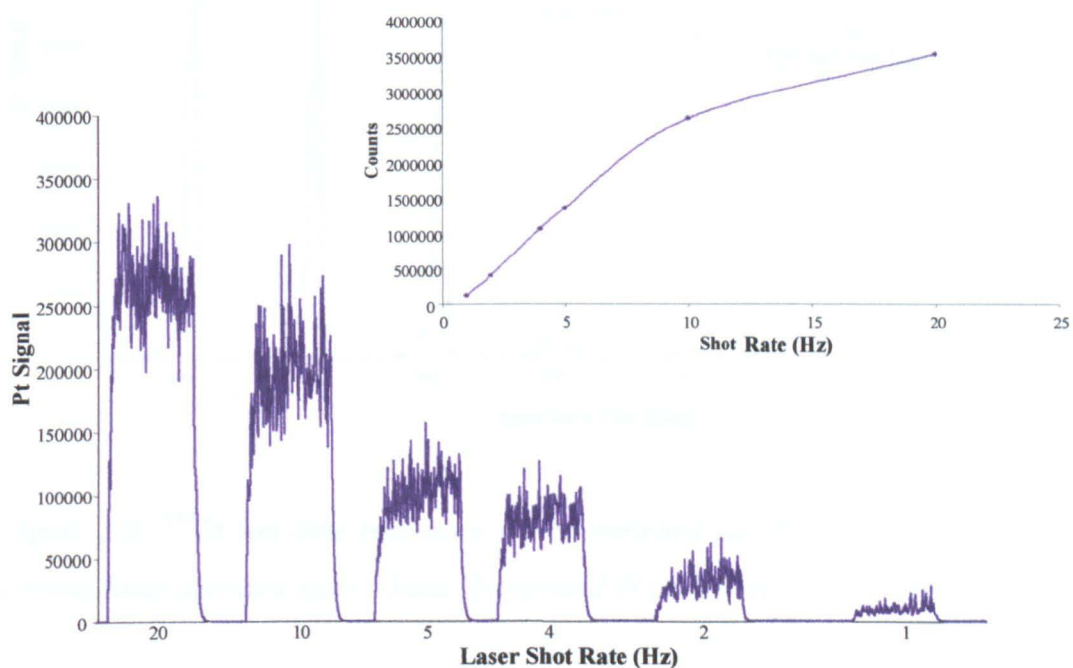


Figure 3.5:  $^{195}\text{Pt}$  Ion time responses for Pt enriched gel ( $\text{PtCl}_4$ ,  $1\ \mu\text{g/mL}$  Pt) at various laser shot rates      Inset: Integrated Pt peak area vs laser shot rate

The LSX200 laser ablation facility can afford a variety of laser beam diameters by varying the aperture settings, i.e. 10  $\mu\text{m}$  - 300  $\mu\text{m}$ . To investigate the effect of aperture size a section of Pt enriched gel ( $\text{PtCl}_4$ , 1  $\mu\text{g}/\text{mL}$  Pt), was interrogated whilst gradually increasing the aperture size. Figure 3.6 shows the ion time response obtained and also the effect of aperture size on signal intensity. It was found that as the aperture size decreased the amount of sample ablated decreased and so the signal intensity decreased. Little or no signal was obtained using apertures below 100  $\mu\text{m}$  (aperture 4). When choosing an aperture size for gel analysis the two main considerations were the sensitivity and maintaining the protein resolution. Since the aperture size is so small relative to the protein band resolution all further work was carried out using the 260  $\mu\text{m}$  aperture.

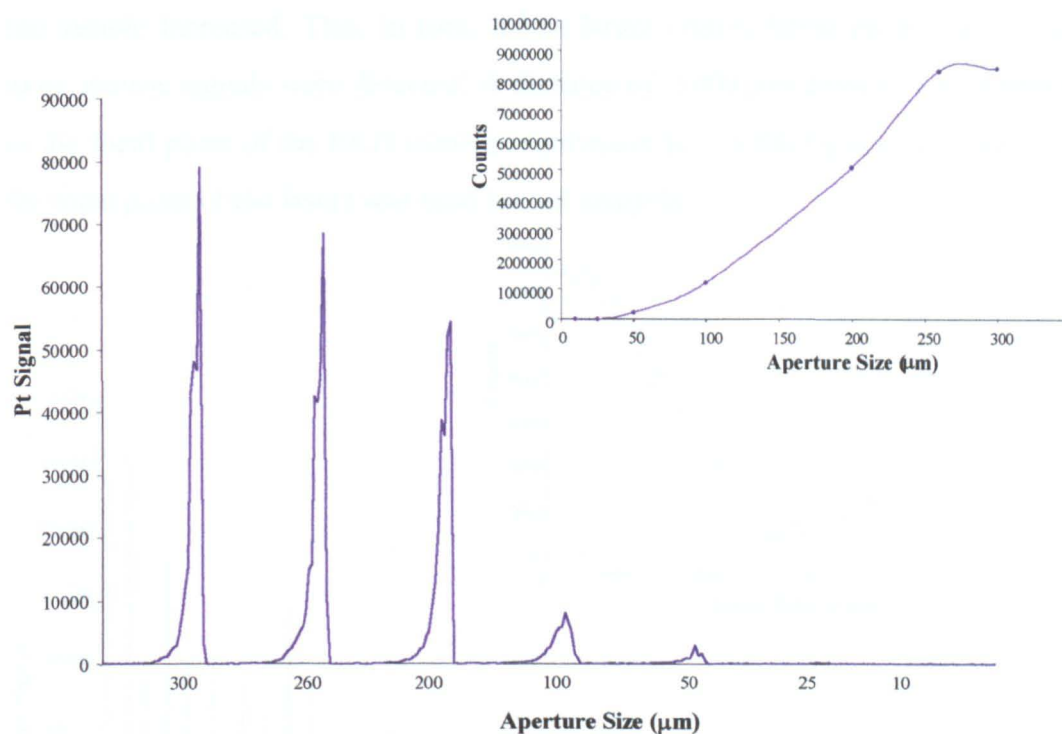


Figure 3.6:  $^{195}\text{Pt}$  Ion time responses for Pt enriched gel ( $\text{PtCl}_4$ , 1  $\mu\text{g}/\text{mL}$  Pt) at various laser aperture sizes Inset: Integrated Pt peak area vs laser aperture size

The LSX-100 laser ablation system controls crater size by varying the focus of the laser on the sample. This is achieved by altering the height of the laser above the sample, see Figure 1.23. This is not an ideal situation as variations in the surface of the gel can alter the crater size and so alter the sensitivity of the system. As

such, variations in the surface nature can lead to variations in the ICP-MS response. The resulting ‘peaks’ may simply be the result of fluctuations in laser focus, not variations in analyte concentration. To minimise this effect the gel surface was kept as smooth as possible whilst drying and was mounted in the ablation chamber using doubled sided tape. The best laser focus for the interrogation of gels was determined by analysing a section of Pt enriched gel ( $\text{PtCl}_4$ ,  $1 \mu\text{g/mL Pt}$ ), whilst systematically altering the laser focus.

Figure 3.7 shows the ion time response obtained. The distances quoted for laser defocus are relative to the focal point of the CCD camera, not the laser. It can be seen that the lasers focal point is  $\sim -3000 \mu\text{m}$  from that of the monitor. As the laser was moved away from its focal point the diameter of the laser beam hitting the sample increased. This, in turn, led to larger craters being produced and so more intense signals were detected. A distance of  $-1000 \mu\text{m}$  defocus with respect to the focal point of the CCD camera (equivalent to  $\sim +2000 \mu\text{m}$  with respect to the focal point of the laser) was used for gel analysis.

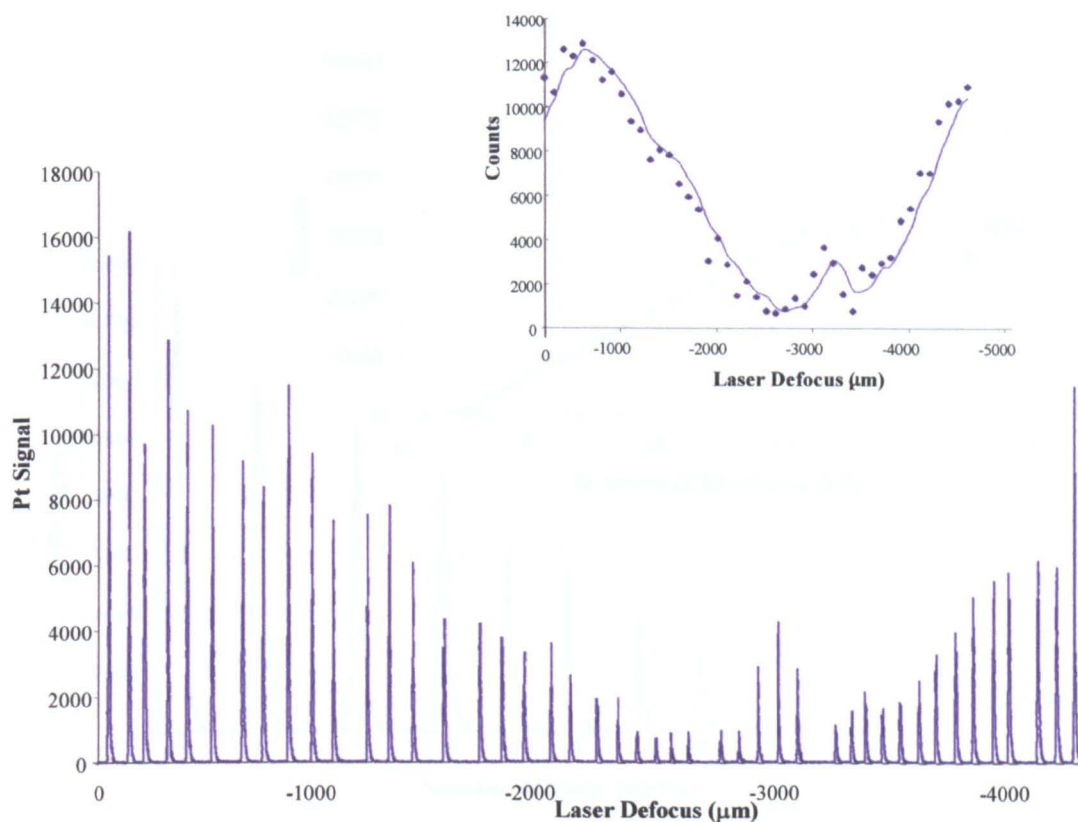


Figure 3.7:  $^{195}\text{Pt}$  Ion time responses for Pt enriched gel ( $\text{PtCl}_4$ ,  $1 \mu\text{g/mL Pt}$ ) at various laser focus settings Inset: Integrated Pt peak area vs laser focus setting



When interrogating gels in a shot-wise manner there is a need to optimize the number of laser shots fired per site. Figure 3.8 shows the ion time response obtained when a Pt enriched gel ( $\text{PtCl}_4$ ,  $1 \mu\text{g/mL Pt}$ ) was interrogated repeatedly whilst gradually altering the number of shots per site. The more laser shots fired per site, the greater the amount of material ablated and so the greater the resultant signal. The finite thickness of the gel limits the amount of material available for ablation, and so an excessive number of shots in one site would result in ablation of the gel support.

Visual examination of the ablated gel indicated that excessive ablation occurred with  $>20$  shots per site. The plot of peak area against number of laser shots per site is linear even when the gel has been excessively ablated, this is probably due to platinum being absorbed by the paper support before drying. At such high shots per site the resultant signal is not representative of the platinum concentration in the gel. For all further work done in the point ablation mode of operation, 20 shots were fired per site.

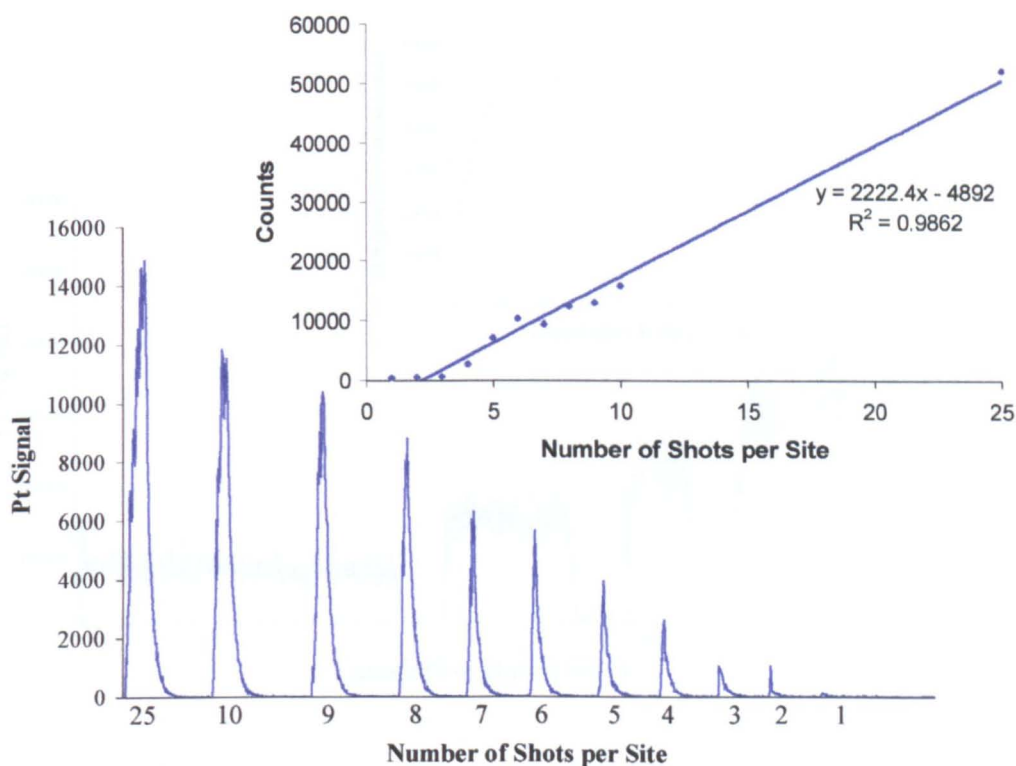


Figure 3.8:  $^{195}\text{Pt}$  Ion time responses for Pt enriched gel ( $\text{PtCl}_4$ ,  $1 \mu\text{g/mL Pt}$ ) for various laser shots Inset: Integrated Pt peak area vs laser shots

The previous experiments were all based on the point ablation mode of operation. An alternative mode of interrogation involves firing the laser at the gel continuously whilst slowly scanning along the length of the gel lane, this was referred to as line rastering. Before interrogating in this manner the translation rate for the gel needed to be optimised. The translation rate was gradually increased from 10  $\mu\text{m/s}$  to a maximum value of 1000  $\mu\text{m/s}$ , all other laser operating parameters being kept constant. In each case equal areas were ablated.

Figure 3.9 shows the ion time responses obtained when a Pt enriched gel ( $\text{PtCl}_4$ , 1  $\mu\text{g/mL}$  Pt) was repeatedly ablated at different translation rates. Each ablation covered a section of the gel approximately 4000  $\mu\text{m}$  in length. Since interrogation time is given by the distance scanned divided by the scan rate, the time taken for successive interrogations decreased. When scanning at 12.5  $\mu\text{m/s}$  the interrogation took 320 s, this decreased to just 4 s when scanning at 1000  $\mu\text{m/s}$ . Figure 3.9 also shows the effect of translation rate on the Pt counts/s detected.

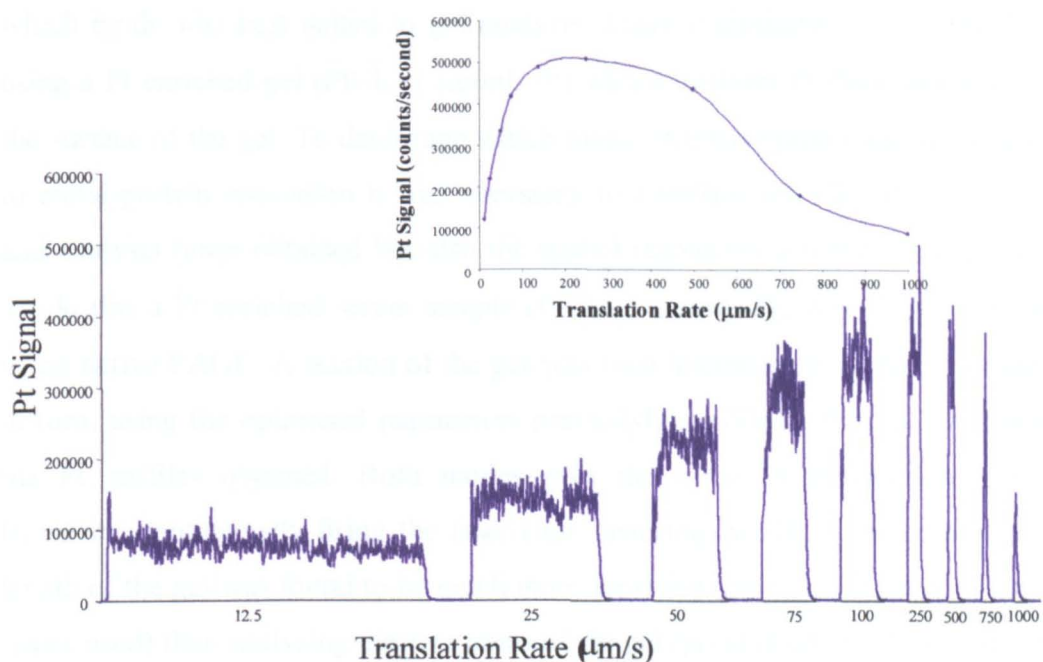
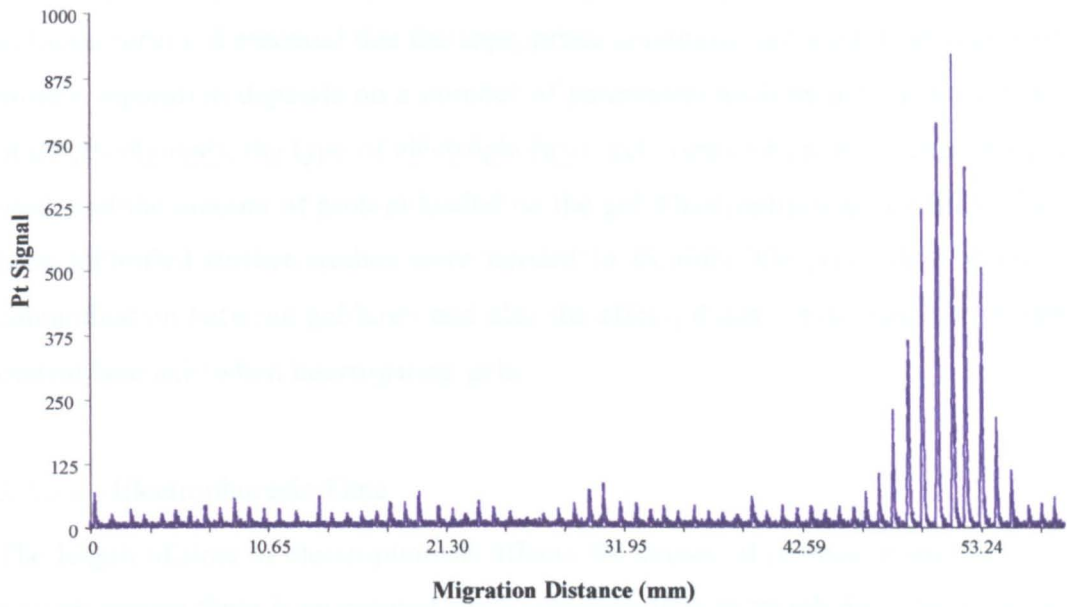


Figure 3.9:  $^{195}\text{Pt}$  Ion time response for Pt enriched gel ( $\text{PtCl}_4$ , 1  $\mu\text{g/mL}$  Pt) at various translation rates Inset: Pt counts per second vs translation rate

To determine the optimal scan rate for line rastering of the gels three factors need to be considered, the counts/s obtained, the analysis time and the spatial resolution. Increasing the scan rate can be seen to increase the counts/s until a maximum signal is achieved (similar in nature to the effect of flow rate in FIA). Increasing the scan rate still further results in a decrease in counts/s as the amount of material ablated decreases. The sensitivity of the system was shown to be maximised at a scan rate of  $\sim 200 \mu\text{m/s}$ . Increasing the translation rate decreased the analysis time (linear relationship) but resulted in the loss of spatial resolution which is essential for metal speciation in gel electrophoresis. A translation rate of  $50 \mu\text{m/s}$  was found to satisfy the three criteria. Whilst the counts/s were not as high as might have been achieved with a faster translation rate, spatial resolution was maintained. This translation rate give a typical analysis time of  $\sim 20$  minutes (1200 s) for a gel lane ( $\sim 60 \text{ mm}$ ) which was found to be acceptable. Thus the compromise translation rate of  $50 \mu\text{m/s}$  was adopted for all further work.

Once the optimised laser parameters for the two modes of laser interrogation (point ablation and line rastering) had been determined it was necessary to decide which mode was best suited to gel analysis. Laser optimisation was carried out using a Pt enriched gel ( $\text{PtCl}_4$ ,  $1 \mu\text{g/mL Pt}$ ) with a uniform Pt distribution across the surface of the gel. To determine which mode of interrogation was most suited to metal-protein speciation it was necessary to compare not only the sensitivity and analysis times obtained but also the spatial resolution achieved in each case. To do this a Pt enriched serum sample ( $\text{PtCl}_4$ ,  $5 \mu\text{g/mL Pt}$ ) was electrophoresed using native PAGE. A section of the gel was then interrogated by the two modes in turn, using the optimised parameters previously described. Figure 3.10 shows the Pt profiles obtained. Both modes give the same Pt distribution profile. However, continuously firing the laser (line rastering) whilst scanning along the length of the gel was found to be much more sensitive (note the different Pt signal scales used) than analysing discrete areas of the gel (point ablation). Line rastering also gave a shorter analysis time ( $\sim 20$  minutes per lane) compared with that needed for point ablation (typically 1 hour per lane), whilst maintaining spatial resolution. Thus for all future work the line raster mode of laser interrogation was employed.

a) Point Ablation



b) Line Rastering

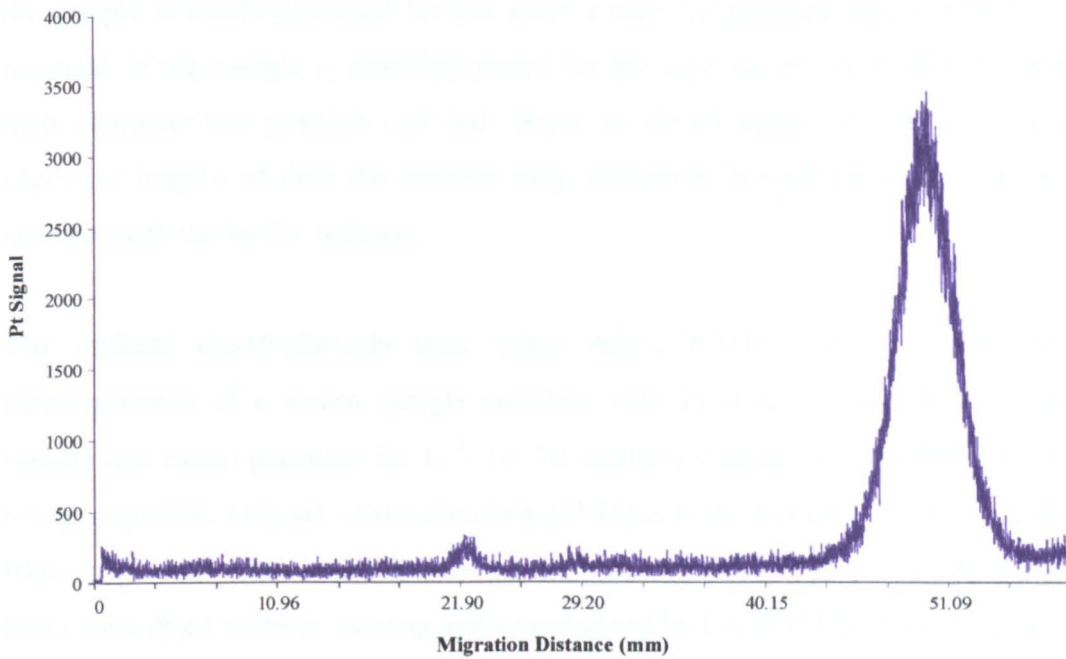


Figure 3.10:  $^{195}\text{Pt}$  Ion time responses for Pt enriched serum ( $\text{PtCl}_4$ ,  $5\ \mu\text{g/mL}$  Pt) interrogated by a) point ablation and b) line rastering

a) Point Ablation (Parameters, 20shots/site, 1.7 mJ,  $-1000\ \mu\text{m}$  defocus, )

b) Line Rastering (Parameters; 1.7 mJ,  $50\ \mu\text{m/s}$ , 20 Hz,  $260\ \mu\text{m}$  aperture)

### 3.2.3 Electrophoresis

When separating proteins, especially in the case of complex protein mixtures such as blood serum, it is essential that the appropriate conditions are used. The degree of protein separation depends on a number of parameters such as the length of time of electrophoresis, the type of electrophoresis, gel composition, the buffer system used, and the amount of protein loaded on the gel. Once optimised conditions had been identified further studies were needed to examine the possibility of cross contamination between gel lanes and also the effect, if any, of deviation from the central lane axis when interrogating gels.

#### 3.2.3.a Electrophoresis Time

The length of time of electrophoresis affects the degree of protein separation. For a given system there is an optimal electrophoresis time at which point the proteins are separated and can be characterised by their migration distance along the gel. If the sample is electrophoresed for too short a time the proteins may not be fully resolved. If the sample is electrophoresed for too long the proteins will over-run their characteristic position and will begin to merge again. If left to run for excessive lengths of time the proteins may eventually run off the end of the gel and mix with the buffer solution.

The optimal electrophoresis time using native PAGE was determined by electrophoresis of a serum sample enriched with Pt ( $\text{PtCl}_4$ , 5  $\mu\text{g/mL}$  Pt). The sample was electrophoresed for 1, 5, 10, 30, and 60 minutes, the experiment being run in duplicate. One set of the resulting gel lanes were stained using Coomassie Blue to give a visual indication of the protein migration. The remaining set of lanes were dried without staining and interrogated by LA ICP-MS monitoring  $m/z$  195 (Pt). The entire procedure was then repeated using an albumin sample (45  $\text{mg/mL}$ ) enriched with Pt ( $\text{PtCl}_4$ , 5  $\mu\text{g/mL}$  Pt).

The stained lanes containing the serum and albumin samples are shown in Figure 3.11. In each case the sample was loaded at the top of the lane and as electrophoresis progressed the proteins migrated down the lane. It can be seen that the migration distance of the proteins increased with increasing electrophoresis

time. Based on the positioning of the stained proteins it can be seen that after 1 minute of electrophoresis the sample was just entering the gel and no protein separation had occurred. From 5-30 minutes of electrophoresis the proteins in the serum migrate further into the gel and separate according to their mass/charge ratio ( $m/z$ ) resulting in the appearance of a number of bands. After 60 minutes of electrophoresis the serum was found to have over run. Such an excessive electrophoresis time caused the protein bands to migrate further but this was at the expense of protein resolution as the protein bands began to broaden and run into each other. Similar behaviour was observed with the albumin samples. The multiple bands observed in the albumin lanes correspond to albumin polymerising to form dimers and trimers etc, possibly promoted by the presence of platinum.

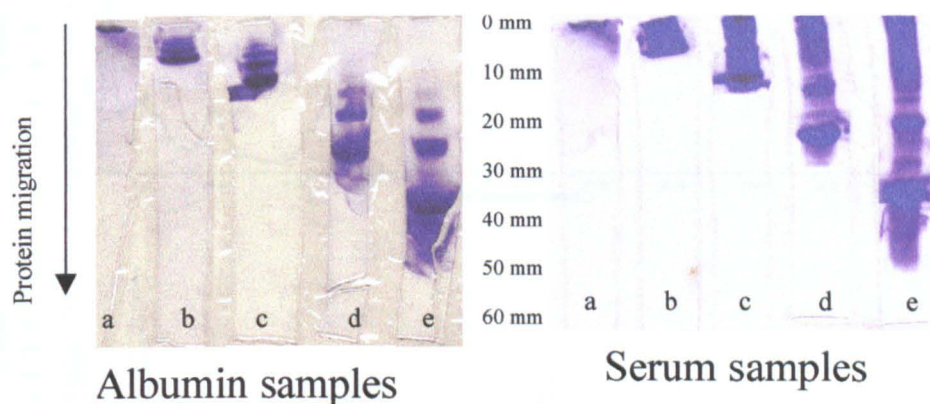


Figure 3.11: Pt enriched albumin and serum samples, ( $PtCl_4$ , 5  $\mu g/mL$  Pt). Stained after electrophoresed for a) 1 min b) 5 min c) 10 min d) 30 min e) 60 min

Figure 3.12 and Figure 3.13 show the Pt signal responses for laser ablation ICP-MS of the Pt enriched serum samples and albumin samples, respectively. It is immediately obvious that some degree of platinum-protein binding occurs in both the pure albumin samples and the serum samples. This is demonstrated by the appearance of platinum peaks along the length of the gels. The platinum peaks progress along the length of the gel as the electrophoresis time is increased in the same way the protein bands were seen to progress along the stained gel. Since charged platinum species are known to migrate with the solvent front during electrophoresis<sup>196</sup>, it is fair to assume that any platinum present on the gel following an 'adequate' electrophoresis time is, therefore, protein bound.

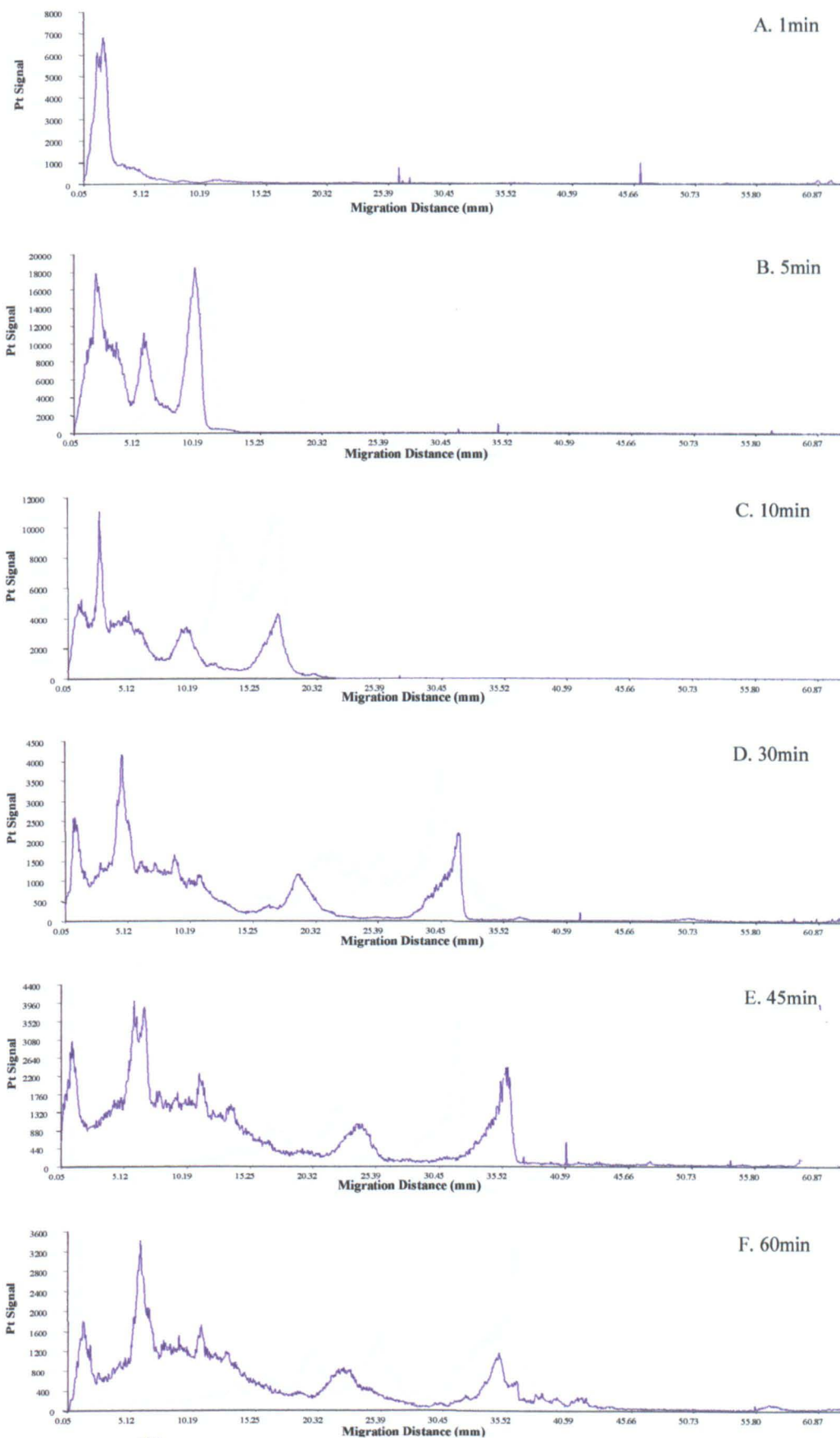


Figure 3.12:  $^{195}\text{Pt}$  profiles for Pt enriched serum samples ( $\text{PtCl}_4$ ,  $5 \mu\text{g/mL Pt}$ ) electrophoresed for a) 1 min b) 5 min c) 10 min d) 30 min e) 45 min f) 60 min

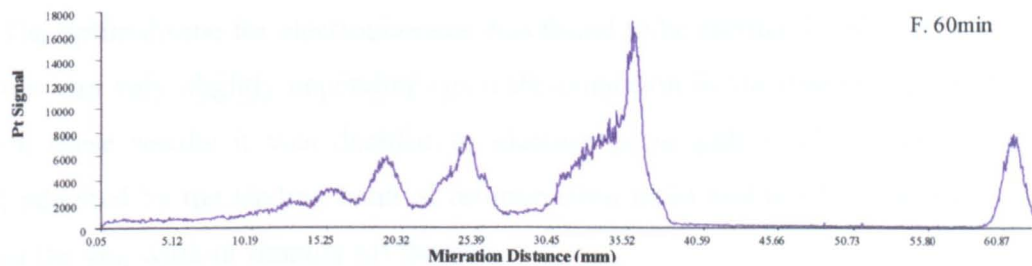
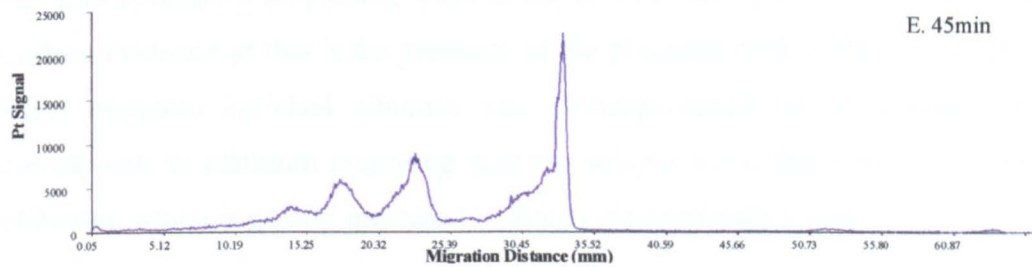
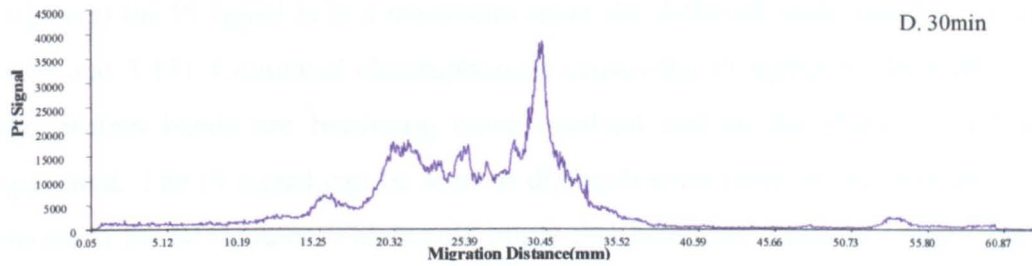
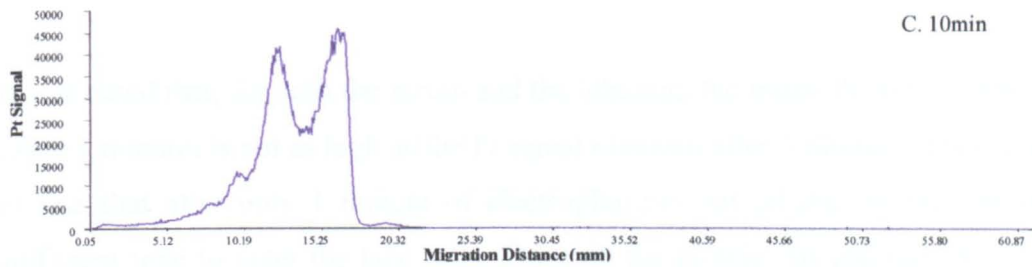
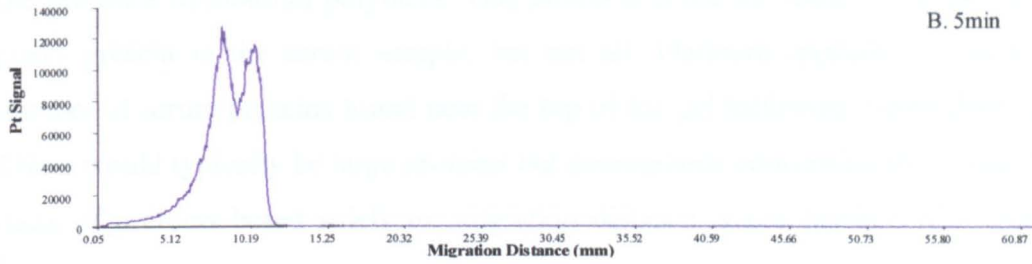
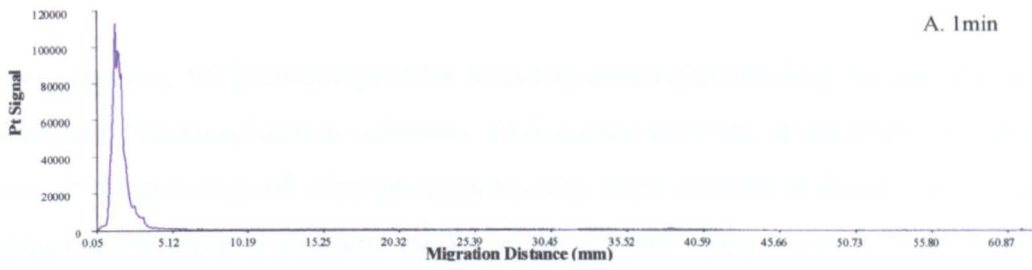


Figure 3.13:  $^{195}\text{Pt}$  profiles for Pt enriched albumin samples ( $\text{PtCl}_4$ ,  $5 \mu\text{g/mL}$  Pt) electrophoresed for a) 1 min b) 5 min c) 10 min d) 30 min e) 45 min f) 60 min



By comparing the platinum profiles from the serum and albumin samples it can be seen that platinum binds to albumin. This occurs not only in the pure protein but also in the presence of other proteins such as those present in human serum. The presence of multiple platinum peaks in the albumin sample can be explained by the presence of albumin polymers. This would account for some of the platinum peaks present in the serum sample, but not all. Platinum appears to bind to a number of serum proteins found near the top of the gel following electrophoresis. These would typically be large proteins but assumptions concerning the molecular mass of proteins based solely on migration distance is not feasible with native PAGE.

It was noted that, for both the serum and the albumin, the initial Pt signal intensity (after 1 minute) is not as high as the Pt signal obtained after 5 minutes. This is due to fact that after only 1 minute of electrophoresis not all the sample has had sufficient time to enter the lane fully. Once all the protein has entered the gel (5 minutes) the Pt signal is at a maximum (note the different scales used in Figures 3.12 and 3.13). Continued electrophoresis causes the Pt signal to diminish since the protein bands are becoming more resolved and so the platinum is being speciated. The Pt signal can be seen to diminish even more as electrophoresis is maintain for 60 minutes. This would imply that extensive electrophoresis, despite the mild conditions employed, leads to the loss of some protein bound platinum. Further evidence of this is the presence of the platinum peak at the end of the gel when platinum enriched albumin was electrophoresed for 60 minutes. This corresponds to platinum migrating with the solvent front, that is to say unbound platinum, which is greatly increased in longer electrophoresis runs.

The optimal time for electrophoresis was found to be around 45 minutes, although this can vary slightly depending upon the condition of the running buffer. Based on these results it was decided to electrophorese gels until the solvent front (indicated by the leading band of bromophenol blue) had reached the lower edge of the gel, without running off the end.

### 3.2.3.b Protein Loading

The amount of protein a gel can tolerate and successfully separate is limited by the gel dimensions. The Mini-Protean electrophoresis system accommodates gels 10 cm x 8 cm x 1 mm (thick) in size. The gels have 10 sample wells, each well being 5 mm wide. Using these gels a range of protein concentrations were electrophoresed to determine the optimal protein loading. Continuous gels were used, made up solely of resolving gel. Discontinuous gels also contain a stacking gel, which acts to focus the samples. The absence of a stacking gel in the continuous system means care must be taken when loading samples. The loaded sample should be in the form of as narrow a plug as is possible to maximise protein resolution. The mini gel wells will hold a sample volume of up to 30  $\mu\text{L}$ , but sample volumes of only 5  $\mu\text{L}$  were loaded to keep the sample band narrow. Smaller volumes were avoided due to the difficulty of accurate pipetting. Serum samples (5  $\mu\text{L}$ , ~70 mg protein /mL), enriched with Pt ( $\text{PtCl}_4$ , 5  $\mu\text{g}/\text{mL}$  Pt), were loaded at the following concentrations; neat, x2 dilution, x5 dilution, x10 dilution, and x20 dilution. After electrophoresis the lanes were stained. The process was then repeated with albumin samples (5  $\mu\text{L}$ , 45 mg albumin /mL) enriched with Pt ( $\text{PtCl}_4$ , 5  $\mu\text{g}/\text{mL}$  Pt).

The stained samples, shown in Figure 3.14, highlight the effect protein concentration has on protein resolution. Since the metals of interest are at very low levels in real serum samples, especially after speciation, it was necessary to maximise sensitivity. This was achieved by loading the highest protein concentration possible without disrupting protein resolution. Low protein concentrations were seen to result in better protein resolution, but this was at the expense of metal ion concentration and so a compromise protein concentration was needed. By comparing the stained lanes it can be seen that as the amount of protein loaded per lane was increased the protein bands became broader. It was decided that x2 dilution of serum was a practically realistic protein loading as it gave a high metal ion concentration without losing too much protein resolution. Loading neat serum is not advisable as this overloads the gel and causes albumin to smear across the gel (the sample is no longer contained within lane width).

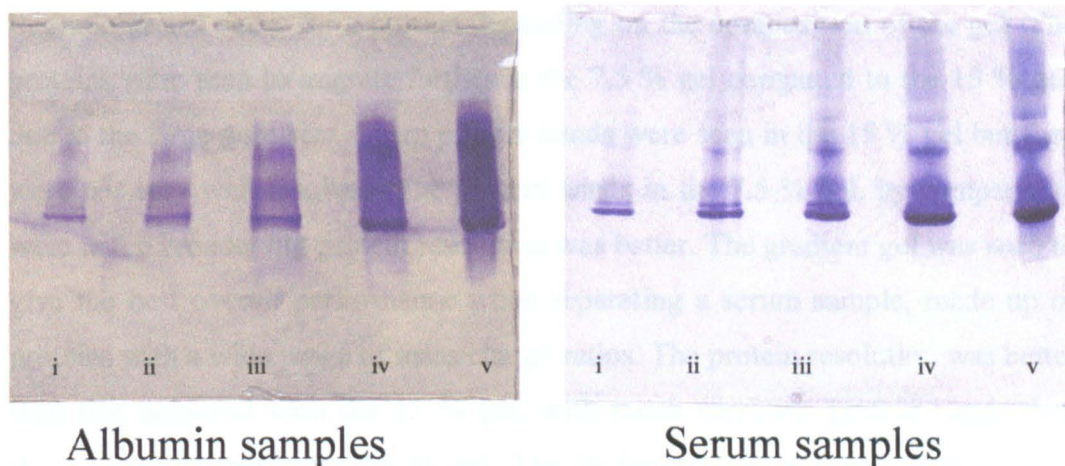


Figure 3.14: Pt enriched albumin and serum samples ( $PtCl_4$ ,  $5 \mu\text{g/mL Pt}$ ) loaded at i, x20 dilution ii, x10 dilution iii, x5 dilution iv, x2 dilution v, neat

### 3.2.3.c Gel Composition

The composition of the gel used in electrophoresis has a large impact upon the degree of protein resolution achieved. Choice of gel composition depends upon the proteins of interest. A low T % gel, with a relatively large pore size, might be well suited to separation of high molecular mass protein mixtures, whilst a high T % gel, with a relatively small pore size, might be more suited to separating low molecular mass mixtures. However, no single T % gel is ideal for the complex mixture of proteins found in serum. Gels are available which have a linear T % gradient increasing along the length of the gel. The gradually decreasing pore size of gradient gels has a sieving effect upon the proteins, thereby increasing resolution in some instances. Three different gels were compared to determine the best gel composition for separating the proteins found in serum. Four different protein samples at physiological concentrations, enriched with Pt ( $PtCl_4$ ,  $5 \mu\text{g/mL Pt}$ ), were run on each gel to show the effect of gel composition on protein migration. The samples run were albumin (relative molecular mass (RMM)  $\sim 69$  kDa), transferrin (RMM  $\sim 75$  kDa),  $\alpha$ -2-macroglobulin (RMM  $\sim 820$  kDa) and serum. All samples were run in duplicate, one set was stained and the other analysed by LA ICP-MS.

From the stained samples, shown in Figure 3.15, it is evident that different migration rates occur for a protein depending on the composition of the gel. The proteins were seen to migrate further in the 7.5 % gel compared to the 15 % gel, due to the large pore size. Sharp protein bands were seen in the 15 % gel but they were not very well resolved. The protein bands in the 7.5 % gel, by comparison, were much broader but protein resolution was better. The gradient gel was seen to give the best overall performance when separating a serum sample, made up of proteins with a wide range of mass/charge ratios. The protein resolution was better than that achieved with the 15 % gel, with much narrower protein bands than those achieved using the 7.5 % gel. The Pt ion responses achieved from laser interrogation of the corresponding protein samples are shown in Figures 3.16-3.19. The platinum profiles also show gradient gels to be the gels most suited to separation of the complex mixture of proteins found in serum.

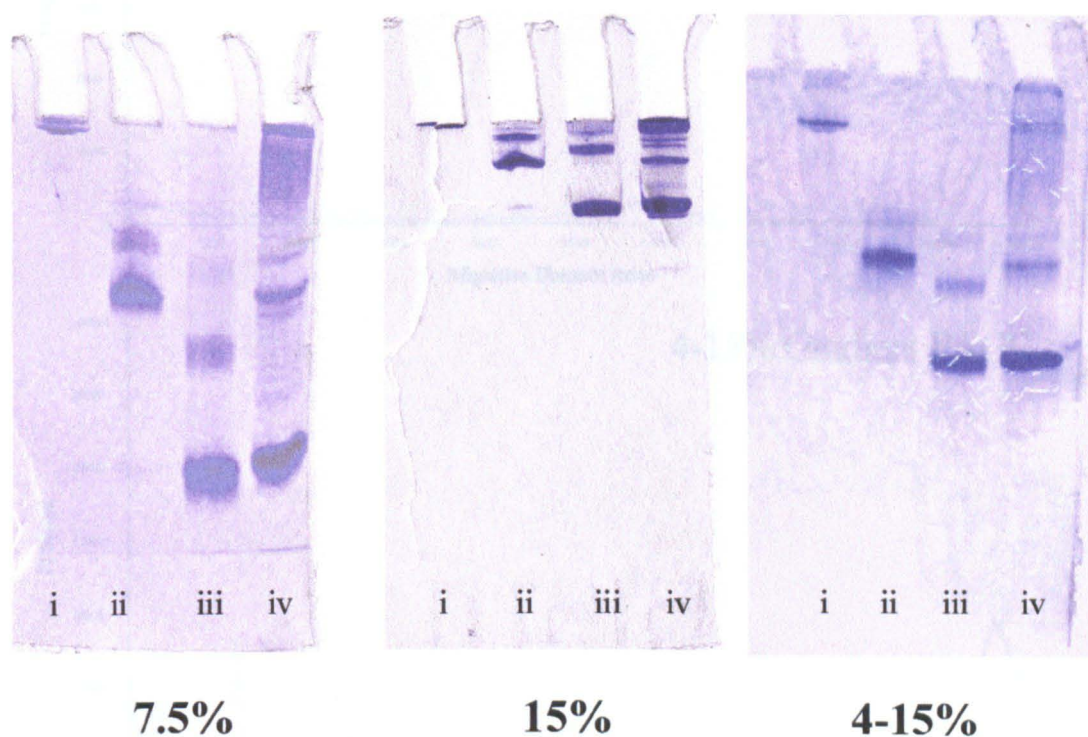


Figure 3.15: Pt enriched protein samples ( $PtCl_4$ , 5  $\mu g/mL$  Pt) run on 7.5 %, 15 % and 4-15 % gels.

Protein samples; i,  $\alpha_2$ -macroglobulin ii, transferrin iii, albumin iv, serum

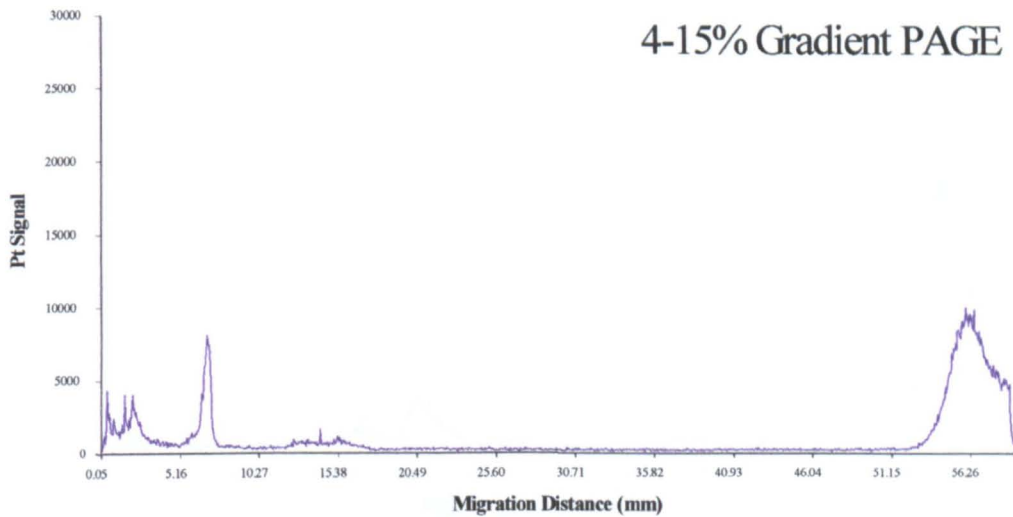
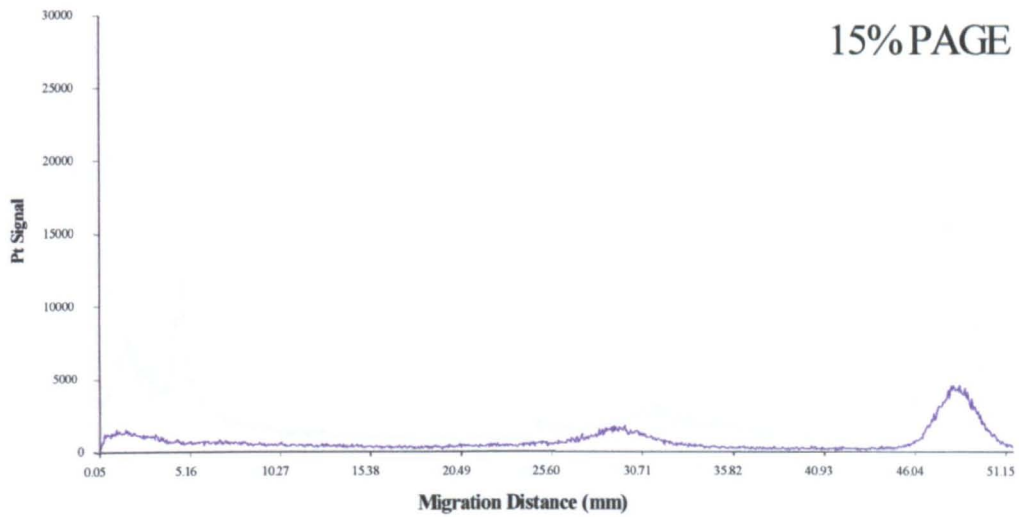
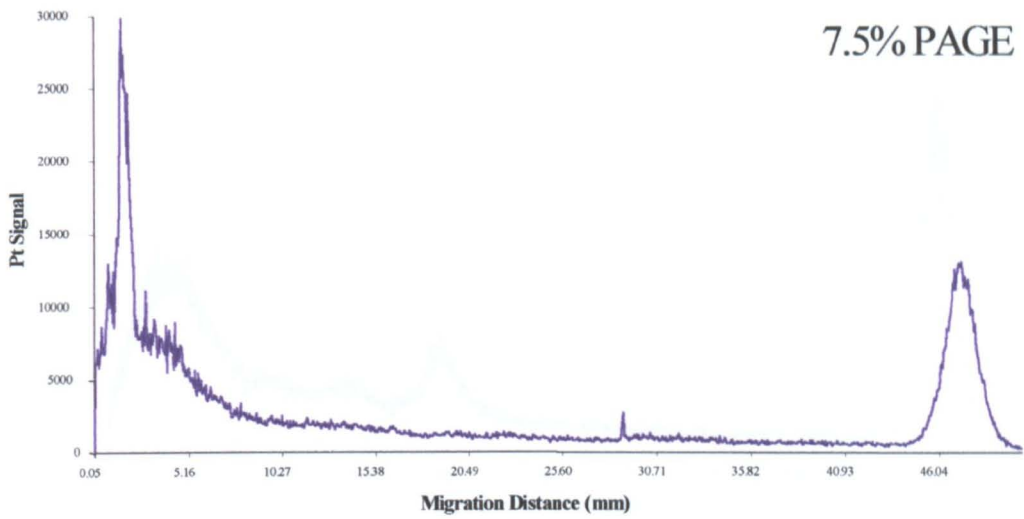


Figure 3.16:  $^{195}\text{Pt}$  profiles for Pt enriched  $\alpha_2$ -macroglobulin ( $\text{PtCl}_4$ , 5  $\mu\text{g/mL}$  Pt) electrophoresed on 7.5 %, 15 % and 4-15 % gels.

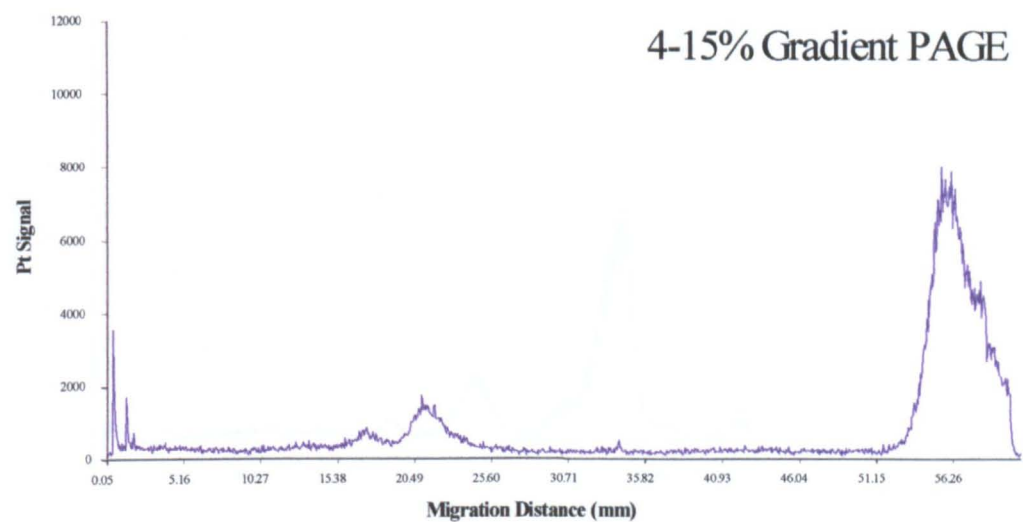
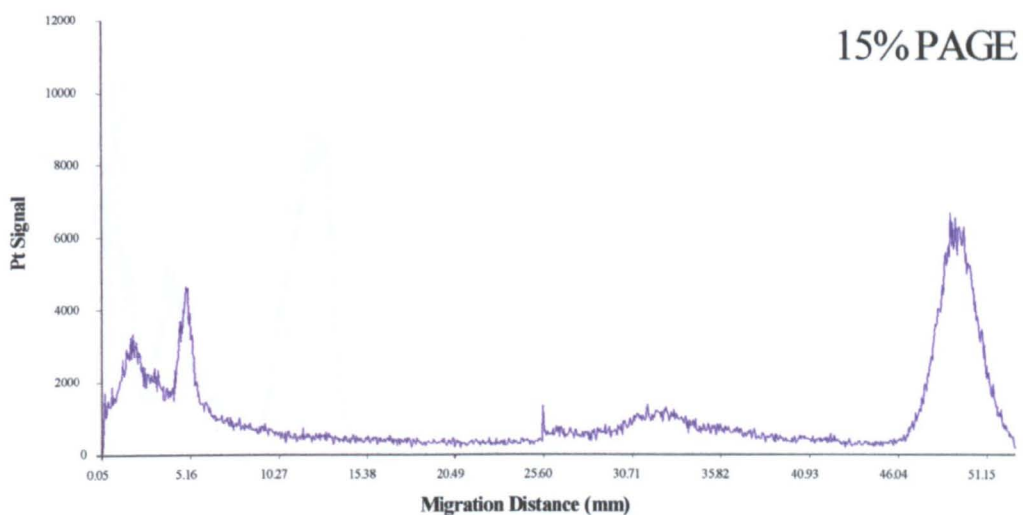
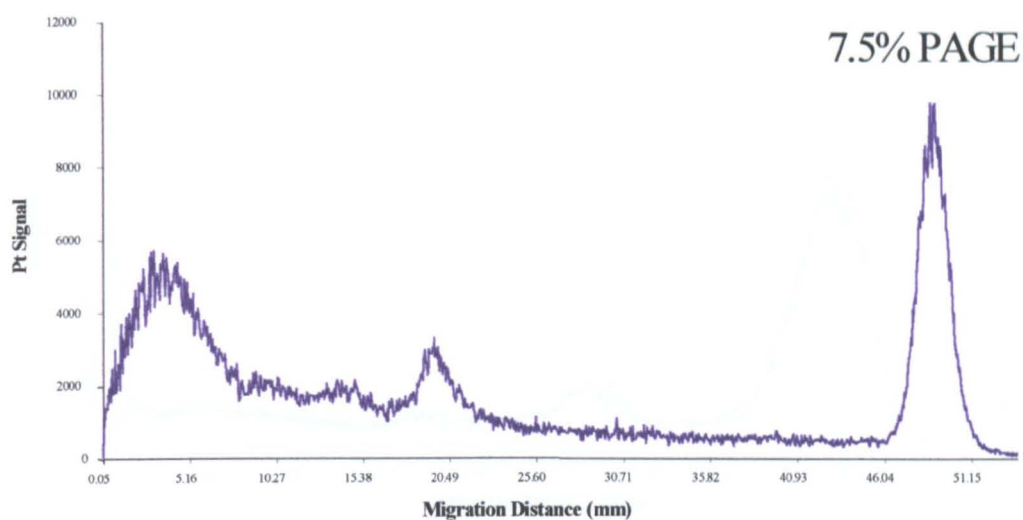


Figure 3.17:  $^{195}\text{Pt}$  profiles for Pt enriched transferrin ( $\text{PtCl}_4$ ,  $5 \mu\text{g/mL Pt}$ ) electrophoresed on 7.5 %, 15 % and 4-15 % gels.

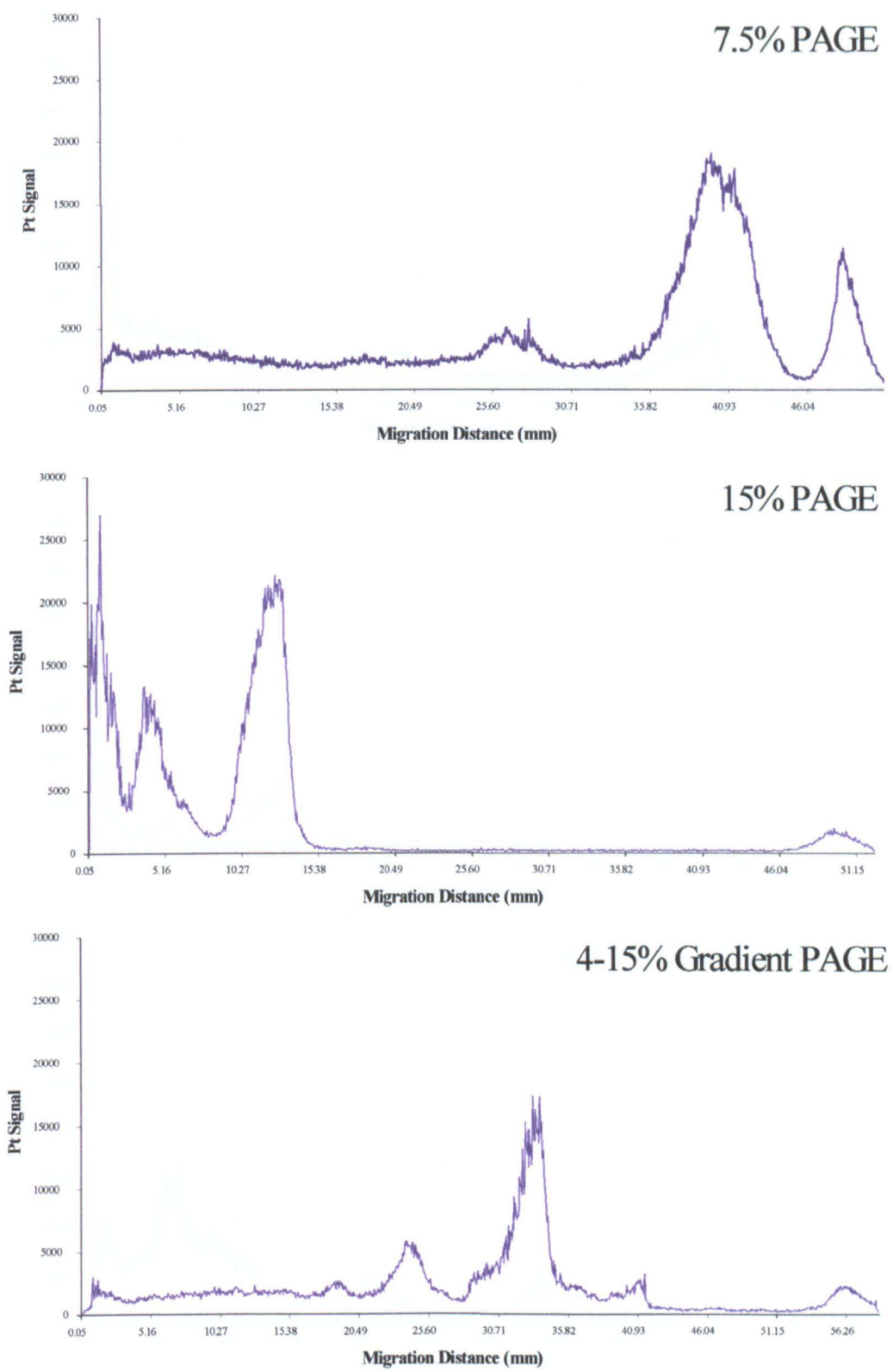


Figure 3.18:  $^{195}\text{Pt}$  profiles for Pt enriched albumin ( $\text{PtCl}_4$ ,  $5 \mu\text{g/mL Pt}$ ) electrophoresed on 7.5 %, 15 % and 4-15 % gels.

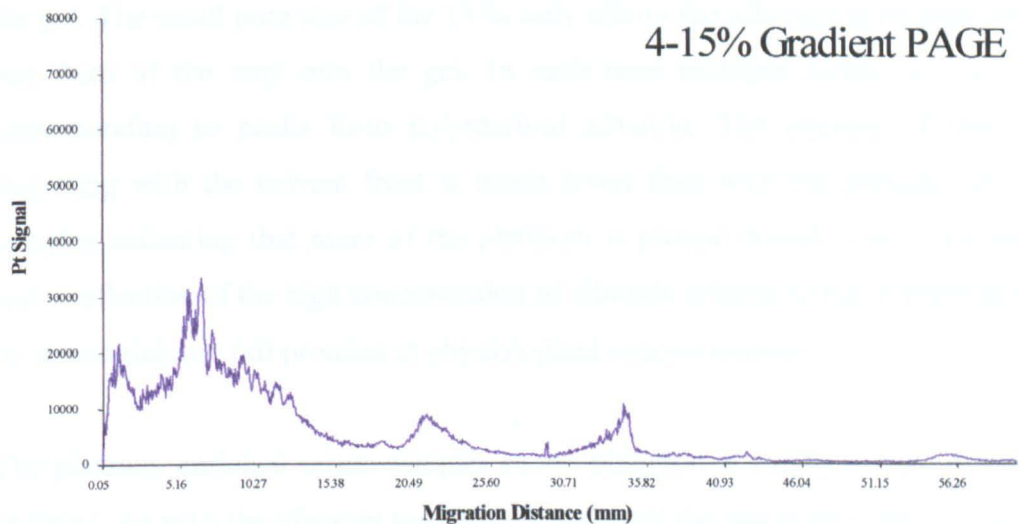
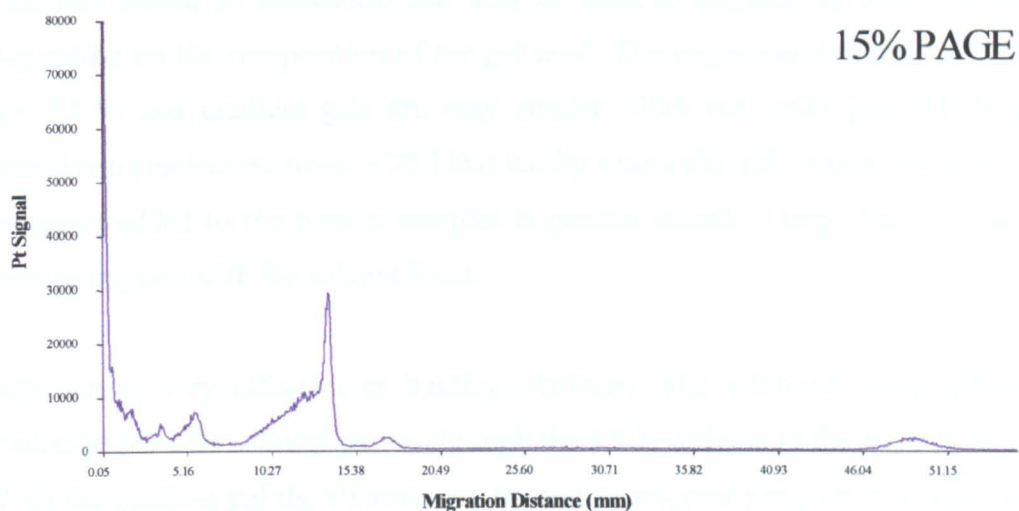
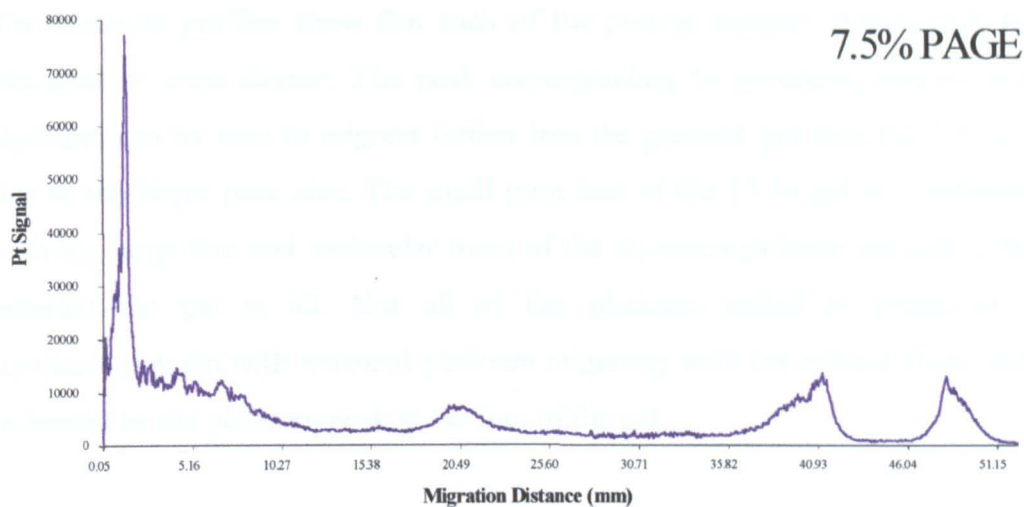


Figure 3.19:  $^{195}\text{Pt}$  profiles for Pt enriched serum ( $\text{PtCl}_4$ , 5  $\mu\text{g/mL}$  Pt) electrophoresed on 7.5 %, 15 % and 4-15 % gels.



The platinum profiles show that each of the protein samples studied will bind platinum to some degree. The peak corresponding to  $\alpha_2$ -macroglobulin bound platinum can be seen to migrate further into the gradient gel than the 7.5 % gel due to the larger pore size. The small pore size of the 15 % gel in combination with the large size and molecular mass of the  $\alpha_2$ -macroglobulin prevent it from entering the gel at all. Not all of the platinum added is bound to the  $\alpha_2$ -macroglobulin with unbound platinum migrating with the solvent front, this is indicated by the platinum peak at the foot of the gel.

Platinum bound to transferrin can also be seen to migrate different distances depending on the composition of the gel used. The migration distances observed for 7.5 % and gradient gels are very similar. With the small pore 15 % gel, transferrin (molecular mass ~ 75 kDa) hardly enters the gel. Again not all of the platinum added to the protein samples is protein bound, a large fraction can be seen to migrate with the solvent front.

Albumin is very effective at binding platinum. The relatively small albumin molecule (69 kDa) almost passes through the 7.5 % gel due to the large pore size. With the gradient gel the albumin can be seen to migrate just over half way along the gel. The small pore size of the 15 % only allows the albumin to migrate about one third of the way into the gel. In each case multiple bands can be seen corresponding to peaks from polymerised albumin. The amount of platinum migrating with the solvent front is much lower than with the previous protein samples indicating that more of the platinum is protein bound. This is probably just a reflection of the high concentration of albumin relative to the transferrin and  $\alpha_2$ -macroglobulin (all proteins at physiological concentrations).

The platinum enriched serum samples shows platinum bound to a range of serum proteins. As with the albumin samples, virtually all the platinum is protein bound (very little platinum migrating with solvent front). The gradient gel gives the best protein distribution, covering about three-quarters of the gel. The 7.5 % gel covers the whole gel but as a result is less sensitive whilst the 15 % gel only uses the first third of the gel and so protein resolution is poor.

### 3.2.3.d Nature of Electrophoresis

The type of electrophoresis system employed to run gels can have a huge impact on the results obtained. Using the Mini-Protean system (Bio-Rad) it is possible to run vertical gels under native, denaturing and IEF conditions. Alternative commercial flatbed systems are available where the gels are held horizontally. Native electrophoresis separates proteins according to a combination of protein size and charge. Reasonable protein resolution may be achieved using native PAGE but protein identification can be difficult. With denaturing electrophoresis, using SDS, protein resolution is improved and protein identification is simplified due to the direct relationship between the migration rate and the molecular mass of the protein. IEF electrophoresis separates proteins according to their isoelectric point. IEF can, therefore, be useful in resolving proteins of similar molecular mass and is often combined with SDS electrophoresis to give 2D electrophoresis.

To show the effect of various electrophoresis styles on protein resolution a number of pure proteins, albumin, transferrin and  $\alpha_2$ -macroglobulin, were run along with serum under both native and denaturing conditions. In each instance 4-15 % gradient gels were used. After electrophoresis the gels were stained, see Figure 3.20. By comparison of the protein distributions achieved using the two systems it is apparent that the SDS system produces narrower protein bands than those achieved using native PAGE. There were significantly more discrete protein bands with the stained SDS gel than with the equivalent sample run under native conditions, an indication of the better resolving power of SDS electrophoresis.

Closer examination of the stained gels shows a difference in migration rates for proteins under the two systems. Using native PAGE, transferrin and albumin have very different migration rates, with albumin travelling much farther into the gel. Under denaturing conditions albumin and transferrin migrate at similar rates due to their similar molecular masses. Albumin is the most abundant protein in human serum, and transferrin is known to bind to a variety of metals so resolution of these two proteins in particular is essential when studying metal speciation in human serum. As a result native PAGE is more suited to this purpose than SDS PAGE.

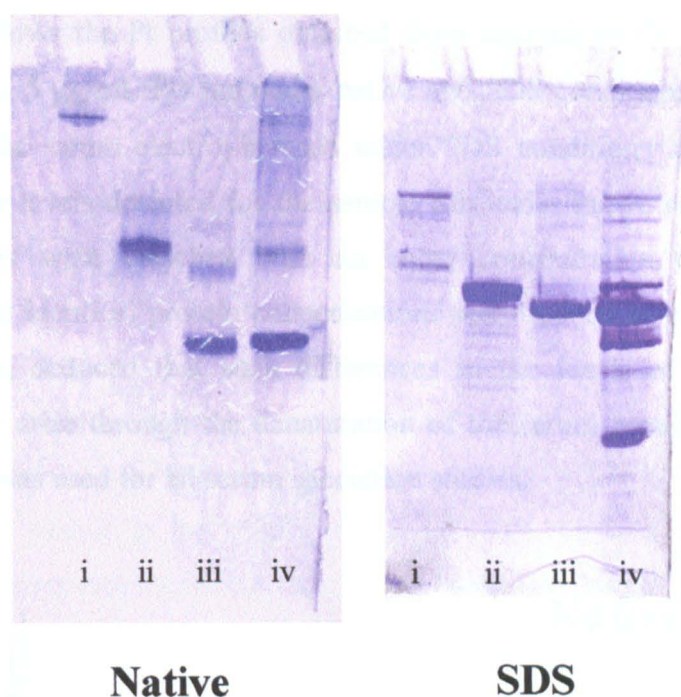


*Figure 3.20: Protein samples electrophoresed by native and SDS PAGE*  
*i,  $\alpha_2$ -macroglobulin ii, transferrin iii, albumin iv, serum*

Under native conditions  $\alpha_2$ -macroglobulin (molecular mass  $\sim 820$  kDa, 4 sub-units) gives a single band. The large size of  $\alpha_2$ -macroglobulin, along with the sieving effect of the gradient gel, means the protein band only migrates a little way into the gel. When run under denaturing conditions  $\alpha_2$ -macroglobulin gives a number of bands that migrate further into the gel than is the case with native PAGE. A possible explanation for this behaviour is the breaking of sulphhydryl bonds during the denaturation of the protein, which could result in separation of the  $\alpha_2$ -macroglobulin sub-units.

Despite the superior resolution of SDS it was decided that native conditions should be used to help maintain protein-metal bonds existing within the serum. SDS acts by binding to the proteins and opening out the protein structure. The effect of this on an existing metal-protein bond is not known. Two detrimental possibilities exist; the opening out of the protein can expose binding sites previously hidden to the metals. This could result in the occurrence of metal-protein binding not present under native conditions. Alternatively the SDS may bind to the proteins at the expense of existing metal-protein bonds.

Figure 3.21 shows the Pt profiles obtained from analysis of Pt enriched serum samples ( $\text{PtCl}_4$ , 5  $\mu\text{g}/\text{mL}$  Pt) run under native and SDS conditions. The Pt levels detected for the serum electrophoresed under SDS conditions are significantly lower than the levels detected for the sample run under native conditions. Both serum samples were enriched with an equal concentration of Pt prior to separation, and identical protein concentrations were loaded in each instance. It was, therefore, deduced that such differences in the levels of protein bound platinum must arise through the denaturation of the serum proteins. As a result native PAGE was used for all serum speciation studies.

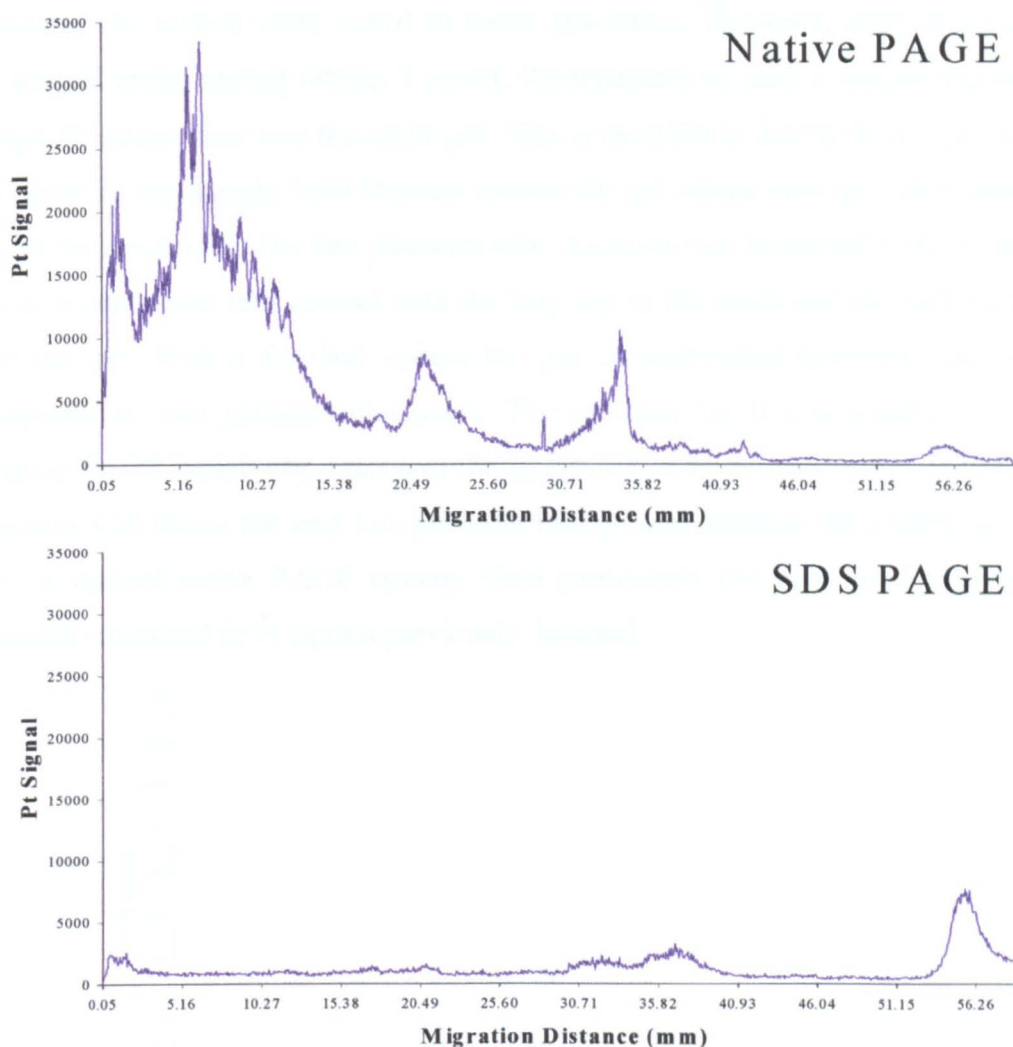


Figure 3.21:  $^{195}\text{Pt}$  profiles for Pt enriched serum ( $\text{PtCl}_4$ , 5  $\mu\text{g}/\text{mL}$  Pt) electrophoresed under native and denaturing conditions.

IEF involves the setting up of a pH gradient. When performing IEF separations on the Mini Protean system the sample is loaded at the top of the gel. As a result, if the pH range is 3-10, proteins may be exposed to pH levels up to 7 pH units away from their isoelectric point. Exposure to such extreme pH levels is highly likely to disrupt the metal-protein bonds of interest. Metal speciation studies were not, therefore, carried out by IEF separation on the Mini-Protean system.

An alternative system for carrying out IEF separation is the flat bed system produced by Pharmacia. Exposure of proteins to extreme pH levels can be avoided by loading the sample in the centre of the gel (~pH 6.5 in a 3-10 pH range) making the system more suited to metal speciation. However, analysis of a Pt enriched serum sample ( $\text{PtCl}_4$ , 5  $\mu\text{g}/\text{mL}$  Pt) separated on such a system showed a high Pt background over the entire gel. This is most likely due to the design of the system. In the upright Mini-Protean system the gel comes into very little contact with the electrodes. The thin platinum wire electrodes are immersed in the buffers, which only come into contact with the very top of the wells and the very bottom of the gel. With a flat bed system the gel is sandwiched between, and so is exposed to, two platinum electrodes. The run time for IEF is greater than for native PAGE which also increases the likelihood of Pt contamination of the gel. Figure 3.22 shows the very low platinum background obtained for a blank gel run on a vertical native PAGE system. Note particularly the very low background counts compared to Pt signals previously detected.

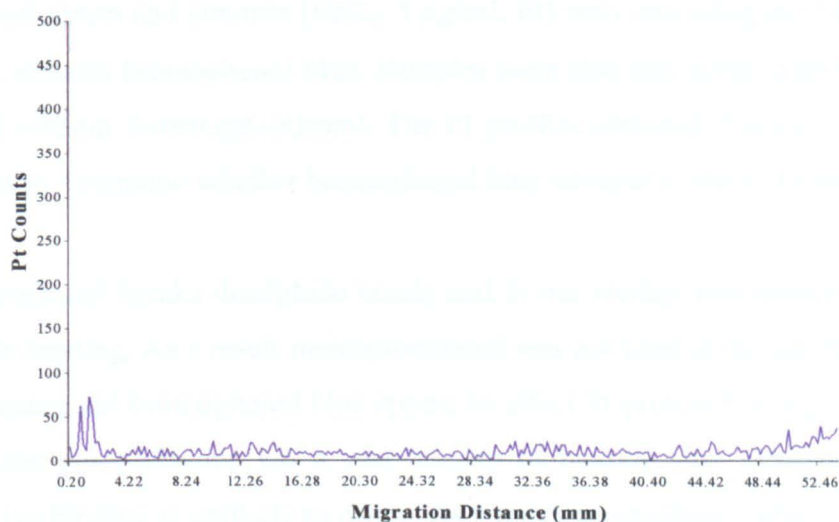
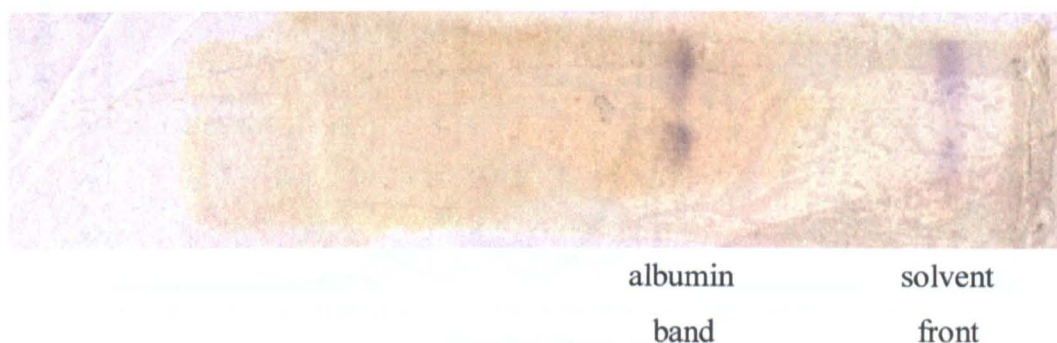


Figure 3.22:  $^{195}\text{Pt}$  profile of blank gel lane from vertical 1-D native PAGE

### 3.2.3.e Buffer System

The sample buffer commonly used in native PAGE contains glycerol to make the sample more dense than the running buffer, thus causing the sample to sink in the sample well. It also contains the tracking dye bromophenol blue, which travels with the solvent front and so can be used to monitor the progression of electrophoresis. In some instances 2-mercaptoethanol is added to break disulphide bonds. When performing native PAGE the bromophenol blue of the tracking dye was seen to migrate with the albumin band as well as the solvent front, as shown in Figure 3.23.



*Figure 3.23: Un-stained gel showing bromophenol blue bound to albumin band*

This would indicate that some degree of albumin-bromophenol blue binding is occurring. To determine the effect of bromophenol blue on metal-protein binding, Pt enriched serum and albumin (PtCl<sub>4</sub>, 5 µg/mL Pt) were run using sample buffers with and without bromophenol blue. Samples were also run using sample buffers with and without 2-mercaptoethanol. The Pt profiles obtained, Figure 3.24, were compared to determine whether bromophenol blue adversely affects Pt binding.

Meraptoethanol breaks disulphide bonds and in our studies was shown to affect Pt-protein binding. As a result meraptoethanol was not used in the sample buffer. In no instance did bromophenol blue appear to affect Pt-protein binding. This is to be expected since albumin has a vast number of binding sites available and so competitive binding is unlikely to occur. As a result bromophenol blue was added to the sample buffer for all further studies.

Not only does bromophenol blue help to indicate the end point of electrophoresis, but the fact that it travels with the albumin band means that  $^{89}\text{Br}$  can be monitored using ICP-MS to help locate the albumin peak. This is more reliable than comparing profiles with stained gels as the dimensions of the gels tend to alter as a result of the staining process where the gel is first dehydrated then rehydrated prior to drying.

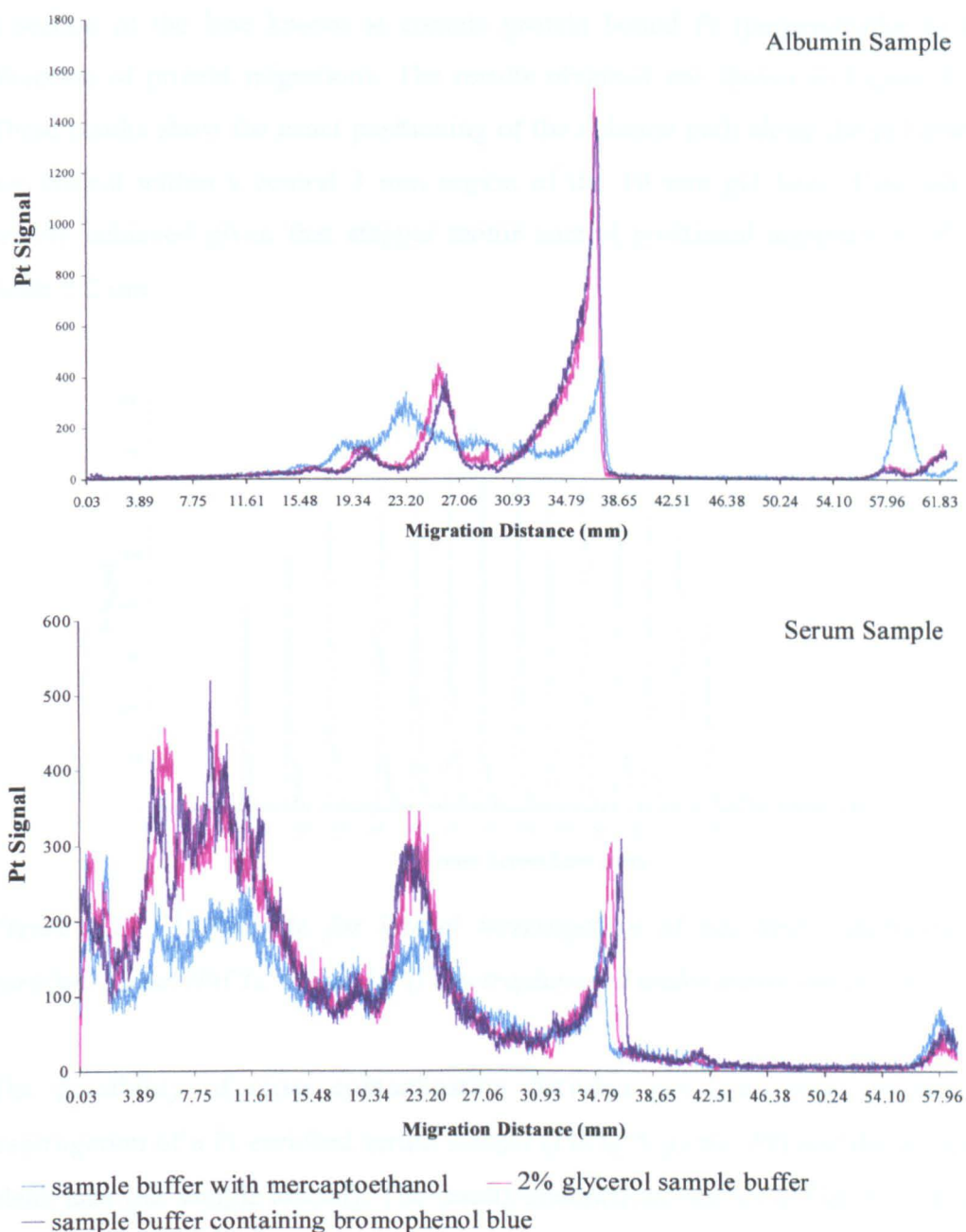


Figure 3.24:  $^{195}\text{Pt}$  profiles for Pt enriched albumin and serum ( $\text{PtCl}_4$ , 5  $\mu\text{g/mL}$  Pt) electrophoresed using various sample buffers.

### 3.2.3.f Additional Studies

After determining the optimal conditions a few additional studies were necessary to check the validity of the technique for metal speciation in biological samples. First the effect of the laser interrogation position within the gel lane upon signal intensity was examined. To perform this experiment a serum sample enriched with Pt ( $\text{PtCl}_4$ ,  $5 \mu\text{g/mL Pt}$ ), was interrogated in a lateral manner, shot-wise across a section of the lane known to contain protein bound Pt (perpendicular to the direction of protein migration). The results obtained are shown in Figure 3.25. These results show the exact positioning of the ablation path along the gel lane is not critical within a central 3 mm region of the 10 mm gel lane. This can be readily achieved given that stepper motor control positional accuracy is of the order  $\pm 2 \mu\text{m}$ .

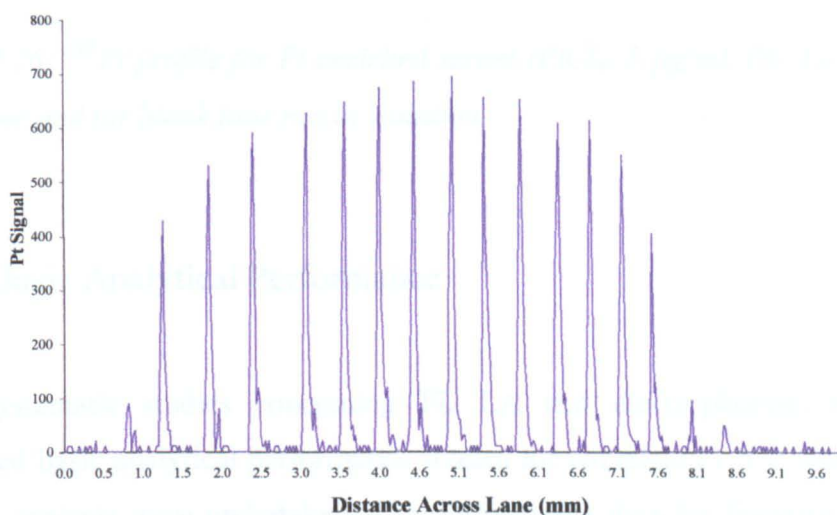


Figure 3.25:  $^{195}\text{Pt}$  profile for lateral interrogation of gel lane containing Pt enriched serum ( $\text{PtCl}_4$ ,  $5 \mu\text{g/mL Pt}$ ) electrophoresed under native conditions.

The possibility of cross contamination between gel lanes was studied by interrogation of a Pt enriched serum sample ( $\text{PtCl}_4$ ,  $5 \mu\text{g/mL Pt}$ ) and the adjacent blank lane (no sample loaded). The results obtained are shown in Figure 3.26. By comparison with the background platinum profile it can be seen that cross contamination between lanes is insignificant when Pt enriched serum is loaded at 2 x dilution,  $5 \mu\text{L/lane}$ .



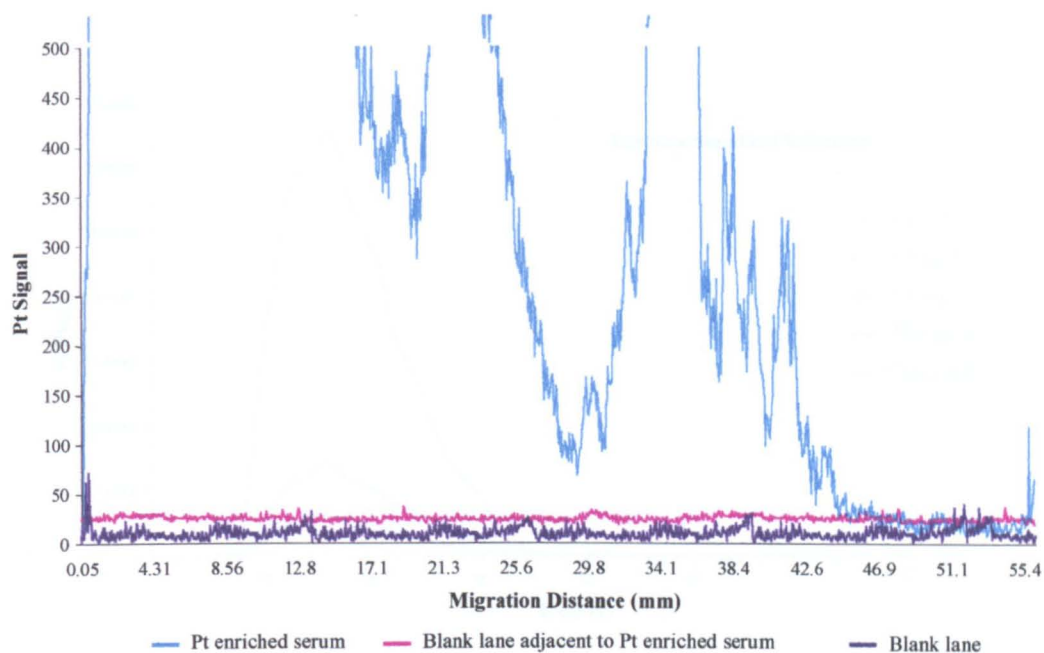


Figure 3.26:  $^{195}\text{Pt}$  profile for Pt enriched serum ( $\text{PtCl}_4$ ,  $5 \mu\text{g/mL Pt}$ ), for adjacent blank lane and for blank lane run in isolation.

### 3.2.4 Basic Analytical Performance

Once systematic studies concerning FI, LA and electrophoresis had been performed basic analytical performance studies for complete FI ICP-MS and LA-ICP-MS analysis were undertaken. The performance data for linearity of signal response, limit of detection, measurement precision and accuracy are reported.

#### 3.2.4.a Flow Injection ICP-MS

##### I. Concentration Dependence

The relationship between signal response with analyte concentration was determined by injecting 0.1 mL injections of aqueous Pt standard solutions at the 0, 10, 50, 100 and 500  $\mu\text{g/L}$  levels (including Rh as an internal standard (IS) at 20  $\mu\text{g/L}$ ). Serum samples enriched with the same Pt concentrations were also injected and analysed by FI ICP-MS. The transient  $^{195}\text{Pt}$  signals are shown in Figure 3.27.

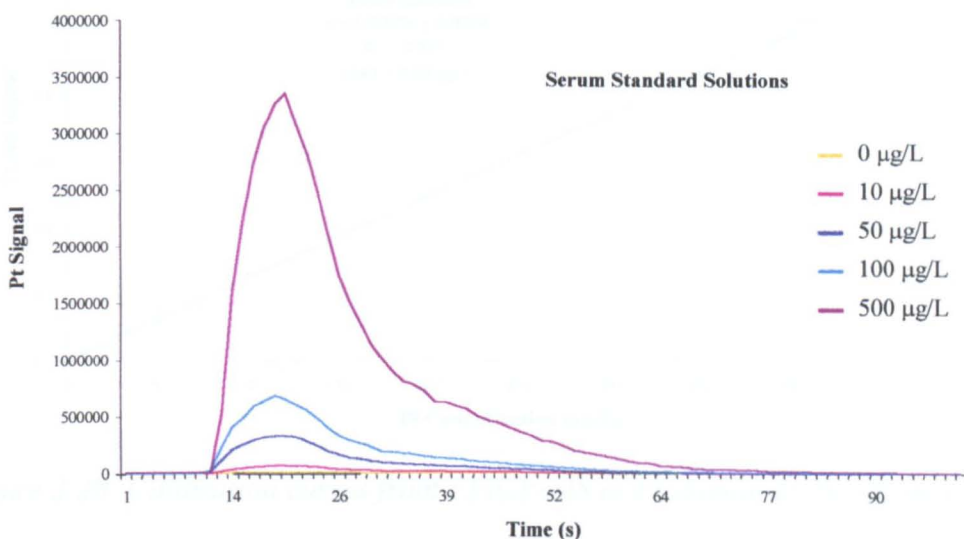
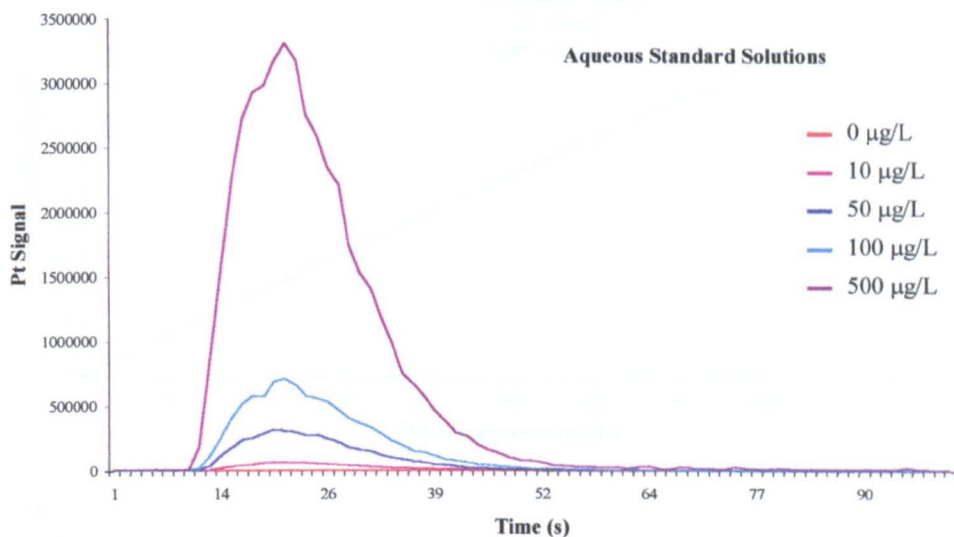


Figure 3.27:  $^{195}\text{Pt}$  time response profiles for various Pt standards (0.1 mL injection volume)

The resulting peak areas were integrated and normalised using the IS, the results were plotted against Pt concentration. The linearity of the line is indicated by the  $R^2$  value, the closer the value is to 1 the better the linearity of the systems concentration response. Figure 3.28 shows that the calibration curves obtained both exhibit good linearity,  $R^2 = 0.998$  and  $R^2 = 0.997$ .

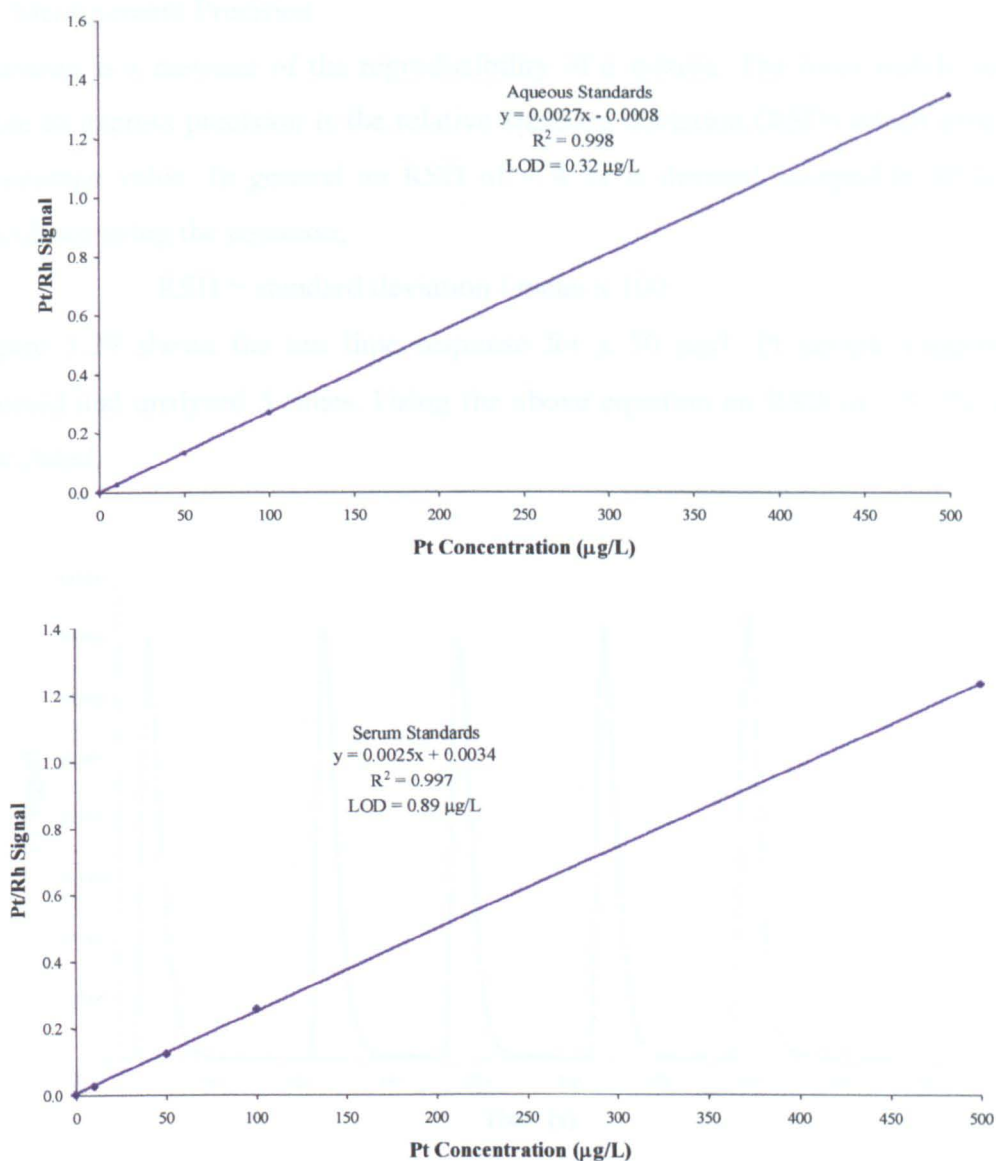


Figure 3.28: Calibration curves from FI ICP-MS of Pt standards (0-500 µg/L)

## II. Limit of Detection

The sensitivity of the technique is generally described using the parameter limit of detection (LOD). The LOD is the lowest analyte concentration above which the analyte content may be reliably quantified. The lower the LOD of a system the more sensitive the system is. A number of different mathematical definitions are in use. However, the most common definition, and the one we shall use here, is the concentration of 3 times the standard deviation ( $3\sigma$ ) of the blank measurements. This definition gave values of 0.32 µg/L and 0.89 µg/L for aqueous standards and serum standards, respectively.

### III. Measurement Precision

Precision is a measure of the reproducibility of a system. The most widely used value to express precision is the relative standard deviation (RSD) which gives a percentage value. In general an RSD of < 4 % is deemed acceptable. RSD is calculated using the equation;

$$\text{RSD} = \text{standard deviation} / \text{mean} \times 100$$

Figure 3.29 shows the ion time response for a 50 µg/L Pt sample (aqueous) injected and analysed 5 times. Using the above equation an RSD of 1.31 % was calculated.

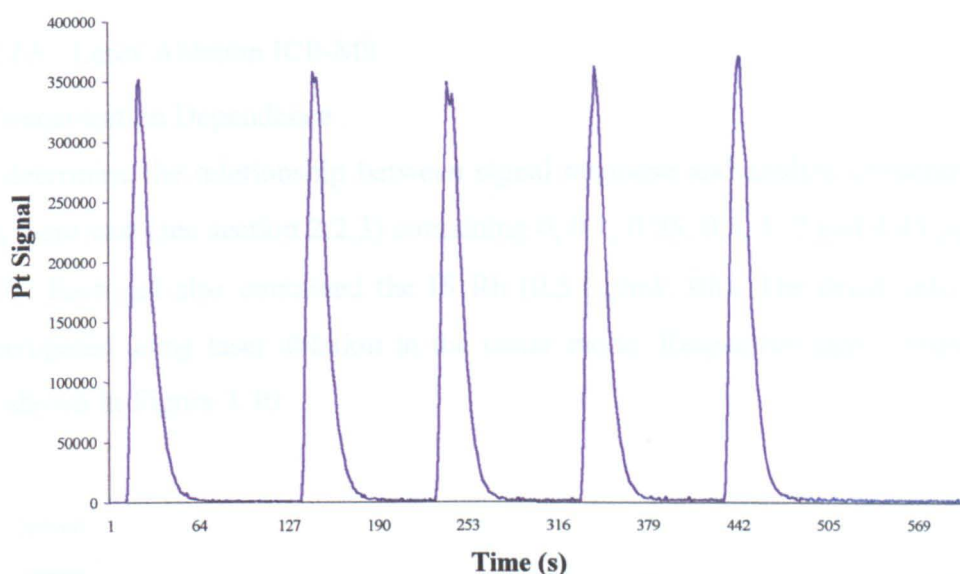


Figure 3.29: Time response profile for injection of 50 µg/L Pt standard solutions

### IV. Accuracy

Accuracy describes the closeness of the result obtained to the true value. The accuracy of the system was obtained by determining the % recovery of spiked samples. Six enriched samples (50 µg/L Pt) were injected and analysed using FI ICP-MS. Percentage recovery was calculated using the following equation;

$$\% \text{ Recovery} = (\text{Concn}_{\text{spiked sample}} - \text{Concn}_{\text{blank}}) / \text{Concn}_{\text{enriched}} \times 100$$

Table 3.2 shows the percentage recoveries obtained. The average recovery is  $101.57 \pm 1.25 \%$ , showing a slight positive bias to the system.

Sample	% Recovery
1	99.19
2	101.41
3	101.90
4	102.10
5	101.99
6	102.81

Table 3.2: Percentage recoveries for 50 µg/L Pt spiked samples

### 3.2.4.b Laser Ablation ICP-MS

#### I. Concentration Dependence

To determine the relationship between signal response and analyte concentration gels were cast (see section 2.2.3) containing 0, 0.1, 0.25, 0.5, 1, 2 and 4.45 µg/mL of Pt. Each gel also contained the IS Rh (0.5 µg/mL Rh). The dried gels were interrogated using laser ablation in the raster mode. Respective signal responses are shown in Figure 3.30

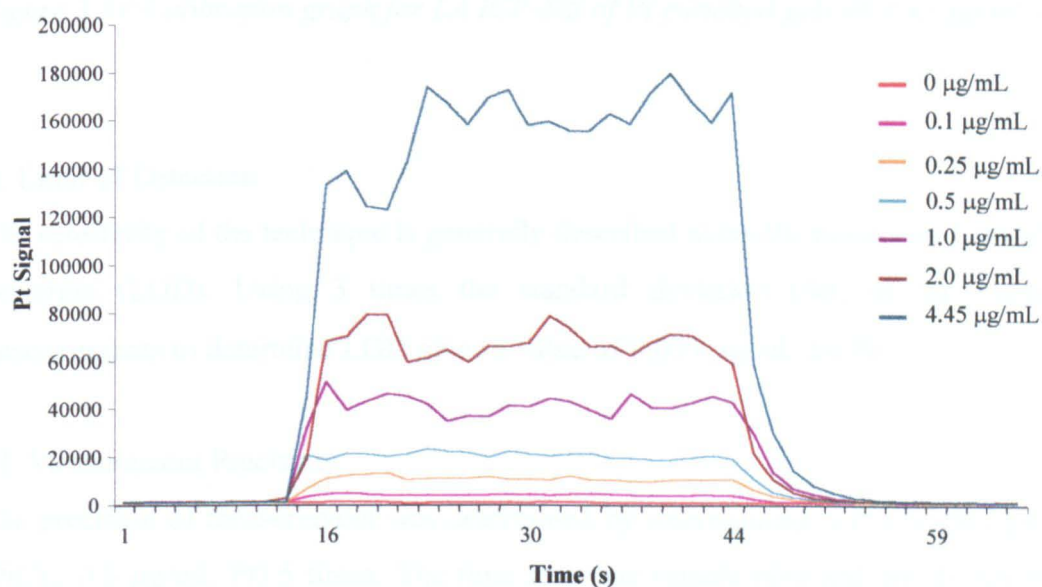


Figure 3.30:  $^{195}\text{Pt}$  time response profiles for laser interrogation of Pt enriched gels

The resulting peak areas were integrated and normalised using the IS, the results were plotted against Pt concentration Figure 3.31 shows the calibration curve, which exhibits good linearity  $R^2 = 0.9983$ .

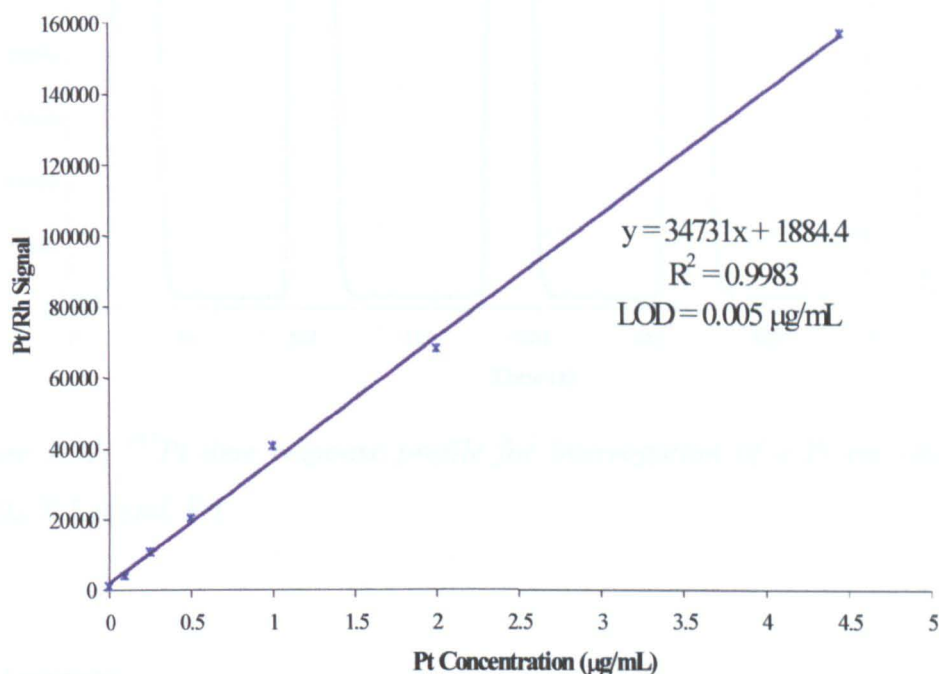


Figure 3.31: Calibration graph for LA ICP-MS of Pt enriched gels (0-4.45  $\mu\text{g/mL}$ )

## II. Limit of Detection

The sensitivity of the technique is generally described using the parameter limit of detection (LOD). Using 3 times the standard deviation ( $3\sigma$ ) of the blank measurements to determine LOD gives a value of  $0.005 \mu\text{g/mL}$  for Pt.

## III. Measurement Precision

The precision of measurement was determined by interrogating a Pt enriched gel ( $\text{PtCl}_4$ ,  $0.5 \mu\text{g/mL}$  Pt) 5 times. The time response signals obtained are shown in Figure 3.32. Using the equation given previously an RSD of 2.15 % was obtained.

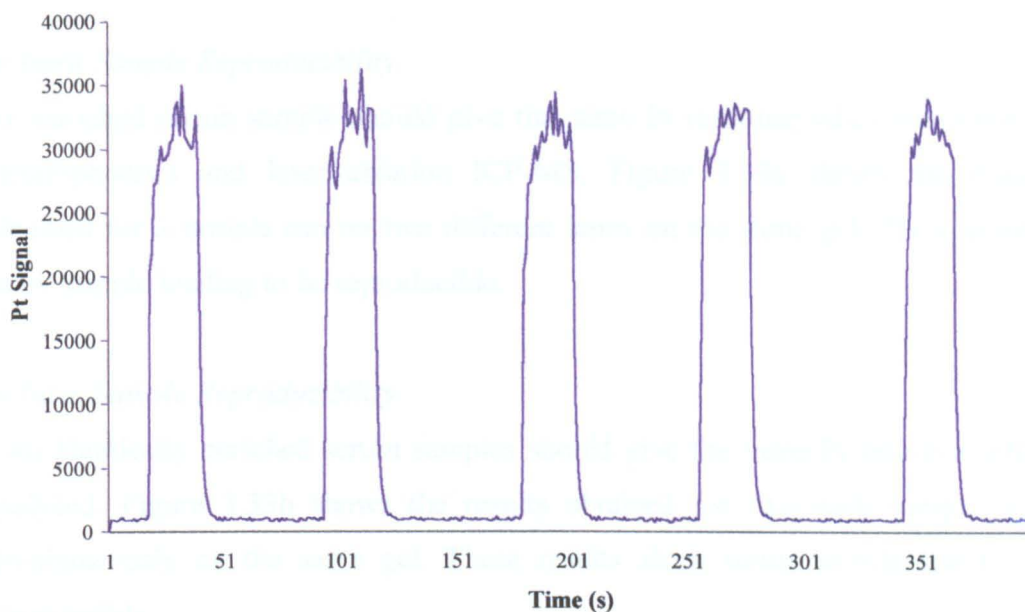


Figure 3.32:  $^{195}\text{Pt}$  time response profile for interrogation of a Pt enriched gel ( $\text{PtCl}_4$ ,  $0.5 \mu\text{g/mL Pt}$ )

#### IV. Accuracy

Accuracy describes the closeness of the result obtained to the true value. The accuracy of a system is best determined using an appropriate certified reference materials (CRM), unfortunately these are not always available. Accuracy can also be determined by analysing spiked samples and determining spike recovery but this approach was not appropriate for the present studies.

##### 3.2.4.c Variability of Gel Interrogation

Having identified a reliable measurement process experiments were conducted to assess the variability / imprecision associated with gel preparation. Pt enriched serum ( $\text{PtCl}_4$ ,  $5 \mu\text{g/mL Pt}$ ) was used throughout this study. The sample separation step needs to be reproducible for the speciation results to be meaningful. Thus there was a need to determine the reproducibility of the electrophoresis step:

*a) Intra-Sample Reproducibility*

An enriched serum sample should give the same Pt response when subjected to electrophoresis and laser ablation ICP-MS. Figure 3.33a shows the results obtained for a sample run on two different lanes on the same gel. These results show sample loading to be reproducible.

*b) Inter-Sample Reproducibility*

Two identically enriched serum samples should give the same Pt response when analysed. Figure 3.33b shows the results obtained for two such samples run simultaneously on the same gel. These results show serum enrichment to be reproducible.

*c) Inter-Gel Reproducibility*

An enriched serum sample should give the same Pt response when run on two separate gels. Figure 3.33c shows the results obtained for such a sample run simultaneously on two separate gels. These results show gels to be reproducible.

*d) Inter-Run Reproducibility*

A sample should give identical results when electrophoresed under identical conditions, even if not run simultaneously. Figure 3.33d shows the results obtained for a sample run on two separate gels at different times. These results show electrophoresis to be reproducible.

*e) Inter-Ablation Reproducibility*

Ablating a gel lane twice should give the same results. Figure 3.33e shows the results obtained when the same lane was ablated. These results show gel ablation to be reproducible.



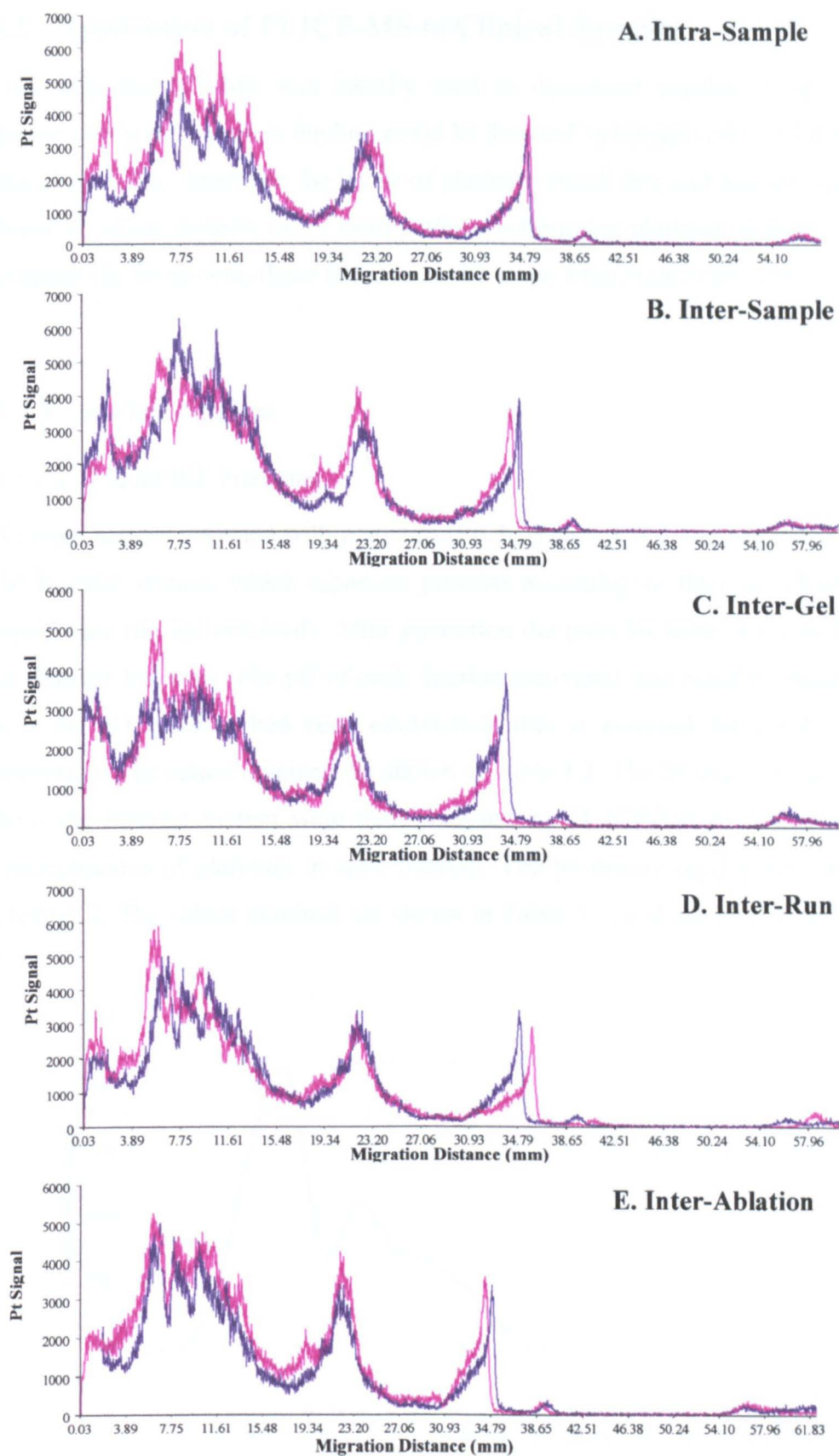


Figure 3.33:  $^{195}\text{Pt}$  profiles for Pt enriched serum ( $\text{PtCl}_4$ , 5  $\mu\text{g/mL}$  Pt) electrophoresed under native conditions.

### 3.3 Application of FI ICP-MS to Clinical Samples

Flow injection ICP-MS was initially used to determine whether a significant degree of platinum-protein binding could be detected in human serum. FI ICP-MS was also used to determine the levels of platinum (total, free and bound) typically found in serum samples taken from patients undergoing platinum therapy and to compare the levels with those found in serum taken from control sources.

#### 3.3.1 *In Vitro* Studies

##### 3.3.1.a Liquid IEF Fractions

A serum sample enriched with platinum ( $\text{PtCl}_4$ , 5  $\mu\text{g/mL}$  Pt) was separated using the Rotofor system, which separates proteins according to their pI whilst in a liquid state (no gel involved). After separation the proteins were 'harvested' into 20 discrete fractions. The pH of each fraction recovered was noted to check how well the pH gradient had been established; this is essential for good protein resolution. The values obtained are shown in Table 3.3. The 20 fractions harvested from the Rotofor system were then analysed by FI ICP-MS to determine the concentrations of platinum in each fraction. The procedure used is described in Chapter 2. The values obtained are shown in Table 3.3, and are plotted in Figure 3.34.

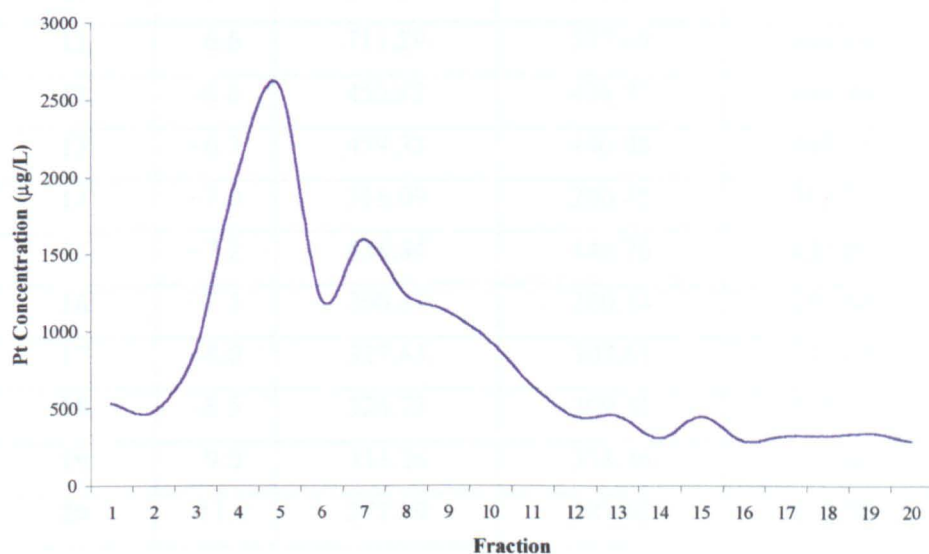


Figure 3.34:  $^{195}\text{Pt}$  concentration in fractions harvested following liquid IEF separation of Pt enriched serum sample ( $\text{PtCl}_4$ , 5  $\mu\text{g/mL}$  Pt)

Figure 3.34 shows that most of the protein bound platinum in the enriched serum sample can be found in fractions 3-6, which cover the pH range of 4.8-5.6. This would correspond to the pI of human serum albumin (see Appendix 1.3). A second peak is visible centred around fraction 7, pH 5.8, which is probably due to platinum-transferrin binding as transferrin has a pI of 5.9. Much of the platinum present in fractions 3-10 is probably bound to albumin. The concentration of albumin in serum is too great to fit in the fractions of the appropriate pH and so it is likely to over-spill into adjacent fractions. The fractions harvested were electrophoresed using native PAGE to gain extra insight into the proteins present in the various fractions, see section 3.4.1.d.

<b>Fraction</b>	<b>pH</b>	<b>Run 1 (<math>\mu\text{g/L}</math>)</b>	<b>Run 2 (<math>\mu\text{g/L}</math>)</b>	<b>Mean (<math>\mu\text{g/L}</math>)</b>
1	~4.5	590.13	469.40	529.76
2	~4.7	481.35	475.68	478.51
3	~4.8	873.59	874.15	873.87
4	~5.0	2058.30	1995.75	2027.02
5	~5.3	2597.90	2587.20	2592.55
6	~5.6	1238.34	1162.21	1200.27
7	~5.8	1591.50	1589.85	1590.68
8	~6.1	1253.09	1212.57	1232.83
9	~6.3	1157.40	1084.04	1120.72
10	~6.4	974.32	888.31	931.32
11	~6.6	711.29	577.69	644.49
12	~6.6	452.83	436.77	444.80
13	~6.7	459.33	440.08	449.71
14	~7.0	316.09	290.45	303.27
15	~7.2	438.84	446.76	442.80
16	~7.5	290.84	280.44	285.64
17	~8.0	327.63	307.61	317.62
18	~8.5	324.73	309.51	317.12
19	~9.0	333.26	338.46	335.86
20	~11.0	277.79	287.62	282.70

*Table 3.3:  $^{195}\text{Pt}$  concentration in fractions harvested following liquid IEF separation of Pt enriched serum sample ( $\text{PtCl}_4$ , 5  $\mu\text{g/mL}$  Pt)*

The actual platinum concentrations found in the fractions are not as high as might be expected. Platinum in serum has been found to be >90% protein bound in under 2 hours<sup>77</sup>. Whilst the conditions in liquid phase IEF electrophoresis are milder than those experienced in IEF PAGE, they are still harsher than those in native PAGE. These harsh conditions may explain the low levels detected by causing metal-protein bonds to break. Further optimisation of operating parameters would be needed before reliable platinum concentrations could be achieved. However, the platinum profile obtained gives some idea of the nature of platinum-protein binding occurring in human serum enriched *in vitro*.

### 3.3.1.b Electro-elution Samples

Serum enriched with inorganic platinum (PtCl<sub>4</sub>, 5 µg/mL Pt) was electrophoresed using a 2D/Prep gel as described in Chapter 2. After electrophoresis the gel was electro-eluted and the 14 resulting fractions were collected. Staining of the 2D/Prep gel after electro-elution showed that a large proportion of the protein was still associated with the gel. The fractions recovered from the electro-elution of the platinum enriched serum sample were analysed using FI ICP-MS to determine the amount of platinum in each fraction. Unfortunately due to the use of large flat bed platinum electrodes in the electro-elution system the background platinum levels were too high to obtain meaningful results.

### 3.3.1.c Samples Enriched with Platinum Compounds

In order to get some idea of the platinum binding potential of serum proteins a serum sample was enriched with inorganic platinum (PtCl<sub>4</sub>), to 0, 1, 5, 10 and 25 µg/mL Pt. After 3 hours of equilibration at room temperature the samples were filtered using ultrafiltration. The ultra-filtrates were collected and analysed using FI ICP-MS to determine the levels of free (unbound platinum). The results obtained are shown in Table 3.4. The amount of bound platinum was calculated using the equation below;

$$\text{Total [Pt]} = \text{Free [Pt]} + \text{Bound [Pt]}$$

Enrichment ( $\mu\text{g/L}$ )	ultrafiltrate 1 ( $\mu\text{g/L}$ )	ultrafiltrate 2 ( $\mu\text{g/L}$ )	mean free Pt ( $\mu\text{g/L}$ )	mean bound Pt ( $\mu\text{g/L}$ )	bound Pt %
0	0.32	0.27	0.30	N/A	N/A
1000	3.06	3.02	3.04	997	99.7
5000	18.5	17.6	18.0	4980	99.6
10000	45.0	43.7	44.4	9960	99.6
25000	10.4	9.62	10.0	25000	99.6

Table 3.4: Pt concentrations for enriched serum samples after filtration (3 sig fig)

It would appear that there is a vast number of potential platinum binding sites in serum. Even at the 25  $\mu\text{g/mL}$  level over 99.6 % of the platinum exists in the bound state, shown in Figure 3.35. As such it is unlikely that there will be saturation of platinum protein binding sites at the levels of platinum occurring in human serum, even at the elevated levels present in serum of patients receiving platinum therapy.

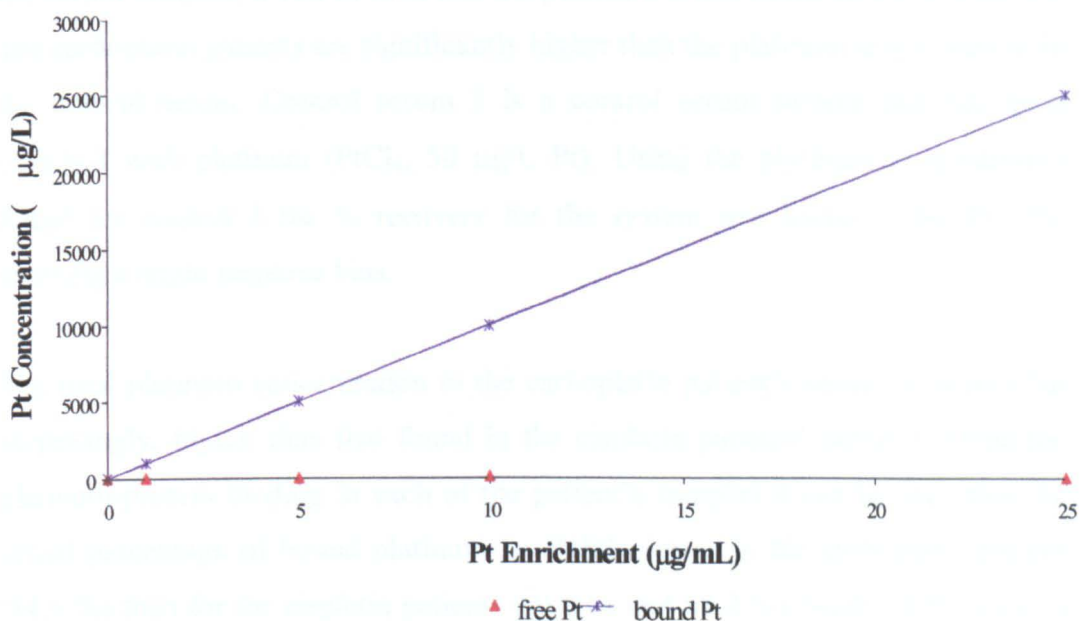


Figure 3.35: Free and bound Pt in enriched serum samples ( $\text{PtCl}_4$ , 0-25  $\mu\text{g/mL}$  Pt)

### 3.3.2 *In Vivo* Studies

Control and platinum patient serum samples were analysed in triplicate using FI-ICP-MS to determine the total platinum levels. Free platinum levels were determined by ultrafiltration of samples prior to analysis. Bound platinum levels were calculated as the difference between the total platinum concentration and the free platinum concentration. The results obtained are shown in Table 3.5.

	<b>Total Pt (<math>\mu\text{g/L}</math>)</b>	<b>Free Pt (<math>\mu\text{g/L}</math>)</b>	<b>Bound Pt (<math>\mu\text{g/L}</math>)</b>	<b>Bound Pt %</b>
<b>Cisplatin Patient</b>	162.34	14.58	147.76	91.0
<b>Cisplatin Patient</b>	107.19	12.61	94.58	88.2
<b>Carboplatin Patient</b>	722.21	111.47	610.74	84.6
<b>Control 1</b>	0.72	0.37	0.35	48.3
<b>Control 2</b>	0.89	0.38	0.51	56.8
<b>Enriched Control</b>	47.33	0.77	46.56	98.4

Table 3.5:  $^{195}\text{Pt}$  concentrations for control and patient serum samples

By comparison of the total Pt concentrations obtained by FI ICP-MS analysis of the serum samples, it can be seen that the platinum levels in the serum of cisplatin and carboplatin patients are significantly higher than the platinum levels present in the control serum. Control serum 3 is a control serum sample that has been enriched with platinum ( $\text{PtCl}_4$ , 50  $\mu\text{g/L}$  Pt). Using the platinum concentration found for control 3 the % recovery for the system was found to be 94.7 %, showing a slight negative bias.

The total platinum concentration in the carboplatin patient's serum is, somewhat surprisingly, higher than that found in the cisplatin patients' serum. Comparing platinum-protein binding in each of the patient's samples it can be seen that the actual percentage of bound platinum is slightly lower in the carboplatin patient (84.6 %) than for the cisplatin patients (91.0 % and 88.2 %). Such a difference in protein binding could help account for the differences in toxicity between the two platinum drugs. In itself these data do not tell us anything about the platinum-protein species being formed in the serum.

### 3.4 Application of LA ICP-MS to Clinical Samples

Flow injection studies can determine total and, in combination with ultrafiltration, free levels of platinum present in serum samples. However, it can not tell us anything about the platinum-species present in the serum. To look at this a more sophisticated separation technique, such as electrophoresis, is needed. The suitability of laser ablation ICP-MS for the speciation of platinum in biological samples separated using PAGE was established during method development. The next step was to apply the technique to 'real' samples. *In vitro* studies were carried out initially to gain some insight into the nature of Pt-protein binding. The binding of inorganic platinum with different proteins was investigated as well as the behaviour of different platinum species in serum. The effect of equilibration time on protein binding was also studied.

Next *in vivo* studies were carried out comparing the platinum-protein binding occurring in control serum with that found in serum taken from patients undergoing platinum therapy. When studying serum samples knowledge of the behaviour of other metals in serum can be helpful, transferrin, for example, is known to be the major protein responsible for iron transport in serum. Human serum typically contains 2-3.2 mg/mL transferrin, which is capable of binding two Fe atoms per molecule<sup>197</sup>. By monitoring the distribution of <sup>57</sup>Fe the location of transferrin in the gel can be inferred. (<sup>57</sup>Fe is monitored despite the greater abundance of <sup>56</sup>Fe due to potential <sup>40</sup>Ar<sup>16</sup>O<sup>+</sup> interference)

#### 3.4.1 *In Vitro* Studies

##### 3.4.1.a Pure Proteins Enriched with Inorganic Platinum

Initial studies were carried out *in vitro* in order to gain a basic understanding of the interaction of platinum with serum proteins. Albumin (50 µg/µL), transferrin (3.0 µg/µL) and α<sub>2</sub>-macroglobulin (4.0 µg/µL), all at physiological concentrations, were enriched with inorganic platinum (PtCl<sub>4</sub>, 5 µg/mL Pt). After a 24 hour equilibration period the samples were electrophoresed and then analysed by laser ablation ICP-MS.

The platinum distribution profiles obtained are shown in Figure 3.36. It was assumed throughout the study that proteins and metal ions found in the same region of the gel are bound. This is not an unreasonable assumption since unbound platinum was found to migrate with the solvent front (migration distance ~55 mm). In all three cases some degree of platinum-protein binding can be observed.

Since all three protein samples were enriched with the same concentration of platinum the degree of protein binding is reflected by the amount of platinum migrating with the solvent front. Hardly any platinum is present at the solvent front of the albumin sample indicating that virtually all the platinum is protein bound. Platinum binding to transferrin and  $\alpha_2$ -macroglobulin is not as abundant, hence the large proportion of platinum migrating with the solvent fronts. This does not, however, imply albumin has a greater affinity for platinum than transferrin and  $\alpha_2$ -macroglobulin. The high degree of platinum-albumin binding may simply reflect the high concentration of albumin present in the sample compared to the other protein samples.

The platinum band for the albumin sample is broad, due to the high concentration of albumin. The band appears to be made up of a number of peaks, this is due to the presence of albumin polymers. The enriched transferrin profile shows platinum binding. The location of the transferrin on the gel (migration distance ~ 22 mm) is confirmed using the  $^{57}\text{Fe}$  profile. All three platinum profiles are plotted on identical y axes and so the platinum peak heights can be directly compared to compare the amount of platinum in each protein band. It can be seen that much less platinum is bound to transferrin than is found bound to albumin.

The platinum profile for enriched  $\alpha_2$ -macroglobulin shows some platinum binding occurs, at a level comparable with transferrin. The occurrence of multiple bands is hard to explain, it may be that on binding platinum the quaternary structure of  $\alpha_2$ -macroglobulin is disrupted causing the constituent sub-units to separate.



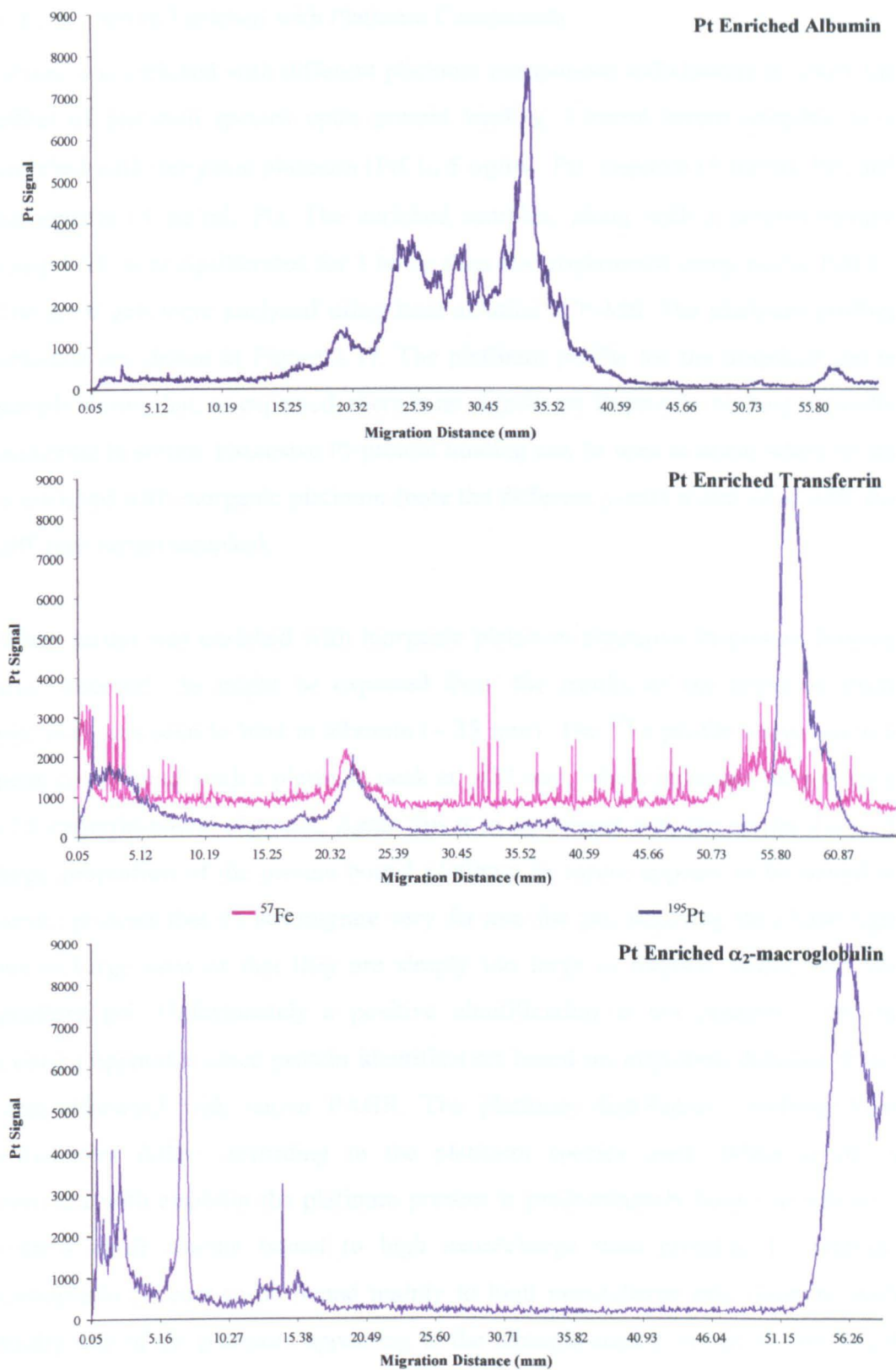


Figure 3.36:  $^{195}\text{Pt}$  &  $^{57}\text{Fe}$  profiles for Pt enriched proteins ( $\text{PtCl}_4$ , 5  $\mu\text{g/mL}$  Pt) electrophoresed under native conditions.

### 3.4.1.b Serum Enriched with Platinum Compounds

Serum was enriched with different platinum compounds individually to study the effect of platinum species upon protein binding. Control serum samples were enriched with inorganic platinum ( $\text{PtCl}_4$ , 5  $\mu\text{g/mL Pt}$ ), cisplatin (5  $\mu\text{g/mL Pt}$ ), and carboplatin (5  $\mu\text{g/mL Pt}$ ). The enriched samples, along with a control sample (unspiked) were equilibrated for 3 hours then electrophoresed using native PAGE. The dried gels were analysed using laser ablation ICP-MS. The platinum profiles obtained are shown in Figure 3.37. The platinum profile for the unspiked serum sample shows that, as expected, there is no significant Pt-protein binding naturally occurring in serum. Extensive Pt-protein binding can be seen to occur when serum is enriched with inorganic platinum (note the different y-axis scales used with the different serum samples).

When serum was enriched with inorganic platinum extensive Pt-protein binding was observed. As might be expected from the results of the previous study platinum was seen to bind to albumin (~ 35 mm). The  $^{57}\text{Fe}$  profile shows an iron peak coincidental with a platinum peak at ~ 22 mm, which indicates the presence of transferrin-bound platinum. Again this is in agreement with the earlier study. A large proportion of the protein bound platinum in serum appears to be bound to serum proteins that do not migrate very far into the gel, implying they have high mass/charge ratio or that they are simply too large to migrate further into the gradient gel. Unfortunately a positive identification is not possible with the existing apparatus since protein identification based on migration distance is not straightforward with native PAGE. The platinum distribution resulting from enrichment differs according to the platinum species used. When serum is enriched with cisplatin the platinum present is predominantly bound to albumin, with a small amount bound to high mass/charge ratio proteins. In contrast, carboplatin appears to be bound mainly to high mass/charge ratio proteins with hardly any of the platinum appearing in the albumin region. It can be concluded that the nature of the platinum species has a strong effect on the protein binding occurring in serum. These apparent differences in the proteins binding cisplatin and carboplatin may relate to the differences in their relative toxicities.

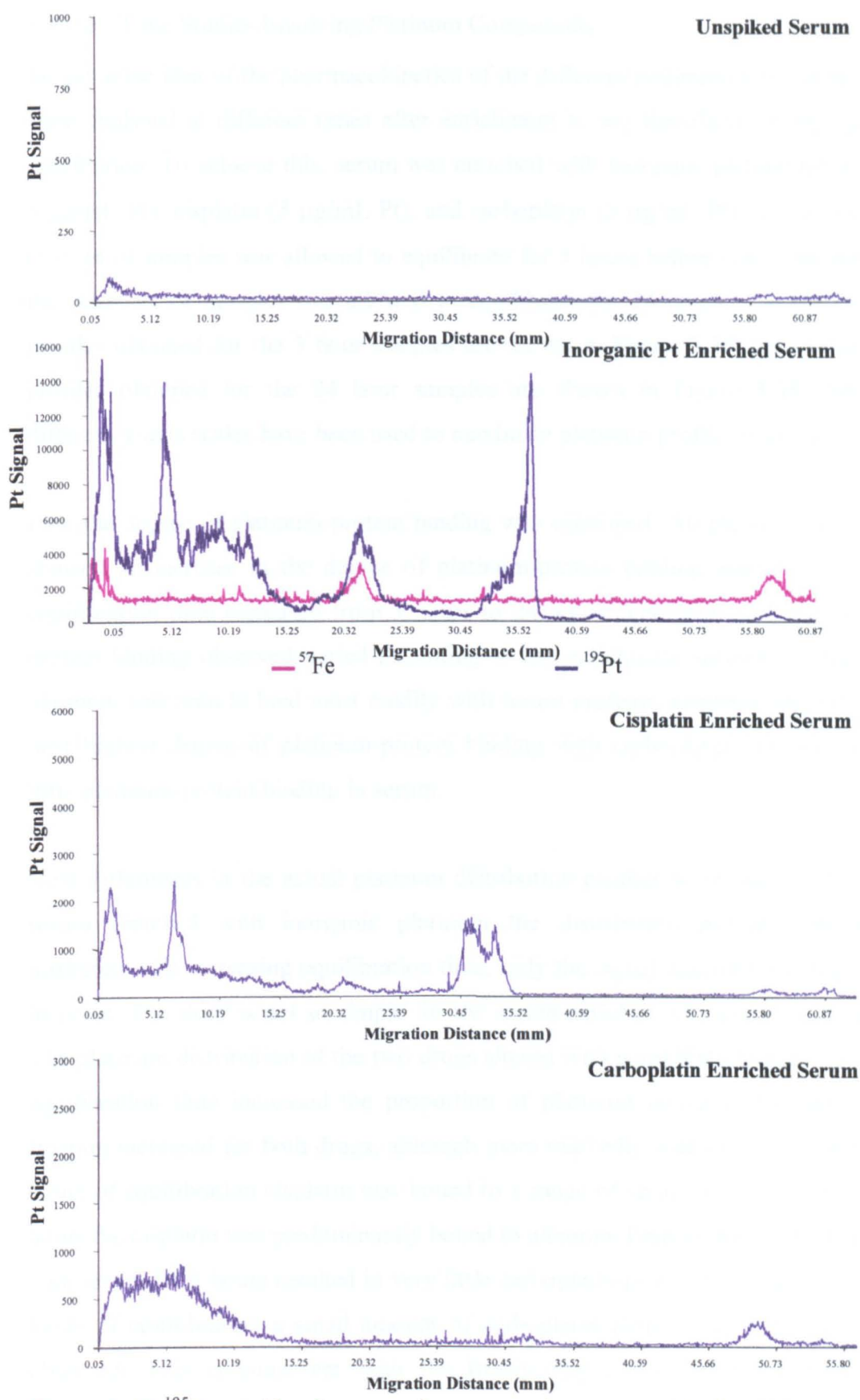


Figure 3.37:  $^{195}\text{Pt}$  profiles for control serum and serum enriched with inorganic platinum, cisplatin and carboplatin ( $5 \mu\text{g/mL Pt}$ ) after 3 hours of equilibration

### 3.4.1.c Time Studies Involving Platinum Compounds

To get some idea of the pharmacokinetics of the different platinum drugs samples were analysed at different times after enrichment to see the effect on platinum distribution. To achieve this, serum was enriched with inorganic platinum ( $\text{PtCl}_4$ , 5  $\mu\text{g/mL Pt}$ ), cisplatin (5  $\mu\text{g/mL Pt}$ ), and carboplatin (5  $\mu\text{g/mL Pt}$ ), in duplicate. One set of samples was allowed to equilibrate for 3 hours before electrophoresis, the other set of samples was allowed to equilibrate for 24 hours. The platinum profiles obtained for the 3 hour samples are shown in Figure 3.37, the platinum profiles obtained for the 24 hour samples are shown in Figure 3.38. Again different y-axis scales have been used to maximise platinum profile examination.

First the degree of platinum-protein binding was examined. All platinum species showed an increase in the degree of platinum-protein binding observed as the equilibration time increased from 3 hours to 24 hours. The degree of platinum-protein binding observed varied according to the enrichment species. Inorganic platinum was seen to bind most readily with serum proteins, cisplatin showed the next highest degree of platinum-protein binding with carboplatin showing very little platinum-protein binding in serum.

Next differences in the actual platinum distribution profiles were examined. For serum enriched with inorganic platinum the distribution pattern remained unaltered with increasing equilibration time, only the signal intensity was seen to increase. The story is not so simple for the serum enriched with platinum drugs. The platinum distribution of the two drugs altered with equilibration time. As the equilibration time increased the proportion of platinum bound to the albumin fraction increased for both drugs, although more markedly with cisplatin. After 3 hours of equilibration cisplatin was bound to a range of serum proteins. After 24 hours the cisplatin was predominantly bound to albumin. Equilibrating carboplatin with serum for 3 hours resulted in very little carboplatin-protein binding. After 24 hours of equilibration a small amount of carboplatin-albumin binding could be observed. This is consistent with the theory that the coplanar structure of carboplatin delays degradation and so slows down the rate of protein binding relative to cisplatin.

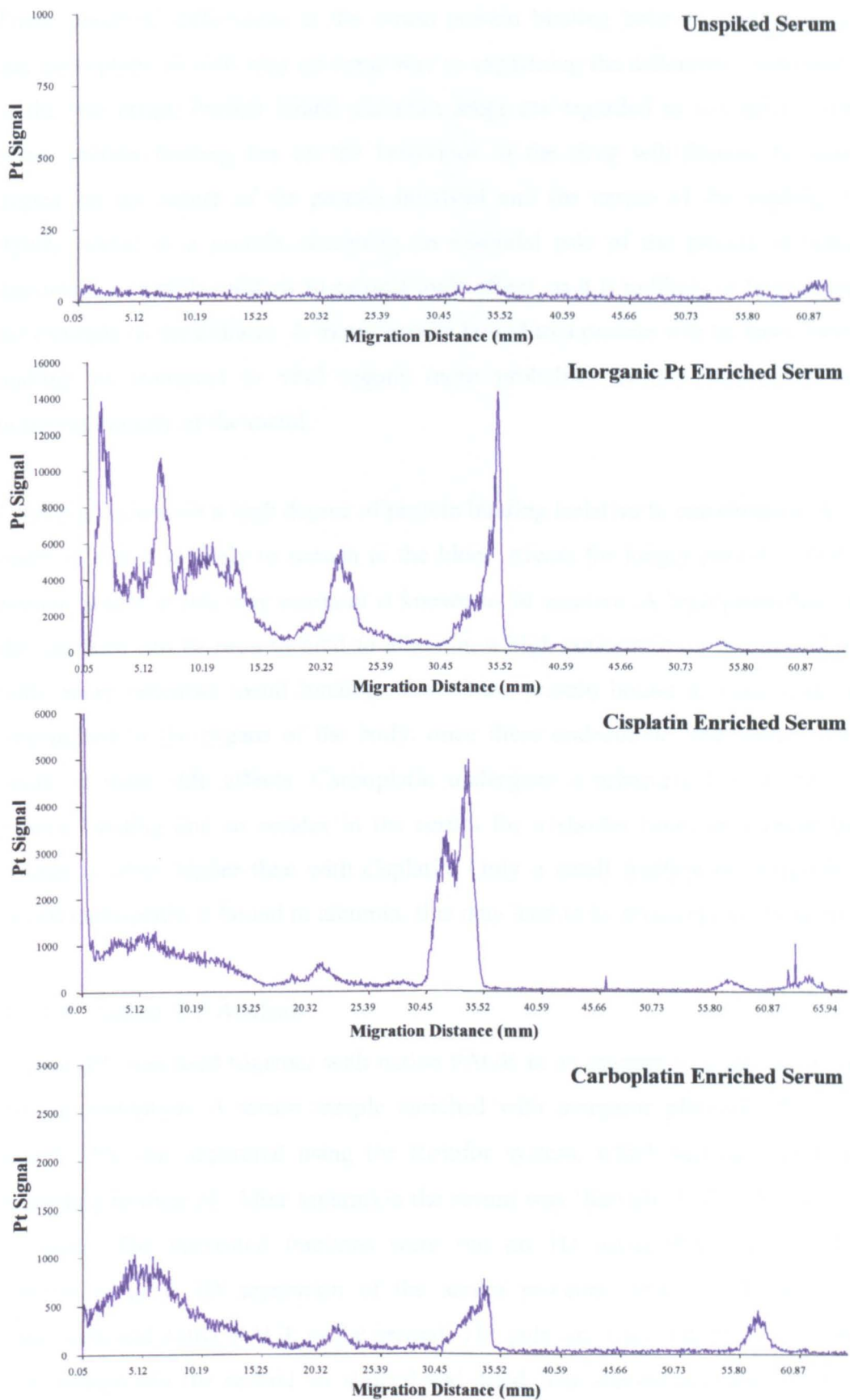


Figure 3.38:  $^{195}\text{Pt}$  profiles for control serum and serum enriched with inorganic platinum, cisplatin and carboplatin ( $5 \mu\text{g/mL Pt}$ ) after 24 hours of equilibration

These observed differences in the serum protein binding behaviour of cisplatin and carboplatin *in vitro* may go some way to explaining the differences in toxicity of the two drugs. Protein bound platinum drugs are regarded as non-active. The effect protein binding has on the behaviour of the drug will depend to some degree on the nature of the protein involved and the nature of the binding. If tightly bound to a protein, assuming no essential role of the protein is being disrupted, a metal is unlikely to cause a toxic effect, as it is unlikely to be released for example to the kidneys. A metal loosely bound to a protein will be more labile making its transport to vital organs more probable, thereby increasing the potential toxicity of the metal.

Cisplatin undergoes a high degree of protein binding (relative to carboplatin). As a result of this it is likely to remain in the blood stream for longer periods. Whilst protein bound in this way cisplatin is known to be inactive. A high proportion of the cisplatin can be seen to bind to albumin, a high concentration serum protein with many potential metal binding sites. Once protein bound a metal may be transported to the organs of the body, once there undesirable interactions may result in toxic side effects. Carboplatin undergoes a relatively low degree of protein binding and so resides in the serum for a shorter time, as a result the dosage is often higher than with cisplatin. Only a small fraction of the protein bound carboplatin is bound to albumin, this may lead to its relatively low toxicity.

#### 3.4.1.d Liquid IEF Analysis

Liquid IEF was used together with native PAGE in an attempt to improve on the protein resolution. A serum sample enriched with inorganic platinum ( $\text{PtCl}_4$ , 5  $\mu\text{g/mL}$  Pt), was separated using the Rotofor system, which separates proteins according to their pI. After separation the serum was 'harvested' into 20 discrete fractions. The harvested fractions were run on 1D native PAGE gels. This effectively gave 2D separation of the serum proteins, with IEF as the first dimension and native PAGE as the second. The gels were run in duplicate, one set was ablated and the second set stained and dried. The stained gels are shown in Figure 3.39. Collected fractions were also analysed using FI ICP-MS as described in section 3.3.1.a.

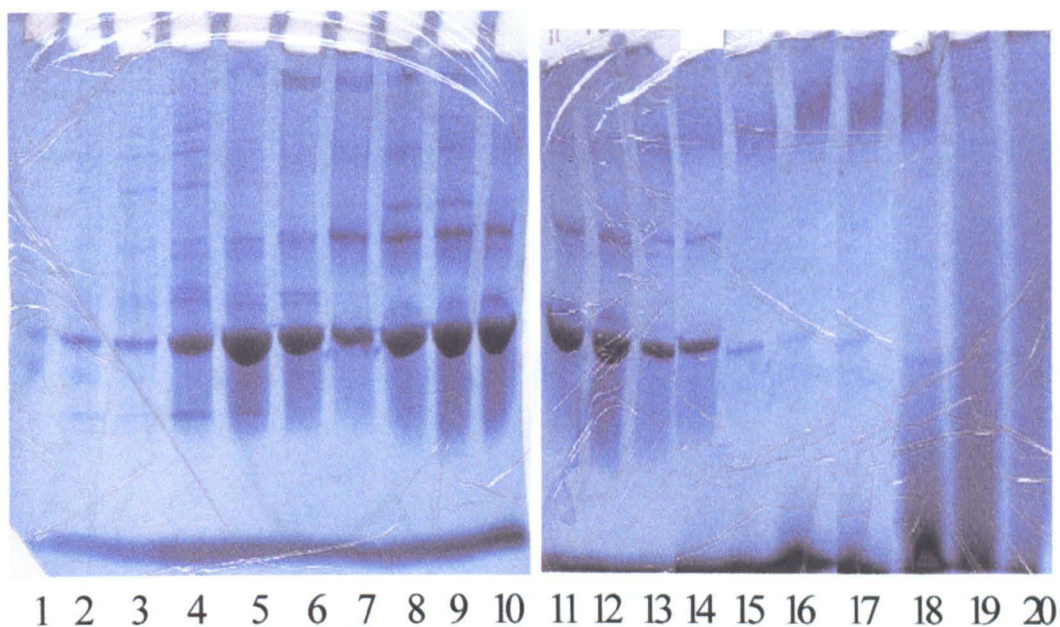


*Figure 3.39: Stained gels of Rotofor fractions run on native PAGE*

The stained gel shows that IEF separation using the Rotofor system was not perfect. The concentration of albumin in the serum was too high despite dilution and as a result albumin was present in virtually every lane. However, a higher degree of protein separation was achieved compared to the use of native PAGE in isolation.

Pt profiles were obtained by interrogation of the 20 gel lanes. To determine how representative the Rotofor harvest was of the original sample the Pt profiles for all 20 lanes were combined. The resultant profile is given in Figure 3.40. By comparing the resultant profile with a Pt profile obtained from analysis of a serum sample enriched with inorganic platinum (such as in Figure 3.37) it can be seen that the distribution profile is almost identical. This shows the harvested fractions are representative of the serum sample being studied. The Pt distribution profiles were also used to construct a 2D contour plot. Platinum signal intensity was plotted against position on the gel. The resultant plot is shown in Figure 3.41. Six discrete regions of high Pt intensity can be made out, further work would be needed to positively identify the associated proteins, but it gives some indication of the complexity of platinum binding.

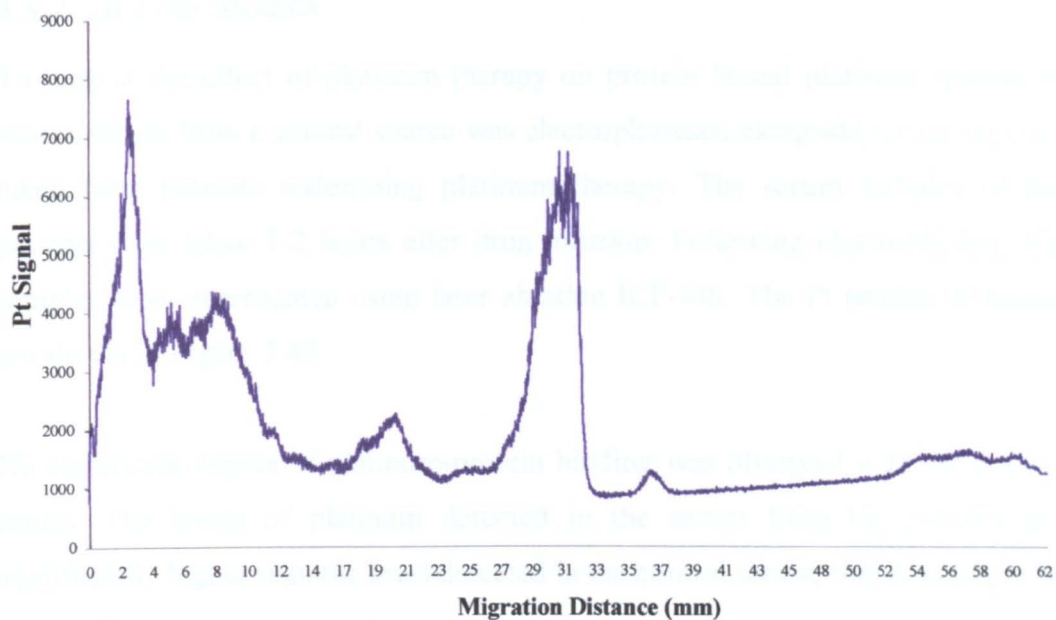


Figure 3.40: Summation of  $^{195}\text{Pt}$  profiles after native PAGE of Rotofor fractions

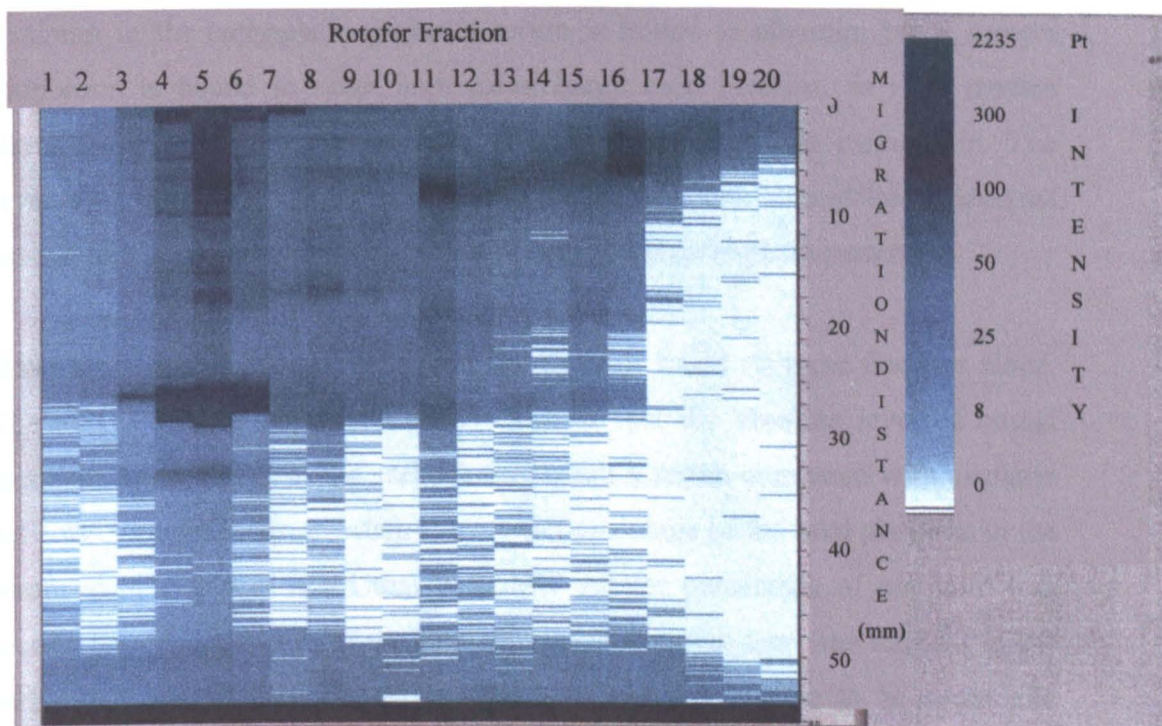


Figure 3.41: 2D plot of  $^{195}\text{Pt}$  distribution in Rotofor fractions after native PAGE



### 3.4.2 *In Vivo* Studies

To look at the effect of platinum therapy on protein bound platinum species in serum, serum from a control source was electrophoresed alongside serum samples taken from patients undergoing platinum therapy. The serum samples of the patients were taken 1-2 hours after drug infusion. Following electrophoresis the samples were interrogated using laser ablation ICP-MS. The Pt profiles obtained are shown in Figure 3.42.

No significant degree of platinum-protein binding was observed with the control serum. The levels of platinum detected in the serum from the patients are significantly higher than the level detected in the control serum, this is as might be expected.

The protein bound platinum in the cisplatin patient's serum is mainly associated with albumin, there is also some binding to higher mass/charge ratio proteins. The platinum in the carboplatin patient's serum is bound to albumin, but a greater proportion is bound to other high mass/charge ratio proteins. *In vitro* studies showed cisplatin bound more readily to serum proteins than carboplatin. The reverse appears to be the case with the patients' serum. The absolute level of protein bound platinum is higher in the serum of the carboplatin patient

However, it is not justifiable to draw conclusions based on these findings alone. The FI ICP-MS results (Section 3.3.2) show that the absolute level of bound platinum to be higher in the carboplatin patient's serum compared with cisplatin patients' serum. However, when taken as a percentage of the total platinum in the serum sample it was noted that a slightly greater percentage of platinum was protein bound in the case of the cisplatin patients' serum than was the case in the carboplatin patient's serum. Other external factors need also to be taken into consideration before reading too much into these results, such factors include the patients general health, the dosage administered and the duration of the therapy.

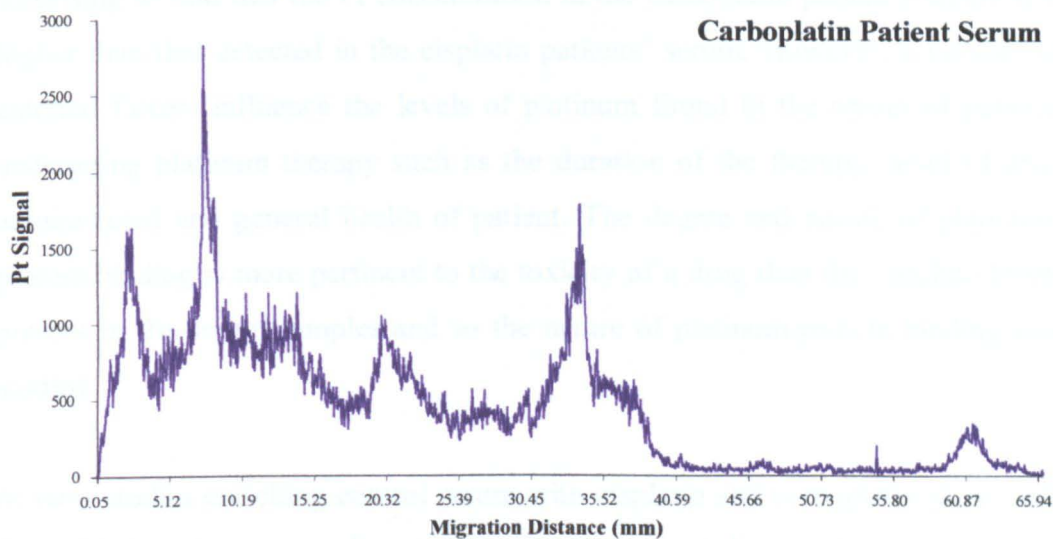
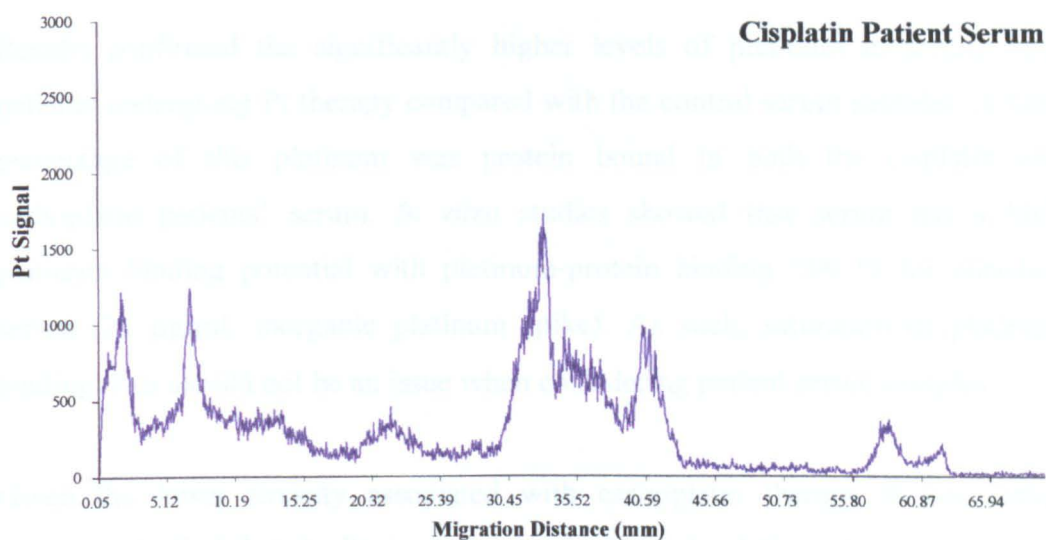
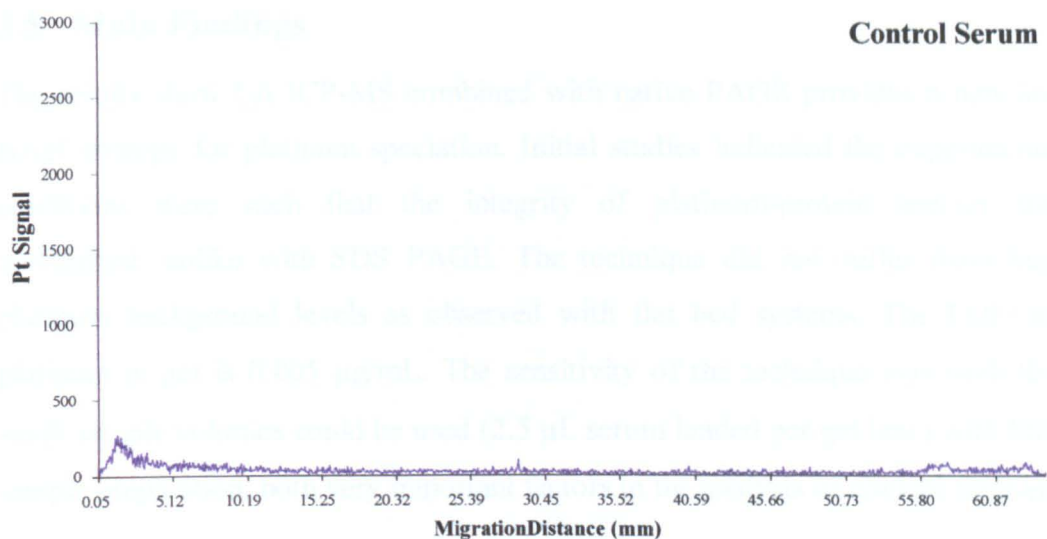


Figure 3.42:  $^{195}\text{Pt}$  profiles for control and platinum patient serum samples

### 3.5 Main Findings

The results show LA ICP-MS combined with native PAGE provides a new and novel strategy for platinum speciation. Initial studies indicated the experimental conditions were such that the integrity of platinum-protein species was maintained, unlike with SDS PAGE. The technique did not suffer from high platinum background levels as observed with flat bed systems. The LOD for platinum in gel is 0.005 µg/mL. The sensitivity of the technique was such that small sample volumes could be used (2.5 µL serum loaded per gel lane) with little sample preparation, both very important factors in the analysis of clinical samples.

Results confirmed the significantly higher levels of platinum in serum from patients undergoing Pt therapy compared with the control serum samples. A high percentage of this platinum was protein bound in both the cisplatin and carboplatin patients' serum. *In vitro* studies showed that serum has a high platinum binding potential with platinum-protein binding >99 % for enriched serum (25 µg/mL inorganic platinum spike). As such, saturation of platinum binding sites should not be an issue when considering patient serum samples.

Given the lower toxicity associated with carboplatin therapy it was rather surprising to find that the Pt concentration in the carboplatin patient's serum was higher than that detected in the cisplatin patients' serum. However, a number of external factors influence the levels of platinum found in the serum of patients undergoing platinum therapy such as the duration of the therapy, level of drug administered and general health of patient. The degree and nature of platinum-protein binding is more pertinent to the toxicity of a drug than the absolute levels present in the serum samples and so the nature of platinum-protein binding was studied.

*In vitro* studies enriching control serum with cisplatin and carboplatin show both drugs bind with a range of proteins. It was observed that cisplatin bound more readily to albumin than was the case for carboplatin. When time studies were carried out with the two drugs differences were observed in the pharmacokinetics of protein binding. Levels of protein bound cisplatin were seen to increase with

time, with proportion bound to albumin increasing. The platinum distribution pattern for carboplatin enriched serum was also seen to alter with time as the proportion of platinum bound to albumin increased. Such a difference in the nature of the protein binding and the observed differences in the mechanistic pathway of the two drugs could go some way to explaining the differences in their associated toxicities. It would appear that Pt-albumin binding is associated with drug toxicity rather than drug efficacy, such a finding is consistent with the fact that albumin bound platinum drugs are known to lose their anti-tumour activity.

LA ICP-MS interrogation of serum samples obtained from cisplatin and carboplatin patients reflects the differences observed between the drugs *in vitro*. The main difference between the profiles obtained is the proportion of platinum bound to albumin. The carboplatin patient's serum contained the highest concentration of protein bound platinum, however, only a small fraction of the protein bound platinum was bound to albumin relative to the cisplatin patients' serum.

Overall the new hyphenated technique developed proved successful in the speciation of platinum species in human serum, in particular clinical samples obtained from patients undergoing platinum therapy. The main limitation of the technique is sufficient protein resolution given the complex nature of the sample, serum typically contains over 100 different proteins<sup>198</sup>. The use of liquid IEF, in the form of the Bio-Rad Rotofor followed by native PAGE was shown to improve protein resolution by the addition of a second separation parameter. The main protein component of serum is albumin (~ 35-45 mg/mL). Such high albumin concentrations can pose problems when trying to study metal binding to other, lower concentration proteins. One way in which such problems can be overcome would be to remove the serum albumin prior to protein separation. The protein concentration of the sample would then be greatly reduced. This would mean serum could be electrophoresed without prior dilution, effectively increasing the sensitivity of the technique as well as improving the potential protein resolution.

# Chapter 4: Characterisation of Gold Enriched Gels

## 4.1 Introduction

The noble metal gold is one of the few metals to exist in nature in the elemental state. Pure gold is a soft, yellow metal with the highest ductility and malleability of any element<sup>199</sup>. Because of its relative inertness gold does not tarnish on exposure to air and so retains its lustre. Such properties meant gold was an unsuitable material from which to make implements, and so primitive man used gold purely for ornamental purposes. Today gold finds more widespread usage. Whilst retaining its ornamental value in coinage and jewellery, gold is also used in the electronics industry, in heterogeneous catalysts, in dental alloys and in modern medicine.

Whilst metallic gold is chemically inert, gold has six discrete oxidation states -I, 0, I, II, III, & V. There is no evidence for the occurrence of states -I, II or V in the environment, whilst the states 0 (metallic gold), I and III are all biologically significant, despite the high toxicity of gold III.

The average concentration of gold in the earth's crust is very low,  $\sim 5 \mu\text{g}/\text{kg}$ <sup>200</sup>, although gold is widely dispersed throughout the environment. Levels of gold released into the environment by man are very low, mainly due to the inertness of gold and the economic incentives. Very low levels of gold naturally occur in plant and animal tissue, although as yet gold has not been identified as an element essential for life<sup>201</sup>. Concentrations of gold in the human body are usually very low, with blood levels of gold in man around  $0.35 \mu\text{g}/\text{L}$ <sup>202</sup>, elevated gold levels can result from wearing gold jewellery<sup>203</sup>, however, or in chrysotherapy<sup>204</sup>. Gold has a long medical history dating back to ancient China. By the late 19<sup>th</sup> century it was being used to treat tuberculosis (TB) and syphilis. The use of chrysotherapy to treat rheumatoid arthritis (RA) was quite fortuitous from the treatment of TB patients.

Treatment of RA is the main application of gold therapy today. All gold drugs are Au(I) compounds since Au(III) is so much more toxic to humans. Gold drugs for the treatment of RA fall into two main groups, oral and parenteral. Auranofin is the only modern orally administered gold drug to have found widespread acceptance. There is a number of parenteral gold drugs available of which the most widely used is Myocrisin.

Chrysotherapy has been used to treat the many millions of people suffering from RA for well over fifty years and is known to induce remission. Despite such widespread usage the exact mode of action of gold drugs is still unknown. It is known, however, that the pharmacokinetics of parenteral and oral gold drugs differ greatly.

The use of all gold therapy is limited by the occurrence of toxic side effects. Such side effects are more common in patients receiving parenteral drugs than with those receiving oral drug treatment. Such toxic side effects are thought to be due to the formation of Au(III) compounds, although this has yet to be proven. Gold levels in the serum and urine of chrysotherapy patients are routinely monitored due to the toxicity associated with the accumulation of high gold levels in the bloodstream.

Gold drugs are difficult to study in solution as gold does not have an observable NMR or ESR spectra. Gold is mono-isotopic, that is to say  $^{197}\text{Au}$  has an abundance of 100 %. ICP-MS uses the detection of individual isotopes to determine analyte concentrations and offers high sensitivity for gold determination. Coupled with the low incidence of isobaric and oxide interferences, ICP-MS is a suitable means of gold determination in clinical samples. This is especially true when coupled with flow injection or laser ablation, which minimise the amount of sample pre-treatment needed. Some techniques require extensive sample pretreatment when analysing biological samples, for examples the presence of proteins can lead to matrix effects when using AAS<sup>205</sup>.

In this chapter the applicability of laser ablation ICP-MS to gold analysis is described and analytical performance documented. Flow injection studies are performed to determine the total and free (unbound) concentrations of gold in serum from chrysotherapy patients and controls. *In vitro* studies have also been carried out to determine the effect of different gold species on protein binding. These studies involved enriching serum samples with inorganic gold (Au(I)), Myocrisin (Au(I)) and colloidal gold (Au(0)).

Au(0) is of interest since there is speculation that it may be the active form of gold in the treatment of RA<sup>206</sup>. Differences between the protein binding of this gold species and inorganic gold may go some way towards explaining the toxic side effects observed with conventional gold drugs. Colloidal gold is known to bind to proteins and is widely used as a protein dye. However, the binding of colloidal gold with proteins is considered non-specific and is very pH dependent<sup>207</sup>. When Au(0)-protein bonds occur they are non-covalent electrostatic interactions. As a result any such interactions occurring in serum should interfere with protein reactivity only minimally. Ion layers around gold colloid particles compress in the presence of strong electrolytes and so they can approach each other closely. Flocculation of the solution can occur once a critical distance is reached. This being the case it is unlikely that colloidal gold will interact with proteins under physiological conditions.

*In vivo* studies were also performed comparing gold distribution in control serum with that observed in serum from patients receiving chrysotherapy.

## 4.2 Method Development

In general the operating parameters determined in the course of the platinum studies were used throughout. FI ICP-MS was identical to that described previously as were the laser parameters utilised to interrogate the gels, as shown in Table 4.1. The electrophoresis time study was repeated using gold enriched serum samples (H(AuCl<sub>4</sub>), 2 µg/mL Au) to check on the overall effectiveness of electrophoretic separation.

Parameter	LSX100	LSX200
Laser Energy	0.65 mJ	0.8 mJ
Laser Shot Rate	20 Hz	20 Hz
Aperture Size	N/A	260 $\mu\text{m}$
Laser Defocus	-3000 $\mu\text{m}$	N/A
Scan Rate	50 $\mu\text{m/s}$	50 $\mu\text{m/s}$

*Table 4.1: Optimised laser ablation parameters for gel interrogation*

#### 4.2.1 Electrophoresis

Figure 4.1 shows the Au signal response for laser ablation ICP-MS of serum samples enriched with Au ( $\text{H}(\text{AuCl}_4)$ , 2  $\mu\text{g/ml}$  Au) and electrophoresed for varying times. Based on the Au distribution it can be seen that after 1 minute the serum is just entering the gel and no separation has occurred. From 5-30 minutes the proteins in the serum migrate further into the gel and begin to separate according to their mass/charge ratio. After 30 minutes a leading peak due to unbound gold present in the solvent front can be observed. After 60 minutes of electrophoresis the sample has over-run, the solvent front is off the end of the gel and the protein bands begin to broaden and run into each other. As with the platinum studies the optimal time for electrophoresis was found to be around 45 minutes, although this time varied depending on the condition of the running buffer. Based on these results it was decided to run the gels until the solvent front (indicated by the leading band of bromophenol blue) had reached the lower edge of the gels, without running off the end of the gel.

Figure 4.2 shows the Au signal response for laser ablation ICP-MS of the albumin samples enriched with Au ( $\text{H}(\text{AuCl}_4)$ , 2  $\mu\text{g/ml}$  Au) and electrophoresed for various times. The results are similar to those obtained with serum, with the optimal electrophoresis time being  $\sim 45$  minutes. It can be seen from the two sets of results that inorganic gold binds to albumin. When serum is enriched with inorganic gold the majority of it is found with the albumin fraction, with a small amount found in two proteins peaks near the top of the gel. Further identification of these proteins was not possible using the system available.



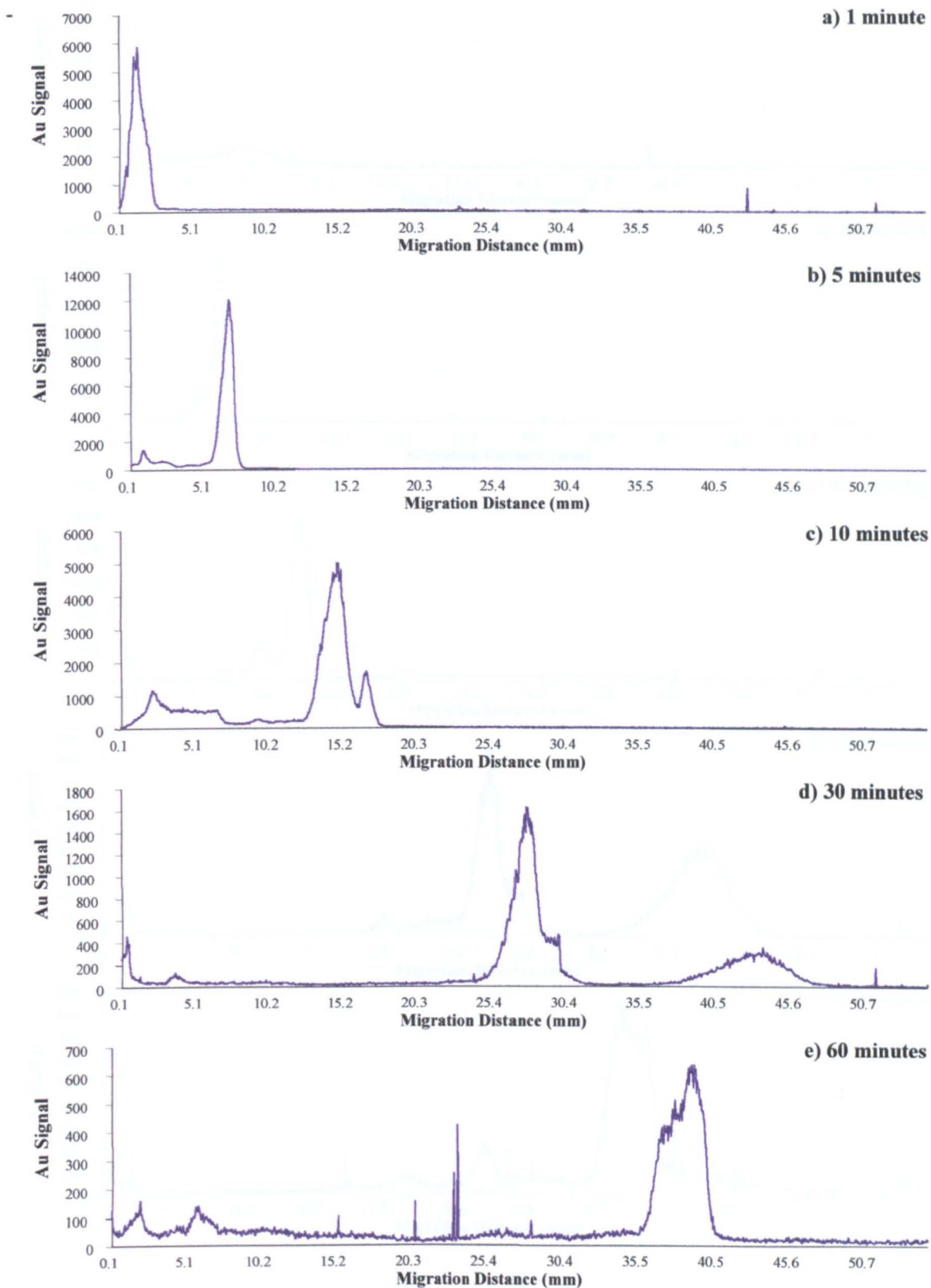


Figure 4.1:  $^{197}\text{Au}$  profiles for Au enriched serum samples ( $\text{H}(\text{AuCl}_4)$ ,  $2\ \mu\text{g/mL Au}$ ) electrophoresed for a) 1min b) 5mins c) 10mins d) 30mins e) 60mins

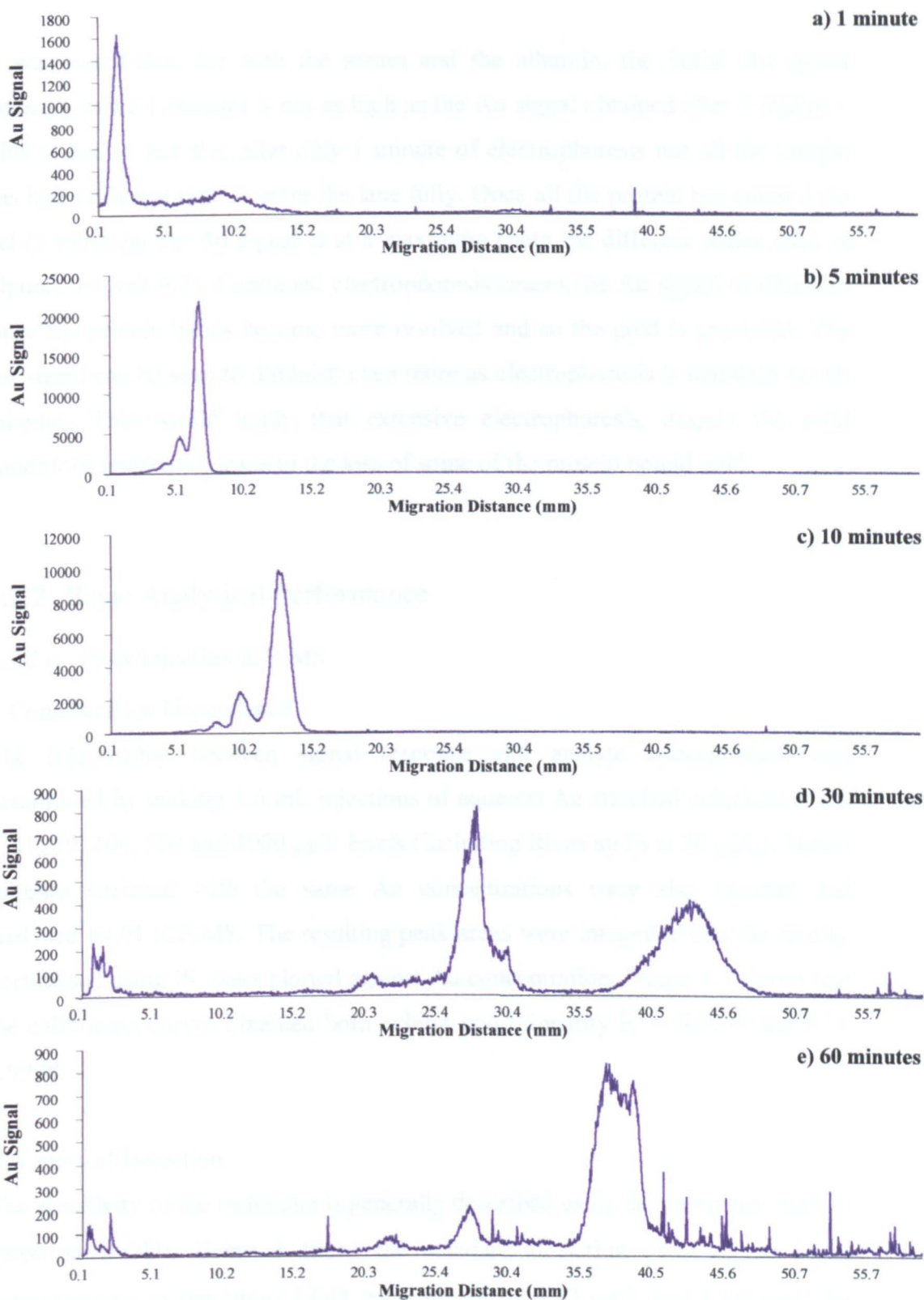


Figure 4.2:  $^{197}\text{Au}$  profiles for enriched albumin samples ( $\text{H}(\text{AuCl}_4)$  2  $\mu\text{g/mL Au}$ ) electrophoresed for a) 1min b) 5mins c) 10mins d) 30mins e) 60mins

It was noted that, for both the serum and the albumin, the initial Au signal intensity (after 1 minute) is not as high as the Au signal obtained after 5 minutes. This is due to fact that after only 1 minute of electrophoresis not all the sample has had sufficient time to enter the lane fully. Once all the protein has entered the gel (5 minutes) the Au signal is at a maximum (note the different scales used in Figures 4.1 and 4.2). Continued electrophoresis causes the Au signal to diminish since the protein bands become more resolved and so the gold is speciated. The Au signal can be seen to diminish even more as electrophoresis is maintain for 60 minutes. This would imply that extensive electrophoresis, despite the mild conditions employed, leads to the loss of some of the protein bound gold.

## 4.2.2 Basic Analytical Performance

### 4.2.2.a Flow Injection ICP-MS

#### I. Concentration Dependence

The relationship between signal response and analyte concentration was determined by making 1.0 mL injections of aqueous Au standard solutions at the 0, 10, 50, 100, 500 and 1000  $\mu\text{g/L}$  levels (including Rh as an IS at 20  $\mu\text{g/L}$ ). Serum samples enriched with the same Au concentrations were also injected and analysed by FI ICP-MS. The resulting peak areas were integrated and the results, normalised using IS, were plotted against Au concentration. Figure 4.3 shows that the calibration curves obtained both exhibit good linearity  $R^2 = 0.9999$  and  $R^2 = 0.9998$ .

#### II. Limits of Detection

The sensitivity of the technique is generally described using the parameter limit of detection (LOD). Using 3 times the standard deviation ( $3\sigma$ ) of the blank measurements to determine LOD gave values of 0.77  $\mu\text{g/L}$  and 0.89  $\mu\text{g/L}$  for aqueous and serum standards, respectively.

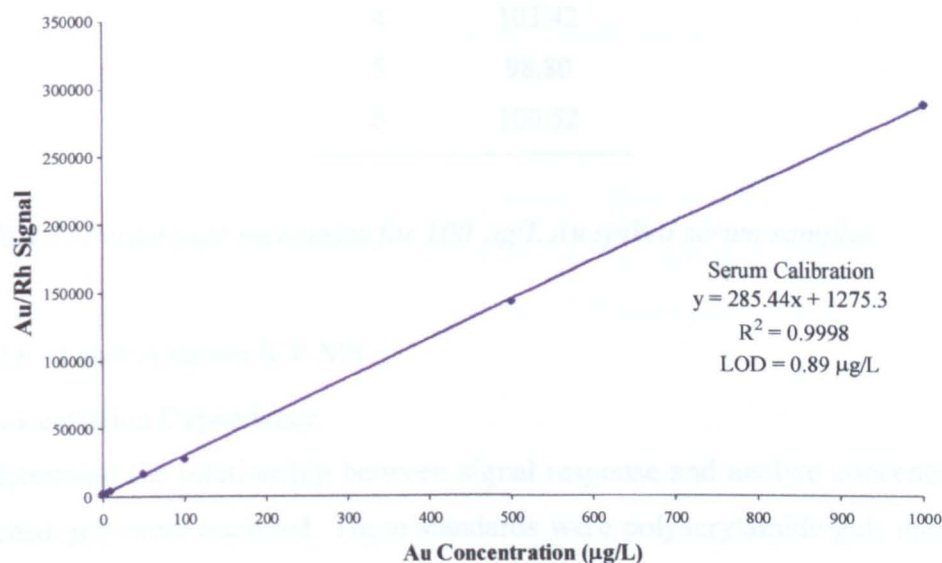
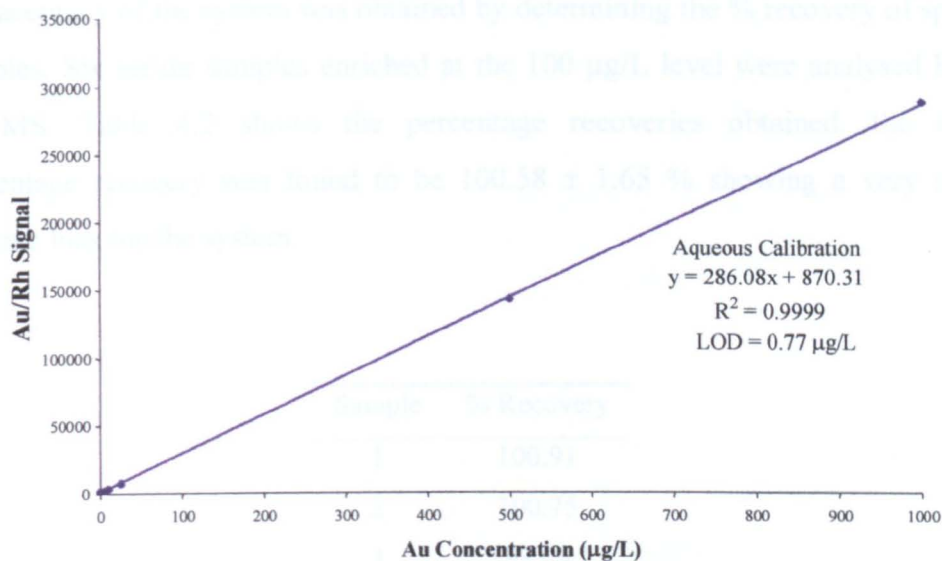


Figure 4.3: Calibration curves for FI ICP-MS of Au standards (0-1000  $\mu\text{g/L}$  Au)

### III. Measurement Precision

Precision is a measure of the reproducibility of a system. The most widely used value to express precision is the relative standard deviation (RSD) which gives a percentage value. The precision of the measurement was determined by injecting an aqueous standard solution (50  $\mu\text{g/L}$  Au) five times. Using the equation given previously an RSD of 1.55 % was calculated.

#### IV. Accuracy

The accuracy of the system was obtained by determining the % recovery of spiked samples. Six serum samples enriched at the 100 µg/L level were analysed by FI ICP-MS. Table 4.2 shows the percentage recoveries obtained. the mean percentage recovery was found to be  $100.58 \pm 1.65$  % showing a very slight positive bias for the system.

Sample	% Recovery
1	100.91
2	100.75
3	99.09
4	103.42
5	98.80
6	100.52

*Table 4.2: Percentage recoveries for 100 µg/L Au spiked serum samples*

#### 4.2.2.b Laser Ablation ICP-MS

##### I. Concentration Dependence

To determine the relationship between signal response and analyte concentration enriched gels were analysed. These standards were polyacrylamide gels enriched with varying levels of the analyte of interest, inorganic Au in this instance. Enriched gels were cast (see Section 2.2.3) containing 0, 0.1, 0.25, 0.5, 1.0, 2.0 and 4.45 µg/mL of Au (including internal standard Rh at 0.5 µg/mL in all gels). The gels were then interrogated using laser ablation in the raster mode.

The resulting peak areas were integrated and the results, normalised using IS, were plotted against Au concentration. The linearity of the line is indicated by the  $R^2$  value, the closer the value is to 1 the better the linearity of the systems concentration response. Figure 4.4 shows the calibration curve obtained, which exhibits good linearity with an  $R^2$  value of 0.9976.

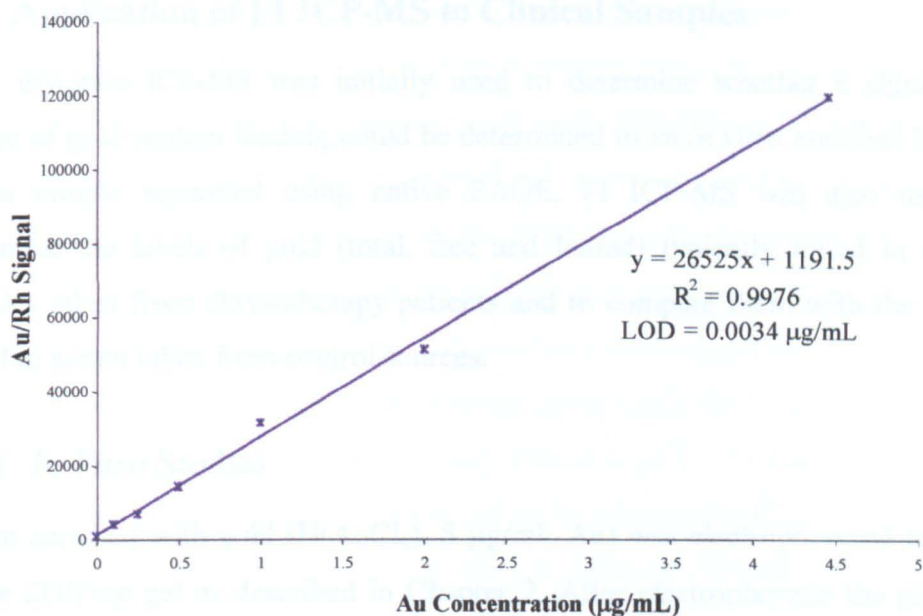


Figure 4.4: Calibration for LA ICP-MS of Au enriched gels (0-4.45 µg/mL Au)

## II. Limit of Detection

The sensitivity of the measurement is generally described using the parameter limit of detection (LOD). Using 3 times the standard deviation ( $3\sigma$ ) of the blank measurements to determine LOD gave a value of 0.0034 µg/mL for Au.

## III. Measurement Precision

The precision of the measurement was determined by interrogating an enriched gel (0.5 µg/mL Au) five times. Using the equation given previously, an RSD of 2.78 % was calculated.

## IV. Accuracy

Accuracy describes the closeness of a result to the true value. The accuracy of a system is best determined using appropriate certified reference materials (CRM), unfortunately these are not always generally available. Accuracy can also be determined by analysing spiked samples and determining spike recovery but this approach was not appropriate for present studies.

### 4.3 Application of FI ICP-MS to Clinical Samples

Flow injection ICP-MS was initially used to determine whether a significant degree of gold-protein binding could be determined in an *in vitro* enriched human serum sample separated using native PAGE. FI ICP-MS was also used to determine the levels of gold (total, free and bound) typically found in serum samples taken from chrysotherapy patients and to compare them with the levels found in serum taken from control sources.

#### 4.3.1 *In Vitro* Studies

Serum enriched with gold ( $H(AuCl_4)$ , 5  $\mu\text{g/mL Au}$ ) was electrophoresed using a native 2D/Prep gel as described in Chapter 2. After electrophoresis the gel was electro-eluted and the 14 resulting fractions were collected. Staining of the 2D/Prep gel after electro-elution showed that a large proportion of the protein was still associated with the gel. The fractions were analysed using FI ICP-MS to determine the amount of gold present in each fraction. The procedure was repeated with an unspiked serum sample. Table 4.3 shows the results obtained.

Fraction	Gold Enriched Serum ( $\mu\text{g/L}$ )	Unspiked Serum ( $\mu\text{g/L}$ )
1	4.536	0.114
2	2.143	0.096
3	1.552	0.134
4	1.928	0.119
5	0.904	0.154
6	0.635	0.131
7	1.302	0.202
8	3.497	0.151
9	6.614	0.209
10	0.764	0.018
11	0.139	0.041
12	0.263	0.004
13	0.177	0.014
14	0.294	0.008

Table 4.3: Au concentrations in electro-elution fractions for Au enriched serum ( $H(AuCl_4)$ , 5  $\mu\text{g/mL Au}$ ) and un-enriched serum

In order to make the electro-elution results meaningful, the protein concentration of each fraction was determined. The protein concentrations for the fractions were calculated using the Bio-Rad protein assay (see Appendix 2.1). The enriched serum ( $H(AuCl_4)$ ,  $5 \mu\text{g/ml Au}$ ) was diluted 1:1 with sample buffer, of this  $75 \mu\text{L}$  were loaded onto the gel. A further 100 fold dilution of the serum occurred during electro-elution. This would result in a final gold concentration of  $25 \mu\text{g/L}$  (assuming all protein eluted from gel). Figure 4.5 shows a graphical representation of the result obtained. Based on the average protein concentration of serum ( $70 \text{ mg/ml}$  before dilution) the protein recovery from the gel by electro-elution is only 25.74 %. This recovery might be improved on by altering the buffer systems and operating parameters, but care must be taken to maintain the metal-protein bonds of interest.

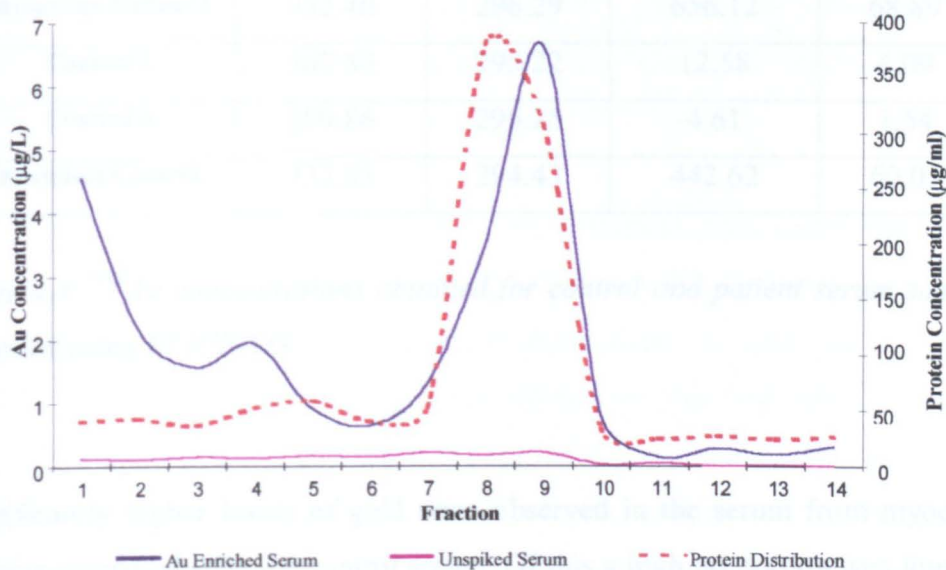


Figure 4.5:  $^{197}\text{Au}$  concentration profile and protein distribution for FI ICP-MS analysis of electro-elution fractions collected following PAGE of Au enriched serum ( $H(AuCl_4)$ ,  $5 \mu\text{g/mL Au}$ ), and un-enriched serum

The horizontal positioning of the fractions in Figure 4.5 correlates directly with the position of the fraction along the gel lane. As a result the plot can be directly compared to the gold profiles obtained using laser ablation ICP-MS. It can be seen that the fractions 8-10 contain the albumin fraction. The plot also shows that hardly any protein bound gold is present in the unspiked serum. This is consistent with other experimental findings (see Figure 4.7).



### 4.3.2 *In Vivo* Studies

Control serum samples and serum samples taken from chrysotherapy patients were analysed in triplicate using FI-ICP-MS. Total and free gold levels were determined by the use of ultrafiltration (as described in Ch2). Using these results levels of bound gold were calculated in each case. The results obtained are shown in Table 4.4.

	<b>Total Au (<math>\mu\text{g/L}</math>)</b>	<b>Free Au (<math>\mu\text{g/L}</math>)</b>	<b>Bound Au (<math>\mu\text{g/L}</math>)</b>	<b>Au Bound %</b>
<b>Myocrisin Patient 1</b>	468.74	295.73	173.01	36.91
<b>Myocrisin Patient 2</b>	952.40	296.29	656.12	68.89
<b>Control 1</b>	307.80	295.22	12.58	4.09
<b>Control 2</b>	299.86	295.25	4.61	1.54
<b>Enriched Control</b>	737.05	294.43	442.62	60.05

*Table 4.4:  $^{197}\text{Au}$  concentrations obtained for control and patient serum samples analysed using FI ICP-MS*

Significantly higher levels of gold were observed in the serum from myocrisin patients compared with the control serum. Of this a high proportion was found to be protein bound although the degree of protein binding varied greatly between the two patients. Very little of the gold present in the control serum was protein bound, this is possibly due to the source of the gold in the control serum. Control 3 was a control serum sample enriched with gold ( $\text{H}(\text{AuCl}_4)$ ,  $500 \mu\text{g/L Au}$ ). The percentage recovery for the system was 85.40 % and so as such the results show a slight negative bias.

## 4.4 Application of LA ICP-MS to Clinical Samples

### 4.4.1 *In Vitro* Studies

*In vitro* studies were carried out initially to gain some insight into the complexation pattern for Au in serum. In an initial study the binding of different gold species with pure proteins was studied. The effect of equilibration time on protein binding was also studied.

#### 4.4.1.a Pure Proteins Enriched with Inorganic Gold

Physiological concentrations of albumin (50 mg/mL), transferrin (3.0 mg/ml) and  $\alpha_2$ -macroglobulin (4.0 mg/mL), were enriched with inorganic gold ( $\text{H}(\text{AuCl}_4)$ , 50  $\mu\text{g/mL}$  Au). After a 24 hour equilibration period the samples were electrophoresed. The dried gels were then analysed using laser ablation ICP-MS. The gold distribution profiles obtained are shown in Figure 4.6.

The level of gold added to the proteins was extremely high, much higher than normal physiological levels encountered,  $\sim 0.35 \mu\text{g/L}^{202}$ . By using such a high gold concentration the relative affinities of the proteins for gold can be studied. By studying the gold profiles obtained it can be seen that both albumin and  $\alpha_2$ -macroglobulin exhibit a high degree of gold binding. The levels of gold found in serum are unlikely to exceed the number of potential binding sites available on the serum proteins. The multiple gold peaks in the albumin profile can be explained by the presence of albumin polymers.

Some form of transferrin-gold interaction can also be observed but to a much lesser degree than that observed with albumin and  $\alpha_2$ -macroglobulin. In the absence of other proteins competing for gold binding only a low level of gold-transferrin binding occurs. It is, therefore, unlikely that a significant degree of gold-transferrin binding will occur in serum where many other proteins are present. Albumin, which is present in serum at high concentrations and readily binds gold, is one such competing protein.

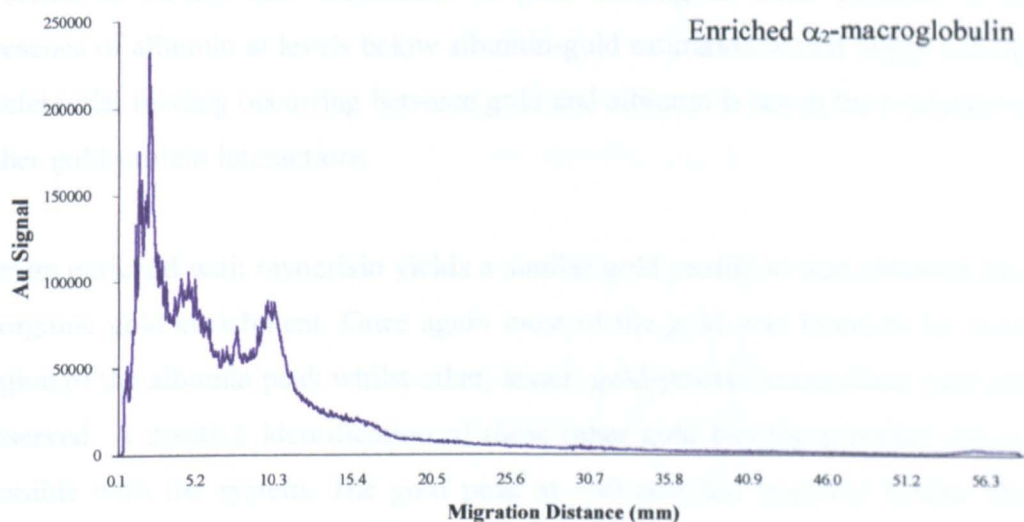
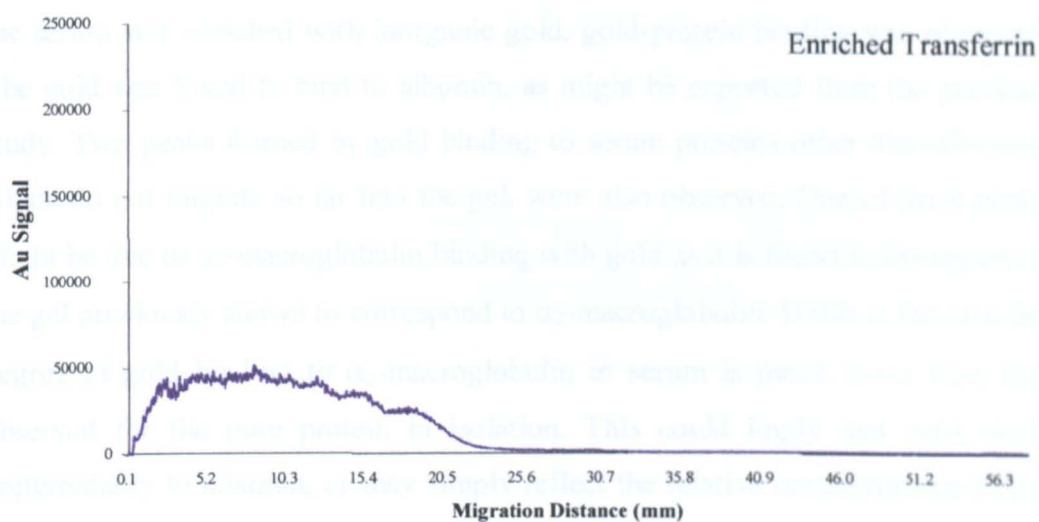
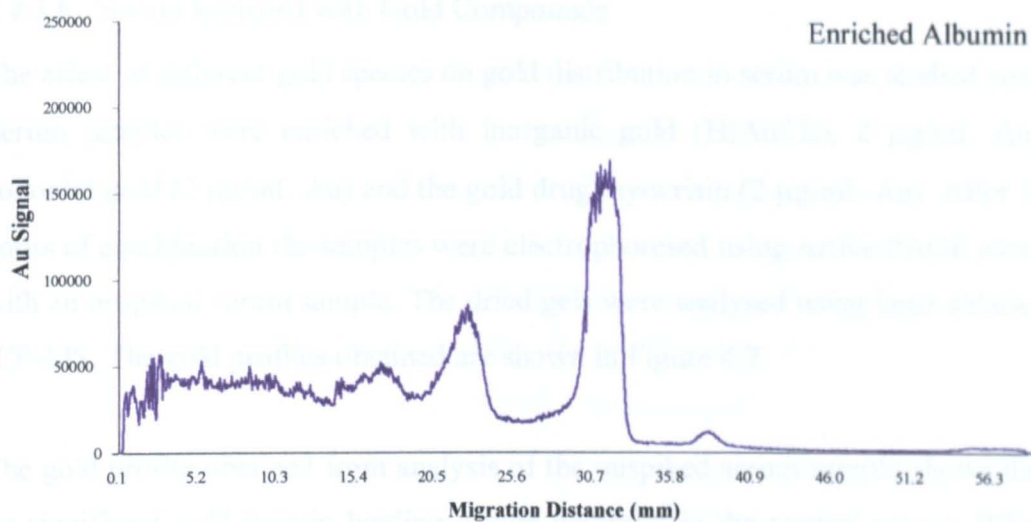


Figure 4.6:  $^{197}\text{Au}$  profiles obtained for pure proteins enriched with inorganic gold, ( $\text{H}(\text{AuCl}_4)$ ,  $50 \mu\text{g/mL Au}$ ).

#### 4.4.1.b Serum Enriched with Gold Compounds

The effect of different gold species on gold distribution in serum was studied next. Serum samples were enriched with inorganic gold ( $\text{H}(\text{AuCl}_4)$ , 2  $\mu\text{g}/\text{mL}$  Au), colloidal gold (2  $\mu\text{g}/\text{mL}$  Au) and the gold drug myocrisin (2  $\mu\text{g}/\text{mL}$  Au). After 24 hours of equilibration the samples were electrophoresed using native PAGE along with an unspiked serum sample. The dried gels were analysed using laser ablation ICP-MS. The gold profiles obtained are shown in Figure 4.7.

The gold profile obtained from analysis of the unspiked serum sample shows that no significant gold-protein binding occurs naturally in the control serum. When the serum was enriched with inorganic gold, gold-protein binding was observed. The gold was found to bind to albumin, as might be expected from the previous study. Two peaks formed by gold binding to serum proteins other than albumin, which do not migrate so far into the gel, were also observed. One of these peaks might be due to  $\alpha_2$ -macroglobulin binding with gold as it is found in the region of the gel previously shown to correspond to  $\alpha_2$ -macroglobulin. If this is the case the degree of gold binding to  $\alpha_2$ -macroglobulin in serum is much lower than that observed for the pure protein in isolation. This could imply that gold binds preferentially to albumin, or may simply reflect the relative concentrations of the proteins in serum. The occurrence of gold binding to other proteins in the presence of albumin at levels below albumin-gold saturation would imply that any preferential binding occurring between gold and albumin is not at the exclusion of other gold-protein interactions.

Serum enriched with myocrisin yields a similar gold profile to that obtained from inorganic gold enrichment. Once again most of the gold was found to be in the region of the albumin peak whilst other, lesser, gold-protein interactions were also observed. A positive identification of these other gold binding proteins was not possible with the system. The gold peak at  $\sim 40$  mm has migrated further than albumin indicating a smaller protein (gradient gel restricts the migration of large proteins). A possible protein associated with this peak is pre-albumin which has a molecular mass of 61 kDa.

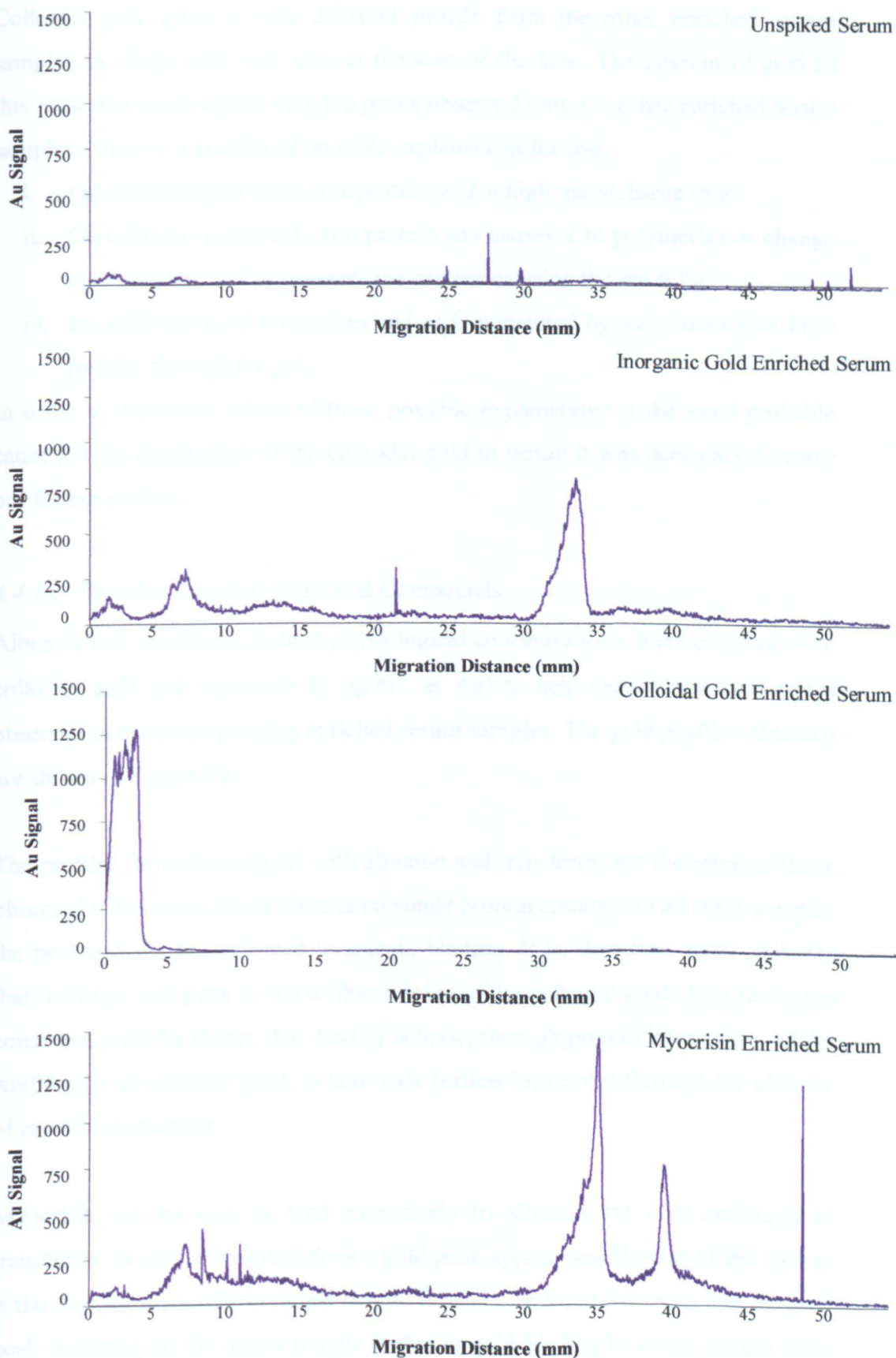


Figure 4.7:  $^{197}\text{Au}$  profiles obtained for profiles for control serum and serum enriched with inorganic gold, colloidal gold and myocrisin ( $2\ \mu\text{g}/\text{mL Au}$ ).

Colloidal gold gives a very different profile from the other enriched serum samples. A single peak was seen at the start of the lane. The amount of gold in this peak was much higher than the peaks observed with the other enriched serum samples. There is a number of possible explanations for this;

- i, the colloidal gold binds to a protein with a high mass/charge ratio
- ii, the colloidal gold binds to a protein and causes it to polymerise or change conformation and so prevents the protein entering the gel fully
- iii, the colloidal gold flocculates and so is prevented by size limitations from passing through the gel.

In order to determine which of these possible explanations is the most probable cause for the distribution of the colloidal gold in serum it was necessary to carry out further studies.

#### *4.4.1.c Proteins Enriched with Gold Compounds*

Albumin and transferrin, both at physiological concentrations, were enriched with colloidal gold and myocrisin (2 µg/mL as Au) to help explain the gold peaks observed in the corresponding enriched serum samples. The gold profiles obtained are shown in Figure 4.8.

The profiles for colloidal gold with albumin and transferrin are the same as those observed with serum. Since there is no single protein common to all three samples the peak can not be attributed to protein binding. It is, therefore, most probable that the large gold peak is due to flocculation of the colloidal gold. This finding is consistent with the theory that Au(III) is toxic, through protein interaction, whilst Au(0) such as colloidal gold, is non-toxic (efficacious even) through the absence of protein interactions.

Myocrisin can be seen to bind extensively to albumin but only sparingly to transferrin. In neither instance does a gold peak appear near the top of the lane as is the case for myocrisin enriched serum. It can be deduced from this that the gold peak occurring in the serum sample is due to gold binding to some protein other than albumin and transferrin.

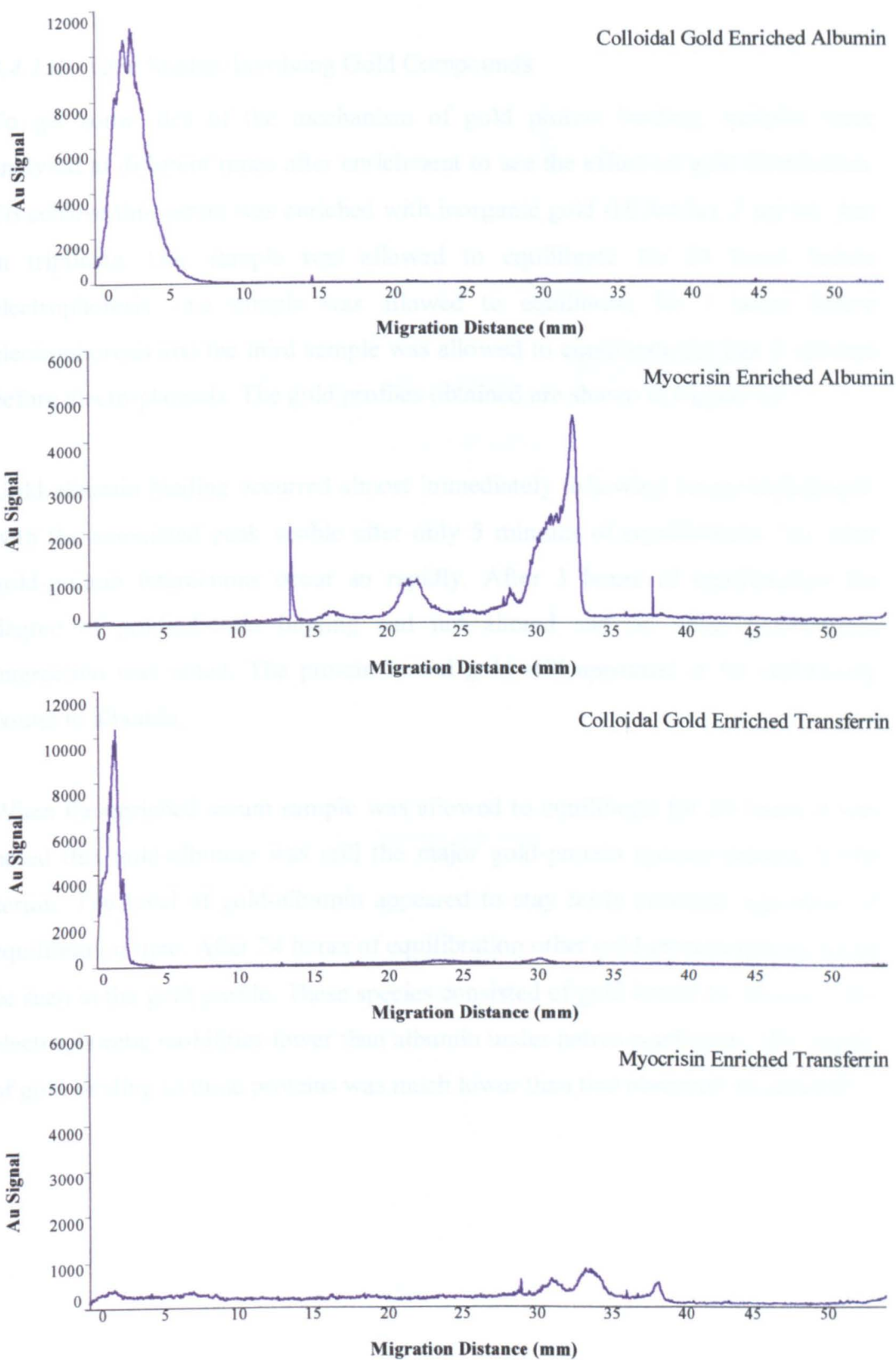


Figure 4.8:  $^{197}\text{Au}$  profiles for albumin and transferrin enriched using colloidal gold and myocrisin ( $2\ \mu\text{g/mL}$ , Au)

#### 4.4.1.d Time Studies Involving Gold Compounds

To get some idea of the mechanism of gold protein binding, samples were analysed at different times after enrichment to see the effect on gold distribution. To achieve this serum was enriched with inorganic gold ( $\text{H}(\text{AuCl}_4)$ , 2  $\mu\text{g}/\text{mL}$  Au) in triplicate. One sample was allowed to equilibrate for 24 hours before electrophoresis, one sample was allowed to equilibrate for 3 hours before electrophoresis and the third sample was allowed to equilibrate for just 5 minutes before electrophoresis. The gold profiles obtained are shown in Figure 4.9.

Gold-albumin binding occurred almost immediately following serum enrichment, with the associated peak visible after only 5 minutes of equilibration. No other gold-protein interactions occur so rapidly. After 3 hours of equilibration the degree of gold-albumin binding had not altered and no other gold-protein interaction was noted. The protein bound gold still appeared to be exclusively bound to albumin.

When the enriched serum sample was allowed to equilibrate for 24 hours it was noted that gold-albumin was still the major gold-protein species present in the serum. The level of gold-albumin appeared to stay fairly constant regardless of equilibration time. After 24 hours of equilibration other gold-protein species could be seen in the gold profile. These species consisted of gold bound to proteins with electrophoretic mobilities lower than albumin under native conditions. The degree of gold binding to these proteins was much lower than that observed for albumin.



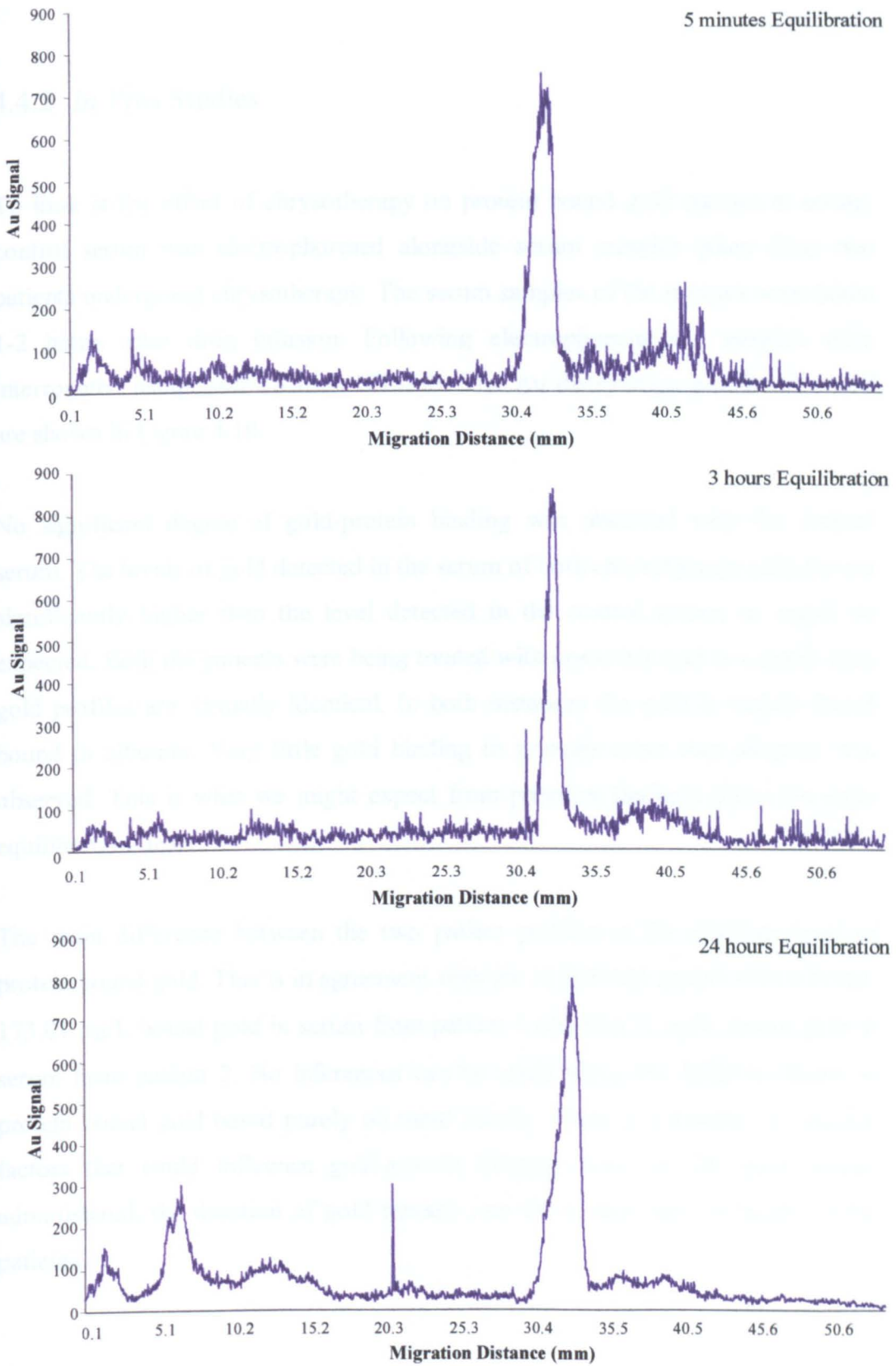


Figure 4.9:  $^{197}\text{Au}$  profiles for Au enriched serum ( $\text{H}(\text{AuCl}_4)$ ,  $2 \mu\text{g/mL Au}$ ) following various equilibration times

#### 4.4.2 *In Vivo* Studies

To look at the effect of chrysotherapy on protein bound gold species in serum, control serum was electrophoresed alongside serum samples taken from two patients undergoing chrysotherapy. The serum samples of the patients were taken 1-2 hours after drug infusion. Following electrophoresis the samples were interrogated using laser ablation ICP-MS. The Au distribution profiles obtained are shown in Figure 4.10.

No significant degree of gold-protein binding was observed with the control serum. The levels of gold detected in the serum of both chrysotherapy patients are significantly higher than the level detected in the control serum, as might be expected. Both the patients were being treated with myocrisin and as a result their gold profiles are virtually identical. In both instances the gold is mainly found bound to albumin. Very little gold binding to proteins other than albumin was observed. This is what we might expect from previous findings given the short equilibration time.

The main difference between the two patient profiles is the absolute level of protein bound gold. This is in agreement with the FI ICP-MS results which found, 173.01  $\mu\text{g/L}$  bound gold in serum from patient 1 and 656.12  $\mu\text{g/L}$  bound gold in serum from patient 2. No inferences can be made about the different levels of protein bound gold based purely on these results. There is a number of external factors that could influence gold-protein binding, such as: the gold dosage administered, the duration of gold therapy and the overall state of health of the patients.

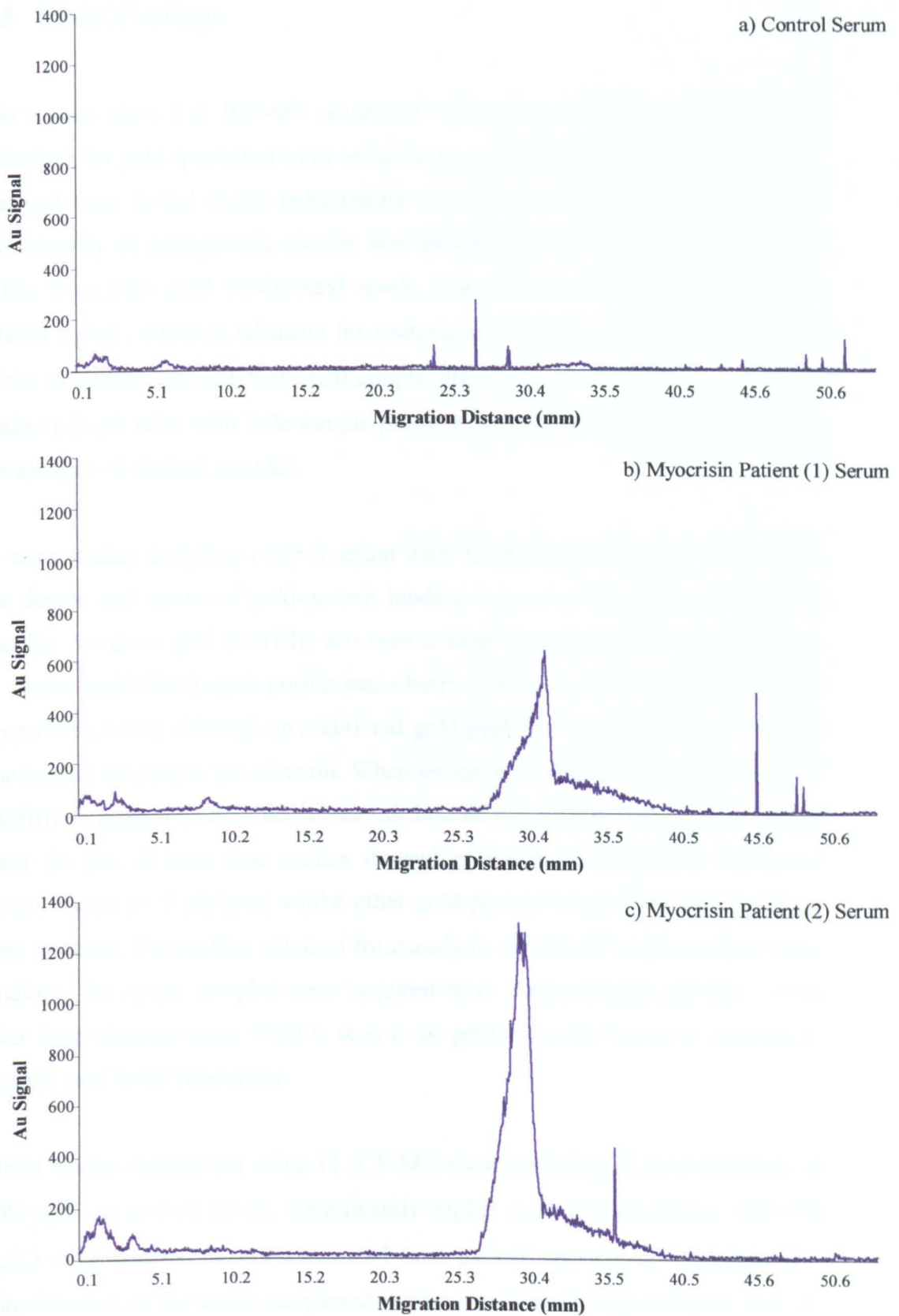


Figure 4.10:  $^{197}\text{Au}$  profiles from analysis of *in vivo* samples.

a) Control serum, b) Myocrisin patient 1, c) Myocrisin patient 2

## 4.5 Main Findings

The results show LA ICP-MS combined with native PAGE to be a suitable technique for gold speciation work using serum samples from patients undergoing chrysotherapy. Initial studies indicated the experimental conditions were such that the integrity of gold-protein species was maintained and the technique did not suffer from high gold background levels. The LOD for gold in the gels was 0.0034  $\mu\text{g/mL}$ , which is adequate for analysis of patient's serum. The sensitivity of the technique was such that small sample volumes could be used (2.5  $\mu\text{L}$  serum loaded per gel lane) with little sample preparation, both very important factors in the analysis of clinical samples.

*In vitro* studies enriching control serum with different gold species showed that the degree and nature of gold-protein binding was very dependent on the gold species. Inorganic gold (Au(III)) was seen to bind most abundantly with albumin. A similar gold distribution profile was observed when serum was enriched with myocrisin (Au(I)) although an additional gold peak was observed which may be due to gold binding to pre-albumin. When serum was enriched with colloidal gold (Au(0)) no protein binding was observed, instead the gold flocculated and did not enter the gel. *In vitro* time studies showed gold-albumin binding to be almost instantaneous (< 5 minutes) whilst other gold-protein interactions took a longer time to occur. The profiles obtained from analysis of clinical samples reflect these findings, the serum samples were acquired from chrysotherapy patients 1 hour after drug administration. Gold is seen to be predominantly bound to albumin as was the case in the time study.

Initial studies carried out using FI ICP-MS show typical gold concentrations of 300  $\mu\text{g/L}$  in control serum. Significantly higher gold concentrations (469-952  $\mu\text{g/L}$ ) were detected in serum obtained from patients undergoing chrysotherapy. Ultrafiltration of the serum samples showed a significantly higher degree of gold-protein binding in the serum of the chrysotherapy patients (37-69 %) compared to that observed in the control serum (~2 %).

The source of serum gold is a possible explanation for the observed differences in the degree of gold-protein binding. In the control, serum gold is likely to result from the subject wearing gold jewellery. Gold in the jewellery is solubilised and absorbed through the skin as  $\text{AuCl}_4^-$ . In the patient's serum samples administration of Au(I) drugs is likely to be the main source of gold. It would appear the absorbed gold species is less inclined to protein binding than the gold drugs.

The large variation in the levels of serum gold and the degree of protein binding in patient's serum can be put down to differences in the length of chrysotherapy, which can, unlike platinum therapy, go on indefinitely. These findings imply absolute gold levels are of little diagnostic use when trying to assess adverse reactions to gold. The degree of protein-bound gold, however, may be more relevant to such studies.

Overall the technique proved successful in the speciation of gold species in human serum, in particular clinical samples obtained from patients undergoing chrysotherapy. It would be interesting to carry out extensive trials into colloidal gold therapy, a study to which this technique could be applied directly.

## **Chapter 5: Multi-Element Studies**

### **5.1 Introduction**

Metals have always been present in mans environment without necessarily posing any health risks. However over the last 200 years man has managed to alter the relative availability and the form in which these metals occur through industrialisation. Two key areas of industrialisation can be used to highlight the emission of metals into the environment. The use of fossil fuels to generate energy creates acid rain, which in turn mobilises aluminium. The mining industry has led to metals being released from their ore deposits into the ambient environment.

The human body functions under homeostatic control, which is to say there is a balanced system of elements present in the cells. Any foreign compounds are a potential risk to this delicate balance. Even otherwise innocuous compounds pose a risk if they are present at excessive concentrations. This means that as a result of anthropogenic emissions health problems can arise caused by elements with significant biological roles as well as those with no apparent biological roles. In 1980 a critical evaluation was written regarding the 'normal levels' of trace elements in human blood and plasma<sup>208</sup>.

Over the last 60 years an enormous effort has been made to investigate the role of trace metals in the biochemical and physiological processes occurring within the human body. In order achieve this it is necessary to determine how different metal species interact with biological molecules and also to determine how different metal species interact with one another within such systems. A wide variety of speciation methods (see Section 1.4) can be used to determine metal metabolites occurring in biological systems. Metals of interest can be roughly grouped according to their naturally occurring concentration in the human body.

The first group of metals of interest are those which occur naturally in the body at trace levels. These metals are usually essential to humans and so a deficiency of such metals can lead to health problems.

The second group of metals of interest includes those that may be present in humans at unnaturally elevated levels. Such an excess of metal can be due to the failure of an intrinsic control mechanism or through unusual environmental exposure. These metals may have some essentiality, but at excessive levels health problems occur. Metal ion antagonism is one example of how these health problems can arise. An example of such an element is cobalt. In the form of Vitamin B<sub>12</sub> cobalt is essential to man. Metal workers are a group particularly at risk of excessive exposure to cobalt. Inhalation of cobalt containing dusts has been found to damage lungs, heart and skin and is an occupational carcinogen.

Assessing the total body status of a particular metal will involve determining its concentration in serum. However, such measurements may not be clinically relevant without further knowledge of the degree and nature of protein binding in the serum sample. In this chapter we look at the speciation of some naturally occurring trace metals in serum using the technique developed in earlier chapters. This technique was also used to detect protein bound metal species in serum sample enriched *in vitro* with metal ions of interest.

## **5.2 Application of LA ICP-MS to Clinical Samples**

It was established in earlier studies that laser ablation ICP-MS was a suitable technique for the speciation of metals in biological samples separated using PAGE. Using the parameters determined in this earlier work, (see chapters 3 and 4) serum samples were analysed to determine the distribution of a variety of metals. The first section of this study looked at metals naturally occurring at trace levels in human serum. Next serum samples were enriched *in vitro* with some metals of interest through anthropogenic emission. Finally serum samples were enriched *in vitro* with multi-element solutions to see how metals interact in serum.

## 5.2.1 Essential Metals Naturally Occurring in Serum

There are a number of metals that naturally occur in serum at trace levels. These elements are essential to life and carry out a number of important roles in metalloenzymes and proteins. Unfortunately for analysis using ICP-MS, most of these elements have relatively low atomic masses (<80) and so fall in the mass region where interference from molecular ions poses a common problem. A classic example of this is calcium, an essential element performing a number of different functions in the body. The most abundant calcium isotope with 96.9 % abundance has a mass of 40 and so is isobaric with Ar used to produce the plasma. Another problem faced when analysing biological samples for such elements is the problem of contamination since these elements are so commonplace.

To get an idea of the distribution of some essential metals in serum a few of the elements more readily detected by ICP-MS were investigated. Care was taken when choosing which mass to monitor bearing in mind any likely interferences. As a result the masses monitored were not necessarily the most sensitive masses available, but were thought to be those with the least interferences associated.

### 5.2.1.a Iron

Iron is the most abundant transition metal on earth, and with regard to its biological activity it is the most versatile of all the elements<sup>209</sup>. In the adult human body there are 3-4 g of functional and stored iron. Less than 0.1 % of total body iron is transferrin bound.

Transferrin is a serum protein used in iron transport and exchange between body tissues. Transferrin has a molecular mass of ~75 kDa and a typical concentration in serum of 2 mg/mL. Each transferrin molecule has two iron binding sites and in general serum transferrin is only 40 % saturated with iron. This gives a rough value of 1.2 µg/mL transferrin bound iron in serum, see Appendix 2.2 for the calculation. Transferrin is known to bind a number of other metals as well as iron and so is of interest in metal speciation.



A control serum sample was made up as described in Section 2.2.2. The serum sample then underwent native PAGE as described in Section 2.2.3. Figure 5.1 shows the Fe distribution profile obtained when the serum sample was interrogated using LA ICP-MS.  $^{57}\text{Fe}$  was monitored despite the relatively low abundance (2.2 %) due the potential interference on  $^{56}\text{Fe}$  (91.7 % abundant) from  $^{40}\text{Ar}^{16}\text{O}^+$ .

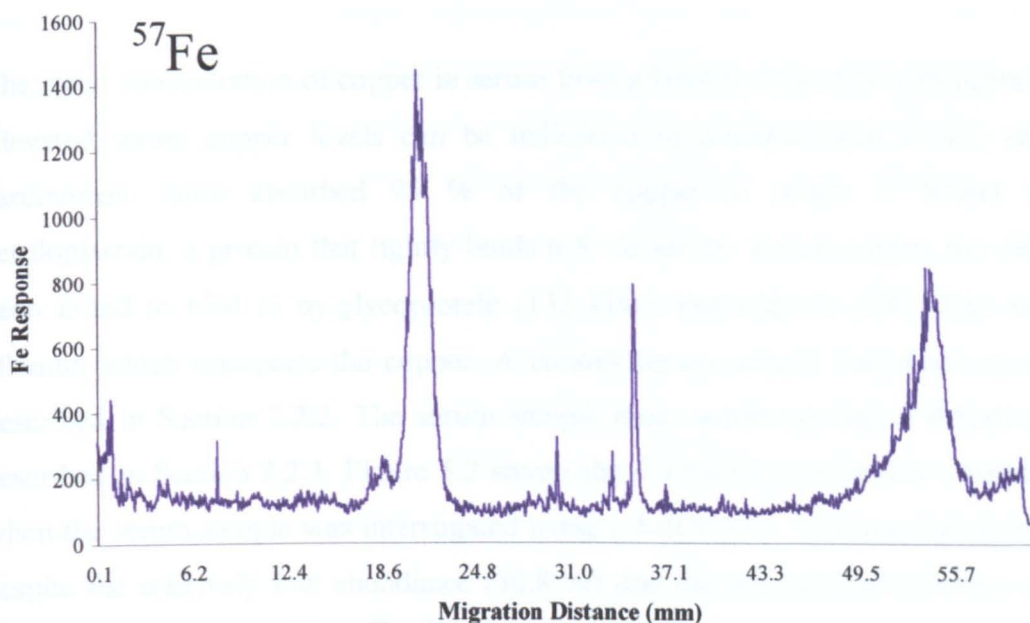


Figure 5.1:  $^{57}\text{Fe}$  profile for unspiked serum

The large iron peak present at  $\sim 23$  mm corresponds with the position of transferrin, the second iron peak (at  $\sim 53$  mm) corresponds with the position of the solvent front. This would indicate that most of the iron present in human serum is bound to transferrin. The remainder of the iron in human serum passes through the gel with the solvent front showing it to be free-iron, that is to say not protein bound (may be bound to low molecular mass fractions of serum). This is consistent with the literature.

### 5.2.1.b Copper

Despite being as inherently toxic as non-essential heavy metals, copper is essential to life. Nature has minimised the potential toxicity of copper by developing processes to eliminate excess ingested copper, by utilising copper only as a prosthetic element tightly bound to specific copper proteins and by interactions with zinc, molybdenum and iron. Copper toxicity seems to be wholly due to free copper ions altering the physiological functions of new copper proteins by combining with them.

The mean concentration of copper in serum from a healthy subject is 1.19  $\mu\text{g/mL}$ . Elevated serum copper levels can be indicative of diseases such as RA and carcinomas. Once absorbed 95 % of the copper in serum is bound to ceruloplasmin, a protein that tightly binds 6-8 Cu atoms. Serum copper has also been found to bind to  $\alpha_2$ -glycoprotein (132 kDa), transcuprein (270 kDa) and albumin which transports the copper. A control serum sample was made up as described in Section 2.2.2. The serum sample then underwent native PAGE as described in Section 2.2.3. Figure 5.2 shows the Cu distribution profile obtained when the serum sample was interrogated using LA ICP-MS.  $^{65}\text{Cu}$  was monitored despite the relatively low abundance (30.8 %) due the potential interference on  $^{63}\text{Cu}$  (69.2 % abundant) from  $^{40}\text{Ar}^{23}\text{Na}^+$ .

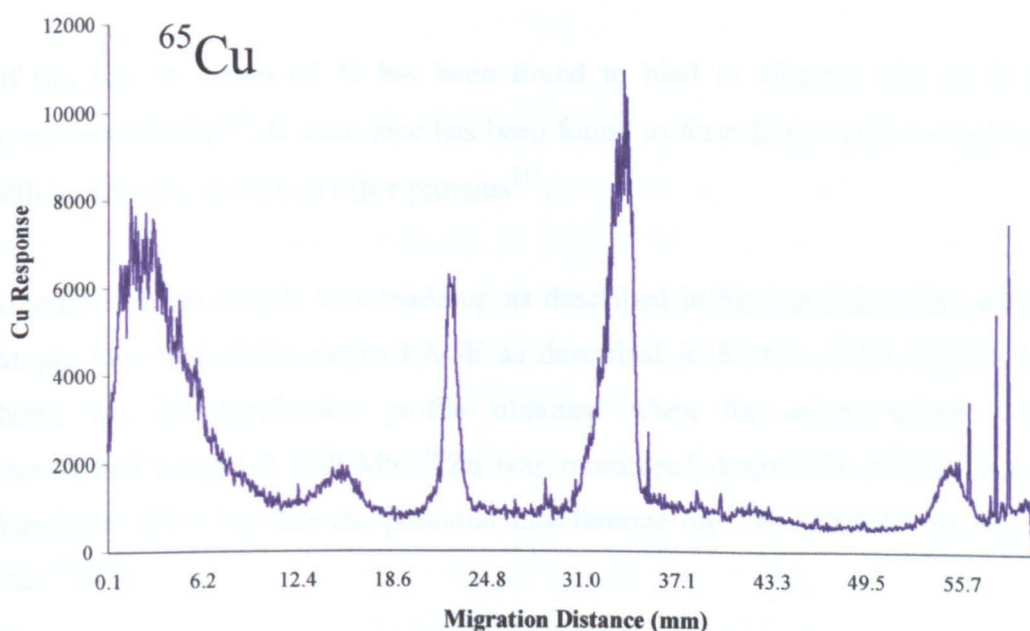


Figure 5.2:  $^{65}\text{Cu}$  profile for unspiked serum

A number of copper peaks can be seen in the profile. The peak at ~54 mm corresponds to the solvent front whilst the peak at ~35 mm corresponds with the position of the albumin peak. Three other copper peaks are also present at; ~22 mm, 16 mm and 4 mm. The first of these peaks is very close to the transferrin peak but does not quite overlap with the position of the iron-transferrin peak. This could be due to the fact that copper binds with transferrin resulting in a slightly different migration rate than for the iron-transferrin species. Alternatively the peak could be due to copper binding to a protein of a similar mass/charge to transferrin. It is possible that these peaks correspond to the copper binding proteins found in serum as mentioned in the literature. In order to positively identify the proteins corresponding to the three copper peaks further work would need to be done.

#### 5.2.1.c Zinc

Zinc is an essential component of over 70 metallo-enzymes. Zinc deficiency can affect growth and reproduction. Typical healthy zinc concentrations in serum are in the range 0.7-1.8 mg/L. AAS can be used to determine total plasma zinc levels but this information is insufficient for the diagnosis of marginal cases of zinc deficiency. There is clearly a need for better understanding of zinc speciation in serum.

Of the zinc in serum 65 % has been found to bind to albumin and 35 % to  $\alpha_2$ -macroglobulin<sup>210</sup>. *In vitro* zinc has been found to form fairly stable complexes with transferrin, as well as other proteins<sup>211</sup>.

A control serum sample was made up as described in Section 2.2.2. The serum sample then underwent native PAGE as described in Section 2.2.3. Figure 5.3 shows the Zn distribution profile obtained when the serum sample was interrogated using LA ICP-MS. <sup>66</sup>Zn was monitored despite the relatively low abundance (27.9 %) due the potential interference on <sup>64</sup>Zn (48.6 % abundant) from <sup>32</sup>S<sup>32</sup>S<sup>+</sup>.

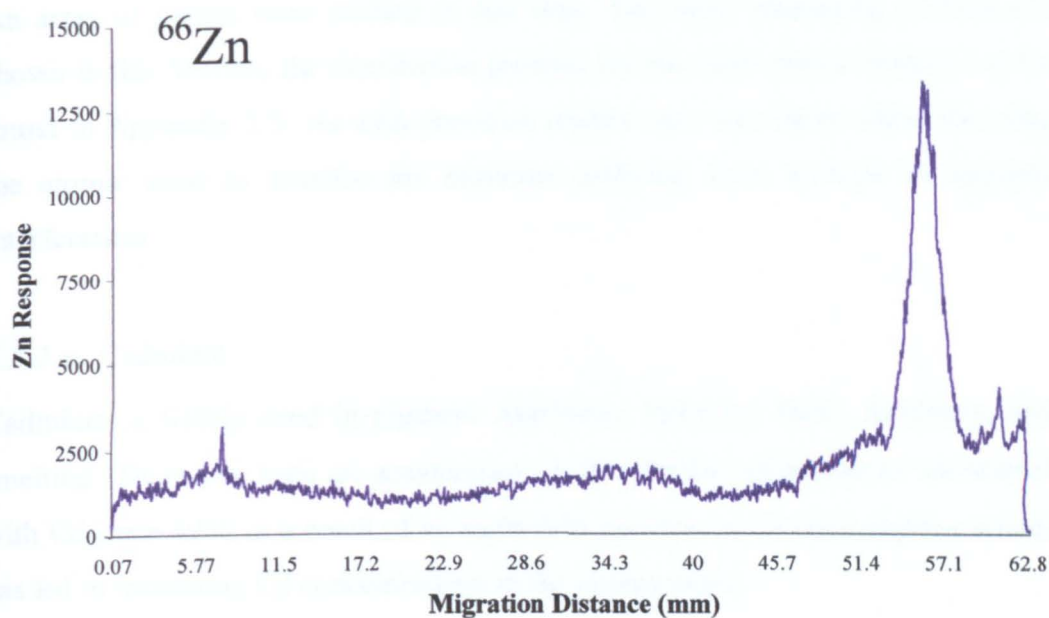


Figure 5.3:  $^{66}\text{Zn}$  profile for unspiked serum

Unlike the studies involving iron and copper no significant zinc-protein binding was observed in the control serum. The zinc peak at  $\sim 55$  mm corresponds to unbound Zn passing through the gel with the solvent front. These findings could imply that Zn-protein bonds naturally occurring in serum are relatively weak or labile and are broken down through electrophoresis.

### 5.2.2 Anthropogenically Enriched Metals

There are a number of metals that occur in serum at ultra-trace levels. These elements are not necessarily essential to healthy life. In general these elements have a higher atomic mass than those elements with biological roles and are not as readily available in the biosphere. Anthropogenic emissions have resulted in humans being exposed to elevated levels of some of these elements. Industrial exposure and metallo-drug therapy are among potential sources of such metals. In order to gain an insight into the distribution of some of these enriched metals in serum, studies were carried out using serum samples enriched (at levels much higher than those found physiologically) *in vitro*. As previously described the samples were analysed using LA ICP-MS.

An array of metals were studied in this way. The most interesting profiles are shown in this Section, the distribution profiles for the other metals studied can be found in Appendix 2.3. As with previous studies care was taken when choosing the atomic mass to monitor for elements suffering from isobaric or spectral interferences.

#### 5.2.2.a Cadmium

Cadmium is widely used in pigment stabilisers, batteries, fuels, fertilisers, and smelting. There has been an acceleration in the number of problems associated with Cd since 1950 as a result of an eight-fold increase in Cd consumption which has led to increasing Cd concentrations in the environment.

Cadmium has no proven essentiality in man but is known to interfere with the normal metabolism of zinc. Cadmium poisoning as a result of industrial exposure is not uncommon, toxicity is thought to be due to competition between Cd and Zn for zinc enzyme cofactor sites. Normal serum Cd levels of 1.1  $\mu\text{g/L}$  – 3.3  $\mu\text{g/L}$  have been reported<sup>212</sup>, whilst levels in workers serum has been reported as eight times higher<sup>213</sup>. Cadmium reacts readily with proteins and other biological molecules. Stored cadmium is thought to bind to the cysteine rich protein metallothionein. Occurrence of low affinity albumin binding<sup>214</sup> and high affinity  $\alpha_2$ -macroglobulin binding<sup>215</sup> has been reported.

A control serum sample was enriched using a Cd standard solution (5  $\mu\text{g/mL}$ , Cd) as described in Section 2.2.2. After 24 hours of equilibration the serum sample underwent native PAGE as described in Section 2.2.3. Figure 5.4 shows the Cd distribution profiles obtained when the Cd enriched serum sample and a control serum sample are interrogated using LA ICP-MS. <sup>111</sup>Cd was monitored despite the relatively low abundance (12.8 %) due to the potential isobaric interference on <sup>114</sup>Cd (28.7 % abundant) from <sup>114</sup>Sn.

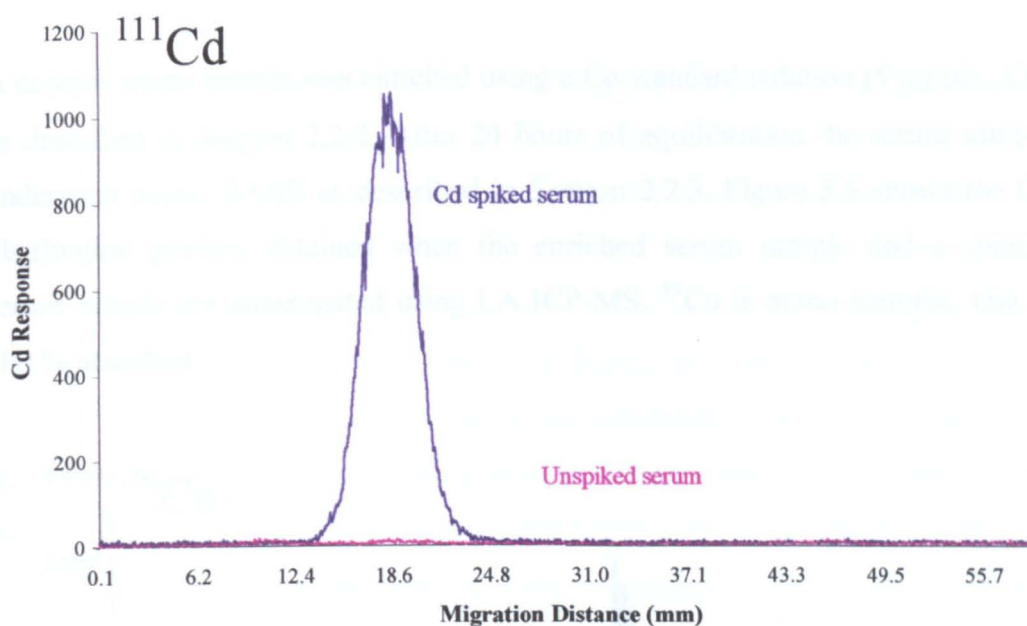


Figure 5.4:  $^{111}\text{Cd}$  profile for serum enriched with inorganic cadmium

The Cd distribution profile shows a single, very intense Cd peak at ~19 mm migration distance. This does not coincide with the two main metal binding proteins in serum, albumin (~ 33 mm) and transferrin (~ 23 mm). It could be due to Cd binding to the cysteine rich metallothionein as the literature suggests. Further work would be necessary to confirm the identity of this protein. Virtually all of the cadmium is protein bound as none migrates with the solvent front (~ 52 mm).

#### 5.2.2.b Cobalt

Cobalt is a component of alloys made to resist high temperatures and stresses. It is used in the glass industry to colour glass and is also used as a chemical catalyst. Exposure of metal workers to elevated levels of cobalt can damage lungs, heart and skin, it is also thought to be an occupational carcinogen.

Cobalt is classed as essential, forming a vital part of Vitamin B<sub>12</sub>. The mean whole blood concentrations of Co were found to be 0.09  $\mu\text{g/L}$  in unexposed subjects and 1.42  $\mu\text{g/L}$  in exposed subjects. The presence of Co can antagonise Fe uptake and so it has been assumed that some binding with transferrin can occur<sup>216</sup>. Co(II) ions bind preferentially to albumin<sup>217</sup>.

### 5.2.2.2. Inorganic Cobalt

A control serum sample was enriched using a Co standard solution (5  $\mu\text{g/mL}$ , Co) as described in Section 2.2.2. After 24 hours of equilibration the serum sample underwent native PAGE as described in Section 2.2.3. Figure 5.5 shows the Co distribution profiles obtained when the enriched serum sample and a control serum sample are interrogated using LA ICP-MS.  $^{59}\text{Co}$  is mono-isotopic, that is 100 % abundant.

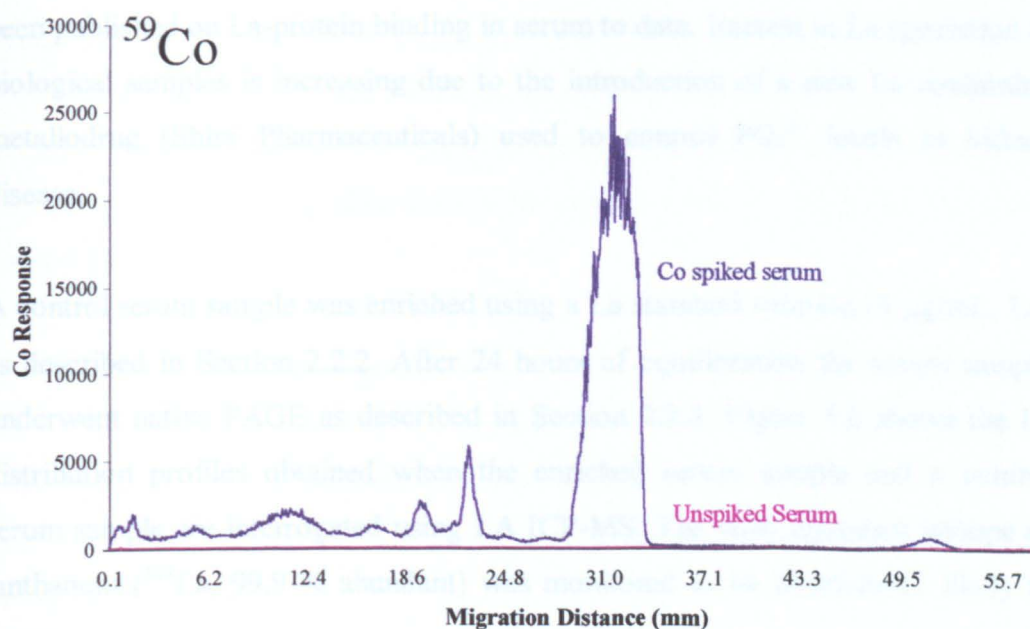


Figure 5.5:  $^{59}\text{Co}$  profile for serum enriched with inorganic cobalt

From the cobalt distribution profile it can be seen that virtually all the cobalt is protein bound as indicated by the small cobalt peak corresponding to the solvent front ( $\sim 52$  mm). The majority of the protein bound cobalt is associated with albumin ( $\sim 34$  mm). A number of other cobalt peaks are present of which the peak at  $\sim 23$  mm is likely to correspond to transferrin bound cobalt. The profile shows cobalt protein binding in serum to be extensive and quite complex, unfortunately it is not possible to positively identify the other proteins binding cobalt from this data alone.

### 5.2.2.c Lanthanum

Lanthanum is used to strengthen steel and to produce superconductors. In exposed workers lanthanum has been found to accumulate in the liver and bone. Lanthanum concentration does not decrease with time after exposure indicating a long biological half-life<sup>218</sup>.

Lanthanum has no known essentiality. It is known to replace Ca in a number of Ca mediated biological processes, but is not considered toxic. Few studies have been published on La-protein binding in serum to date. Interest in La speciation in biological samples is increasing due to the introduction of a new La containing metallodrug (Shire Pharmaceuticals) used to control  $\text{PO}_4^{3-}$  levels in kidney disease.

A control serum sample was enriched using a La standard solution (5  $\mu\text{g}/\text{mL}$ , La) as described in Section 2.2.2. After 24 hours of equilibration the serum sample underwent native PAGE as described in Section 2.2.3. Figure 5.6 shows the La distribution profiles obtained when the enriched serum sample and a control serum sample are interrogated using LA ICP-MS. The most abundant isotope of lanthanum ( $^{139}\text{La}$ , 99.9 % abundant) was monitored as no interference likely to occur.

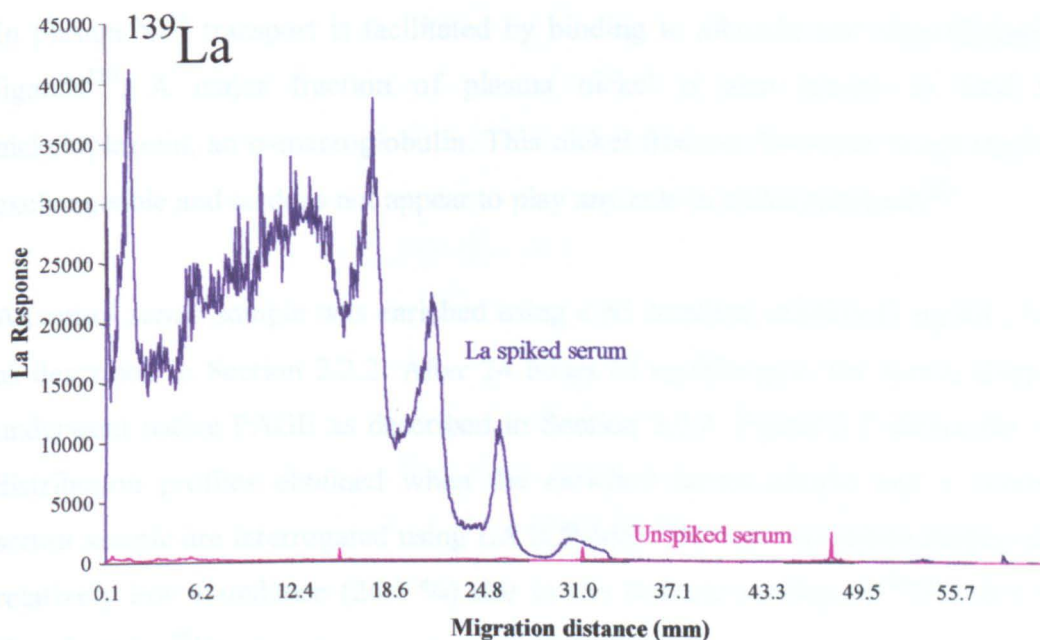


Figure 5.6:  $^{139}\text{La}$  profile for serum enriched with inorganic lanthanum



The lanthanum profile shows extensive protein binding in serum with very little lanthanum present in the solvent front (~ 52 mm). None of the peaks appear to correspond with the position of the albumin band (~ 35 mm), unless the lanthanum is causing the albumin to polymerise on binding. One of the peaks coincides with transferrin (~ 23 mm) but unfortunately positive identification of the other lanthanum binding proteins is not possible from data obtained alone.

#### 5.2.2.d Nickel

Nickel is used in stainless steel, jewellery, electroplating, batteries, dental prosthetics, data storage and chemical catalysis. Nickel emissions result from mining, refining, metal consumption in industrial processes and waste incineration. Atmospheric nickel levels are directly linked to fossil fuel and petrol consumption.

Whilst nickel is generally regarded as toxic it has some essentiality at trace levels. The toxicity of nickel depends on the nature of the nickel compound exposed to. Contact dermatitis is a common complaint especially among women with nickel containing jewellery. A typical serum level of  $0.28 \mu\text{g/L}$ <sup>219</sup> has been reported in unexposed subjects.

In plasma  $\text{Ni}^{2+}$  transport is facilitated by binding to albumin and ultra-filterable ligands<sup>220</sup>. A major fraction of plasma nickel is also known to bind to nickeloplasmin, an  $\alpha$ -macroglobulin. This nickel fraction, however, is not readily exchangeable and so does not appear to play any role in nickel transport<sup>221</sup>.

A control serum sample was enriched using a Ni standard solution ( $5 \mu\text{g/mL}$ , Ni) as described in Section 2.2.2. After 24 hours of equilibration the serum sample underwent native PAGE as described in Section 2.2.3. Figure 5.7 shows the Ni distribution profiles obtained when the enriched serum sample and a control serum sample are interrogated using LA ICP-MS.  $^{60}\text{Ni}$  was monitored despite the relatively low abundance (26.1 %) due to the isobaric overlap of  $^{58}\text{Ni}$  (68.3 % abundant) by  $^{58}\text{Fe}$ .

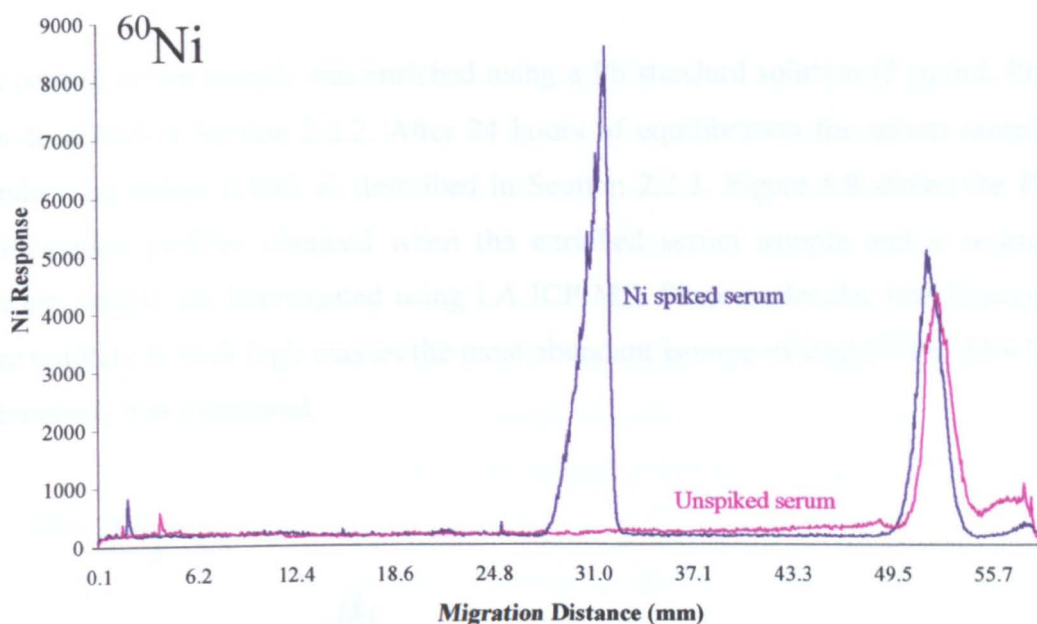


Figure 5.7:  $^{60}\text{Ni}$  profile for serum enriched with inorganic nickel

From the nickel profile it can be seen that a large portion of the nickel is bound to a single protein which coincides with the albumin band (~ 32 mm) and the rest of the nickel migrates with the solvent front (~53 mm). This is consistent with the literature.

#### 5.2.2.e Lead

Lead has a wide variety of uses, a few of which include batteries, petrol, paints and glassware. Over the past 50 years there has been an increase in the amount of lead extracted, used and so emitted into the environment by man. As a result lead levels are now many times higher than they used to be which has in turn led to increased health risks.

Lead has no known essentiality, and is found to interfere with several enzymes involved in haeme synthesis. Once absorbed by the body lead enters the blood stream. Typical lead levels in blood are 5-20  $\mu\text{g}/100\text{ mL}$  for unexposed subjects, of this >95 % is bound to erythrocytes. In plasma almost all the lead is protein bound, in particular to albumin and some high molecular mass globulins.

A control serum sample was enriched using a Pb standard solution (5 µg/ml, Pb) as described in Section 2.2.2. After 24 hours of equilibration the serum sample underwent native PAGE as described in Section 2.2.3. Figure 5.8 shows the Pb distribution profiles obtained when the enriched serum sample and a control serum sample are interrogated using LA ICP-MS. Since molecular interferences are unlikely at such high masses the most abundant isotope of lead ( $^{208}\text{Pb}$ , 52.4 % abundant) was monitored.

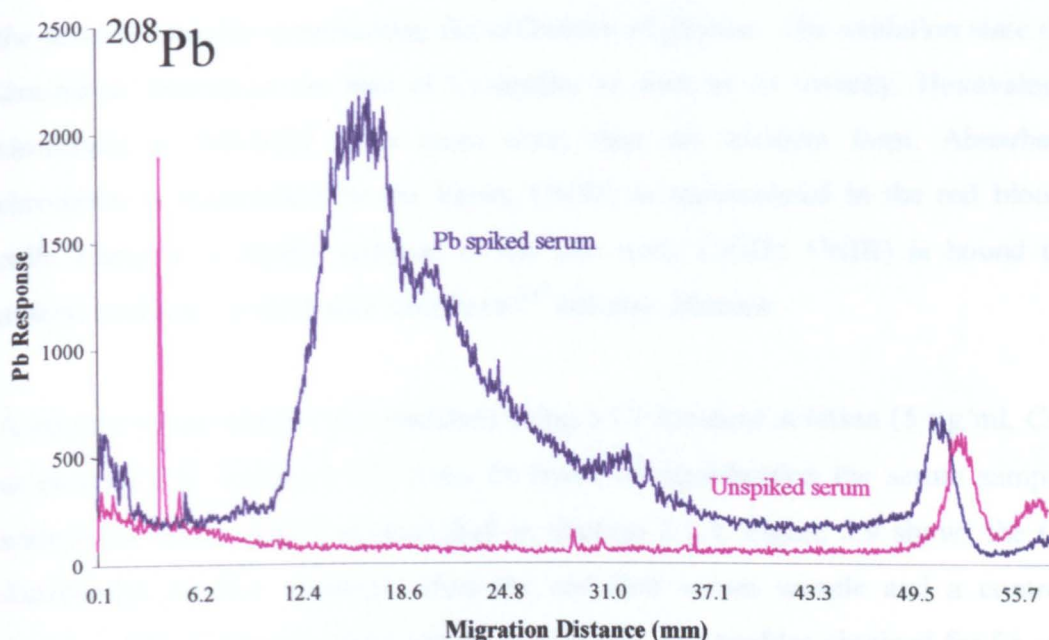


Figure 5.8:  $^{208}\text{Pb}$  profile for serum enriched with inorganic lead

From the lead profile it can be seen that a small fraction of the lead migrates with the solvent front, whilst the remainder of the lead appears in a very broad band (from ~ 15-35 mm) with the main peak at ~ 15 mm. Given these migration distances it is possible albumin and transferrin are involved to some degree, however, it is difficult to say what protein binding is actually occurring within the serum from these results alone. It does show that protein-lead binding occurs in serum and so may be of clinical interest.

### 5.2.2.f Chromium

Chromium is used in stainless steel production, metal finishing, paint, tanning, chemical catalysis and data storage. Increased quantities of chromium have been used by man and released into the environment over several decades. Welders are exposed to chromium via inhalation as well as running the risk of allergic contact dermatitis. Normal concentration range of chromium in human blood is found to be 0.1-1  $\mu\text{g/L}$ <sup>222</sup>. There is a danger volatile chromium species may be lost when using analytical techniques requiring sample digestion, this is not an issue with LA ICP-MS. Chromium is known to be essential, Cr(III) is thought to potentiate the action of insulin in promoting the utilisation of glucose. The oxidation state of chromium influences the rate of Cr-uptake as well as its toxicity. Hexavalent chromium is 100-1000 times more toxic than the trivalent form. Absorbed chromium is transported by the blood, Cr(VI) is accumulated in the red blood cells where it is rapidly reduced to the less toxic Cr(III). Cr(III) is bound to plasma proteins, in particular transferrin<sup>223</sup> but also albumin.

A control serum sample was enriched using a Cr standard solution (5  $\mu\text{g/ml}$ , Cr) as described in Section 2.2.2. After 24 hours of equilibration the serum sample underwent native PAGE as described in Section 2.2.3. Figure 5.9 shows the Cr distribution profiles obtained when the enriched serum sample and a control serum sample are interrogated using LA ICP-MS. The profiles obtained for Fe are also shown to demonstrate the effect of enriched Cr on other metal-protein binding in serum. <sup>53</sup>Cr was monitored despite the relatively low abundance (9.5 %) due the potential interference on <sup>52</sup>Cr (83.8 % abundant) from <sup>40</sup>Ar<sup>12</sup>C<sup>+</sup>.

The profile shows Cr binding to three proteins in serum, with some Cr migrating with the solvent front (~55 mm). The main Cr binding protein is albumin (~34 mm) closely followed by transferrin (~23 mm). The third Cr binding protein (~2 mm) is likely to be a large protein or one with a high mass/charge ratio but a positive identification can not be made with the data available. It can be seen that Fe is lost from transferrin on binding Cr, a process that may be detrimental to health.

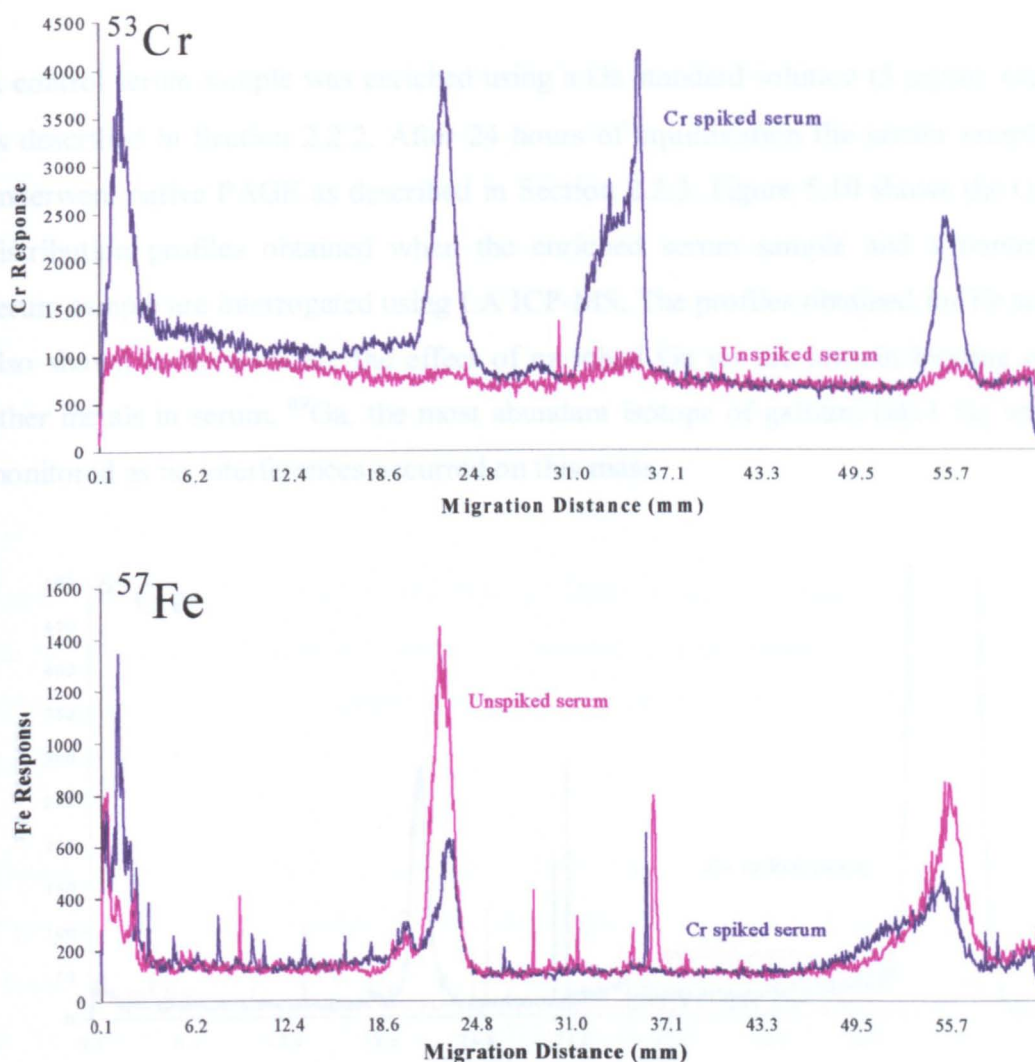


Figure 5.9:  $^{53}\text{Cr}$  and  $^{57}\text{Fe}$  profiles for serum enriched with inorganic chromium

#### 5.2.2.g Gallium

Gallium is used as a chemotherapeutic and radio-imaging agent and also as a component of super-fast integrated circuits. Technological developments that call for the use of more semi-conductors are likely to lead to an increase in gallium emissions.

Gallium has no known essentiality and has toxic effects such as nephrotoxicity. When administered intravenously gallium binds rapidly to plasma proteins in particular transferrin<sup>224</sup>, where it competes with iron, and ceruloplasmin. The level of gallium in healthy human plasma was found to be around  $0.1 \mu\text{g/L}$ <sup>225</sup>.

A control serum sample was enriched using a Ga standard solution (5  $\mu\text{g}/\text{ml}$ , Ga) as described in Section 2.2.2. After 24 hours of equilibration the serum sample underwent native PAGE as described in Section 2.2.3. Figure 5.10 shows the Ga distribution profiles obtained when the enriched serum sample and a control serum sample are interrogated using LA ICP-MS. The profiles obtained for Fe are also shown to demonstrate the effect of enriched Ga on the protein binding of other metals in serum.  $^{69}\text{Ga}$ , the most abundant isotope of gallium (60.1 %) was monitored as no interferences occurred on this mass.

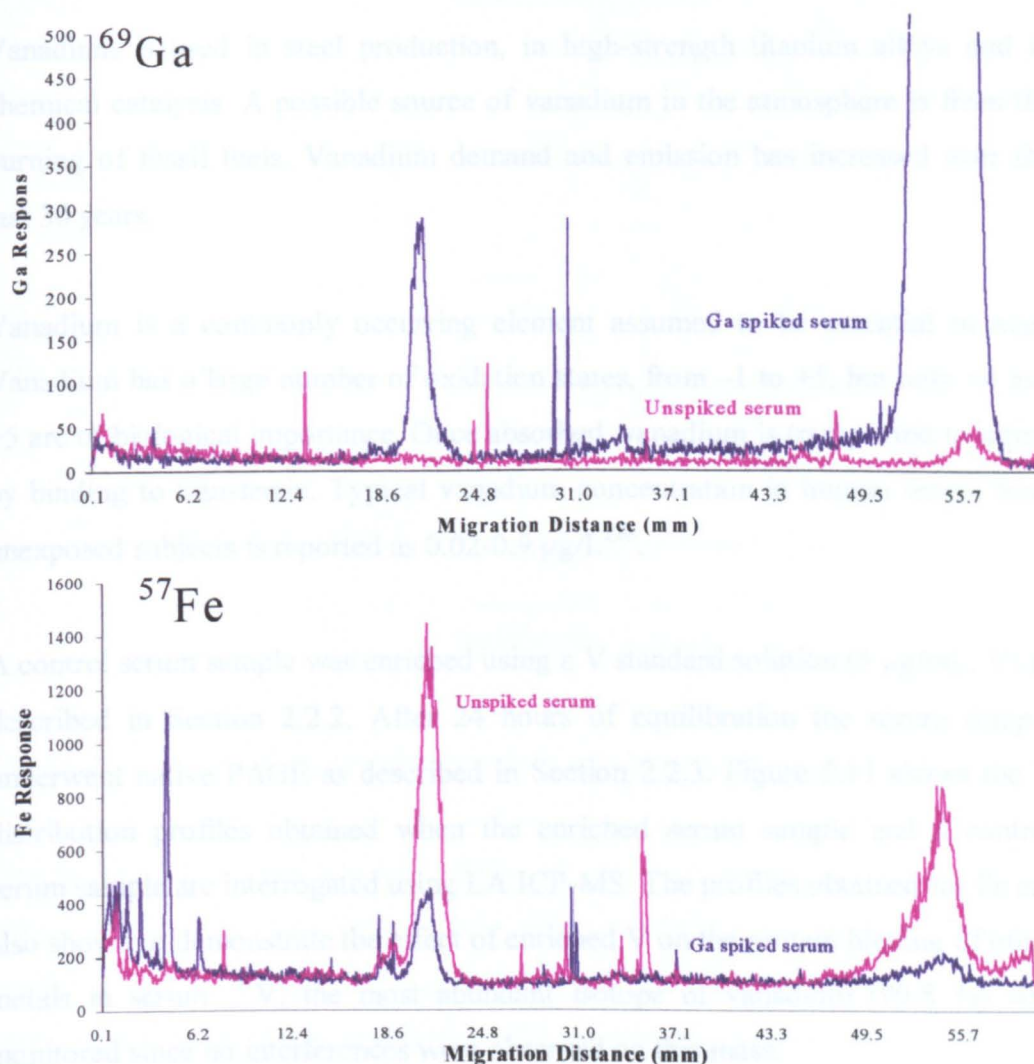


Figure 5.10:  $^{69}\text{Ga}$  and  $^{57}\text{Fe}$  profiles for serum enriched with inorganic gallium

From the profile it can be seen that a small fraction of gallium in serum is protein bound, the remainder migrates with the solvent front (~ 53 mm). A small Ga peak is clearly visible at ~23 mm coinciding with the transferrin band. A Ga peak at ~34 mm can just be made out coinciding with the albumin band. By comparing the iron profiles of unspiked and Ga enriched serum it can be seen that transferrin bound iron is lost on gallium binding. This could be of clinical interest and so could for the basis of further research.

#### 5.2.2.h Vanadium

Vanadium is used in steel production, in high-strength titanium alloys and in chemical catalysis. A possible source of vanadium in the atmosphere is from the burning of fossil fuels. Vanadium demand and emission has increased over the last 30 years.

Vanadium is a commonly occurring element assumed to be essential in man. Vanadium has a large number of oxidation states, from -1 to +5, but only +4 and +5 are of biological importance. Once absorbed, vanadium is transported in serum by binding to transferrin. Typical vanadium concentration in human serum from unexposed subjects is reported as 0.02-0.9  $\mu\text{g/L}$ <sup>226</sup>.

A control serum sample was enriched using a V standard solution (5  $\mu\text{g/mL}$ , V) as described in Section 2.2.2. After 24 hours of equilibration the serum sample underwent native PAGE as described in Section 2.2.3. Figure 5.11 shows the V distribution profiles obtained when the enriched serum sample and a control serum sample are interrogated using LA ICP-MS. The profiles obtained for Fe are also shown to demonstrate the effect of enriched V on the protein binding of other metals in serum. <sup>51</sup>V, the most abundant isotope of vanadium (99.8 %) was monitored since no interferences were observed on this mass.

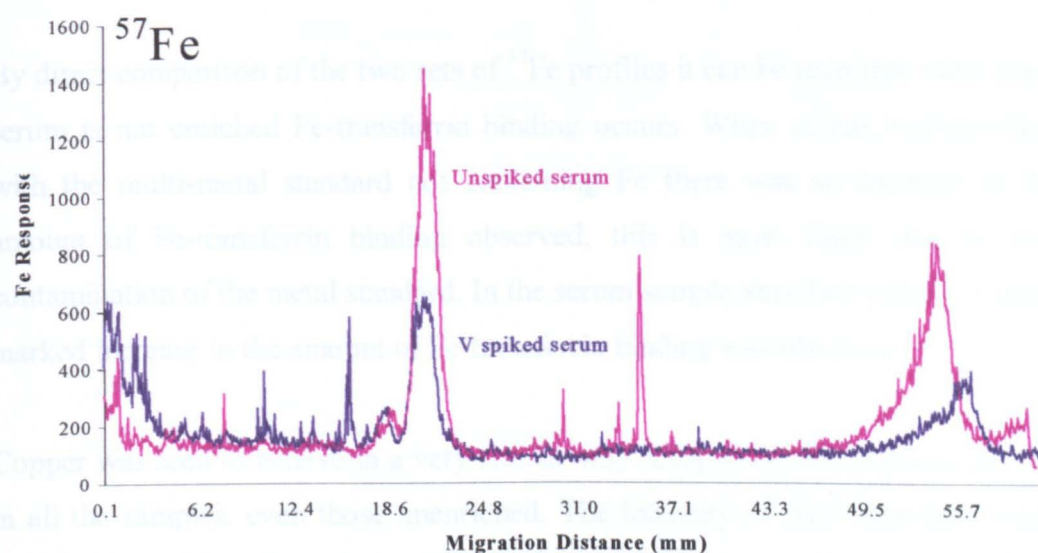
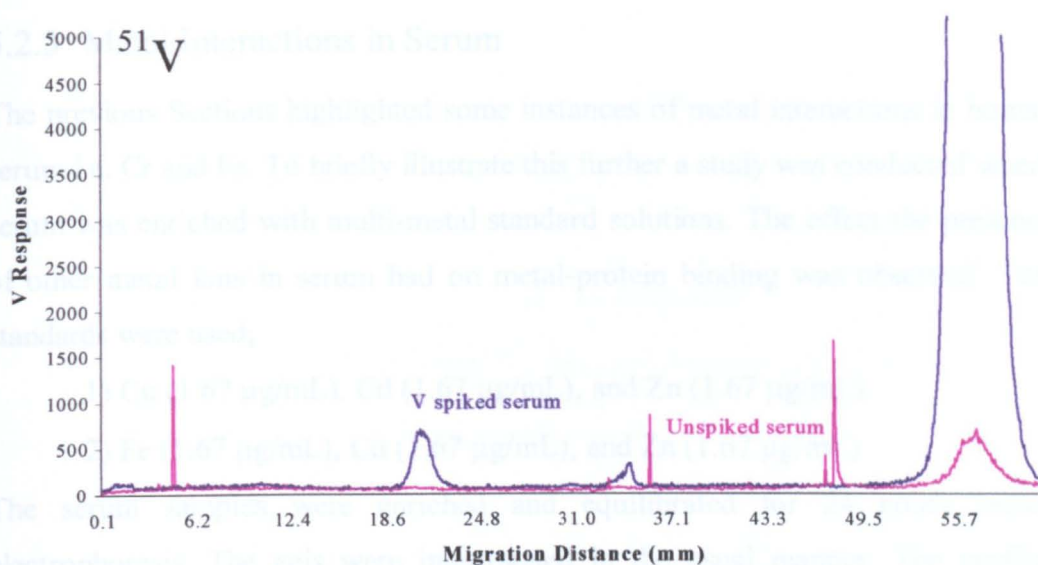


Figure 5.11:  $^{51}\text{V}$  and  $^{57}\text{Fe}$  profiles for serum enriched with inorganic vanadium

The profile shows that a small degree of vanadium-protein binding occurs in serum, with the majority of the V migrating with the solvent front (~55 mm). A small V peak can be seen at ~22 mm which coincides with the transferrin band. A very small V peak is just visible at ~35 mm which coincides with the albumin band. The Fe profile shows transferrin bound iron is lost when V is bound to transferrin. Such interactions are unlikely to occur at normal physiological levels, but may become more important when serum levels are elevated through exposure.



### 5.2.3 Metal Interactions in Serum

The previous Sections highlighted some instances of metal interactions in human serum i.e. Cr and Fe. To briefly illustrate this further a study was conducted where serum was enriched with multi-metal standard solutions. The effect the presence of other metal ions in serum had on metal-protein binding was observed. Two standards were used;

1) Cu (1.67  $\mu\text{g/mL}$ ), Cd (1.67  $\mu\text{g/mL}$ ), and Zn (1.67  $\mu\text{g/mL}$ )

2) Fe (1.67  $\mu\text{g/mL}$ ), Cd (1.67  $\mu\text{g/mL}$ ), and Zn (1.67  $\mu\text{g/mL}$ )

The serum samples were enriched and equilibrated for 24 hours before electrophoresis. The gels were interrogated in the usual manner. The profiles obtained for the two samples are shown in Figures 5.12 and 5.13, respectively.

By direct comparison of the two sets of  $^{57}\text{Fe}$  profiles it can be seen that even when serum is not enriched Fe-transferrin binding occurs. When serum was enriched with the multi-metal standard not containing Fe there was an increase in the amount of Fe-transferrin binding observed, this is most likely due to iron contamination of the metal standard. In the serum sample enriched with Fe a more marked increase in the amount of Fe-transferrin binding was observed.

Copper was seen to behave in a very similar way. Cu-protein binding was present in all the samples, even those unenriched. The intensity of the Cu-protein peaks increased slightly when the serum was enriched with a multi-metal standard containing no copper, this is again most probably due to copper contamination. The greatest increase in Cu-protein peak intensity was observed when serum was enriched with the multi-metal standard containing copper.

No specific Zn-protein binding is evident with the unspiked serum samples. Both serum samples enriched with the multi-metal standard containing zinc showed signs of Zn-protein binding. However, despite the two samples being enriched with zinc to a concentration of 1.67  $\mu\text{g/mL}$  the  $^{66}\text{Zn}$  profiles obtained differ. It can be seen that the presence of additional copper in the serum sample appears to facilitate zinc binding to an unidentified protein, which migrates only a little way into the gel (~ 8 mm).

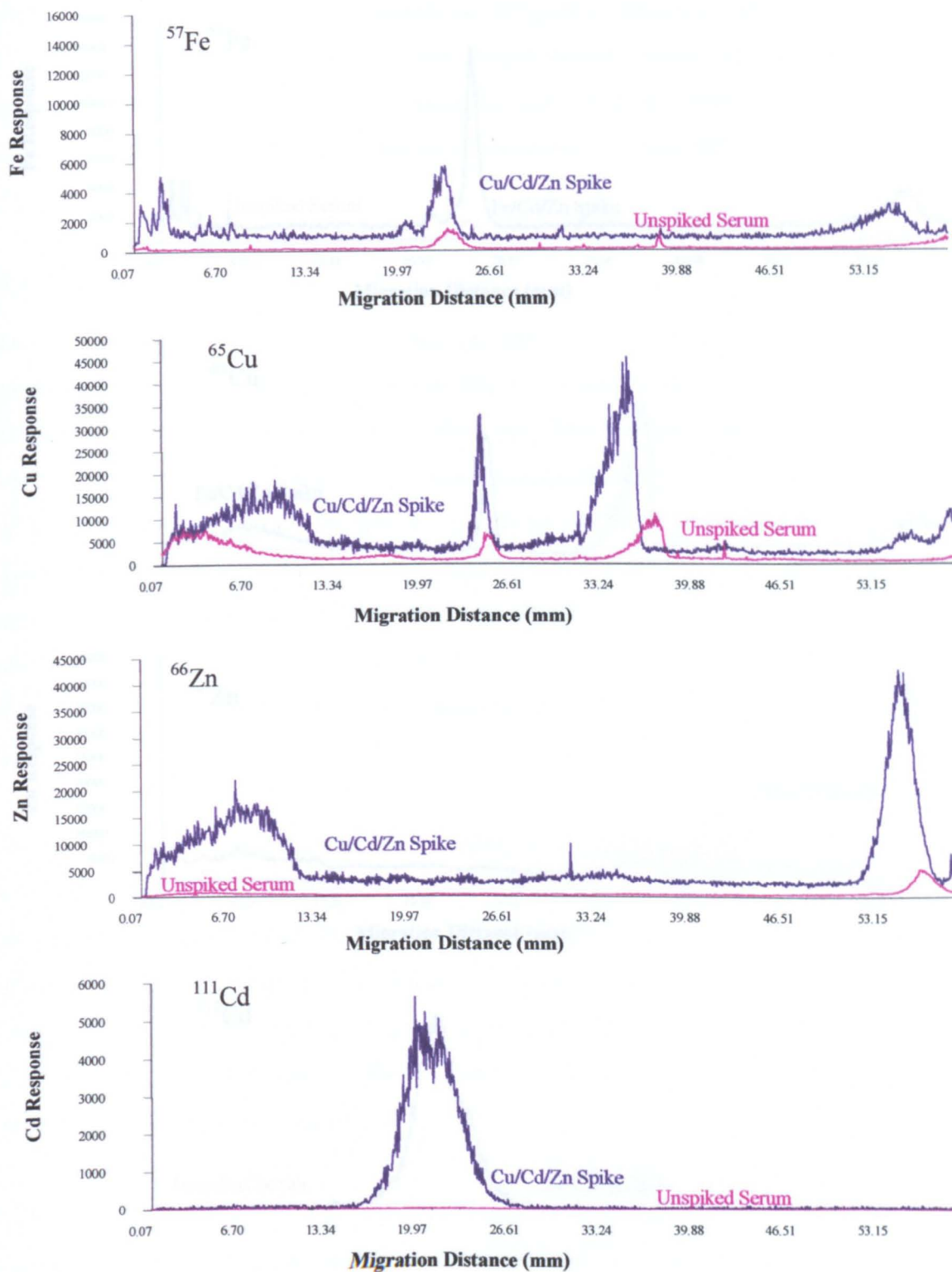


Figure 5.12:  $^{57}\text{Fe}$ ,  $^{65}\text{Cu}$ ,  $^{66}\text{Zn}$  and  $^{111}\text{Cd}$  Profiles for Serum Enriched with Cu, Cd and Zn (1.67 mg/L)

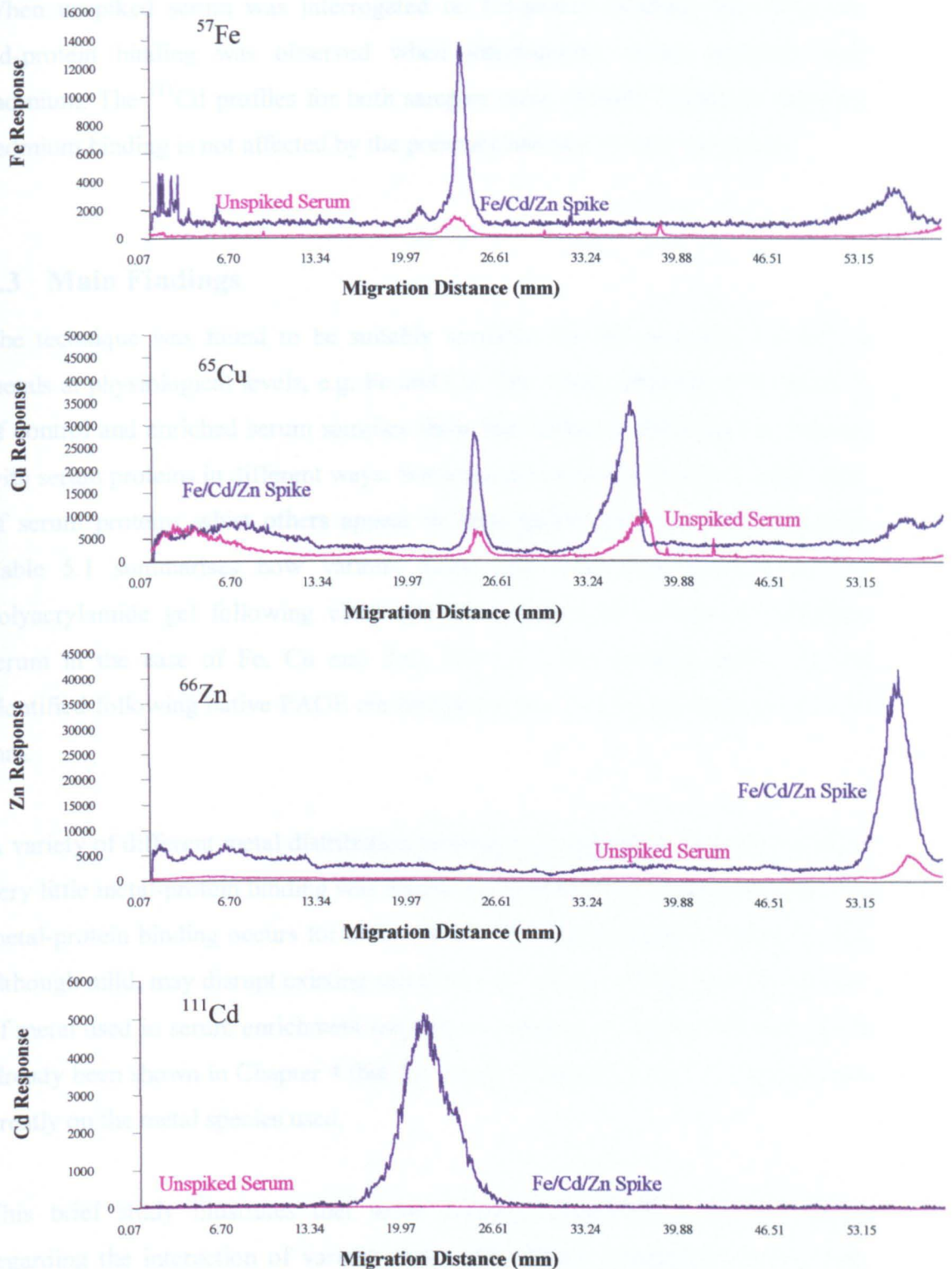


Figure 5.13:  $^{57}\text{Fe}$ ,  $^{65}\text{Cu}$ ,  $^{66}\text{Zn}$  and  $^{111}\text{Cd}$  Profiles for Serum Enriched with Fe, Cd and Zn (1.67 mg/L)

When unspiked serum was interrogated no Cd-protein binding was observed. Cd-protein binding was observed when interrogating serum enriched with cadmium. The  $^{111}\text{Cd}$  profiles for both samples were virtually identical, implying cadmium binding is not affected by the presence/absence of iron and copper.

### **5.3 Main Findings**

The technique was found to be suitably sensitive for the speciation of certain metals at physiological levels, e.g. Fe and Cu. The results obtained from analysis of control and enriched serum samples show that different metal species interact with serum proteins in different ways. Some metals appear to bind to a wide range of serum proteins whilst others appear to bind specifically to a single protein. Table 5.1 summarises how various metal ions were distributed along the polyacrylamide gel following electrophoresis of enriched serum (or unspiked serum in the case of Fe, Cu and Zn). The two main proteins which can be identified following native PAGE are transferrin at ~ 24 mm and albumin at ~ 36 mm.

A variety of different metal distribution profiles were observed. In some instances very little metal-protein binding was observed. This does not necessarily imply no metal-protein binding occurs for these metals. The experimental conditions used, although mild, may disrupt existing metal-protein bonds. Alternatively the species of metal used in serum enrichment may not be suitable for protein binding. It has already been shown in Chapter 4 that the nature of metal-protein binding depends greatly on the metal species used.

This brief study illustrates that some complex interactions occur in serum regarding the interaction of various metal ions. These interactions can, in turn, affect the degree/nature of metal-protein binding. Such interactions must be considered when interpreting metal-protein binding data obtained from the analysis of complex biological samples such as serum.

		Migration Distance (mm)																	
		3	6	9	12	15	18	21	24	27	30	33	36	39	42	45	48	51	54
<sup>57</sup> Fe									**										*
<sup>65</sup> Cu		*				*		**					*						*
<sup>66</sup> Zn													*						**
<sup>111</sup> Cd							**												
<sup>59</sup> Co		*	*	*		*		*					**						*
<sup>139</sup> La		*			*	**	*	*		*			*						*
<sup>60</sup> Ni													**						*
<sup>208</sup> Pb		*				**		**					*						*
<sup>53</sup> Cr		*							*				*						*
<sup>69</sup> Ga									*				*						**
<sup>51</sup> V									*										**

Table 5.1: Metal distribution in enriched serum samples. \* denotes metal present in protein fraction, \*\* denotes metal signal intensity relatively high

# **Chapter 6: Conclusions and Recommendations for Future Work**

## **6.1 Conclusions**

Certain criteria were outlined in the aims of the study, which the gel electrophoresis/laser ablation combination needed to fulfill in order for it to be deemed suitable for metal speciation in biological samples. The four key criteria were as follows.

- Mild conditions to maintain integrity of metal-protein species
- Selective separation step to separate species
- High sensitivity metal species detection
- Small sample volume requirements

All of these criteria were considered during the method development step. PAGE was chosen for its high selectivity in separating serum proteins and the small sample volumes required. To ensure sample integrity, serum samples were separated under native conditions. ICP-MS was chosen as the detection system because of its multi-element capability as well as its high sensitivity. Laser ablation provided a novel route for sample introduction permitting rapid interrogation of gels and acquisition of mass spectra. In situ analysis of the gels helped to maintain both the metal-protein species integrity and protein resolution.

LA ICP-MS analysis of native electrophoresis gels was found to compare favourably with competitive techniques. Method development studies showed both the electrophoresis step and the metal detection step to be robust and have good reproducibility. The design of the electrophoresis system meant the background platinum signal was suitably low. The multi-element capability of the technique means a variety of elements were monitored simultaneously, reducing the need for replicate gel interrogations. As a result multi-element data from an electrophoresed sample can be acquired relatively rapidly at around 20 minutes.

Pt-protein binding was observed in serum samples acquired from patients undergoing platinum therapy. Analysis of control serum showed no such binding. Cisplatin and carboplatin, two popular platinum anti-tumour drugs, were studied. LA ICP-MS combined with native PAGE showed there to be differences in the protein binding of these two drugs. *In vitro* studies enriching control serum with cisplatin and carboplatin show both drugs binding with a range of proteins. It was observed that cisplatin bound more readily to albumin than was the case for carboplatin. Time studies carried out with the two drugs highlighted differences in their protein binding mechanisms. Levels of protein bound cisplatin were seen to increase with time, with the majority of the platinum always bound to albumin.

The platinum distribution pattern for carboplatin enriched serum was seen to alter over time with the proportion of albumin bound platinum increasing. These differences in protein binding were also observed in serum samples acquired from patients undergoing platinum therapy. Such differences in protein binding and mechanistic pathways of the two drugs could go some way to explaining the differences in their associated toxicities. It would appear that Pt-albumin binding is associated with drug toxicity rather than drug efficacy; such a finding is consistent with the fact that albumin bound platinum drugs are known to lose their anti-tumour activity.

The degree and nature of gold-protein binding was found to be very dependent upon the gold species present. Au(III) and Au(I) were both found to bind almost instantaneously with albumin when studied *in vitro*. However, when serum was enriched with colloidal gold (Au(0)) no protein binding was observed, instead the gold flocculated and did not enter the gel. The profiles obtained from analysis of clinical samples are consistent these findings.

The FI ICP-MS studies established gold concentrations of 300 µg/L in control serum whilst significantly higher gold concentrations (469-952 µg/L) were detected in serum from patients undergoing chrysotherapy. Gold-protein binding was found to be significantly higher in the patients' serum (37-69 %) than in the control (~2 %), reflecting the source of serum gold.

The main source of gold in serum obtained from chrysotherapy patients is the administration of Au(I) drugs. Au(I) is thought to disproportionate in serum to give Au(0) and Au(III), which has been shown to bind readily with serum proteins. With reference to the control serum the majority of the gold has been shown not to be protein bound. This finding would imply inorganic gold is not the main source of gold. These findings demonstrate how absolute gold levels are of little diagnostic use when trying to assess adverse reactions to gold. The degree of protein-bound gold, however, may be more relevant to such studies.

When the technique was applied to serum enriched with a range of multi-elements *in vitro*, a variety of metal distribution profiles was observed signifying extensive metal-protein binding. These results are summarised in Appendix 2.4. In some instances very little metal-protein binding was observed. This does not necessarily imply no metal-protein binding occurs for these metals. The experimental conditions used, although mild, may disrupt existing metal-protein bonds. Alternatively the species of metal used in serum enrichment may not be suitable for protein binding. The study also illustrated some of the complex interactions occurring in serum with regards the interactions of various metal ions. Such interactions can, in turn, affect the degree/nature of metal-protein binding. The possibility of metal-metal interactions must be considered when interpreting metal-protein binding data obtained from the analysis of complex biological samples such as serum.

Overall the technique proved suitable for the metal speciation of biological samples. It was successfully applied to the detection of metal species in human serum enriched *in vitro* with a variety of metals. The technique was also used to speciate metals occurring in serum at trace levels, such as Fe and Cu. Finally the technique was successfully used to analyse clinical samples obtained from patients undergoing platinum and gold therapy. Meaningful data was obtained which could be compared to that obtained from the analysis of control serum.



## 6.2 Recommendations for Future Work

Recommendations for future work focus firstly upon improving the technique and then on further clinical studies. Although the technique met the criteria laid out in the aims of the study it still had a number of limitations, which might be improved upon. The main limitations of the technique include:

- high concentration of albumin in serum obscures other serum proteins and so necessitates sample dilution
- limited protein identification given the use of native PAGE
- limited protein resolution given the complex nature of the sample, serum typically contains more than 100 proteins.

The main protein component of serum is albumin (~ 35 mg/mL). Such high albumin concentrations can pose problems when trying to look at metal binding to other, lower concentration proteins. One way in which such problems can be overcome would be to remove the serum albumin prior to protein separation. Albumin removal can be achieved by passing the serum through an affinity gel such as the one produced by Bio-Rad<sup>227</sup>. Removal of albumin in this way will greatly reduce the total protein concentration of the serum, thus removing the need for sample dilution. This would effectively increase the sensitivity of the technique as well as improving the potential protein resolution. Investigation would need to be carried out to check if the integrity of the metal species was maintained.

Protein identification is difficult when using native PAGE as the migration distance of the protein is not simply a function of molecular mass. A method of protein identification which could be used in conjunction with LA ICP-MS of polyacrylamide gels is matrix assisted laser desorption/ionisation time of flight mass spectrometry (MALDI TOF)<sup>228</sup>. In this process a laser is used to remove molecules, intact, from the target and the molecular mass of the molecule is determined using time of flight MS. An initial test was carried out using albumin on the target and promising results were obtained, see Appendix 2.5.

MALDI has been used to analyse proteins directly from the polyacrylamide gels<sup>229</sup>. The process requires the use of a matrix, which allows the sample to be desorbed by the laser energy. Investigations into the best matrix for the system would be needed. By using MALDI TOF the molecular mass of a protein, from a region of the gel where high metal concentrations were detected, could be determined. Such information may help identify the proteins binding metal ions.

The protein resolution achievable with native PAGE is limited by factors such as the gel size and the protein concentration. Albumin removal might go some way to improving resolution of the remaining proteins. Increasing the size of the gels, whilst it would improve the protein resolution would also increase the electrophoretic run time, increasing the likelihood of metal-protein binding loss. It would also increase the interrogation time. Another way in which protein resolution can be improved is to use a different separation technique. The use of liquid IEF, in the form of the Bio-Rad Rotofor followed by native PAGE was shown to improve protein resolution by the addition of a second separation parameter. This technique was found to work with platinum samples. Its applicability to other metals would have to be determined to check sample integrity. Another analytical technique for rapid protein separation requiring small sample volumes is capillary electrophoresis (CE). Coupling of CE to ICP-MS was until quite recently troublesome. Recent advances have made it more easily achievable<sup>154, 230</sup>. CE coupled to ICP-MS would combine rapid protein identification with sensitive multi-element detection. The main draw back with this technique compared with LA ICP-MS of polyacrylamide gels is that the sample is totally destroyed by analysis whereas the gel can be re-analysed after suitable storage if required.

Future work in the applications of the technique to clinical samples should include a more extensive time study of both the platinum and gold patients. Analysis of samples from colloidal gold trials would also be interesting. Table 1.5 shows a sample of the metallo-drugs currently used and so the potential clinical applications of this technique are numerous.




# **Appendix 1**

<b>Appendix 1.1: Elemental Composition of a Reference Person</b>	<b>p 192</b>
<b>Appendix 1.2: The Natural Protein Amino Acids</b>	<b>p 193</b>
<b>Appendix 1.3: Metallo-drugs used in Sample Enrichment</b>	<b>p 194</b>
<b>Appendix 1.4: Properties of Serum Proteins</b>	<b>p 195</b>
<b>Appendix 1.5: Metal Standards used in Sample Enrichment</b>	<b>p 196</b>
<b>Appendix 1.6: Laser Ablation Parameters</b>	<b>p 197</b>
<b>Appendix 1.7: Composition of SRM612</b>	<b>p 198</b>

## Appendix 1.1: Elemental Composition of a Reference Person

<i>Class</i>	<i>Element</i>	<i>g/70 kg</i>	<i>moles/70 kg</i>
<b>Bulk Elements</b>	C	12600	1050
	H	7000	3500
	N	2100	75
	O	45500	1425
<b>Macronutrients</b>	Ca	1050	26.2
	Cl	105	2.96
	K	140	3.58
	Mg	35	1.44
	Na	105	4.6
	P	700	22.5
	S	175	5.5
<b>Trace Elements</b>			
<b>Essential</b>	Co	0.003	0.00005
	Cr	0.005	0.0001
	Cu	0.11	0.0016
	F	0.8	0.021
	Fe	4.2	0.075
	I	0.03	0.00024
	Mn	0.02	0.00036
	Mo	0.005	0.00005
	Se	0.02	0.00025
	Zn	2.33	0.036
	<b>Possibly Essential</b>	Ni	0.01
Si		1.4	0.05
Sn		0.03	0.00025
V		0.02	0.00039
<b>Non-Essential</b>	Al	0.1	0.0037
	As	0.014	0.00019
	B	0.01	0.00092
	Ba	0.016	0.00012
	Cd	0.03	0.00027
	Li	0.0007	0.0001
	Pb	0.08	0.00038
	Rb	1.1	0.013
	Sb	0.07	0.00057
	Sr	0.14	0.0016

## Appendix 1.2: The Natural Protein Amino Acids

<i>Name</i>	<i>Character</i>	<i>Metal-binding</i>	<i>Sidechain</i>
Aspartic acid, Asp	Acid	M <sup>2+</sup> , M <sup>3+</sup>	-CH <sub>2</sub> -COOH
Glutamic acid, Glu	Acid	M <sup>2+</sup>	-CH <sub>2</sub> -CH <sub>2</sub> -COOH
Tyrosine, Tyr	Neutral	Mn <sup>3+</sup> , Fe <sup>3+</sup>	-CH <sub>2</sub> -  -O-H
Alanine, Ala	Neutral		-CH <sub>3</sub>
Asparagine, Asn	Neutral,		-CH <sub>2</sub> -CO-NH <sub>2</sub>
Cysteine, Cys	Neutral	Zn, Cu, Fe, Ni, Mo	-CH <sub>2</sub> -SH
Glutamine, Gln	Neutral		-CH <sub>2</sub> -CH <sub>2</sub> -CO-NH <sub>2</sub>
Serine, Ser	Neutral	M <sup>+</sup> ?	-CH <sub>2</sub> OH
Threonine, Thr	Neutral	M <sup>+</sup> ?	-CH-CH <sub>3</sub>   OH
Histidine, His	Neutral Basic	Zn, Cu, Mn, Fe, Ni anion binding	-CH <sub>2</sub> -C=CH         NH    NH <sup>+</sup>         CH    =
Arginine, Arg	Basic	anion binding	-(CH <sub>2</sub> ) <sub>3</sub> -NH-C-NH <sub>2</sub>    NH <sub>2</sub> <sup>+</sup>
Lysine, Lys	Basic	anion binding	-(CH <sub>2</sub> ) <sub>4</sub> -NH <sub>3</sub> <sup>+</sup>
Glycine, Gly	Non-polar		-H
Isoleucine, Ile	Non-polar		-CH-CH <sub>2</sub> -CH <sub>3</sub>   CH <sub>3</sub>
Leucine, Leu	Non-polar		-CH <sub>2</sub> -CH   CH <sub>3</sub>   CH <sub>3</sub>
Methionine, Met	Non-polar	Cu, Fe	-CH <sub>2</sub> -CH <sub>2</sub> -S-CH <sub>3</sub>
Phenylalanine, Phe	Non-polar		-CH <sub>2</sub> - 
Proline, Pro	Non-polar		amino group replaced by cyclic imino group
Tryptophan, Trp	Non-polar		-CH <sub>2</sub> - 
Valine, Val	Non-polar		-CH   CH <sub>3</sub>   CH <sub>3</sub>

### **Appendix 1.3: Metallo-drugs used in Sample Enrichment**

#### **Cisplatin**

Cisplatin injection solution. Concentration 1 mg/mL, presented in 10 mL Onco-Tain™ vials. Each mL contains 1 mg of cisplatin, 9 mg of sodium chloride B.P. 1 mg of mannitol B.P. and water for injections B.P. Distributed in UK by Faulding Pharmaceuticals plc trading as David Bull Laboratories.

#### **Carboplatin**

Paraplatin™ injection solution. Concentration 10 mg/mL, presented in 15 mL vials. Also contains water for injections. Distributed in UK by Bristol-Myers Pharmaceuticals.

#### **Myocrisin**

Myocrisin™ injection solution. Concentration 10 % presented in 0.5 mL ampoules. The injection solution also contains phenylmercuric nitrate and water for injections. Distributed in UK by JHC Healthcare Limited.

## Appendix 1.4: Properties of Serum Proteins

<b>Protein</b>	<b>pI</b>	<b>Molecular Mass</b>	<b>mg/100 mL (in serum)</b>
<b><math>\alpha_1</math>-Acid glycoprotein</b>	2.7	44 100	75-100
<b>haptoglobin</b>	4.1	100 000	30-190
<b>ceruloplasmin</b>	4.4	160 000	27-63
<b>prealbumin</b>	4.7	61 000	28-35
<b>albumin</b>	4.9	69 000	3500-4500
<b><math>\alpha_2</math>-macroglobulin</b>	5.4	820 000	220-380
<b>transferrin</b>	5.9	75 000	200-320

## Appendix 1.5: Metal Standards used in Sample Enrichment

As	1000 µg/mL As in 2 % HNO <sub>3</sub>
Au	1000 µg/mL Au in HCl
Bi	1000 µg/mL Bi in 2 % HNO <sub>3</sub>
Cd	1000 µg/mL Cd in 2 % HNO <sub>3</sub>
Co	1000 µg/mL Co in 2 % HNO <sub>3</sub>
Cr	1000 µg/mL as (NH <sub>4</sub> ) <sub>2</sub> Cr <sub>2</sub> O <sub>7</sub> in HNO <sub>3</sub>
Cu	1000 µg/mL Cu in 2 %
Fe	1000 µg/mL Fe in 2 % HNO <sub>3</sub>
Ga	1000 µg/mL Ga in HNO <sub>3</sub>
Gd	1000 µg/mL as Gd <sub>2</sub> O <sub>3</sub> in HNO <sub>3</sub>
Hg	1000 µg/mL Hg in 2 % HNO <sub>3</sub>
In	1000 µg/mL In in 2 % HNO <sub>3</sub>
La	1000 µg/mL as La <sub>2</sub> O <sub>3</sub> in HNO <sub>3</sub>
Li	1000 µg/mL as Li <sub>2</sub> CO <sub>3</sub> in HNO <sub>3</sub>
Lu	1000 µg/mL as Lu <sub>2</sub> O <sub>3</sub> in HNO <sub>3</sub>
Mn	1000 µg/mL Mn in 2 % HNO <sub>3</sub>
Mo	1000 µg/mL Mo in 2 % HNO <sub>3</sub>
Ni	1000 µg/mL Ni in 2 % HNO <sub>3</sub>
Pb	1000 µg/mL as Pb(NO <sub>3</sub> ) <sub>2</sub> in HNO <sub>3</sub>
Pd	1000 µg/mL Pd in HCl
Pt	1000 µg/mL Pt in HCl
Ru	1000 µg/mL as RuCl <sub>3</sub> .3H <sub>2</sub> O in HCl
Sb	1000 µg/mL Sb in 2 % HNO <sub>3</sub>
Se	1000 µg/mL Se in 2 % HNO <sub>3</sub>
Sn	1000 µg/mL Sn in HNO <sub>3</sub> tr. HF
Sr	1000 µg/mL as Sr(NO <sub>3</sub> ) <sub>2</sub> in HNO <sub>3</sub>
V	1000 µg/mL V in 2 % HNO <sub>3</sub>
Zn	1000 µg/mL Zn in 2 % HNO <sub>3</sub>



## Appendix 1.6: Laser Ablation Parameters

### LSX 200 Energy Values

1	0 mJ	11	1.9 mJ
2	0 mJ	12	2.2 mJ
3	0.1 mJ	13	2.7 mJ
4	0.2 mJ	14	3.1 mJ
5	0.4 mJ	15	3.3 mJ
6	0.6 mJ	16	3.4 mJ
7	0.8 mJ	17	3.7 mJ
8	1.1 mJ	18	4.0 mJ
9	1.3 mJ	19	4.2 mJ
10	1.7 mJ	20	4.6 mJ

### LSX 200 Aperture Diameters

1	10 $\mu\text{m}$	5	200 $\mu\text{m}$
2	25 $\mu\text{m}$	6	260 $\mu\text{m}$
3	50 $\mu\text{m}$	7	300 $\mu\text{m}$
4	100 $\mu\text{m}$		

## Appendix 1.7: Composition of SRM612

<b>Element</b>	<b>Certified Value (mg/kg)</b>
<b>Barium</b>	(41)
<b>Boron</b>	(32)
<b>Cerium</b>	(39)
<b>Cobalt</b>	(35.5)
<b>Copper</b>	(37.7)
<b>Dysprosium</b>	(35)
<b>Erbium</b>	(39)
<b>Europium</b>	(36)
<b>Gadolinium</b>	(39)
<b>Gold</b>	(5)
<b>Iron</b>	51
<b>Lanthanum</b>	(36)
<b>Lead</b>	38.57
<b>Manganese</b>	(39.6)
<b>Neodymium</b>	(36)
<b>Nickel</b>	38.8
<b>Potassium</b>	(64)
<b>Rubidium</b>	31.4
<b>Samarium</b>	(39)
<b>Silver</b>	22
<b>Strontium</b>	78.4
<b>Thallium</b>	(15.7)
<b>Thorium</b>	37.79
<b>Titanium</b>	(50.1)
<b>Uranium</b>	37.38
<b>Ytterbium</b>	(42)

Values in brackets not certified

## **Appendix 2**

<b>Appendix 2.1: Protein Assay</b>	<b>p 200</b>
<b>Appendix 2.2: Calculation of Iron Concentration</b>	<b>p 203</b>
<b>Appendix 2.3: Metal Profiles for Enriched Serum</b>	<b>p 204</b>
<b>Appendix 2.4: Metal Distribution in Enriched Serum</b>	<b>p 209</b>
<b>Appendix 2.5: MALDI TOF Spectra from Albumin Analysis</b>	<b>p 211</b>

## Appendix 2.1: Protein Assay

The Bio-Rad protein assay is based on a method first developed by Bradford<sup>231</sup>. It is used to determine the total protein concentration of a sample based on the proportional binding of Coomassie<sup>®</sup> Brilliant Blue G-250 dye to proteins. The binding of the dye to a protein causes a shift in the absorption maximum of the dye from 465 nm (doubly protonated red form) to 595 nm (unprotonated blue form). The protein concentration of a sample is determined by comparison of the absorbance max at 595 nm to a linear absorbance profile produced by a series of calibration standards. The microassay procedure is very sensitive with a working range of 5-100 µg/ml.

The method is a rapid, simple one-step procedure in which the reagent is added to the sample and the absorbance measured at 595 nm. This assay has the advantage of being faster, involving fewer mixing steps, not requiring heating and giving a more stable colorimetric response than other assays commonly used. However, as with other assays the results can be influenced by non-protein sources such as detergents and response becomes progressively non-linear at the high end of the protein concentration range. The procedure also exhibits a significant dependence on protein amino acid composition and this has recently been shown to be a consequence of the dye binding primarily to basic (especially arginine) and aromatic amino acid residues<sup>232</sup>.

The system was calibrated using lyophilised bovine serum albumin (BSA) reconstituted in deionised water. Five working standards were prepared in linear range (1.2-20 µg/mL). To 800 µL of each standard and sample solution 200 µL of dye reagent concentrate were added. Samples were mixed using a vortex spinner then incubated at room temperature for 5 minutes – 1 hour. The absorbance maximum at 595 nm was then measured. A calibration graph plotted with Absorbance at 595 nm vs [protein] for the BSA standard solutions, see Figure A2.1. The protein concentrations of the samples were then determined using the calibration curve, values obtained shown in Table A2.1.

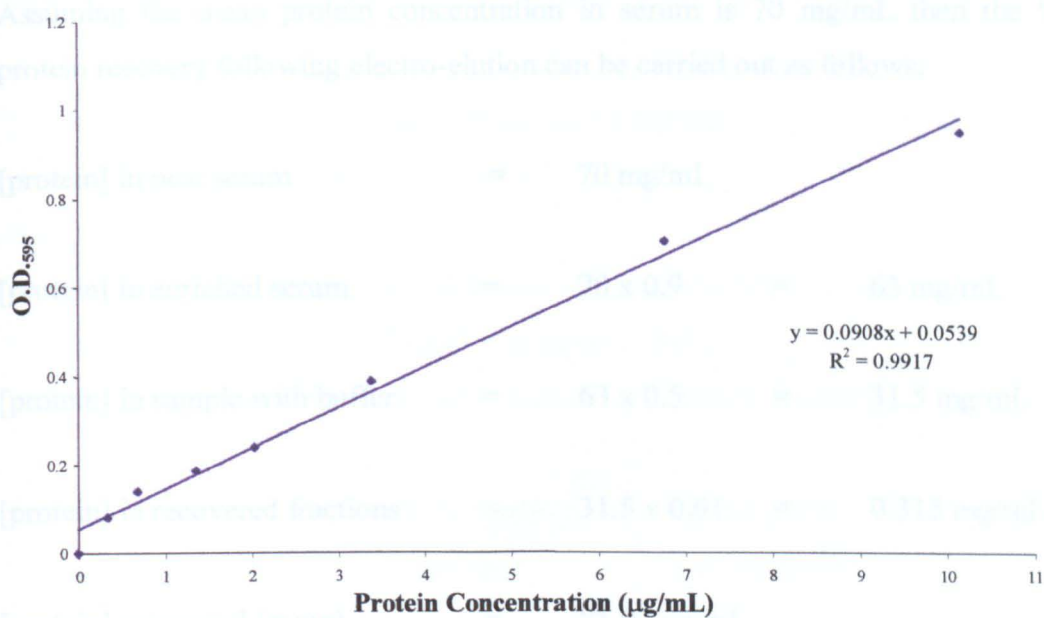


Figure A2.1: Standard Curve for Bio-Rad protein assay using BSA

Electro-elution Fraction	Protein Concentration (µg/mL)
1	39.93
2	41.93
3	35.97
4	51.28
5	58.02
6	39.70
7	51.51
8	378.62
9	306.62
10	32.46
11	23.82
12	25.93
13	23.32
14	25.84
Mean	81.07

Table A2.1: Protein Concentrations in Electro-elution Fractions

Assuming the mean protein concentration in serum is 70 mg/mL then the % protein recovery following electro-elution can be carried out as follows;

$$\text{[protein] in neat serum} = 70 \text{ mg/mL}$$

$$\text{[protein] in enriched serum} = 70 \times 0.9 = 63 \text{ mg/mL}$$

$$\text{[protein] in sample with buffer} = 63 \times 0.5 = 31.5 \text{ mg/mL}$$

$$\text{[protein] in recovered fractions} = 31.5 \times 0.01 = 0.315 \text{ mg/mL}$$

$$\text{[protein] recovered (mean)} = 81.07 \text{ } \mu\text{g/mL}$$

$$\% \text{ protein recovery} = 100/0.315 \times 0.08107 = 25.74 \%$$

## Appendix 2.2: Calculation of Iron Concentration

Typical concentration of transferrin in serum = 2 mg/mL

Molecular mass of transferrin = ~ 75 kDa

Atomic mass of iron = 56

Number of iron binding sites per molecule of transferrin = 2

Typical saturation of iron binding sites in serum = 40%

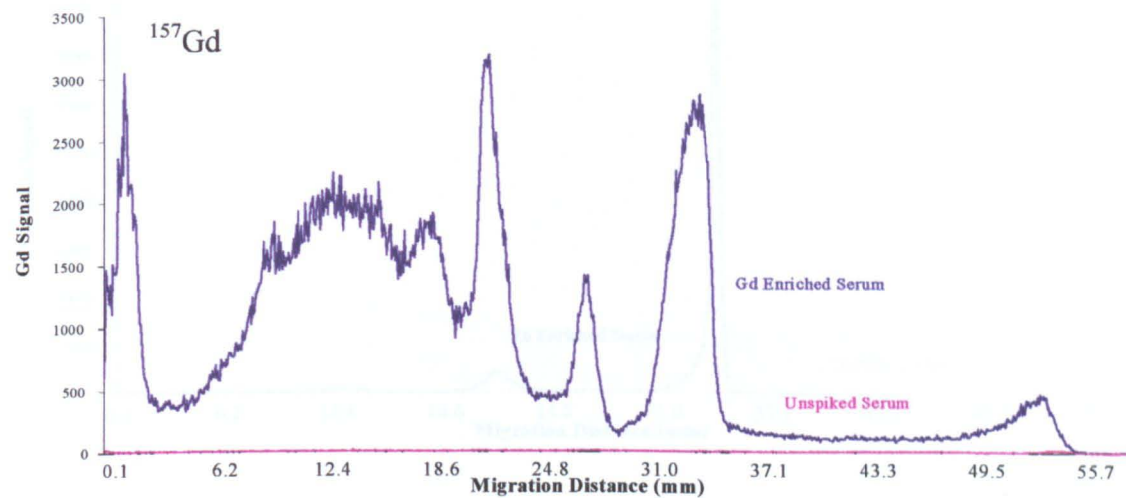
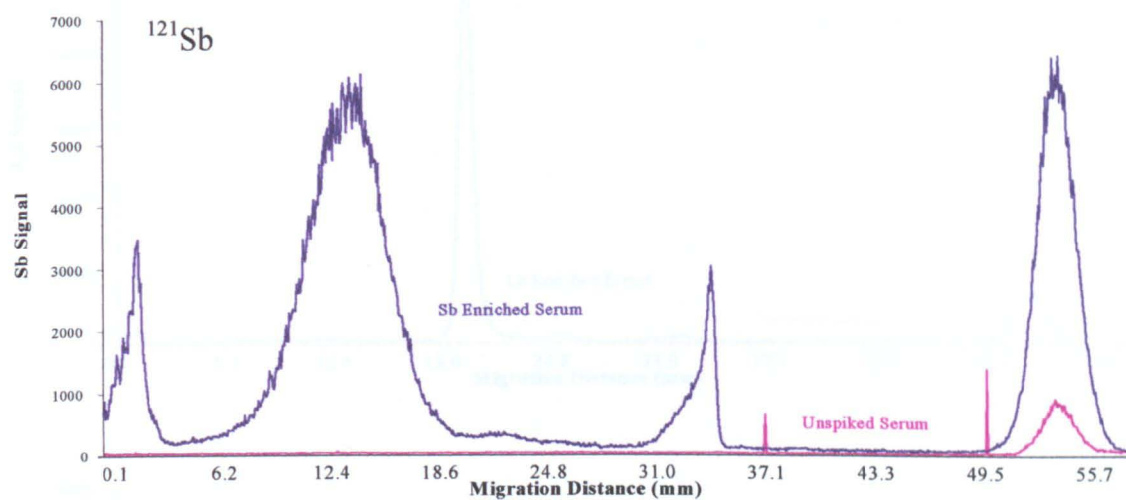
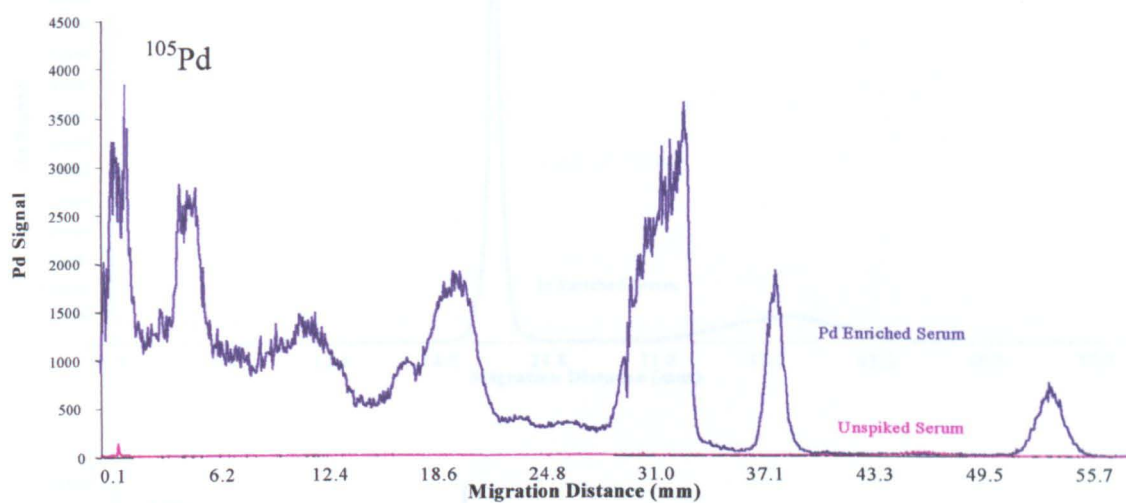
Typical concentration of iron bound to transferrin in serum given by;

$$\begin{aligned} [\text{Fe-transferrin}] &= \text{no molecules transferrin} \times \text{no Fe atoms per molecule} \times \text{atomic mass Fe} \\ \text{in serum} &= 0.002 / 75000 \times (2 \times 40 / 100) \times 56 \\ &= 1.194 \times 10^{-6} \text{ g/mL} \\ &= 1.194 \mu\text{g/mL} \end{aligned}$$

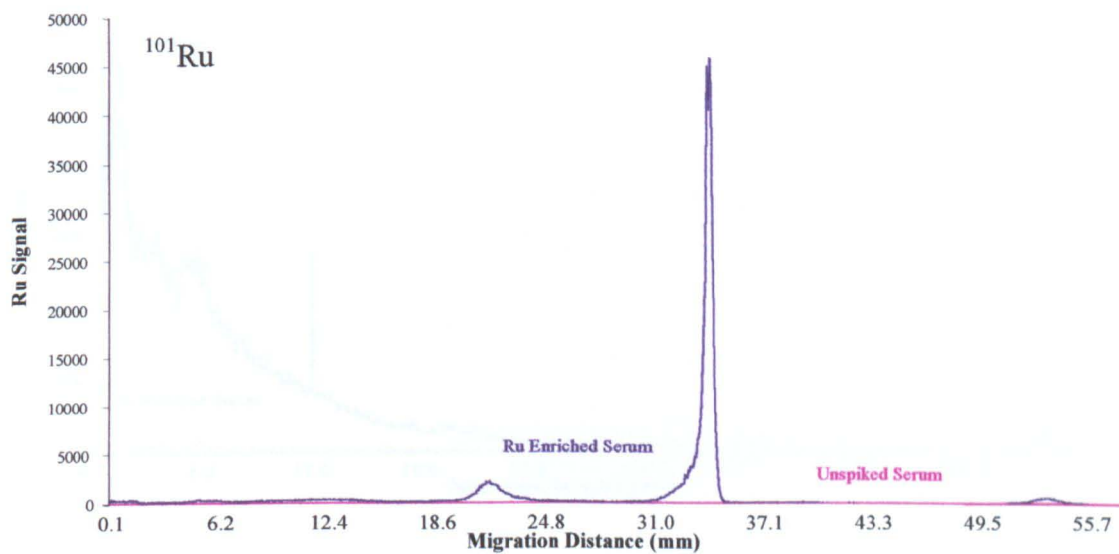
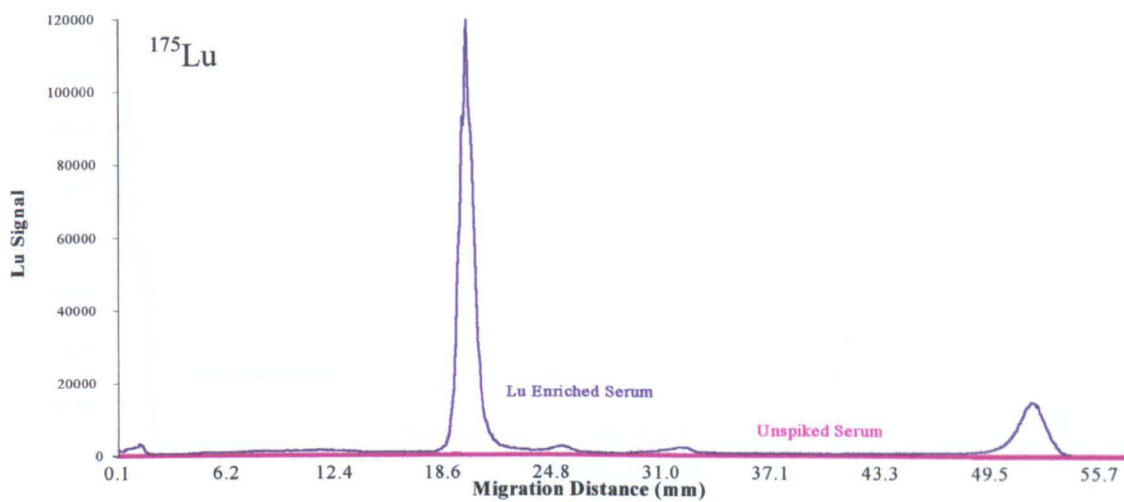
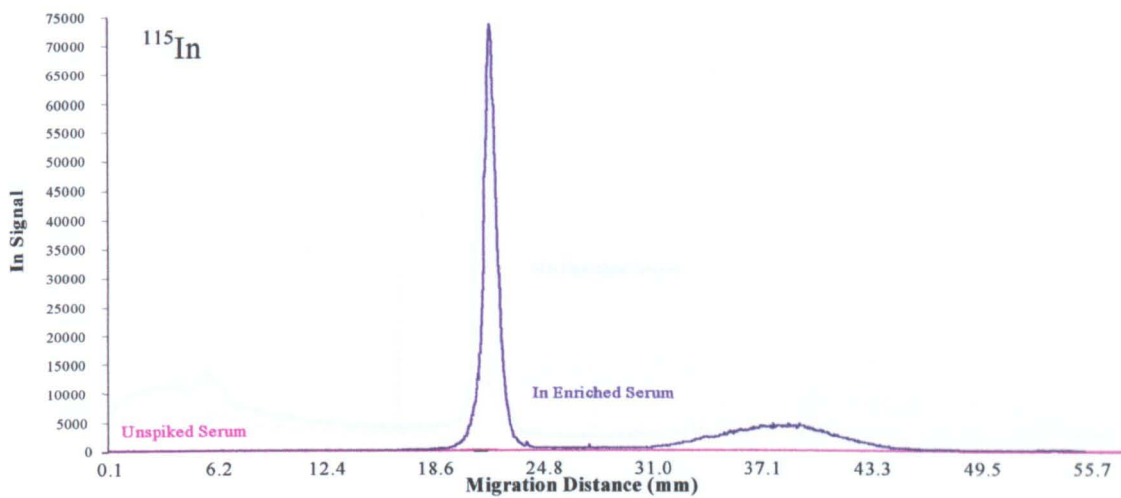
typical amount of Fe-transferrin loaded per PAGE lane is given by;

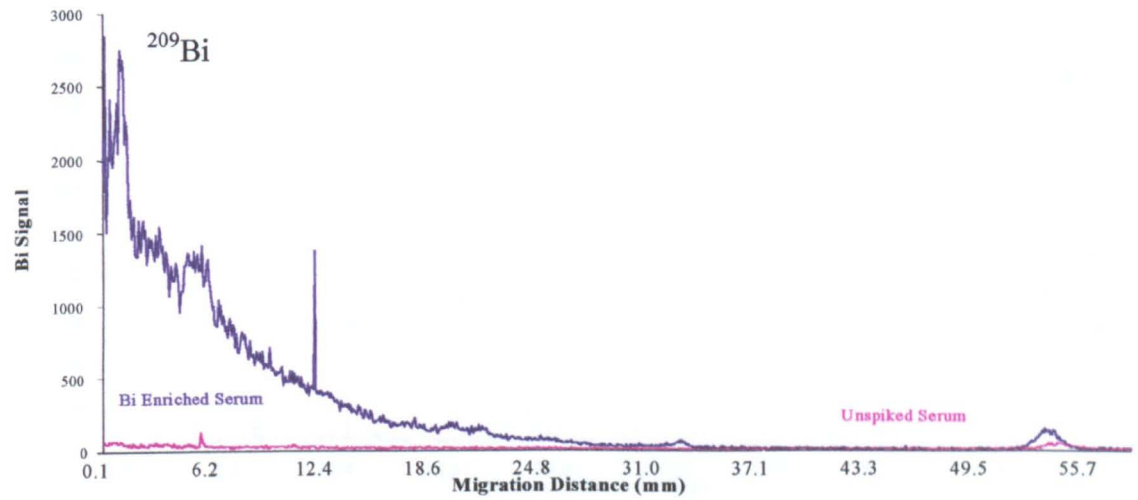
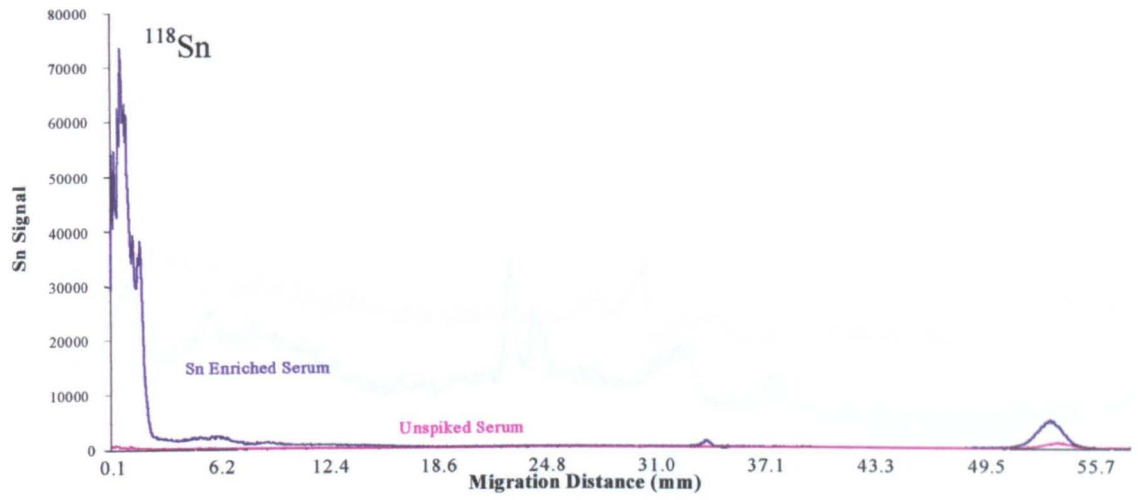
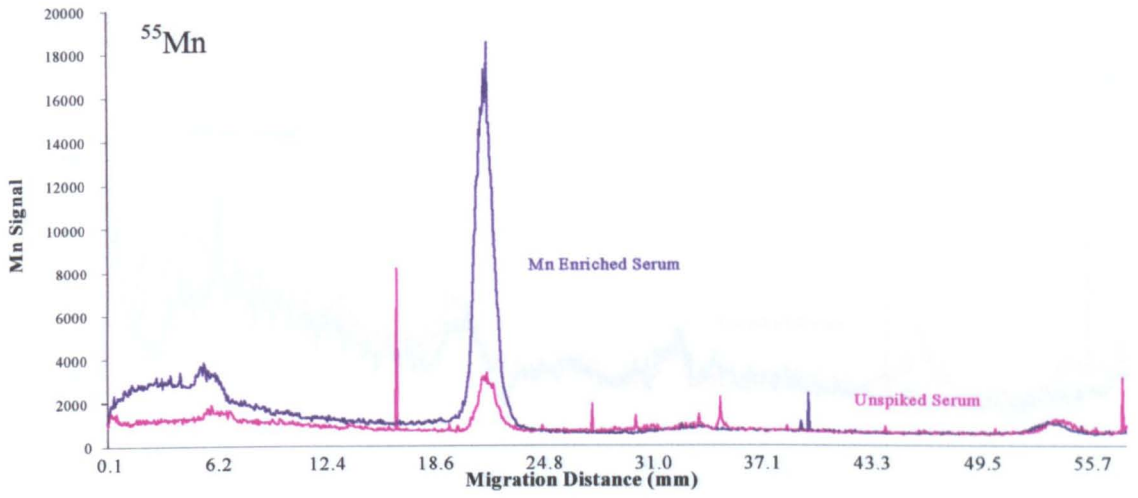
$$\begin{aligned} \text{Fe-transferrin mass} &= [\text{Fe-transferrin}] \text{ in serum} \times \text{serum volume} \\ &= 1.194 \times 0.00225 \\ &= 0.0027 \mu\text{g} \\ &\approx 3 \text{ ng Fe-transferrin/lane} \end{aligned}$$

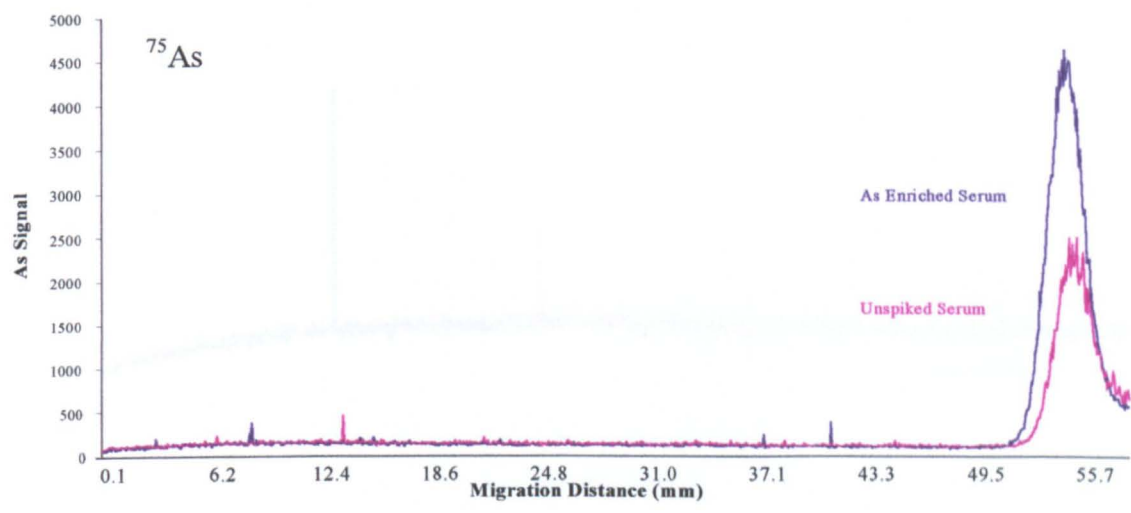
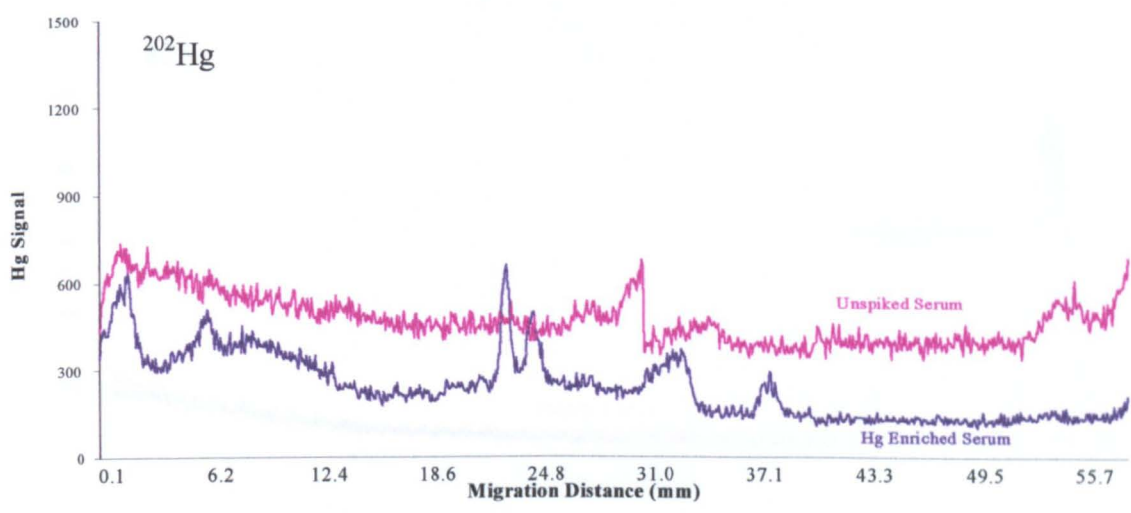
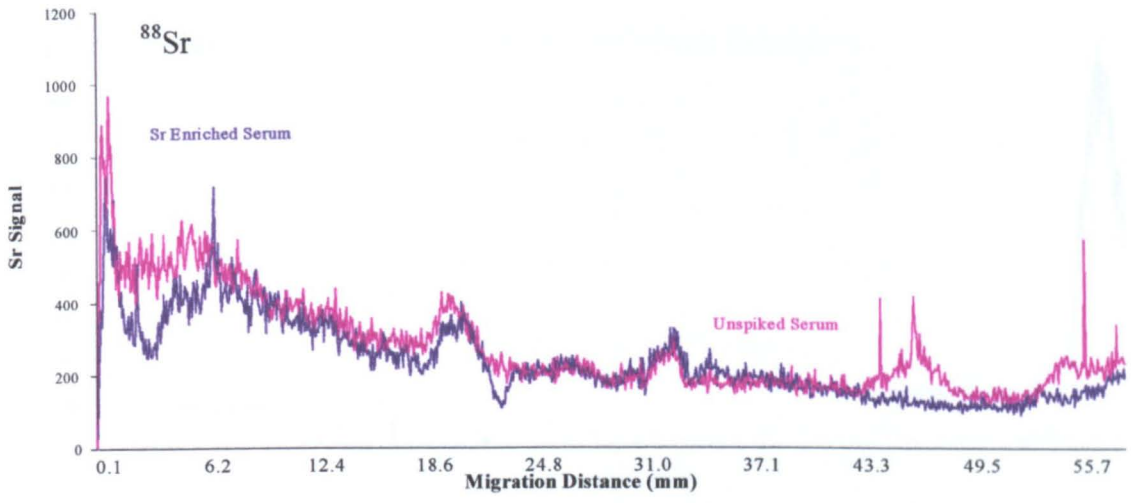
## Appendix 2.3: Metal Profiles for Enriched Serum











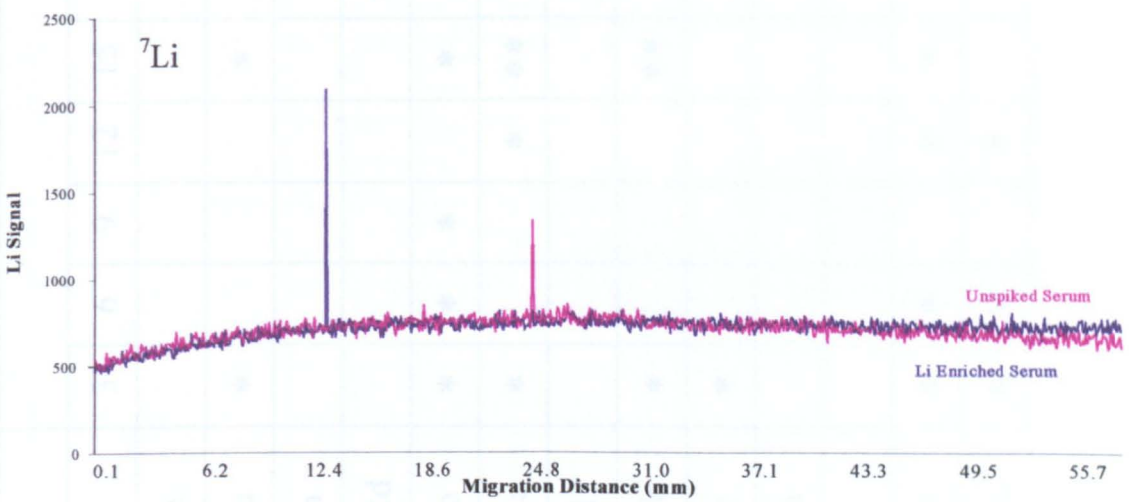
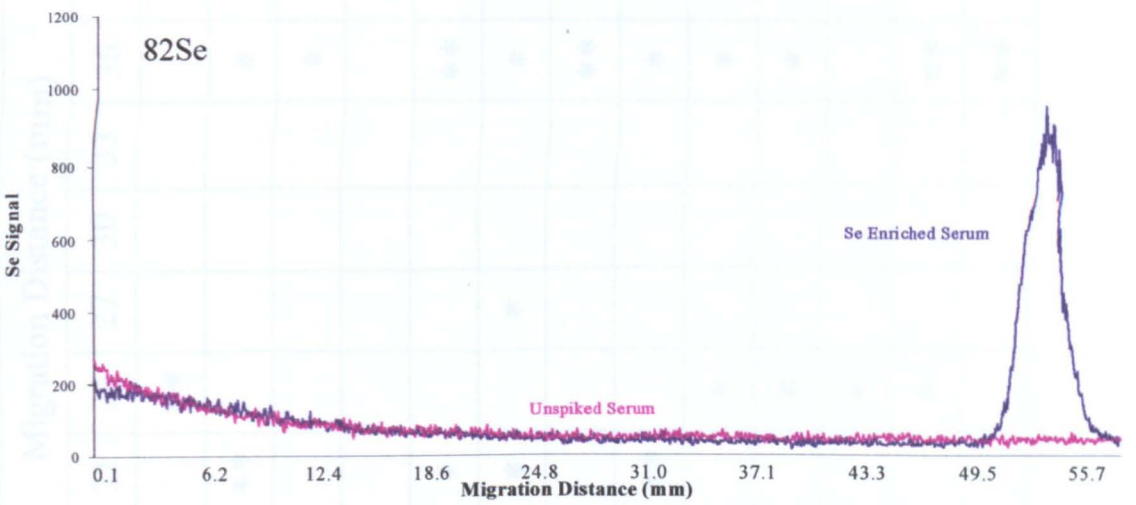
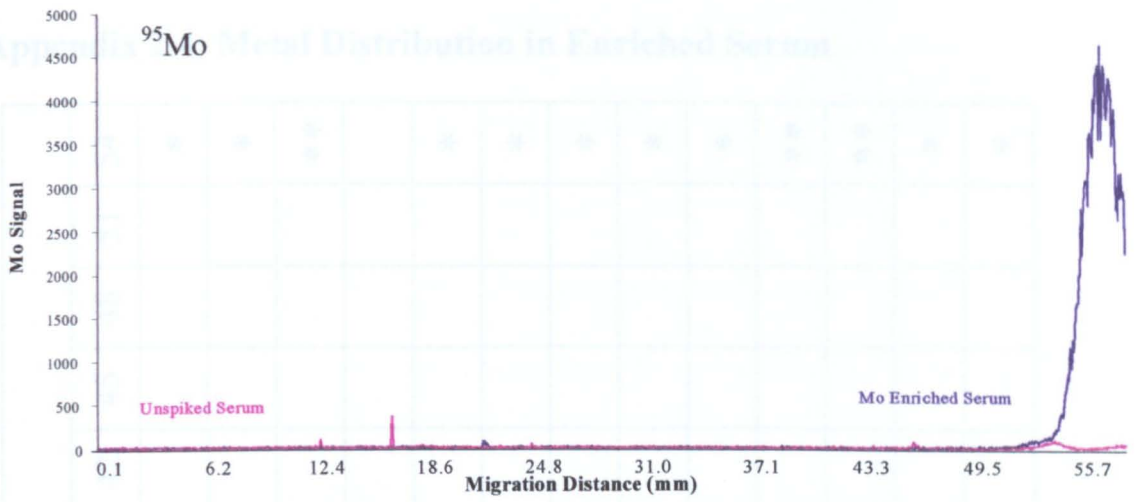


Table A3.2: Metal distribution in enriched serum samples present in protein fraction. \* denotes initial signal in unenriched serum

## Appendix 2.4: Metal Distribution in Enriched Serum

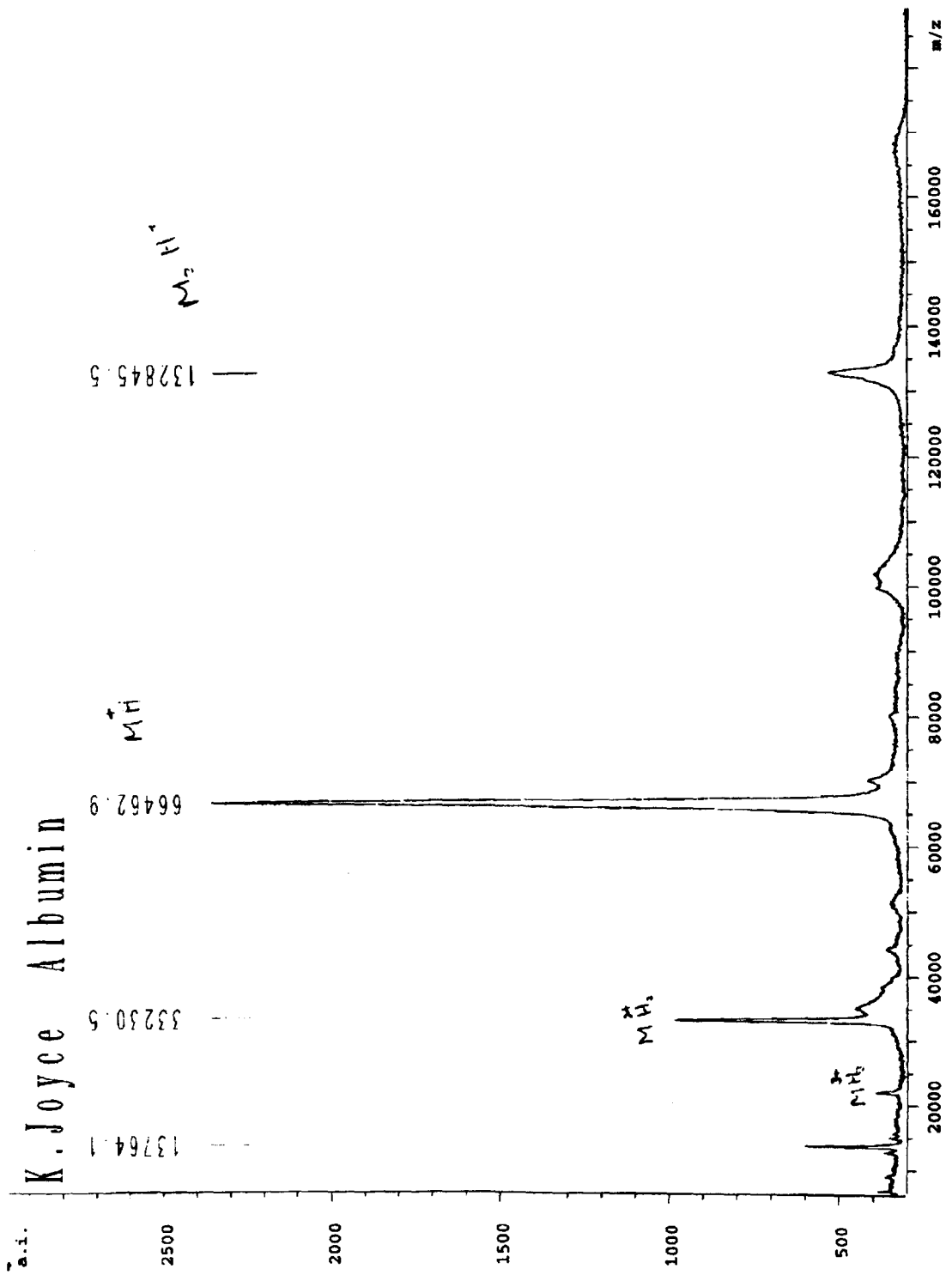
	Migration Distance (mm)																	
	3	6	9	12	15	18	21	24	27	30	33	36	39	42	45	48	51	54
<sup>57</sup> Fe							**											*
<sup>65</sup> Cu	*				*		**					*						*
<sup>66</sup> Zn												*						**
<sup>111</sup> Cd						**												
<sup>59</sup> Co	*	*	*		*		*					**						*
<sup>139</sup> La	*			*	**	*	*		*			*						*
<sup>60</sup> Ni												**						*
<sup>208</sup> Pb	*				**		**					*						*
<sup>53</sup> Cr	*											*						*
<sup>69</sup> Ga												*						**
<sup>51</sup> V													*					**
<sup>195</sup> Pt	*	*		*	*	*						**						*
<sup>197</sup> Au	*	*		*								**						*

Table A2.2: Metal distribution in enriched serum samples. \* denotes metal present in protein fraction, \*\* denotes metal signal intensity relatively high

	Migration Distance (mm)																	
	3	6	9	12	15	18	21	24	27	30	33	36	39	42	45	48	51	54
<sup>105</sup> Pd	*	*		*			*	*			**		*					*
<sup>121</sup> Sb	*				**							*						**
<sup>157</sup> Gd	*		*	*	*		**	**	*		**	**						*
<sup>115</sup> In							**	**					*					
<sup>175</sup> Lu	*						**	**	*			*						*
<sup>101</sup> Ru								*				**						*
<sup>55</sup> Mn		*						**										*
<sup>118</sup> Sn	**											*						*
<sup>209</sup> Bi	**	*	*									*						*
<sup>88</sup> Sr	*	*							*			*						
<sup>202</sup> Hg	*							*				*	*					*
<sup>75</sup> As																		**
<sup>95</sup> Mo								*										**
<sup>82</sup> Se																		**
<sup>7</sup> Li																		**

Table A2.3: Metal distribution in enriched serum samples. \* denotes metal present in protein fraction, \*\* denotes metal signal intensity relatively high

# Appendix 2.5: MALDI TOF Spectra from Albumin Analysis



## Bibliography

- (1) Frausto da Silva, J. J. R.; Williams, R. J. P. In *The Biological Chemistry of the Elements. Inorganic Chemistry of Life.*; Frausto da Silva, J. J. R., Williams, R. J. P., Eds.; Clarendon Press: Oxford, 1993, pp 3.
- (2) Mertz, W. *Science* **1981**, *213*, 1332-1338.
- (3) WHO In *Trace Elements in Human Nutrition, Tech. Rep. Ser. No. 532*: Geneva, 1973.
- (4) Morgan, J. J.; Stumm, W. In *Metals and Their Compounds in the Environment*; Merian, E., Ed.; VCH: Weinheim, 1991, pp 96.
- (5) Department of Health Report No.41, HMSO: London, 1991.
- (6) Frausto da Silva, J. J. R.; Williams, R. J. P. In *The Biological Chemistry of the Elements. Inorganic Chemistry of Life.*; Frausto da Silva, J. J. R., Williams, R. J. P., Eds.; Clarendon Press: Oxford, 1993, pp 541.
- (7) Seiler, H. G.; Sigel, A.; Sigel, H. In *Handbook on Metals in clinical and Analytical chemistry*; Seiler, H. G., Sigel, A., Sigel, H., Eds.; Marcel Dekker: New York, 1994, pp 10.
- (8) Kieffer, F. In *Metals and Their Compounds in the Environment*; Merian, E., Ed.; VCH: Weinheim, 1991, pp 487.
- (9) Langmuir, I. *J. Amer. Chem. Soc.* **1916**, *38*, 2221-2295.
- (10) Langmuir, I. *J. Amer. Chem. Soc.* **1917**, *39*, 1848-1906.
- (11) Albert, A. In *Selective Toxicity*, 3rd ed.; Albert, A., Ed.; Methuen & Co. Ltd: London, 1965, pp 133.
- (12) Albert, A. *Biochem. J.* **1952**, *50*, 690.
- (13) Tanford, C. *J. Amer. Chem. Soc.* **1952**, *74*, 211-215.
- (14) Cornelis, R. *Ann. Clin. Lab. Sci.* **1996**, *26*, 252-263.
- (15) Cornelis, R.; De Kimpe, J. *JAAS* **1994**, *9*, 945-950.
- (16) Templeton, D. M.; Ariese, F.; Cornelis, R.; Danielsson, L.-G.; Muntau, H.; Van Leewen, H. P.; Lobinski, R. *Pure Appl. Chem* **2000**, *72*, 1453-1470.
- (17) Stubbs, R. L. *Cadmium-81 1981, Edited Proceedings 3rd International Cadmium Conference, Miami*, 3-7.
- (18) Nielsen, T. In *Biological Effects of Organolead Compounds*; Grandjean, P., Ed.; CRC Press: Boca Raton, Florida, 1984, pp 43-62.
- (19) Kendrick, M. J.; May, M. T.; Plishka, M. J.; Robinson, K. D. In *Metals in Biological Systems*; Kendrick, M. J., May, M. T., Plishka, M. J., Robinson, K. D., Eds.; Ellis Horwood: London, 1992, pp 158-159.
- (20) Rosenberg, B.; Van Camp, L.; Krigas, T. *Nature* **1965**, *205*, 698.
- (21) Rosenberg, B.; Van Camp, L.; Trosko, J. E.; Mansour, V. H. *Nature* **1969**, *222*, 385-386.
- (22) Rosenberg, B.; Van Camp, L.; Grimley, E. B.; Thomson, A. J. *J. Biol. Chem.* **1967**, *242*, 1347.
- (23) Lippert, B. In *Cisplatin - Chemistry and Biochemistry of a Leading Anticancer Drug*; Lippert, B., Ed.; Wiley-VCH: Weinheim, 1999.
- (24) Roberts, J. J.; Thomson, A. J. *Prog. Nucleic Acid Res. Mol. Biol.* **1979**, *22*, 71-133.
- (25) Madias, N. E.; Harrington, J. T. *Am. J. Med.* **1978**, *65*, 307.
- (26) Borch, R. F.; Pleasants, M. *Proc. Natl. Acad. Sci. USA* **1979**, *76*, 6611.
- (27) Bodenner, D.; Dedon, P.; Keng, P.; Katz, J. *Cancer Res.* **1986**, *46*, 2751.



- (28) Bodenner, D.; Dedon, P.; Keng, P.; Borch, R. *Cancer Res.* **1986**, *46*, 2745-2750.
- (29) Hayes, D. M.; Cvitovic, E.; Golbey, R. B.; Scheiner, E.; Helson, L.; Krakoff, B. I. H. *Cancer* **1977**, *39*, 1372.
- (30) Johnson, S. W.; Ferry, K. V.; Hamilton, T. C. *Drug Resist. Updates* **1998**, *1*, 243-254.
- (31) Kelland, L. R.; Sharp, S. Y.; O'Neill, C. F.; Raynaud, F. I.; Beale, P. J.; Judson, I. R. *J. Inorg. Biochem.* **1999**, *77*, 111-115.
- (32) Knox, R. J.; Friedlos, F.; Lydall, D. A.; Roberts, J. J. *Cancer Res.* **1986**, *46*, 1972-1979.
- (33) Kaim, W.; Schwederski, B. In *Bioinorganic Chemistry: Inorganic Elements in the Chemistry of Life, An Introduction and Guide*; Kaim, W., Schwederski, B., Eds.; John Wiley and Sons: New York, 1996, pp 366.
- (34) Kaim, W.; Schwederski, B. In *Bioinorganic Chemistry: Inorganic Elements in the Chemistry of Life an Introduction and Guide*; Schwederski, B., Ed.; John Wiley & Sons: New York, 1991, pp 367.
- (35) Johnson, N. P.; Hoeschele, J. D.; Rahn, R. O. *Chem.-Biol. Inter.* **1980**, *30*, 151.
- (36) Nagai, N.; Okuda, R.; Kinoshita, M.; Ogata, H. *J. Pharm. Pharmacol.* **1996**, *48*, 918-924.
- (37) Litterst, C. L.; Gram, T. E.; Dedrick, R. L.; Leroy, A. F.; Guarino, A. M. *Cancer Res.* **1976**, *36*, 2340-2344.
- (38) DeConti, R. C.; Toftness, B. R.; Lange, R. C.; Creasey, W. A. *Cancer Res.* **1973**, *33*, 1310.
- (39) Hoshino, T.; Misaki, M.; Yamamoto, M.; Shimizu, H.; Ogawa, Y.; Toguchi, H. *J. Cont. Rel.* **1995**, *37*, 75-81.
- (40) Takahashi, I.; Ohnuma, T.; Kavy, S.; Bhardwaj, S.; Holland, J. F. *Brit. J. Cancer* **1980**, *41*, 602-608.
- (41) Manaka, R. C.; Wolf, W. *Chem.-Biol. Inter.* **1978**, *22*, 353-358.
- (42) Pascoe, J. M.; Roberts, J. J. *Biochem. Pharmacol.* **1974**, *23*, 1345-1357.
- (43) Brouwer, J.; Vandeputte, P.; Fichtingerschepman, A. M. J.; Reedjik, J. *Proc. Natl. Acad. Sci. USA - Biological Sciences* **1981**, *78*, 7010-7014.
- (44) McAuliffe, C. A.; Sharma, H. L.; Tinker, N. D. In *Chemistry of the Platinum Group Metals*; Hartley, F. R., Ed.; Elsevier: New York, 1991, pp 546-593.
- (45) Lippert, B. *Progr. Inorg. Chem.* **1989**, *37*, 1-97.
- (46) Lippard, S. J. *Science* **1982**, *218*, 1075-1082.
- (47) Kline, T. P.; Marzilli, L. G.; Live, D.; Zon, G. *J. Amer. Chem. Soc.* **1989**, *111*, 7057-7068.
- (48) Cohen, S. M.; Lippard, S. J. *Prog. Nucleic Acid Res. Mol. Biol.* **2001**, *67*, 93-130.
- (49) Hambley, T. W.; Jones, A. R. *Coordin. Chem. Rev.* **2001**, *212*, 35-59.
- (50) Repta, A. J.; Long, D. F. In *Cisplatin Current Status and Developments*; Prestayko, A. W., Crooke, S. T., Carter, S. K., Eds.; Academic Press: New York, 1980, pp 285-304.
- (51) Van der Vijgh, W. J. F.; Klein, I. *Cancer Chemother. Pharmacol.* **1986**, *18*, 129-132.
- (52) Ivanov, A. I.; Christodoulou, J.; Parkinson, J. A.; Barnham, K. J.; Tucker, A.; Woodrow, J.; Sadler, P. J. *J. Biol. Chem.* **1998**, *273*, 14721-14730.

- (53) Mustonen, R.; Hietanen, P.; Leppala, S.; Takala, M.; Hemminki, K. *Arch. Tox.* **1989**, *63*, 361-366.
- (54) Gormley, P. E.; Bull, J. M.; Le Roy, A. F.; Cysyk, R. *Clin. Pharmacol. Ther.* **1979**, *25*, 351-357.
- (55) Bannister, S. J.; Sternson, L. A.; Repta, A. J. *Clin. Chem.* **1978**, *24*, 877.
- (56) Chang, Y.; Sternson, L. A.; Repta, A. J. *Anal. Lett.* **1978**, *11*, 449.
- (57) Nineham, A. W. *Arch. Interamerican Rheum.* **1963**, *6*, 113.
- (58) Wigley, R. A.; Brooks, R. R. In *Noble Metals and Biological Systems Their Role in Medicine, Mineral Exploration and the Environment*; Brooks, R. R., Ed.; CRC Press: London, 1992, pp 279.
- (59) Koch, R. *Deut. Med. Wochenschr.* **1927**, *16*, 756.
- (60) Feldt, A. *Ber. Klin. Wochenschr* **1917**, *54*, 1111.
- (61) Lande, K. *Munch. Med. Woch.* **1927**, *74*, 1132.
- (62) Forestier, J. B. *Soc. Med. Hop. Paris* **1929**, *53*, 323.
- (63) Forestier, J. *Lancet* **1934**, *2*, 646.
- (64) Simon, T. M.; Kunishima, D. H.; Vibert, G. J.; Lorber, A. *Cancer* **1979**, *44*, 1965.
- (65) Wackers, F. J.; Giles, R. W.; Hoffer, P. B.; Lange, R. C.; Berger, H. J.; Zaret, B. L. *Am. J. Cardiol.* **1982**, *50*, 89-94.
- (66) Fricker, S. P. *Gold Bull.* **1996**, *29*, 53-60.
- (67) Shaw III, C. F. *Comm. Inorg. Chem.* **1989**, *8*, 233-267.
- (68) Best, S. L.; Sadler, P. J. *Gold Bull.* **1996**, *29*, 87-93.
- (69) Rodman, G. P. In *Primer on the Rheumatic Diseases*, 7th ed.; The Arthritis Foundation: New York, 1973.
- (70) Empire; Rheumatism; Council *Ann. Rheum. Dis.* **1961**, *20*, 315-354.
- (71) Sadler, P. J. *Struct. Bonding* **1976**, *29*, 171-214.
- (72) Brown, D. H.; Smith, W. E. *Chem. Soc. Rev.* **1980**, *9*, 217-240.
- (73) Shaw III, C. F. *Inorg. Pers. Biol. Med.* **1979**, *2*, 287-355.
- (74) Gottlieb, N. L. *J. Rheumatol. Sup.* **1982**, *9*, 99-109.
- (75) Walz, D. T.; Griswold, D. E.; DiMartino, M. J.; Bumbier, E. E. *J. Rheumatol.* **1980**, *7*, 820-824.
- (76) Guo, Z. J.; Sadler, P. J. *Angewandte Chemie - Int. Ed.* **1999**, *38*, 1513-1531.
- (77) Danpure, C. J.; Fyfe, D. A.; Gumpel, J. M. *Ann. Rheum. Dis.* **1979**, *38*, 364-370.
- (78) Ghdially, E. N.; Orschak, A. F.; Mitchell, D. M. *Ann. Rheum. Dis.* **1976**, *35*, 67-72.
- (79) Brown, D. H.; Smith, W. E. In *Platinum, Gold, and Other Metal Chemotherapeutic Agents*; Lippard, S. J., Ed.; American Chemical Society: Washington, D.C., 1983, pp 401-418.
- (80) Ishida, K.; Orimo, H. In *Handbook on Metals in Clinical and Analytical Chemistry*; Seiler, H. G., Sigel, A., Sigel, H., Eds.; Marcel Dekker: New York, 1994, pp 394.
- (81) Herrlinger, J. D.; Alsen, C.; Beress, R.; Hecker, U.; Weikert, W. *J. Rheumatol. Sup.* **1982**, *9*, 81-89.
- (82) Christodoulou, J.; Sadler, P. J.; Tucker, A. *Euro. J. Biochem.* **1994**, *225*, 363-368.
- (83) Christodoulou, J.; Sadler, P. J.; Tucker, A. *FEBS Letters* **1995**, *376*, 1-5.
- (84) Schmitz, G.; Minkel, D. T.; Gingrich, D.; Shaw III, C. F. *J. Inorg. Biochem.* **1980**, *12*, 293.

- (85) Chayen, J.; Bitensky, L. *Ann. Rheum. Dis.* **1971**, *30*, 522.
- (86) Lawrence, J. S. *Ann. Rheum. Dis.* **1961**, *20*, 341.
- (87) Kaim, W.; Schwederski, B. In *Bioinorganic Chemistry: Inorganic Elements in the Chemistry of Life An Introduction and Guide*; Schwederski, B., Ed.; John Wiley & Sons: New York, 1991, pp 375.
- (88) Gleichmann, E.; Schumann, D.; Kubickamuranyi, M. *Euro. J. Pharmacol.* **1990**, *183*, 78-79.
- (89) Schuhmann, D.; Kubickamuranyi, M.; Mirtschewa, J.; Gunther, J.; Kind, P.; Gleichmann, E. *J. Immunol.* **1990**, *145*, 2132-2139.
- (90) Zou, J.; Guo, Z.; Parkinson, J. A.; Chen, Y.; Sadler, P. J. *J. Inorg. Biochem.* **1999**, *74*, 352-352.
- (91) Witkiewicz, P. L.; Shaw III, C. F. *J. Chem. Soc. - Chem. Comm.* **1981**, *21*, 1111-1114.
- (92) Abraham, G. E.; Himmel, P. B. *J. Nut. Env. Med.* **1997**, *7*, 295-305.
- (93) Cornelis, R.; Borguet, F.; De Kimpe, J. *Anal. Chim. Acta* **1993**, *283*, 183-189.
- (94) Guo, Z.; Sadler, P. J. *Advances in Inorganic Chemistry* **2000**, *49*, 183-306.
- (95) Stoepler, M. In *Metals and Their Compounds in the Environment*; Merian, E., Ed.; VCH: Weinheim, 1991, pp 122.
- (96) Greenberg, R. R.; Fleming, R. F.; Zeisler, R. *Environ. Int.* **1984**, *10*, 129-136.
- (97) Houk, R. S.; Fassel, V. A.; Flesch, G. D.; Svec, H. J.; Gray, A. L.; Taylor, C. E. *Anal. Chem.* **1980**, *52*, 2283-2289.
- (98) Greaves, E. D.; Parra, L. M. M.; Rojas, A.; Sajo-Bohus, L. *X-ray Spectrometry* **2000**, *29*, 349-353.
- (99) Jonson, R.; Mattsson, S.; Unsgaard, B. *Physics in Medicine and Biology* **1988**, *33*, 847-857.
- (100) Pietra, R.; Sabbioni, E.; Gallorini, M.; Orvini, E. *J. Radioanal. Nuc. Chem. - Articles* **1986**, *102*, 69-98.
- (101) Ensslin, A. S.; Pethran, A.; Schrierl, R.; Fruhmann, G. *Int. Arch. Occup. Env. Health* **1994**, *65*, 339-342.
- (102) Vaughan, G. T.; Florence, T. M. *Sci. Tot. Environ.* **1992**, *111*, 47-58.
- (103) Evetts, I.; Milton, D.; Mason, R. *Biol. Mass Spec.* **1991**, *20*, 153-159.
- (104) Egila, J.; Littlejohn, D.; Smith, W. E.; Sturrock, R. D. *J. Pharm. Biomed. Anal.* **1992**, *10*, 639-644.
- (105) Massarella, J. W.; Waller, E. S.; Crout, J. E.; Yakatan, G. J. *Biopharm. Drug Disp.* **1984**, *5*, 101-107.
- (106) Melethil, S.; Schoepp, D. *Pharm. Res.* **1987**, *4*, 332-336.
- (107) Morrison, J. G.; White, P.; McDougall, S.; Firth, J. W.; Woolfrey, S. G.; Graham, M. A.; Greenslade, D. *J. Pharm. Biomed. Anal.* **2000**, *24*, 1-10.
- (108) Cairns, W. R. L.; McLeod, C. W.; Hancock, B. *Spectros.* **1997**, *12*, 16.
- (109) Christodoulou, J.; Kashani, M.; Keohane, B. M.; Sadler, P. J. *JAAS* **1996**, *11*, 1031-1035.
- (110) Farago, M. E.; Kavanagh, P.; Blanks, R.; Kelly, J.; Kazantzis, G.; Thornton, I.; Simpson, P. R.; Cooke, J. M.; Delves, H. T.; Hall, G. E. M. *Analyst* **1998**, *123*, 451-454.
- (111) Vanhoe, H.; Vandecasteele, C.; Versieck, J.; Dams, R. *Anal. Chem.* **1989**, *61*, 1851-1857.
- (112) Alimonti, A.; Petrucci, F.; Fioravanti, S.; Laurenti, F.; Caroli, S. *Anal. Chim. Acta* **1997**, *342*, 75-81.

- (113) Patriarca, M.; Lyon, T. D. B.; Delves, H. T.; Howatson, A. G.; Fell, G. S. *Analyst* **1999**, *124*, 1337-1343.
- (114) Lim, H. B.; Han, M. S.; Lee, K. J. *Anal. Chim. Acta* **1996**, *320*, 185-189.
- (115) McLeod, C. W.; Worsford, P. J.; Cox, A. G. *Analyst* **1984**, *109*, 327-332.
- (116) Melton, L. A.; Tracy, M. L.; Moller, G. *Clin. Chem.* **1990**, *36*, 247-250.
- (117) Mianzhi, Z.; Barnes, R. M. *Applied Spectroscopy* **1984**, *38*, 635-644.
- (118) Taylor, D. M.; Williams, D. R. In *Trace Element Medicine and Chelation Therapy*; Taylor, D. M., Williams, D. R., Eds.; Royal Society of Chemistry: Cambridge, 1995, pp 38.
- (119) Lobinski, R.; Szpunar, J. *Anal. Chim. Acta* **1999**, *400*, 321-332.
- (120) Cave, M. R.; Butler, O.; Cook, J. M.; Cresser, M. S.; Garden, L. M.; Miles, D. L. *JAAS* **2000**, *15*, 181-235.
- (121) Kalac, P.; Svoboda, L. *Food Chemistry* **2000**, *69*, 273-281.
- (122) Menon, N. N.; Balchand, A. N.; Menon, N. R. *Hydrobiologia* **2000**, *430*, 149-183.
- (123) Szpunar-Lobinski, J.; Witte, C.; Lobinski, R.; Adams, F. C. *Fresenius J. Anal. Chem.* **1995**, *351*, 351-377.
- (124) Lobinski, R. *App. Spectros.* **1997**, *51*, 260A-278A.
- (125) Kot, A.; Namiesnik, J. *TRAC* **2000**, *19*, 69-79.
- (126) Szpunar, J. *Analyst* **2000**, *125*, 963-988.
- (127) Tiselius, A. T. *Faraday Soc.* **1937**, *33*, 524.
- (128) Ornstein, L. *Ann. N.Y. Acad. Sci.* **1964**, *121*, 321-349.
- (129) Davis, B. J. *Ann. N.Y. Acad. Sci.* **1964**, *121*, 404-427.
- (130) Margolis, J.; Kenrick, K. G. *Nature* **1967**, *214*, 1334.
- (131) Sharpiro, A. L.; Vinuela, E.; Maizel, J. V. J. *Biochem. Biophys. Res. Commun.* **1967**, *28*, 815-820.
- (132) Laemmli, U. K. *Nature* **1970**, *227*, 680-685.
- (133) Reynolds, J. A.; Tanford, C. J. *Biol. Chem.* **1970**, *245*, 5161-5167.
- (134) Svensson, H. *Acta Chem. Scand.* **1961**, *15*, 325-341.
- (135) Bjellqvist, B.; Ek, K.; Righetti, P. G.; Gianazza, E.; Gorg, A.; Westermeier, R.; Postel, W. J. *Biochem. Biophys. Methods* **1982**, *6*, 317-339.
- (136) Svensson, H. *Acta Chem. Scand.* **1962**, *16*, 456-466.
- (137) Gianazza, E.; Righetti, P. G. *J. Chromatogr.* **1980**, *193*, 1.
- (138) O'Farrell, P. H. *J. Biol. Chem.* **1975**, *50*, 4007-4021.
- (139) Van Loon, J. C. *Anal. Chem.* **1979**, *51*, A1139.
- (140) Himmelhoch, S. R.; Sober, H. A.; Vallee, B. L.; Peterson, E. A.; Fuwa, K. *Biochem.* **1966**, *5* (5), 2523-2530 (2523).
- (141) Teape, J.; Kamel, H.; Brown, D. H.; Ottaway, J. M.; Smith, W. E. *Clin. Chim. Acta* **1979**, *94*, 1-8.
- (142) Scott, B. J.; Bradwell, A. R. *Clin. Chem.* **1983**, *29*, 629-633.
- (143) Nielsen, J. L.; Poulsen, O. M.; Abildtrup, A. *Electrophoresis* **1994**, *15*, 666-671.
- (144) Kamel, H.; Brown, D. H.; Ottaway, J. M.; Smith, W. E. *Analyst* **1977**, *102*, 645-657.
- (145) Delves, H. T. *Clin. Chim. Acta* **1976**, *71*, 495-500.
- (146) Harrison, I.; Littlejohn, D.; Fell, G. S. *Analyst* **1996**, *121*, 189-194.
- (147) Shaw III, C. F.; Schaeffer-Memmel, N.; Krawczak, D. J. *Inorg. Biochem.* **1986**, *26*, 185-195.

- (148) Zhang, X. R.; Cornelis, R.; De Kimpe, J.; Mees, L. *JAAS* **1996**, *11*, 1075-1079.
- (149) Zhao, Z.; Tepperman, K.; Dorsey, J. G.; Elder, R. C. *J. Chromatogr. B - Biomed. App.* **1993**, *615*, 83-89.
- (150) Falter, R.; Wilken, R.-D. *Sci. Tot. Environ.* **1999**, *225*, 167-176.
- (151) Owen, L. M. W.; Rauscher, A. M.; Fairweather-Tait, S. J.; Crews, H. M. *Biochem. Soc. Trans.* **1996**, *24*, 947-952.
- (152) Zhao, Z.; Jones, W. B.; Tepperman, K.; Dorsey, J. G.; Elder, R. C. *J. Pharm. Biomed. Anal.* **1992**, *10*, 279-287.
- (153) Coni, E.; Alimonti, A.; Bocca, A.; La Torre, F.; Menghetti, E.; Miraglia, E.; Caroli, S. *Trace Elem. Electrol.* **1996**, *13*, 26-32.
- (154) Michalke, B.; Schramel, P. *Electrophoresis* **1999**, *20*, 2547-2553.
- (155) Lustig, S.; De Kimpe, J.; Cornelis, R.; Schramel, P. *Fresenius J. Anal. Chem.* **1999**, *363*, 484-487.
- (156) Lustig, S.; De Kimpe, J.; Cornelis, R.; Schramel, P.; Michalke, B. *Electrophoresis* **1999**, *20*, 1627-1633.
- (157) Neilsen, J. L.; Abildtrup, A.; Christensen, J.; Watson, P.; Cox, A. G.; McLeod, C. W. *Spectrochimica Acta B - Atomic Spectroscopy* **1998**, *53*, 339-345.
- (158) McLeod, C. W.; Clarke, P. A.; Mowthorpe, D. J. *Spectrochim. Acta B* **1986**, *41*, 63-71.
- (159) Hull, D. R.; Horlick, G. *Spectrochim. Acta B* **1984**, *39*, 843-850.
- (160) Farnsworth, P. B.; Hieftje, G. M. *Anal. Chem.* **1983**, *55*, 1414-1417.
- (161) Thompson, M.; Goulter, J. E.; Sieper, F. *Analyst* **1981**, *106*, 32-39.
- (162) Moenke-Blankenberg, L. *Spectrochim. Acta Rev.* **1993**, *15*, 1-37.
- (163) Russo, R. E.; Mao, X. L.; Borisov, O. V. *TRAC* **1998**, *17*, 461-469.
- (164) Horlick, G.; Montaser, A. In *Inductively Coupled Plasma Mass Spectrometry*; Montaser, A., Ed.; Wiley-VCH: New York, 1998, pp 525.
- (165) Abercrombie, F. N.; Silvester, M. D.; Murray, A. D.; Barringer, A. R. In *Applications of Inductively Coupled Plasma to Emission Spectroscopy*; Barnes, R. M., Ed.; Franklin Institute Press: USA, 1978, pp 121-145.
- (166) Gray, A. L. *Analyst* **1985**, *110*, 551-556.
- (167) Tye, C.; Gordon, J.; Webb, P. *Int. Lab.* **1987**, *12*, 34.
- (168) Chenery, S.; Cooke, J. M. *JAAS* **1993**, *8*, 299-303.
- (169) Longerich, H. P.; Jackson, S. E.; Fryer, B. J.; Strong, D. F. *Geosci. Can.* **1993**, *20*, 21-27.
- (170) Hoffmann, E.; Ludke, C.; Scholze, H.; Stepanowitz, H. *Fresenius J. Anal. Chem.* **1994**, *350*, 253-259.
- (171) Gunther, D.; Frischknecht, R.; Muschenborn, H. J.; Heinrich, C. A. *Fresenius J. Anal. Chem.* **1997**, *359*, 390-393.
- (172) Perkins, W. T.; Fuge, R.; Pearce, N. J. G. *JAAS* **1991**, *6*, 445-449.
- (173) Pearce, N. J. G.; Perkins, W. T.; Abell, I.; Duller, G. A. T.; Fuge, R. *JAAS* **1992**, *7*, 53-57.
- (174) Huang, Y.; Shibata, Y.; Morita, M. *Anal. Chem.* **1993**, *65*, 2999-3003.
- (175) Simon, K.; Wiechert, U.; Hoefs, J.; Grote, B. *Fresenius J. Anal. Chem.* **1997**, *359*, 458-461.
- (176) Gunther, D.; Frischknecht, R.; Heinrich, C. A.; Kahlert, H.-J. *JAAS* **1997**, *12*, 939-944.
- (177) Mao, X. L.; Ciocan, A. C.; Russo, R. E. *App. Spectros.* **1998**, *52*, 913-918.

- (178) Andrews, D. L. In *Lasers in Chemistry*, 2nd ed.; Andrews, D. L., Ed.; Springer-Verlag: London, 1990.
- (179) Jarvis, K. E.; Gray, A. L.; Houk, R. S. In *Handbook of Inductively Coupled Plasma Mass Spectrometry*; Jarvis, K. E., Gray, A. L., Houk, R. S., Eds.; Blackie: Glasgow, 1992, pp 294.
- (180) Veillon, C.; Patterson, K. Y.; Bryden, N. A. *Anal. Chim. Acta* **1984**, *164*, 67-76.
- (181) Dewaal, W. A. J.; Maessen, F. J. M. J.; Kraak, J. C. J. *Pharm. Biomed. Anal.* **1990**, *8*, 1-30.
- (182) Ruzicka, J.; Hansen, E. H. In *Flow Injection Analysis*; John Wiley and Sons: New York, 1981.
- (183) Fergusson, J. E. In *Noble Metals and Biological Systems Their Role in Medicine, Mineral Exploration and the Environment*; Brooks, R. R., Ed.; CRC Press: Ann Arbor, 1992, pp 94.
- (184) Messerschmidt, J.; Alt, F.; Tolg, G.; Angerer, J.; Schaller, K. H. *Fresenius J. Anal. Chem.* **1992**, *343*, 391-394.
- (185) Artelt, S.; Creutzenberg, O.; Kock, H.; Levsen, K.; Nachtigall, D.; Heinrich, U.; Ruhle, T.; Schlogl, R. *Sci. Tot. Environ.* **1999**, *228*, 219-242.
- (186) Luedke, C.; Hoffmann, E.; Skole, J.; Artelt, S. *Fresenius J. Anal. Chem.* **1996**, *355*, 261.
- (187) Ma, R.; Staton, I.; McLeod, C. W.; Gomez, M. B.; Gomez, M. M.; Palacios, M. A. *JAAS* **2001**, *16*, 1070-1075.
- (188) Farago, M. E.; Kavanagh, P.; Blanks, R.; Kelly, J.; Kazantzis, G.; Thornton, I.; Simpson, P. R.; Cooke, J. M.; Parry, S.; Hall, G. E. M. *Fresenius J. Anal. Chem.* **1996**, *354*, 660.
- (189) Lustig, S.; Zang, S.; Michalke, B.; Schramel, P.; Beck, W. *Science of the Total Environment* **1996**, *188*, 195.
- (190) Schofer, J.; Hannker, D.; Eckhardt, J.-D.; Stuben, D. *Science of the Total Environment* **1998**, *215*, 59.
- (191) Kummerer, K.; Helmers, E. *Sci. Tot. Environ.* **1997**, *193*, 179-184.
- (192) Begerow, J.; Turfield, M.; Dunemann, L. *JAAS* **1996**, *11*, 913-916.
- (193) Krachler, M.; Alimonti, A.; Petrucci, F.; Irgolic, K. J.; Forastiere, F.; Caroli, S. *Anal. Chim. Acta* **1998**, *363*, 1-10.
- (194) Begerow, J.; Dunemann, L. *JAAS* **1996**, *11*, 303-306.
- (195) Litterst, C. L. *Pharmacol. Ther.* **1988**, *38*, 215-251.
- (196) Cole, W. C.; Wolf, W. *Chem.-Biol. Inter.* **1980**, *30*, 223-235.
- (197) Sun, H.; Cox, M. C.; Li, H.; Mason, A. B.; Woodworth, R. C.; Sadler, P. J. *FEBS Letters* **1998**, *422*, 315-320.
- (198) Bhagavan, N. V. In *Medical Biochemistry*, 4th ed.; Bhagavan, N. V., Ed.; Harcourt/Academic Press: London, 2001, pp 949.
- (199) Ishida, K.; Orimo, H. In *Handbook on Metals in Clinical and Analytical Chemistry*; Seiler, H. G., Sigel, A., Sigel, H., Eds.; Marcel Dekker: New York, 1994, pp 388.
- (200) Shaw III, C. F. In *Metals and Their Compounds in the Environment*; Merian, E., Ed.; VCH: Weinheim, 1991, pp 931.
- (201) Perrelli, G.; Piolatto, G. *Sci. Tot. Environ.* **1992**, *120*, 93-96.
- (202) Smith, P. M.; Smith, E. M.; Gottlieb, N. L. *J. Lab. Clin. Med.* **1973**, *82*, 930-937.
- (203) Brown, D. H.; Smith, W. E.; Fox, P.; Sturrock, R. D. *Inorg. Chim. Acta - Bioinorg. Chem.* **1982**, *67*, 27-30.

- (204) Doner, G.; McLeod, C. W.; Bax, D. In *Plasma Source Mass Spectrometry Development and Applications*; G., H., Tanner, S. D., Eds.; Royal Society of Chemistry: Cambridge, 1997, pp 175-181.
- (205) Dietz, A. A.; Rubenstein, H. M. *Clin. Chem.* **1969**, *15*, 787.
- (206) Shaw III, C. F. In *Metals and Their Compounds in the Environment*; Merian, E., Ed.; VCH: Weinheim, 1991, pp 934.
- (207) Beesley, J. E. In *Colloidal Gold: A New Perspective for Cytochemical Marking*; Beesley, J. E., Ed.; Oxford University Press: London, 1989, pp 8.
- (208) Versieck, J.; Cornelis, R. *Anal. Chim. Acta* **1980**, *116*, 217-254.
- (209) Huebers, H. A. In *Metals and Their Compounds in the Environment*; Merian, E., Ed.; VCH: Weinheim, 1991, pp 945-958.
- (210) Parisi, A. F.; Vallee, B. L. *Am. J. Clin. Nutr.* **1969**, *22*, 1222-1239.
- (211) Prasad, A. S.; Oberleas, D. *J. Lab. Clin. Med.* **1970**, *76*, 416-425.
- (212) Raptis, S.; Muller, K. *Clin. Chim. Acta* **1978**, *88*, 393-402.
- (213) Bernard, A.; Roels, H.; Hubermont, G.; Buchet, J. P.; Masson, P. L.; Lauwerys, R. R. *Int. Arch. Occup. Env. Health* **1976**, *38*, 19-30.
- (214) Giroux, E. L.; Henkin, R. I. *Bioinorg. Chem.* **1972**, *2*, 125-133.
- (215) Watkins, S. R.; Hodge, R. M.; Cowman, D. C.; Wickman, P. P. *Biochem. Biophys. Res. Commun.* **1977**, *74*, 1403-1410.
- (216) Thomson, A. B. R.; Valberg, L. S. *Am. J. Physiol.* **1972**, *223*, 1327-1329.
- (217) Nandekar, A. K. N.; Basu, P. K.; Friedberg, F. *Bioinorg. Chem.* **1972**, *2*, 149-157.
- (218) Gerhardsson, L.; Wester, P. O.; Nordberg, G. F.; Brune, D. *Sci. Tot. Environ.* **1984**, *37*, 233-246.
- (219) Sunderman, F. W. J. In *Handbook on Toxicity of Inorganic Compounds*; Seiler, H. G., Sigel, H., Sigel, A., Eds.; Marcel Dekker: New York, 1986, pp 453-468.
- (220) Van Soestbergen, M.; Sunderman, F. W. J. *Clin. Chem.* **1972**, *18*, 1478-1484.
- (221) Nomoto, S.; McNeely, M. D.; Sunderman, F. W. J. *Biochem.* **1971**, *10*, 1647-1651.
- (222) Anderson, R. A. *Sci. Tot. Environ.* **1981**, *17*, 13-22.
- (223) Langard, S. In *Biological and Environmental Aspects of Chromium*; Langard, S., Ed.; Elsevier: Amsterdam, 1982, pp 149-169.
- (224) Hartman, R. E.; Hayes, R. L. *J. Pharmacol. Exp. Ther.* **1969**, *168*, 193-198.
- (225) Hamilton, E. I.; Miniski, M. J.; Cleary, J. J. *Sci. Tot. Environ.* **1972**, *1*, 1-14.
- (226) Lagerkvist, B.; Nordberg, G. F.; Vouk, V. In *Handbook on the Toxicology of Metals*, 2nd ed.; Lagerkvist, B., Nordberg, G. F., Vouk, V., Eds.; Elsevier: Amsterdam, 1986, pp 638-663.
- (227) Rengarajan, K.; de Smet, M. D.; Wiggert, B. *Biotech.* **1996**, *20*, 30-32.
- (228) Fenselau, C. *Anal. Chem.* **1997**, *11*, 661A-665A.
- (229) Ogorzalek Loo, R. R.; Stevenson, T. I.; Mitchell, C.; Loo, J. A.; Andrews, P. C. *Anal. Chem.* **1996**, *68*, 1910-1917.
- (230) Olesik, J. W.; LKinzer, J. A.; Olesik, S. V. *Anal. Chem.* **1995**, *67*, 1-12.
- (231) Bradford, M. B. *Anal. Biochem.* **1976**, *72*, 248-254.
- (232) Compton, S. J.; Jones, C. G. *Anal. Biochem.* **1985**, *151*, 369.